OXYGEN, CARBON, AND HYDROGEN ISOTOPE STUDIES OF CONTACT METAMORPHISM

Thesis by

Yuch-Ning Shieh

In Partial Fulfillment of the Requirements

For the Degree of

Doctor of Philosophy

California Institute of Technology

Pasadena, California

1969

(Submitted July 15, 1968)

ACKNOWLEDGEMENTS

I wish to thank Dr. Hugh P. Taylor, Jr. for encouragement and guidance throughout the course of this research.

I am indebted to Dr. S. Epstein for the use of his mass spectrometer laboratory and facilities.

Drs. T. E. Bridge, R. R. Compton, S. R. Hart, R. H. Steiger, and G. R. Tilton generously contributed specimens for analysis.

I am grateful for valuable discussions I have had with Drs. A. L. Albee, S. Epstein, S. M. Savin, S. M. F. Sheppard, L. T. Silver, and R. H. Steiger. Dr. R. H. Steiger also aided me in collecting samples from the Eldora area.

Assistance with the construction and maintenance of the apparatus was received from Messrs. C. Bauman, E. V. Nenow, and P. Yanagisawa.

I would like to express my thanks to my wife, Tiee-leou, for her encouragement and assistance during this study.

This research was supported by grant from the National Science Foundation (Grant Number GA 992) and by the Atomic Energy Commission Contract Number AT (04-3) - 427.

ABSTRACT

The O^{18}/O^{16}, C^{13}/C^{12}, and D/H ratios have been determined for rocks and coexisting minerals from several granitic plutons and their contact metamorphic aureoles in northern Nevada, eastern California, central Colorado, and Texas, with emphasis on oxygen isotopes. A consistent order of O^{18}/O^{16}, C^{13}/C^{12}, and D/H enrichment in coexisting minerals, and a correlation between isotopic fractionations among coexisting mineral pairs are in general observed, suggesting that mineral assemblages tend to approach isotopic equilibrium during contact metamorphism. In certain cases, a correlation is observed between oxygen isotopic fractionations of a mineral pair and sample distance from intrusive contacts. Isotopic temperatures generally show good agreement with heat flow considerations. Based on the experimentally determined quartz-muscovite O^{18}/O^{16} fractionation calibration curve, temperaturesare estimated to be 525 to 625°C at the contacts of the granitic stocks studied.

Small-scale oxygen isotope exchange effects between intrusive and country rock are observed over distances of 0.5 to 3 feet on both sides of the contacts; the isotopic gradients are typically 2 to 3 per mil per foot. The degree of oxygen isotopic exchange is essentially identical for different coexisting minerals. This presumably occurred through a diffusion-controlled recrystallization process. The size of the oxygen isotope equilibrium systems in the small-scale exchanged zones vary from about 1.5 cm to 30 cm. A xenolith and a re-entrant of country rock projecting into an intrusive have both undergone much more extensive isotopic exchange (to hundreds of feet);

they also show abnormally high isotopic temperatures. The marginal portions of most plutons have unusually high O^{18}/O^{16} ratios compared to "normal" igneous rocks, presumably due to large-scale isotopic exchange with metasedimentary country rocks when the igneous rocks were essentially in a molten state. The isotopic data suggest that outward horizontal movement of H_2O into the contact metamorphic aureoles is almost negligible, but upward movement of H_2O may be important. Also, direct influx and absorption of water from the country rock may be significant in certain intrusive stocks.

Except in the exchanged zones, the O^{18}/O^{16} ratios of pelitic rocks do not change appreciably during contact metamorphism, even in the cordierite and sillimanite grades; this is in contrast to regional metamorphic rocks which commonly decrease in O^{18} with increasing grade. Low O^{18}/O^{16} and C^{13}/C^{12} ratios of the contact metamorphic marbles generally correlate well with the presence of calc-silicate minerals, indicating that the CO_2 liberated during metamorphic decarbonation reactions is enriched in both O^{18} and C^{13} relative to the carbonates.

The D/H ratios of biotites in the contact metamorphic rocks and their associated intrusions show a geographic correlation that is similar to that shown by the D/H ratios of meteoric surface waters, perhaps indicating that meteoric waters were present in the rocks during crystallization of the biotites.

TABLE OF CONTENTS

I. INTRODUCTION

1.1 Statement of the problem

Studies of the variations of oxygen isotopes, and to a lesser extent carbon and hydrogen isotopes, in rocks and minerals have been made in recent years. Such studies are useful in interpreting geologic processes. From previous work, it is known that igneous rocks and minerals are generally lowest in O^{18}/O^{16} ratios, while sedimentary rocks and minerals are highest. Metamorphic rocks and minerals have intermediate O^{18}/O^{16} ratios. The purpose of the present study is to investigate how the isotopic compositions of rocks and minerals change during contact metamorphic processes. In contact metamorphic aureoles, one commonly can trace a single lithologic unit from an area where the rocks are essentially unaffected to a locality where the rocks are in contact with intrusive igneous bodies. The physical parameters, particularly the temperature, can be at least qualitatively inferred from the spatial configurations of the country rocks and the intrusions. More specifically, the present studies aim to determine:

(1) The O^{18}/O^{16}, C^{13}/C^{12}, and D/H ratios of contact metamorphic minerals and rocks.

(2) The extent of isotopic exchange between the country rock and the intrusive.

(3) The effect of metamorphic reactions upon the isotopic compositions of metamorphic rocks.

(4) The isotopic compositions of H_2O and CO_2 liberated by contact metamorphic reactions.

(5) Whether isotopic geothermometers are applicable in a contact metamorphic environment.

1.2 Previous work

Early researches on the oxygen isotopic compositions of rocks and minerals are those of Silverman (1951), Baertschi (1950), Baertschi and Silverman (1951), and Schwander (1953). These investigators found large variations of O^{18}/O^{16} ratios among geologic materials.

Baertschi (1957) made a thorough study of the oxygen and carbon isotopes of carbonate rocks with emphasis on metamorphic marbles. He found both O^{18}/O^{16} and C^{13}/C^{12} ratios usually decreased as the limestones were metamorphosed. Clayton and Epstein (1958), and Engel, Clayton, and Epstein (1958) analyzed the oxygen isotopic compositions of coexisting quartz, calcite, and dolomite in various types of Leadville limestone, including hydrothermal dolomites and contact metamorphic marbles. They found a systematic decrease in the oxygen isotopic fractionations between quartz and calcite in the vicinity of ore bodies and obvious conduits. James and Clayton (1962) measured the O^{18}/O^{16} ratios of magnetite, hematite, quartz, and calcite from the metamorphosed iron formations of the Lake Superior region and in other iron-rich rocks. Isotopic fractionations were observed to decrease systematically up to the garnet grade, but at higher grades, no correlation was observed between metamorphic grade and isotopic fractionations. Taylor and Epstein (1962) showed that isotopic fractionations among coexisting minerals in metamorphic rocks were larger than in igneous rocks, but that equilibrium was generally not completely attained in either rock types. Also they

showed that regional metamorphism tended to reduce O^{18}/O^{16} ratios of metasedimentary rocks. Taylor, Albee, and Epstein (1963) analyzed the oxygen isotopic compositions of coexisting minerals in kyanite-zone pelitic schists from the Lincoln Mountain quadrangle, Vermont. They found that the isotopic compositions in a particular mineral from rocks several hundred meters apart are identical within experimental error. Perry and Bonnichsen (1966) analyzed coexisting quartz and magnetite in the contact metamorphic aureole of the Duluth gabbro. They found a systematic increase of fractionation between the two minerals outward from the contact. Schwarcz (1966) studied the O^{18}/O^{16} and C^{13}/C^{12} ratios in coexisting dolomite and calcite from metamorphic rocks in Vermont. He found no consistent correlation between metamorphic grade and isotopic fractionations, but the Mg-content in calcite is related to carbon isotopic fractionation between dolomite and calcite. Garlick and Epstein (1967), after making a general survey of the oxygen isotopic compositions in coexisting minerals of regional metamorphic rocks, concluded that there is generally a consistent correlation between grade of metamorphism and oxygen isotopic fractionations among coexisting minerals. Sharma, Mueller, and Clayton (1965) demonstrated that the O^{18}/O^{16} ratios of quartz, magnetite, amphibole, and pyroxene in the metamorphosed Quebec iron formations are rather high, indicating major retention of the original sedimentary O^{18}/O^{16} ratios during metamorphism. On the other hand, Taylor (1968 a) has shown that the anorthosite body in the Adirondack Mountains is enriched in O^{18}/O^{16} ratio by 2 to 4 per mil compared to normal un-metamorphosed anorthosite, suggesting isotopic exchange with O^{18}/O^{16} rich pore fluids. Taylor and Coleman (1968) studied the O^{18}/O^{16} ratios of coexisting

minerals in glaucophane-bearing metamorphic rocks. They found that the fractionations among minerals are quite systematic, being larger than the corresponding minerals in the pelitic schists of the biotite zone or higher grades. Equilibration and homogenization of isotopes were observed in a few cases. Anderson (1967) showed that oxygen isotopic equilibrium is commonly not attained during regional metamorphism over dimensions of more than a few mm or cm.

The results of Taylor and Epstein (1962) on the oxygen isotopic compositions of minerals from plutonic igneous rocks are pertinent to the present study. They found that regardless of the igneous rock type in which a mineral occurred, its isotopic composition is confined to a narrow range. Quartz is invariably the mineral richest in O^{18}, and magnetite is the lowest. Other coexisting minerals have intermediate O^{18}/O^{16} ratios; the usual sequence is: quartz, K-feldspar, plagioclase, pyroxene, hornblende, biotite, and magnetite. The consistencies are observed in all the rock types, regardless of age or geographic location.

Hydrogen isotope variations in igneous minerals have been studied by Godfrey (1962), Friedman et al. (1964a), and Taylor and Epstein (1966). Little or no D/H fractionation is observed between coexisting biotite and hornblende, but large variations exist between different rocks. Taylor and Epstein (1966) also measured the D/H ratios in metamorphic minerals. They found that muscovite is invariably enriched in deuterium relative to biotite and hornblende, whereas chlorite has intermediate values.

The experimental calibrations of mineral - H_2O or mineral - CO_2 systems have been carried out by several workers. The calcite-water system

was determined by Clayton (1961) and O'Neil and Clayton (1964). Other mineral - H_2O or mineral - CO_2 systems which have been done include: dolomite-calcite by Northrop and Clayton (1966) and O'Neil and Epstein (1966), quartz-water and magnetite-water by O'Neil and Clayton (1964), alkali feldspar-water and anorthite-water by O'Neil and Taylor (1967), and muscovite-water by O'Neil and Taylor (1966) for various temperatures from 250° to 800°C.

II. THEORETICAL CONSIDERATIONS

2.1 Terminology

The fractionation factor α_{A-B} between two chemical compounds or phases A and B is defined by:

$$\alpha_{A-B} = R_A / R_B$$

where $R_A = (O^{18}/O^{16})_A$ or $(C^{13}/C^{12})_A$, or $(D/H)_A$;

$$R_B = (O^{18}/O^{16})_B, \text{ or } (C^{13}/C^{12})_B, \text{ or } (D/H)_B.$$

The experimental data are reported in terms of the quantity δ defined by

$$\delta_A = \frac{R_A - R_{std}}{R_{std}} \times 1000$$

where R_{std} is the reference standard. For oxygen and hydrogen, the standard is Standard Mean Ocean Water (SMOW) defined by Craig (1961). For carbon, the standard is PDB carbonate standard (Craig, 1957).

α is related to δ by the following equation:

$$\alpha_{A-B} = \frac{1000 + \delta_A}{1000 + \delta_B}$$

If α_{A-B} is very close to unity, then

$$\ln \alpha_{A-B} \approx \alpha_{A-B} - 1 = \frac{\delta_A - \delta_B}{1000 + \delta_B}$$

therefore,

$$1000 \ln \alpha_{A-B} \approx \delta_A - \delta_B$$

For abbreviation, $1000 \ln \alpha_{A-B}$ will commonly be denoted by Δ_{A-B}.

The following equation is useful in relating the δ -values of a sample measured against different standards:

$$\delta(A\text{-}S1) = \delta(A\text{-}S2) + \delta(S2\text{-}S1) + 10^{-3}\ \delta(A\text{-}S2)\ \delta(S2\text{-}S1)$$

where (A-S1) is sample A measured against standard S1; (A-S2) is sample A measured against standard S2; and (S2-S1) is standard S2 measured against standard S1.

2.2 Isotopic fractionations

A. Equilibrium isotopic fractionation

Consider the following isotopic exchange reaction:

$$aA_1 + bB_2 = aA_2 + bB_1$$

where A and B are two molecules having an element as a common constituent, and the subscripts 1 and 2 indicate that the molecule contains only the light or the heavy isotope, respectively. The number of the reacting molecules is indicated by a and b. For this reaction, the equilibrium constant is equal to

$$K = \left(\frac{Q_{A_2}}{Q_{A_1}}\right)^a \Big/ \left(\frac{Q_{B_2}}{Q_{B_1}}\right)^b$$

where the Q's are the partition functions of the molecules containing the various isotopic species. The calculation for a single partition function is very complicated; but actually only the ratios of the partition functions for isotopic molecules enter into the equilibrium constant. Urey (1947) and Bigeleisen and Mayer (1947) made various approximations and showed that the ratios of partition functions can be calculated from a knowledge of vibrational frequencies alone. Their approximated formulas predict that:

(1) At low temperatures or high frequencies, ln K is proportional to $1/T$.

(2) At high temperatures or low frequencies, ln K is proportional to $1/T^2$.

(3) At extremely high temperatures, ln K approaches 0.

Theory also shows that it is possible for the equilibrium constant of certain reactions to change with temperature from a region in which K is greater than 1 to a region where K is less than 1. In other words, the equilibrium constant may show a "cross-over" at some temperature.

The pressure effect is not expected to alter appreciably the equilibrium isotopic fractionations, because the volume change accompanying the isotopic substitution is very small. Hoering (1961) found that the oxygen isotopic fractionation between bicarbonate ion and water at 4 Kb differed from the atmospheric-pressure determinations by only 0.2 ± 0.2 per mil.

The equilibrium isotopic fractionation factor α is related to the equilibrium constant K by the equation:

$$\alpha = K^{1/n}$$

where n is the number of equivalent exchangeable atoms in the reaction. If the chemical reaction is written with the proper stoichiometric coefficients such that only one atom is exchanged, then $\alpha = K$.

B. Kinetic isotopic fractionation

Kinetic isotopic fractionations are due to differences in translational velocities or reaction rates. The subject has been treated by Bigeleisen (1949). When different isotopic atoms are chemically bound as molecules in the reacting species, the light molecule will usually have a greater rate constant than

the heavy molecule. An example of this type is the electrolytic decomposition of H_2O and D_2O. There are, however, also reactions in which the rate of the heavy isotope is higher than that of the light isotope.

The most important reactions which might be accompanied by kinetic isotopic fractionations in metamorphic processes are dehydration and decarbonation reactions. Unfortunately, our knowledge upon the isotopic effects of these reactions is exceedingly limited, because quantitative predictions of kinetic-fractionation phenomena are very difficult.

2.3 Diffusion processes

Diffusion is a spontaneous process by which molecules, atoms, or ions, driven by a chemical potential gradient, move from point to point in an attempt to reach a constant chemical potential everywhere.

The relations of concentration with time and space are governed by Fick's First Law and Second Law of diffusion. In one dimension, the two Fick's laws have the following form:

$$S_x = - D \frac{\partial c}{\partial x}$$

$$\frac{\partial c}{\partial t} = \frac{\partial}{\partial x} \left(D \frac{\partial c}{\partial x} \right)$$

where S_x is the net flow of material through unit cross section in unit time, c is the concentration, x is the distance, t is the time, and D is the diffusion coefficient.

The average distance travelled by the diffusing particles after time t is given by:

$$\overline{x^2} = 2Dt$$

where $\overline{x^2}$ is the mean square displacement.

The dependence of diffusion coefficient on temperature obeys the Arrhenius Equation:

$$D = D_o \, e^{-Q/RT}$$

where D_o is a constant, Q is the activation energy, R is the gas constant, and T is the absolute temperature.

Three types of diffusion in solids will be distinguished: lattice diffusion, grain boundary diffusion, and surface diffusion. Lattice diffusion coefficients are in general several orders of magnitude smaller than grain-boundary diffusion coefficients, which are in turn much smaller than surface diffusion coefficients. The diffusion coefficient in a liquid is commonly several orders of magnitude larger than the diffusion coefficient in a solid.

The diffusion coefficients in solids are usually very small quantities. For example, Choudhury et al. (1965) determined the diffusion coefficient of oxygen in quartz parallel to the c-axis to be 4×10^{-12} cm^2/sec, using the nuclear reaction O^{18} (p, α) N^{15} method at 667° C and 820 bars. It was determined by Verhoogen (1952) at 500° C to be 3×10^{-11} cm^2/sec, using electric conductivity measurements. Haul and Dümbgen (1962) employed isotopic exchange rates between oxygen and quartz, in the temperature range of 1010 to 1220° C, to obtain the diffusion coefficient of oxygen in quartz. By extrapolating their data to 667° C by means of the Arrhenius Equation, a value of 1.0×10^{-21} cm^2/sec is obtained; this is about 9 orders of magnitude smaller than that determined by Choudhury et al. (1965). The diffusion

coefficients in silicate melts have been determined by Bowen (1921) to be of the order of 10^{-6} to 10^{-7} cm^2/sec. Therefore, material transport by diffusion alone is limited to very short distances, particularly if only solid diffusion is considered.

When two or more isotopes of a specific element are transported by diffusion, a change in isotopic abundance ratio might be expected because of the velocity differences of isotopes of a given element. Verbeek and Schreiner (1967) have cited the variations of K^{39}/K^{41} ratios in a granite-amphibolite contact as having resulted from such an effect. However, no evidence of diffusion-induced fractionation of oxygen isotopes in natural processes has yet been observed.

2.4 Heat flow models

A. General statement

In contact metamorphic aureoles, heat flow calculations can usually give us some idea about: (1) the maximum temperature attained in a sample at a certain distance away from the intrusive contact; (2) how long the sample will remain above a certain specific temperature; and (3) the temperature gradient in the contact aureoles. It is also desirable to compare temperatures calculated from heat flow models with those from oxygen isotopic geothermometers and those from mineral parageneses to justify the validity of various assumptions made in the heat flow models.

B. Heat flow equation and its solutions

The differential equation of heat conduction in rectangular coordinates has the following form:

$$\frac{\partial T}{\partial t} = H\left(\frac{\partial^2 T}{\partial x^2} + \frac{\partial^2 T}{\partial y^2} + \frac{\partial^2 T}{\partial z^2}\right) \qquad (1)$$

where T is temperature, t is time, and H is thermal diffusivity defined by:

$$H = k/\rho c$$

where k is thermal conductivity, ρ is density, and c is specific heat.

In an infinite region of constant k, ρ, and c, with a prescribed initial temperature $f(x, y, z)$ at time $t = 0$, the temperature T at x, y, z at time t is given by Carslaw and Jaeger (1959):

$$T = 1/8(\pi Ht)^{-3/2} \int_{-\infty}^{\infty}\int_{-\infty}^{\infty}\int_{-\infty}^{\infty} f(x',y',z') \exp\left\{\frac{(x-x')^2+(y-y')^2+(z-z')^2}{4\,H\,t}\right\} dx'dy'dz' \qquad (2)$$

The initial temperature $f(x', y', z')$ may be continuous or step-wise in the space coordinates. The following situations are pertinent to the present research:

(1) An infinite dike $-d < x < d$ with constant initial temperature T_o and zero temperature outside. In this case

$$T(x,t) = 1/2\ T_o \left\{\operatorname{erf} \frac{\xi+1}{2\,\tau^{\frac{1}{2}}} - \operatorname{erf} \frac{\xi-1}{2\,\tau^{\frac{1}{2}}}\right\} \qquad (3)$$

where ξ and τ are the dimensionless quantities:

$$\xi = x/d$$

$$\tau = Ht/d^2$$

and erf u is the error function defined by:

$$\operatorname{erf} u = 2\,\pi^{-\frac{1}{2}} \int_0^u e^{-\xi^2}\, d\xi$$

The contact temperature, by letting $x = d$, is

$$Tc = T(d, t) = 1/2\ T_o \operatorname{erf}(\tau^{-1/2}) \qquad (4)$$

(2) Constant initial temperature T_o over the infinite cylinder of rectangular cross section $-d_1 < x < d_1$, $-d_2 < y < d_2$, and zero initial temperature outside. The temperature in this case is:

$$T = \tfrac{1}{4} T_o \left\{ \operatorname{erf} \frac{\xi_1 + 1}{2\tau_1^{\frac{1}{2}}} - \operatorname{erf} \frac{\xi_1 - 1}{2\tau_1^{\frac{1}{2}}} \right\} \left\{ \operatorname{erf} \frac{\xi_2 + 1}{2\tau_2^{\frac{1}{2}}} - \operatorname{erf} \frac{\xi_2 - 1}{2\tau_2^{\frac{1}{2}}} \right\} \qquad (5)$$

where $\xi_1 = x/d_1$, $\xi_2 = y/d_2$, $\tau_1 = Ht/d_1^2$, $\tau_2 = Ht/d_2^2$

(3) Constant initial temperature T_o over the region $|y| < x \tan \theta$, $x > 0$ which forms a wedge of angle 2θ, zero initial temperature outside the wedge. The contact temperature at $x = 0$, $y = 0$ is given by Jaeger (1964):

$$T_c = \theta T_o / \pi \qquad (6)$$

All the solutions discussed above apply to the situation where the thermal conductivity k, specific heat c, and density ρ are constant in the region of interest. There is also no latent heat involved.

If difference in thermal properties and latent heat are taken into account, the problem usually cannot be solved analytically. However, there are a few special cases where exact solutions are obtainable.

(1) Liquid magma initially intruded as an infinite dike at temperature T_o, with k_1, H_1, respectively, the thermal conductivity and diffusivity of the country rock, and k_2, H_2 those of magma (liquid and solidified). The initial contact temperature is given by Jaeger (1964):

$$T_c = \sigma T_o / (1 + \sigma) \qquad (7)$$

where $\sigma = (k_2 H_1^{1/2}) / (k_1 H_2^{1/2})$

(2) The latent heat L can be taken into account by assuming

that the same quantity of heat would be contained in the magma in the case of an exaggeration of the initial temperature by L/c degrees, i.e., the initial magma temperature is replaced by a fictitious temperature T_o':

$$T_o' = T_o + L/c \qquad (8)$$

and subsequently treated as a case of no latent heat.

(3) Liquid magma initially intruded as an infinite dike at a fixed melting point T_1 with latent heat L, and equal thermal properties in the country rock and magma. The distance x_o of the surface of solidification from the contact is given by Carslaw and Jaeger (1959, section II.2):

$$x_o = 2\lambda\,(Ht)^{1/2} \qquad (9)$$

where λ is the root of

$$\lambda\,(1+\operatorname{erf}\lambda)\,e^{\lambda^2} = c\,T_1 / L\,\pi^{1/2} \qquad (10)$$

The temperature before complete solidification of the dike is

$$T = T_1, \quad \text{for } 0 < |x| < d - 2\lambda\,(Ht)^{1/2}$$

$$T = T_1 \left\{ 1 + \operatorname{erf} \frac{d-x}{2(Ht)^{1/2}} \right\} / (1+\operatorname{erf}\lambda),$$

$$\text{for } |x| > d - 2\lambda\,(Ht)^{1/2} \qquad (11)$$

At contact ($x = d$)

$$T_c = T_1 / (1 + \operatorname{erf}\lambda) \qquad (12)$$

C. Numerical examples

Some of the numerical results of temperature vs. time curves in the country rock are given in Figure 1. The calculations were based on the assumption of equal thermal properties of country rock and intrusive, with

Figure 1. Temperature vs. time curves for various heat flow models, assuming magma temperature = 700°C, country rock temperature = 100°C, and diffusivity = 0.009 cm^2/sec. Latent heat of solidification accounted for by exaggeration of intrusive temperature by 300°C. Model A: infinite dike of thickness 8000 feet, sample distance measured perpendicular to the dike. Model B: infinite cylinder of square cross section 8000 x 8000 feet, distance measured perpendicular to one side from the midpoint. Model C: same as model B except distance measured diagonally from the vertex.

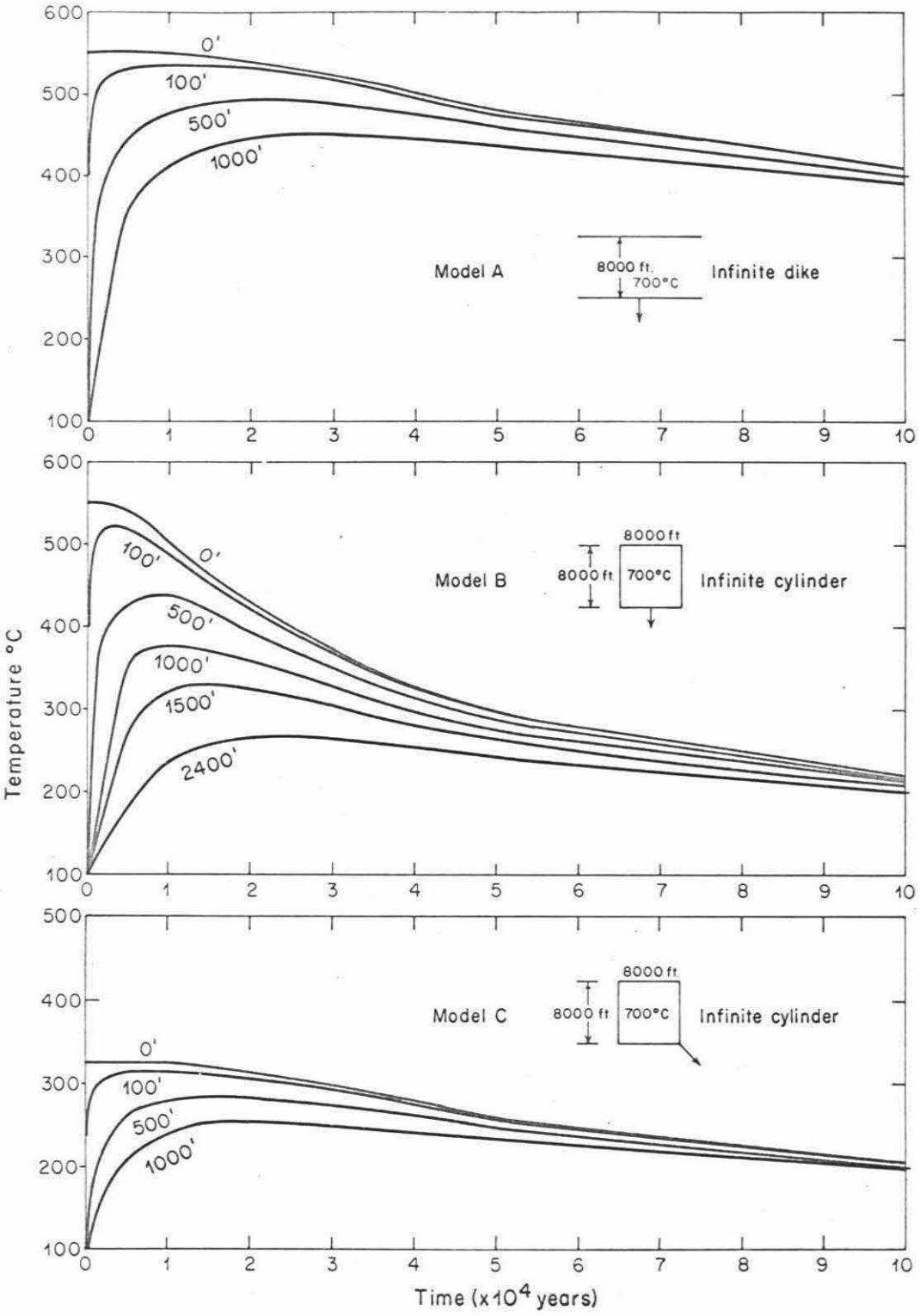
Temperature °C
Time (x10⁴ years)
Model A
8000 ft.
700°C
Infinite dike
0'
100'
500'
1000'
Model B
8000 ft
8000 ft
700°C
Infinite cylinder
0'
100'
500'
1000'
1500'
2400'
Model C
8000 ft
8000 ft
700°C
Infinite cylinder
0'
100'
500'
1000'

Figure 1

thermal diffusivity H = 0.009 cm^2/sec. The latent heat was accounted for by exaggeration of intrusive temperature by L/c = 300° C (L = 80 to 100 cal/gm, c = 0.25 to 0.3). The initial country rock temperature was taken to be 100° C.

Model A. Infinite dike of thickness 8000 feet, initial intrusive temperature 700°C, distance measured perpendicular to the dike. The solution is given in equation (3).

Model B. Infinite cylinder of square cross section 8000 x 8000 feet, initial intrusive temperature 700° C, distance measured perpendicular to the edge from the mid-point. The solution is given in equation (5).

Model C. Same as model B except distance measured diagonally from the vertex. The solution is given in equation (5).

Two pertinent features are to be noted: (1) The contact temperatures, as well as temperatures in the country rock, depend greatly on their locations with respect to the geometry of the intrusion (compare temperatures in model B and model C). (2) Although cooling rates are different for different models, and within the same model different for different locations and times, they are generally very slow. As an example, the 100-foot sample in model B, which will attain a maximum temperature of 520°C, will remain above 510°C for 5000 years.

III. EXPERIMENTAL TECHNIQUES

3.1 Sample collections

Most of the samples analyzed in this research were collected by the author. The exact locations and field relations of the samples are very important in order to interpret the isotopic data, particularly for samples near the intrusive contacts. For samples less than 1 foot from the contact, the distances were marked before they were broken from the outcrop. The rock samples adjoining each contact were sliced at 1/2 to 1 inch intervals parallel to the contact surface before they were crushed for mineral separation.

Sample-distances within 50 feet of the contact were measured by a steel tape. Sample-distances greater than 50 feet from the contact were measured by pacing. At distances greater than 500 feet, sample localities were located on a geologic or topographic map. Whenever possible, samples of a traverse were collected along the strike of a single bed or lithologic unit.

3.2 Sample preparations

For oxygen isotope analysis, mineral separations were made on as small a volume of rock as possible. This is particularly important for samples very close to the contact because of the steep isotopic compositional gradient. If samples are very coarse-grained, hand-picking was used. Otherwise, routine magnetic and heavy liquid procedures were performed. The platy minerals can further be purified by sliding over a sheet of paper. Quartz was separated from feldspars by dissolving away the feldspars in cold hydrofluoric acid for a few minutes. By combining the above methods, a purity of better

than 95% was usually obtained except for very fine mineral grains. In the latter case, a correction was made for the isotopic composition of the impurity by point counting. In some instances, the purity was checked by x-ray diffraction.

For hydrogen isotope analysis, purity is not too critical. Muscovite can easily be separated from biotite by passing through a Frantz isodynamic separator.

3.3 Oxygen extraction from silicates and oxides

The extraction of oxygen from silicates and oxides was performed by reacting with BrF_5 at 500 to 650° C in nickel reaction vessels, as described by Clayton and Mayeda (1963) and Garlick (1964). Mass spectrometric analyses were performed on CO_2 gas obtained from oxygen by combustion with a resistance-heated graphite rod as described by Taylor and Epstein (1962).

For most silicates, a grain size as coarse as 50 to 100 mesh is easily reacted with BrF_5 at a temperature of 500°C and a time of 8 hours. However, andalusite, magnetite, garnet, and forsterite are exceptions. These minerals have to be ground very fine (suspended in acetone) in order to obtain high yields. If coupled with higher reaction temperatures (~630°C) and longer reaction time (24 to 48 hours), near 100% yields can usually be obtained in most cases. Fortunately, the isotopic compositions of the oxygen liberated from these minerals are insensitive to the stoichiometric yield of oxygen. Andalusite was not analyzed previous to the present study; a study of yields vs. isotopic compositions was therefore made (Table 1). As can be seen, the oxygen isotopic compositions are, within experimental error, almost independent of percent yields.

TABLE 1

Comparison of oxygen isotopic compositions and oxygen yields from andalusite

Sample No.	Grain Size	Reaction Temperature °C	Reaction Time Hours	Yield %	δO^{18} permil
SRO-19 B	<200 mesh	616	22	75	15.74
SRO-19 B	Suspend in acetone	632	17	92	15.61
SRO-19 B	Suspend in acetone	640	30	100	15.84
SRO-15 B	Sink in acetone	610	21	78	15.26
SRO-15 B	Suspend in acetone	614	22	97	15.14
SRO-22 A	< 200 mesh	619	17	51 } 81	14.04
SRO-22 A	Residue from above run	648	22	30	13.76

3.4 Oxygen and carbon extractions from carbonates

The isotopic analysis of carbonates was determined by the mass spectrometric analysis of CO_2 liberated by reacting carbonate with anhydrous H_3PO_4 at 25°C as described by McCrea (1950). In this reaction, only 2/3 of the oxygen is liberated, but the oxygen isotopic fractionation in this reaction is a constant at a given temperature. The acid fractionation factors used are 1.01008 for calcite and 1.01090 for dolomite (Sharma and Clayton, 1965).

No physical separation of dolomite from calcite was attempted. A chemical separation technique developed by Epstein et al. (1964) was used, which allowed CO_2 evolved from calcite and dolomite to be collected separately. The method is based on the markedly faster reaction rate of calcite relative to dolomite during phosphoric acid treatment.

3.5 Hydrogen extraction

The experimental technique for extraction of hydrogen from OH-bearing minerals is similar to that described by Friedman (1953) and Godfrey (1962). Samples, after degassing at room temperature under high vacuum for about 1 hour, were heated by an induction furnace to a maximum temperature of 1300 to 1500°C to liberate hydrogen and water. Water was converted to hydrogen by passing it over hot uranium at about 750°C. The volume of total hydrogen evolved was measured and the gas was then ready for mass spectrometric analysis.

3.6 Mass spectrometry, correction factors, and standards

Mass spectrometric analyses of oxygen and carbon isotopes are

performed on CO_2 gas. The mass spectrometer used is a 60 degree, single-focusing, double-collecting and dual gas-feed instrument of the type described by Nier (1947) with modifications by McKinney et al. (1950).

For oxygen the mass spectrometer measures the ratio of the mass 46 beam to the mass 44 plus 45 beam, and for carbon the mass spectrometer measures the ratio of the mass 45 beam to the mass 44 beam, whereas the desired ratios are O^{18}/O^{16} and C^{13}/C^{12}. Therefore , one has to correct for the contribution of O^{17} and C^{13} to beam 45 and 46. The correction formulas have been derived by Craig (1957). Another correction factor one has to apply to the raw data is the background and mixing of standard and sample gas in the mass spectrometer because of slight imperfections in the valve system; a factor of 1.023 was used in this research.

During the course of this research, a working standard (St. Peter sandstone) was usually included in each set of six samples analyzed. The δO^{18}-value of St. Peter sandstone is taken as 10.9 per mil relative to Standard Mean Ocean Water (SMOW). The δ-value of all the samples were then normalized to the δ-value of St. Peter sandstone by comparing them with the mass spectrometer reference gas.

Mass spectrometric analyses of hydrogen isotopes are performed on hydrogen gas. The ratio of mass 3 to mass 2 is measured. Because the mass 3 beam consists of both HD^+ and H_3^+ ions, a correction has been made for the contribution of H_3^+ ions as described by Friedman (1953). The mass spectrometer background and leakage through the switching valves were also corrected using a correction factor of 1.01.

The precision of the mass spectrometers is about 0.1 per mil for

oxygen and carbon, and 1 per mil for hydrogen. The analytical error for oxygen and carbon samples in this research is about 0.1 to 0.2 per mil and for hydrogen samples about 2 to 3 per mil. The oxygen and hydrogen isotope data reported in this work are relative to Standard Mean Ocean Water (SMOW) as defined by Craig (1961) and Clayton and Mayeda (1963). The carbon isotope data are relative to the Chicago Pee Dee Belemnite (PDB) calcite standard (see Craig, 1957).

IV. ANALYTICAL RESULTS AND PETROGRAPHY

In the following are given a description of analyzed rocks and tabulation of isotopic data. The modes are in volume percent, and H_2O- contents of minerals and whole-rock samples are in weight percent. Analytical errors shown represent average deviation from the mean. Numbers in parentheses indicate the number of separate determinations.

4.1 Santa Rosa Range, Nevada

A. Sawtooth stock and its aureole

Traverse I

SRO-18. Medium-grained trondhjemite, 50 feet inward from contact. Quartz: 20%, anhedral, 1.5 - 2mm. Microcline: 15%, anhedral, 1.5mm. Plagioclase (An_{15}): 55%, subhedral, 2mm. Biotite: 8%, anhedral, 1.5mm. Muscovite: 2%, anhedral, 0.5mm. Opaques: trace, dust, 0.1mm.

Mineral	δO^{18} per mil	δD per mil
Quartz	11.7 ± 0.1 (3)	
Plagioclase (An_{15})	9.2 (1)	
Biotite (H_2O = 4.6%)	5.5 ± 0.1 (6)	-95 ± 0 (2)
Magnetite	-0.3 ± 0.1 (2)	

SRO-17. Coarse-grained leucocratic variety of trondhjemite, 10 feet inward from contact. Crosscut by quartz vein 2 inches in thickness.

Mineral	δO^{18} per mil
Quartz vein	11.8 ± 0.1 (2)
Plagioclase (An_{15})	9.7 (1)

SRO-16. Quartz vein crosscutting trondhjemite, 8 feet inward from contact.

Mineral	δO^{18} per mil
Quartz vein	11.5 ± 0.2 (2)

SRO-19AI. Medium grained equigranular trondhjemite, 6 inches from contact. Plagioclase (An_{15}): 50%, subhedral, zoned, 1.5 mm. Microcline: 5%, subhedral, zoned, 1.5 mm. Quartz: 25%, anhedral, 1.5 mm. Biotite: 10% anhedral, 1 - 1.5 mm. Muscovite: 10%, Flaky, 1 - 1.5 mm. Opaques: trace, dust, 0.01 mm.

Mineral	δO^{18} per mil	δD per mil
Quartz	14.5 ± 0.2 (3)	
Plagioclase (An_{15})	12.1 (1)	
Muscovite	11.2 ± 0.1 (3)	-64 (1)
Biotite (H_2O = 4.1%)	7.9 ± 0.1 (4)	-105 ± 1 (2)
Magnetite	0.2 ± 0.0 (2)	

SRO-15 C. Trondhjemite similar to SRO-19AI, 2 inches from contact.

Mineral	δO^{18} per mil	δD per mil
Quartz	16.0 ± 0.1 (4)	
Plagioclase (An_{15})	13.4 (1)	
Muscovite	12.7 ± 0.2 (3)	-62 (1)
Biotite (H_2O = 3.6%)	9.7 ± 0.1 (2)	-104 ± 2 (2)

SRO-15A. Trondhjemite similar to SRO-19AI, 0.5 inches from contact.

Mineral	δO^{18} per mil	δ D per mil
Quartz	15.9 ± 0.1 (4)	
Plagioclase (An_{15})	14.2 (1)	
Muscovite	13.1 ± 0.1 (4)	-66 (1)
Biotite (H_2O = 3.7%)	10.0 ± 0.1 (2)	-103 ± 4 (2)

SRO-15B. Porphyroblastic andalusite schist, 1 inch from contact. Andalusite: 15%, euhedral to subhedral, 3-10 mm, pink pleochroic core. Biotite: 35%, flaky, 0.5 - 1 mm. Quartz: 40%, two distinct sizes, 0.1 mm (granular) and 1 mm (irregular). Muscovite: 10%, flaky, 1 mm. Opaques: trace, dust. Biotite and muscovite locally abundant adjacent to the contact.

Mineral	δO^{18} per mil	δD per mil
Quartz	16.1 ± 0.2 (4)	
Andalusite	15.2 ± 0.1 (2)	
Muscovite	13.2 ± 0.1 (5)	-65 (1)
Biotite (H_2O = 4.3%)	9.9 ± 0.1 (5)	-97 ± 1 (2)
Whole rock (H_2O = 2.9%)	13.5 (calc.)	-75 (1)

SRO-19AII. Porphyroblastic staurolite-sillimanite-andalusite schist, 6 inches from contact. Andalusite: 10%, subhedral to anhedral, 3 - 6 mm, pleochroic in core. Biotite: 40%, anhedral or flaky, anhedral grains with abundant quartz inclusions, 0.5 - 1 mm. Quartz: 40%, two grain sizes (0.1 and 1 mm), anhedral. Muscovite: 7%, flaky, 1 mm. Staurolite: 1%, subhedral, 1 mm, as inclusions in andalusite. Sillimanite: 1%, fibrous aggregates pseudomorph after biotite or peripheral to andalusite. Opaques: 1%, 0.05 mm, as inclusions in other minerals.

Mineral	δO^{18} per mil	δD per mil
Quartz	16.7 ± 0.0 (2)	
Andalusite	14.4 ± 0.1 (2)	
Muscovite	14.1 ± 0.2 (4)	-59 ± 0 (2)
Biotite (H_2O = 3.6%)	10.9 ± 0.1 (4)	-86 ± 3 (8)
Magnetite	0.3 (1)	
Whole rock	14.5 (1)	

SRO-19B. Porphyroblastic andalusite schist, 1 foot from contact. Andalusite: 14%, 3 - 10 mm subhedral to anhedral, pleochroic in core. Muscovite: 30%, flaky, 0.5 - 1.5 mm. Biotite: 30%, flaky, 0.5 mm. Quartz: 25%, 2 mm (anhedral), 0.1 mm (granular). Opaques: 1%, 0.1 mm, equigranular, as inclusions or surrounding mica flakes.

Mineral	δO^{18} per mil	δD per mil
Quartz	18.7 ± 0.1 (2)	
Andalusite	15.8 ± 0.1 (4)	
Muscovite (H_2O = 4.6%)	15.3 ± 0.2 (3)	-57 ± 2 (2)
Biotite (H_2O = 4.4%)	11.8 ± 0.2 (4)	-110 ± 2 (2)
Whole rock (H_2O = 2.6%)	15.9 (1)	-83 (1)

SRO-19b: Aplite dike, 1/2 inch thick, crosscutting SRO-19B. Quartz: 40%, equigranular, 0.3 mm. Plagioclase (An_{10}): 50%, equigranular, 0.3 mm. Muscovite: 10%, flaky, 0.4 mm.

Mineral	δO^{18} per mil
Quartz	17.4 ± 0.2 (2)
Muscovite	16.1 ± 0.2 (2)
Whole rock	17.1 (1)

SRO-19C: Andalusite schist, 50 feet from contact. Minerals well oriented. Andalusite: 5%, 3 - 6 mm, subhedral. Biotite: 30%,

slender flakes, 0.2 mm. Muscovite: 15%, slender flakes, 0.2 mm. Quartz: 40%, 0.1 - 0.2 mm, granular, somewhat elongated. Plagioclase: 8%, 0.1 - 0.2 mm, elongated. Opaques: 2%, probably graphite, aggregates around margins of mineral grains.

Mineral	δO^{18} per mil	δ D per mil
Quartz	19.2 ± 0.1 (2)	
Muscovite	15.5 ± 0.1 (2)	-69 (1)
Biotite (H_2O = 4.3%)	12.0 ± 0.0 (3)	-98 ± 0 (2)
Whole rock (H_2O = 1.5%)	16.6 (1)	-81 (1)
Quartz pod	18.0 ± 0.1 (3)	

SRO-19D: Porphyroblastic phyllite, 600 feet from contact. Marked compositional banding. Andalusite gaining space by pushing other minerals to the side. Andalusite: 10%, euhedral to subhedral, 2 - 10 mm, most of them altered to white mica. White mica: 30%, 0.02 mm tiny slender aggregates, well oriented, some flaky muscovite derived from andalusite may attain 0.5 mm in size. Chlorite: 20%, subhedral to anhedral, 0.3 mm or less. Quartz and feldspar: 35%, 0.02 mm or less, oriented. Biotite: 1%, anhedral, 0.05 mm. Opaques: 4%, probably graphite, granular or fine dust dissipated in other minerals.

Mineral	δO^{18} per mil	δD per mil
Quartz	19.1 ± 0.2 (2)	
Andalusite	16.2 ± 0.1 (2)	
Muscovite	16.4 ± 0.1 (2)	-73 ± 2 (2)
Chlorite	12.2 ± 0.1 (2)	
Whole rock (H_2O = 3.6%)	16.8 (1)	-79 (1)
Quartz in quartzite	18.6 ± 0.1 (3)	

SRO-19E, SRO-19F, SRO-20A. Very fine-grained phyllites, collected 2000, 2500, and 7000 feet, respectively, from the contact. Low-grade regional metamorphic rocks unaffected by the intrusion of the stock. Grain-size less than 0.01 mm. Microfolded, marked compositional bandings. SRO-20A equivalent to Compton's No. 1A and 1B samples: Quartz 37%, Plagioclase 3.5%, Muscovite 15%, Grey mica 40%, Chlorite 3%, Ores 0.5%, Graphite 0.5%, Apatite 0.1%.

Sample No.	Mineral	δO^{18} per mil		δ D per mil	
SRO-19E	Whole rock (H_2O = 0.8%)	19.8	(1)	-63	(1)
SRO-19F	Whole rock (H_2O = 3.0%)	16.2	(1)	-80	(1)
	Quartz	18.9± 0.0	(2)		
	Grey mica*	14.0	(1)		
	Muscovite (calc.)**	15.0			
	Chlorite (calc.)**	11.0			
SRO-20A	Whole rock (H_2O = 2.4%)	18.0	(1)	-79	(1)

* X-ray diffraction shows: muscovite ~75%, chlorite ~25%.

** Assuming δ muscovite - δ chlorite = 4.

Traverse II

SRO-22F. Medium-grained equigranular trondhjemite, 50 feet from contact. Megascopically and microscopically similar to SRO-18 of traverse I.

Mineral	δO^{18} per mil	
Quartz	11.4± 0.1	(2)
Plagioclase (An_{15})	9.4	(1)
Biotite	5.3 ± 0.1	(2)

SRO-22E. Medium-grained equigranular trondhjemite, 1.5 feet inward from contact.

Mineral	δO^{18} per mil
Quartz	11.3 ± 0.0 (2)
Plagioclase	9.8 (1)
Biotite	5.6 ± 0.0 (2)

SRO-22D. Gneiss, 2 inches away from contact. Gneissic texture. White mica pods 5 - 10 mm of size conspicuous. Muscovite: 15%, 0.2 - 0.5 mm, flakes. Biotite: 40%, 0.2 mm, flakes. Quartz: 40%, anhedral, 0.1 - 0.3 mm. Plagioclase: 5%, anhedral, 0.1 - 0.3 mm. Muscovite aggregates very often assume oval shape, some are pseudomorphs after andalusites.

Mineral	δO^{18} per mil
Quartz	12.1 ± 0.1 (2)
Muscovite	9.2 ± 0.0 (2)
Biotite	6.5 ± 0.0 (2)
Whole rock	10.2 (1)

SRO-22C. Porphyroblastic andalusite schist, 5 feet from contact. Quartz: 35%, two grain sizes: 0.2 mm (granular) and 2 mm (irregular shape). Andalusite: 10%, 6 mm, euhedral. Muscovite: 15%, two grain sizes: 0.5 mm (small flakes) and 2 mm (long flakes usually surrounding andalusite porphyroblasts). Biotite: 28%, flaky, 0.5 mm. Plagioclase: 10%, anhedral, 0.2 mm. Opaques: 2%, 0.01 mm, granular or dusty.

Mineral	δO^{18} per mil
Quartz	15.1± 0.0 (3)
Andalusite	14.3 ± 0.0 (2)
Muscovite	12.6 ± 0.2 (2)
Biotite	9.7 ± 0.1 (2)
Whole rock	14.3 (1)

SRO-22A. Porphyroblastic staurolite-andalusite schist, 85 feet from contact. Matrix very fine-grained. Staurolite: 3%, subhedral, 2 mm. Andalusite: 7%, euhedral, 6 mm. Muscovite: 20%, flakes, 0.2 mm. Biotite: 20%, anhedral or flaky, 0.3 mm. Quartz: 40%, anhedral, two distinct grain sizes of 0.1 and 0.5 mm. Plagioclase: 8%, anhedral, 0.1 mm. Opaques: 2%, granular or dusty.

Mineral	δO^{18} per mil
Quartz	15.3 ± 0.0 (2)
Andalusite	14.0 ± 0.0 (2)
Muscovite	13.3 ± 0.2 (2)
Biotite	10.3 ± 0.1 (2)
Whole rock	13.9 (1)

SRO-25b. Chloritoid phyllite, 2000 feet from contact. Porphyroblastic euhedral chloritoid of 1.5 mm long embedded in a very fine grained, microfolded matrix. Equivalent to Compton's sample No. 2A: Quartz 39%, Plagioclase 10%, Muscovite 13%, Grey mica 30%, Chlorite 3%, Chloritoid 4%, Ores 0.5%, Graphite 0.5%, Apatite 0.2%.

Mineral	δO^{18} per mil
Quartz	18.0 (1)
Grey mica*	14.3 (1)
Whole rock	15.7 (1)
Muscovite (calc.) **	15.3
Chlorite (calc.) **	11.3

* X-ray diffraction shows a mixture of muscovite and chlorite roughly in a proportion of 3:1.

** Assuming δ muscovite - δ chlorite = 4.

SRO-25. Phyllite, 100 feet apart from SRO-25b. No chloritoid.

Mineral	δO^{18} per mil
Whole rocks	14.9 (1)

SRO-24. Staurolite phyllite, 2000 feet from contact. Euhedral to subhedral staurolite porphyroblasts 1 to 2 mm long embedded in a fine-grained matrix consisting of quartz, plagioclase, muscovite, chlorite, and biotite.

Mineral	δO^{18} per mil
Quartz	17.7 ± 0.1 (2)
Grey mica*	14.6 (1)
Quartz pod	17.6 (1)
Muscovite (calc.)**	15.6
Chlorite (calc.)**	11.6

* X-ray diffraction shows a mixture of muscovite and chlorite in roughly 3:1 ratio.

** Assuming δ muscovite - δ chlorite = 4.

South side of stock

SRO-A. Medium-grained equigranular trondhjemite, 500 feet inward from contact. Mineralogy and texture similar to those of SRO-18.

Mineral	δO^{18} per mil
Quartz	11.4 ±0.1 (2)
Plagioclase (An_{15})	9.5 (1)
Biotite	5.3 ± 0.1 (2)

SRO-B. Porphyroblastic andalusite schist, 1 foot from contact. Andalusite: 20%, subhedral, 4 - 8 mm, surrounded by muscovite flakes, usually having pleochroic pink core. Muscovite: 25%, flakes 5 - 6 mm long.

Biotite: 25%, anhedral, 0.2 mm, oriented. Quartz: 25%, anhedral, 0.2 - 0.5 mm. Plagioclase: 5%, anhedral, 0.2 - 0.5 mm.

Mineral	δO^{18} per mil
Quartz	15.8 ± 0.0 (2)
Andalusite	14.8 ± 0.0 (2)
Muscovite	12.2 ± 0.1 (2)
Biotite	9.4 ± 0.0 (2)

SRO-C. Garnet hornfels. Collected a few feet from the contact. Garnet: 30%, irregular and fragmental. Quartz: 60%, 0.2 mm, anhedral. Calcite: 3%, 0.2 mm, anhedral. Diopside: 3%, 0.2 mm, anhedral. Graphite: 4%, bordering quartz grains.

Mineral	δO^{18} per mil
Quartz	19.3 (1)

SRO-D: Pegmatite dike 3 inches thick crosscutting country rock (schist) a few feet away from contact. A pure quartz core about 0.5 inch thick bordered on both sides by extremely coarse-grained K-feldspar, muscovite, and minor quartz.

Mineral	δO^{18} per mil
Pure quartz core	18.3 (1)
Quartz	17.8 (1)
K-feldspar	12.4 (1)
Muscovite	15.7 (1)

B. Flynn stock and its aureole

North traverse

SRO-4. Medium-grained granodiorite, 300 feet inward from

contact. A leucocratic band (mainly K-feldspar) crosscutting the rock. Quartz: 25%, anhedral, 1 - 1.5 mm. Plagioclase (An_{30}): 45%, subhedral, 1 - 1.5 mm. Microcline: 20%, anhedral, 1 - 1.5 mm. Biotite: 8%, anhedral, 0.5 - 1 mm. Chlorite: 2%, 0.5 - 1 mm, alteration product of biotite.

Mineral	δO^{18} per mil
Quartz	12.6 ± 0.1 (3)
Feldspar	10.0 (1)
Biotite	6.6 ± 0.2 (3)
K-feldspar (leucocratic band)	11.8 ± 0.1 (3)

SRO-3C. Medium-grained granodiorite, 15 feet inward from contact. Plagioclase (An_{20}) 75%, subhedral, 1 - 3 mm, zoned. Quartz: 7%, anhedral, 0.5 mm. Hornblende: 15%, euhedral to subhedral, 1 mm. Biotite: 1%, alteration product of hornblende, 0.5 mm. Sphene: 2%, euhedral, 0.5 mm. Chlorite: trace, alteration product of hornblende.

Mineral	δO^{18} per mil
Quartz	14.3 ± 0.0 (2)
Plagioclase (An_{20})	11.6 ± 0.2 (2)
Hornblende	9.4 ± 0.1 (3)
Biotite	8.9 ± 0.1 (2)

SRO-3A-1. Medium-grained granodiorite, 6 inches inward from contact. Plagioclase (An_{20}): 55%, subhedral, zoned, 1 - 3 mm. Quartz: 15% anhedral, irregular size, average 1 mm. Hornblende: 20%, subhedral, 1.5 mm. Biotite: 10%, anhedral, 1.5 mm. Chlorite: trace, alteration product of biotite.

Mineral	δO^{18} per mil	δ D per mil
Quartz	14.5 ± 0.2 (3)	
Plagioclase (An_{20})	12.3 ± 0.1 (3)	
Hornblende	9.1 ± 0.2 (3)	-91 (1)
Biotite	9.2 ± 0.1 (3)	

SRO-3A-2. Amphibolite, 6 inches from contact. Hornblende: 40%, euhedral to subhedral, 0.5 - 1 mm. Plagioclase: 50%, 0.5 mm, lath. Biotite: 1%, anhedral, alteration product of hornblende. Chlorite: 4%, anhedral, alteration product. Quartz: 5%, anhedral, 0.5 mm.

Mineral	δO^{18} per mil	δ D per mil
Quartz	14.8 (1)	
Plagioclase	12.9 ± 0.1 (3)	
Hornblende	9.6 ± 0.1 (3)	-90 (1)
Chlorite	8.8 ± 0.2 (3)	

SRO-3B. Amphibolite, 10 feet from contact. Hornblende: 60%, euhedral to subhedral, 0.5 - 1 mm. Plagioclase: 35%, subhedral, 0.5 mm. Biotite: 4%, anhedral. Chlorite: 1%, anhedral. Biotite and chlorite are secondary after hornblende; they occur in minor amounts peripheral to or along cleavage cracks in the hornblende.

Mineral	δO^{18} per mil
Plagioclase	12.3 ± 0.2 (4)
Hornblende	8.6 ± 0.1 (4)
Biotite	8.5 ± 0.2 (3)

SRO-9. Amphibolite, 250 feet from contact. Mineralogy and texture similar to those of SRO-3B.

Mineral	δO^{18} per mil
Plagioclase	12.3 ± 0.1 (4)
Hornblende	8.0 ± 0.2 (4)
Biotite	8.5 (1)

SRO-5, SRO-7. Very fine-grained semi-hornfelses, 5 feet and 20 feet, respectively, from contact. Biotite: 40%, tiny flakes, 0.02 mm, well oriented. Quartz and Feldspar: 40%, anhedral, 0.02 mm. White mica: 10%, tiny flakes, 0.02 mm. Cordierite: 8%, 2 mm porphyroblasts, most of them have altered to white mica. Opaques: 1%, as inclusions in cordierite. Tourmaline: 1%, subhedral, 0.2 mm.

SRO-8, SRO-10. Very fine-grained semi-hornfelses. 150 and 400 feet, respectively, from contact. Differ from SRO-5 and SRO-7 in that they do not contain cordierite.

SRO-12. Porphyroblastic phyllite, 800 feet from contact. Cordierite porphyroblasts all have altered to white mica. Very fine-grained matrix composed of quartz, feldspar, grey mica, and chlorite.

SRO-11, SRO-13. Very fine-grained phyllite, collected 3000 and 5000 feet, respectively, away from contact.

Sample No.	Distance from Contact, feet	Rocks	δO^{18} per mil
SRO-5	5	Semi-hornfels	16.7 ± 0.1 (2)
SRO-7	20	Semi-hornfels	16.5 ± 0.0 (2)
SRO-8	150	Semi-hornfels	17.3 ± 0.0 (2)
SRO-10	400	Semi-hornfels	17.2 ± 0.1 (2)
SRO-12	800	Porphyro-phyllite	16.7 ± 0.1 (2)
SRO-11	3000	Phyllite	16.3 ± 0.2 (2)
SRO-13	5000	Phyllite	16.6 ± 0.2 (2)

South traverse

SRO-39. Medium-grained granodiorite, 75 feet inward from contact. Plagioclase (An_{30}): 55%, subhedral, strongly zoned, 2 - 3 mm, rarely 6 mm. K-feldspar: 15%, anhedral, 2 mm. Quartz: 15%, anhedral, 1 mm. Hornblende: 6%, subhedral, 1 - 2 mm. Biotite: 8%, subhedral to anhedral, 1 mm. Opaques: 1%, granular, 0.1 mm.

Mineral	δO^{18} per mil	δ D per mil
Quartz	10.7 ± 0.1 (2)	
Hornblende	6.4 (1)	
Biotite	5.0 ± 0.1 (2)	-90 (1)

SRO-38. Granodiorite, 35 feet inward from contact. Petrography the same as SRO-39.

Mineral	δO^{18} per mil
Quartz	10.5 (1)
Plagioclase (An_{30})	8.2 (1)
Hornblende	5.9 (1)
Biotite	4.6 (1)

SRO-37. Cordierite hornfels, 45 feet from contact. Cordierite: 25%, 2 - 3 mm, oval, abundant quartz and opaque inclusions. Quartz: 28%, anhedral, 0.1 mm. K-feldspar: 2%, anhedral, 0.2 mm. Plagioclase: 18%, anhedral, 0.1 mm. Biotite: 15% irregular shape, 0.2 mm. Muscovite: 8%, 0.2 mm, slender flakes. Opaques: 4%, 0.01 mm granular.

Mineral	δO^{18} per mil
Quartz	17.3 ± 0.1 (2)
Muscovite	15.2 ± 0.2 (2)
Biotite	12.0 ± 0.1 (2)

SRO-36. Andalusite-cordierite hornfels, 150 feet from contact. Cordierite: 30%, 2 - 3 mm, oval, abundant inclusions. Andalusite: 5%, anhedral, 0.5 mm. Biotite: 12%, irregular shape, 0.2 mm. Muscovite: 4%, 0.2 mm, slender flakes or irregular outline. Quartz: 28%, anhedral, 0.1 mm. Plagioclase: 15%, anhedral 0.1 mm. K-feldspar: 2%, anhedral, 0.1 mm. Sillimanite: trace, as needles in biotite and quartz. Opaques: 4%, granular, 0.01 mm.

Mineral	δO^{18} per mil
Quartz	17.3 ± 0.1 (2)
Andalusite	15.0 ± 0.1 (2)
Biotite	12.2 ± 0.0 (2)

SRO-42. Andalusite-cordierite hornfels, 200 feet from contact. Andalusite: 15%, euhedral, 5 mm long. Cordierite: 20%, oval, 2 - 3 mm. Quartz: 25%, anhedral, 0.1 mm. Plagioclase: 20%, anhedral, 0.1 mm. Biotite: 10%, anhedral, 0.2 mm,rarely 0.8 mm. Muscovite: 7%, slender flakes or irregular shape, 0.2 mm. Opaques: 3%, 0.01 mm, granular.

Mineral	δO^{18} per mil
Quartz	17.1 ± 0.2 (2)
Andalusite	15.0 ± 0.1 (2)
Muscovite	15.5 (1)
Biotite	12.2 (1)

SRO-46. Porphyroblastic phyllite, 3200 feet from contact. Euhedral andalusite porphyroblasts of 10 - 15 mm in length and oval-shaped white mica aggregates of 2 mm in size embedded in a very fine-grained chlorite, quartz, feldspar, and micas matrix. Some biotite also occurs as small oval (about 0.2 mm size).

Mineral	δO^{18} per mil
Quartz	16.9 (1)
Andalusite	14.8 ± 0.1 (2)

SRO-48. Porphyroblastic phyllite, 4500 feet from contact. Slender euhedral andalusites of 10 - 15 mm in length embedded in very fine-grained phyllitic matrix. No cordierite.

Mineral	δO^{18} per mil
Andalusite	15.1 ± 0.1 (2)
Whole rock	16.3 (1)

SRO-49, SRO-50. Phyllites, collected 5000 and 5300 ft., respectively, away from contact. Oval-shaped chlorite of 0.2 mm in diameter embedded in very fine-grained micro-folded matrix.

Sample No.	Mineral	δO^{18} per mil
SRO-49	Whole rock	15.6 (1)
SRO-50	Whole rock	16.3 (1)

C. Santa Rosa stock and its aureole

SRO-29F. Medium-grained granodiorite, 150 feet inward from contact. Plagioclase (An_{20}): 65%, subhedral, 1 mm, some phenocrysts 6 mm, strongly zoned. K-feldspar: 10%, anhedral, 1 mm. Quartz: 15%, anhedral, 0.5 - 1 mm, rarely 4 mm. Hornblende: 1%, anhedral, 1 mm. Chlorite: 1%, anhedral, 0.5 mm, alteration product of biotite.

Mineral	δO^{18} per mil
Quartz	13.1 ± 0.2 (2)
Plagioclase (An_{20})	10.4 (1)
Biotite (groundmass)	6.8 ± 0.1 (2)
Biotite (phenocryst)	7.7 (1)

SRO-29A. Migmatized hornfels. 1 inch from contact. Plagioclase: 35%, 0.1 mm, anhedral, also as 2 mm strongly zoned porphyroblasts. Quartz: 30%, 0.1 mm, anhedral, also as 0.5 mm irregular grains. Biotite: 25%, 0.5 - 1 mm, flakes or irregular grains. Muscovite: 5%, 0.5 mm, flakes. Cordierite: 5%, ill-defined oval, 1.5 mm, abundant inclusions.

Mineral	δO^{18} per mil
Quartz	14.6 ± 0.1 (2)
Muscovite	11.5 ± 0.1 (2)
Biotite	8.6 ± 0.1 (2)
Whole rock	11.8 (1)

SRO-29B. Migmatized hornfels, 5 inches from contact. Mineralogy similar to SRO-29A, but texture more hornfelsic.

Mineral	δO^{18} per mil
Whole rock	11.8 (1)

SRO-29C. Fine-grained hornfels, 11 inches from contact. Quartz and feldspar: 50%, anhedral, 0.1 mm. Biotite: 30%, tiny flakes or anhedral, 0.1 mm. Muscovite: 5%, tiny flakes, 0.1 mm. Cordierite: 10%, oval, 1.5 mm, abundant inclusions, most of them altered to micas. Tourmaline: 2%, subhedral, 0.5 mm. Opaques: 3%, 0.05 mm, granular.

Mineral	δO^{18} per mil
Whole rock	13.6 (1)

SRO-29D. Fine-grained hornfels,2 feet from contact. Petrography similar to SRO-29C.

Mineral	δO^{18} per mil
Quartz	16.9 ± 0.0 (2)
Muscovite	13.7 ± 0.0 (2)

Biotite	10.7 ± 0.1 (2)
Whole rock	14.0 (1)

SRO-29E. Fine-grained hornfels, 30 feet from contact. Petrography similar to SRO-29C.

Mineral	δO^{18} per mil
Whole rock	15.7 (1)

SRO-28. Dike-hornfels contact, 30 feet from the main stock. A fine-grained homogeneous hornfels similar to SRO-29E was crosscut by a 5-inch thick medium-grained (1 mm) granitic dike. The contact is extremely sharp. No contact effect is observed in the hornfels due to the intrusion of the dike. Isotopic analyses were made on the whole rock samples of the hornfels and the dike at various distances from the contact.

Sample No.	Rock	Distance from contact, inches	δO^{18} per mil
SRO-28-1	dike	2	12.2 (1)
SRO-28-2	dike	0.1	13.4 (1)
SRO-28-3	Hornfels	0.2	13.6 (1)
SRO-28-4	Hornfels	2	14.9 (1)
SRO-28-5	Hornfels	5	15.7 (1)
SRO-28-6	Hornfels	20	15.0 ± 0.2 (2)

SRO-31. Very fine-grained semi-hornfels, 2500 feet from contact. Composed of quartz, feldspar, biotite, muscovite, and oval cordierite now replaced by micas.

Mineral	δO^{18} per mil
Whole rock	16.1 (1)

SRO-32. Semi-hornfels, 2600 feet from contact. Petrography similar to SRO-31.

Mineral	δO^{18} per mil
Whole rock	16.1 (1)

SRO-34. Medium-grained granodiorite, collected from center of a small intrusive plug of exposed area 300 x 600 feet located 2000 feet from the main stock. Petrography similar to SRO-29F.

Mineral	δO^{18} per mil
Quartz	14.0 ± 0.1 (2)
Biotite	8.1 ± 0.1 (2)

13-85-7a. Medium-grained adamellite, 1.7 miles inward from contact. Collected by R.R. Compton. Plagioclase (An_{20}): 40%, subhedral, 2 - 4 mm, strongly zoned. Microcline: 25%, 4 mm, anhedral. Quartz: 15%, anhedral, 4 mm. Biotite: 14%, 2 - 4 mm, flakes. Hornblende: 4%, subhedral, 1 - 2 mm. Sphene: 1%, subhedral, 1 mm. Opaques: 1%, granular, 0.5 mm.

Mineral	δO^{18} per mil	δD per mil
Quartz	9.5 ± 0.0 (2)	
Plagioclase (An_{20})	8.0 ± 0.1 (2)	
Biotite	4.4 ± 0.1 (2)	-92 (1)

13-85-8. Medium-grained adamellite, 1 mile inward from contact. Collected by R. R. Compton. Petrography similar to 13-85-7a.

Mineral	δO^{18} per mil
Quartz	9.6 ± 0.1 (2)
Plagioclase (An_{20})	7.9 (1)
Biotite	4.6 (1)

4.2 Birch Creek, Deep Springs Valley, California

Traverse BC-27

BC-27G. Medium-grained biotite granite, 4.5 feet from contact. Microcline: 35%, as phenocrysts, subhedral, 3 - 5 mm, rarely 10 mm. Plagioclase (An_{10}) 27%, subhedral, faintly zoned, 1 mm. Quartz: 20%, anhedral, 1 mm. Biotite: 15%, flaky, 0.5 - 1 mm, slightly altered to chlorite. Chlorite: 2%, 0.5 mm, intergrown with biotite. Sphene: 1%, subhedral, 0.2 mm. Apatite: trace, 0.1 mm.

Mineral	δO^{18} per mil	δD per mil
Quartz	12.2 ± 0.2 (3)	
K-feldspar	10.4 ± 0.0 (2)	
Biotite (H_2O = 3.4%)	6.4 ± 0.1 (2)	-98 (1)

BC-27AI. Medium-grained equigranular biotite granite, 5 inches from contact. Mineralogy the same as BC-27G except microcline no longer as phenocrysts.

Mineral	δO^{18} per mil	δD per mil
Quartz	12.7 ± 0.0 (2)	
Biotite (H_2O = 3.3%)	7.0 ± 0.1 (3)	-84 ± 3 (2)

BC-27AII. Hornblende-biotite schist, 3 inches from contact. Quartz: 30%, anhedral, 0.1 mm, rarely 1 mm. Plagioclase: 25%, anhedral, 0.1 mm. Microcline: 5%, anhedral, 0.1 mm. Hornblende: 20%, subhedral or granular, 0.1 mm. Biotite: 20%, small flakes, 0.1 mm, prefer-oriented.

Mineral	δO^{18} per mil	δD per mil
Quartz	14.0 ± 0.1 (2)	
Hornblende	9.6 ± 0.2 (3)	

Biotite (H_2O = 3.9%)	8.1 ± 0.2 (2)	-96 ± 4 (2)
Whole rock (H_2O = 1.5%)	11.3 (1)	-94 (1)

BC-27B. Hornblende-biotite schist, 2 feet from contact. Mineralogy essentially the same as BC-27AII, except the proportion of biotite to hornblende increased to 3:1. Biotite markedly oriented. Oval shape of quartz and microcline 1 - 2 mm long elongate parallel to the foliation of the rock.

Mineral	δO^{18} per mil	δD per mil
Quartz	19.4 ± 0.0 (2)	
Biotite (H_2O = 5.4%)	12.6 ± 0.0 (2)	-75 (1)
Whole rock (H_2O = 2.0%)	16.0 (1)	-75 (1)

BC-27C. Hornblende-biotite schist, 4 feet from granite and 1 foot from marble. Mineralogy and texture similar to BC-27B.

Mineral	δO^{18} per mil
Quartz	17.7 ± 0.1 (2)
Biotite	11.4 ± 0.1 (2)
Whole rock	14.9 (1)

BC-27D1: Biotite-hornblende schist, 4.6 feet from granite and 0.4 feet from marble. The rock is essentially the same as BC-27C except that hornblende becomes predominant over biotite (3:1), and quartz occurs in minor amounts.

Mineral	δO^{18} per mil
Plagioclase	13.9 ± 0.2 (3)
Hornblende	11.9 ± 0.0 (2)
Biotite	9.9 ± 0.1 (2)
Whole rock	13.2 (1)

BC-27DII. Zoned skarn, 3 inches thick, formed along the schist-marble contact. Diopside: 50%, granular, 0.05 - 0.2 mm. Plagioclase: 50%, anhedral, 0.1 - 2 mm, diopside commonly as inclusions. Biotite: trace.

Mineral	δO^{18} per mil
Plagioclase	12.2 ± 0.1 (3)
Diopside	10.4 ± 0.1 (2)

BC-27E. Dolomite marble, 7 feet from granite, 2 feet from schist. Dolomite: 90%, anhedral, 6 mm. Calcite: 10%, anhedral, 6 mm.

Mineral	δO^{18} per mil	δC^{13} per mil
Dolomite	20.5 ± 0.0 (2)	0.1 ± 0.0 (2)
Calcite	19.6 ± 0.2 (2)	-0.4 ± 0.0 (2)

BC-27F. Dolomite marble, 10.5 feet from granite, 5.5 feet from schist.

Mineral	δO^{18} per mil	δC^{13} per mil
Dolomite	20.2 ± 0.1 (2)	0.7 ± 0.1 (2)
Calcite	19.9 ± 0.0 (2)	-0.1 ± 0.0 (2)

Traverse BC-28

BC-28J. Medium-grained biotite granite, 60 feet inward from contact. Microcline: 30%, 1 - 2 mm, anhedral. Plagioclase (An_{10}): 30%, subhedral, 1 - 1.5 mm, faintly zoned. Quartz: 25%, anhedral, 1 mm. Biotite: 12%, flaky or anhedral, 0.5 mm. Sphene: 1%, euhedral, 0.2 mm. Chlorite: 1%, alteration product of biotite. Opaques: 1%, granular, 0.2 mm.

Mineral	δO^{18} per mil	δD per mil
Quartz	11.1 ± 0.2 (3)	

K-feldspar	9.3 ± 0.2 (2)	
Biotite (H_2O = 4.0%)	5.5 ± 0.1 (2)	-102 (1)

BC-28I. Medium-grained biotite granite, 10 feet inward from contact. Mineralogy essentially the same as BC-28J, except that biotite reduced to about 4% of total rock, and microcline is more abundant than plagioclase.

Mineral	δO^{18} per mil
Quartz	12.9 ± 0.1 (2)

BC-28H. Medium-grained alaskite, 2.5 feet inward from contact. Microcline: 50%, 1 - 3 mm, anhedral, most of them altered to white mica. Quartz: 15%, anhedral, 1 mm. White mica: 32%, 0.05 mm, alteration product of feldspar. Calcite: 2%, interstitial. Opaques: 1%, irregular grains.

Mineral	δO^{18} per mil
Quartz	12.9 ± 0.1 (2)

BC-28A: Hornblende-biotite schist, 3 inches from intrusive contact. Quartz: 40%, anhedral, average size 0.1~ 0.05 mm, rarely 2 mm. Plagioclase: 15%, anhedral, 0.1 - 0.05 mm. Biotite: 35%, 0.1 mm, flakes, well oriented. Hornblende: 9%, granular, 0.1 - 0.5 mm. Opaques: 1%, irregular size.

Mineral	δO^{18} per mil	δ D per mil
Quartz	14.1 ± 0.0 (2)	
Biotite	8.1 ± 0.1 (2)	
Whole rock (H_2O = 2.1%)	12.2 (1)	-91 ± 1 (2)

BC-28B. Medium-grained biotite granite, from a granitic sill of 1 foot in thickness intruded into schist 2 feet from main contact. Microcline:

54%, anhedral, 2 - 3 mm, plagioclase laths as inclusions. Plagioclase (An_{10}): 10%, subhedral, 2 mm, also occurs as inclusions (0.5 mm) in microcline. Quartz: 30%, 2 mm, anhedral. Biotite: 6%, subhedral to anhedral, 1 - 2 mm, slightly chloritized.

Mineral	δO^{18} per mil
Quartz	12.9 ± 0.1 (3)
K-feldspar	11.5 ± 0.2 (2)
Biotite	6.9 ± 0.1 (4)

BC-28C: Hornblende-biotite schist, 6 feet from intrusive contact. Mineralogy and texture similar to BC-28A.

Mineral	δO^{18} per mil
Quartz	19.2 ± 0.0 (2)
Biotite	13.0 ± 0.1 (2)
Whole rock	16.4 (1)

BC-28D. Hornblende-biotite schist, 9 feet from intrusive contact. Mineralogy and texture similar to BC-28A.

Mineral	δO^{18} per mil
Whole rock	16.4 (1)

BC-28E. Hornblende-biotite schist, 13 feet from intrusive contact, 4 feet to the marble unit. Mineralogy and texture identical to BC-28A, except that the proportion of hornblende to biotite increased to 1 : 1 and some microcline recrystallized to a size of about 1 mm.

Mineral	δO^{18} per mil	δD per mil
Quartz	19.1 ± 0.1 (2)	
Biotite	12.8 ± 0.0 (2)	
Whole rock (H_2O = 0.9%)	16.4 (1)	-90 ± 2 (2)

BC-28F: Dolomite marble, 18 feet from igneous contact, and 1 foot from the schist. Coarse-grained (6 mm) dolomite > 95%. Calcite < 5%.

Mineral	δO^{18} per mil	δC^{13} per mil
Dolomite	23.0 ± 0.0 (2)	0.7 ± 0.0 (2)

BC-28G: Dolomite marble similar to BC-28F, 30 feet from granite, 13 feet from schist.

Mineral	δO^{18} per mil	δC^{13} per mil
Dolomite	21.3 ± 0.1 (2)	0.9 ± 0.1 (2)

Traverse BC-29-30-7-31

Four additional samples were collected along the strike of the hornblende-biotite schist unit south of traverse BC-28. The mineralogy and texture of these four samples are similar to those of samples from traverse 28. The isotopic results are shown below:

Sample No.	Distance from intrusive, feet	Mineral	δO^{18} per mil
BC-29	20	Whole rock	16.9 (1)
BC-30	50	Whole rock	15.2 ± 0.2 (2)
BC-7	70	Whole rock	17.4 ± 0.3 (2)
		Quartz	19.9 ± 0.1 (2)
		Biotite	13.5 ± 0.1 (3)
BC-31	75	Whole rock	17.8 (1)

Xenolith (10 x 50 feet)

BC-22. Medium-grained biotite schist, poorly foliated, collected near the center of the xenolith. Minerals appear to be completely recrystallized. Plagioclase (An_5): 48%, subhedral, 1 - 2 mm. Quartz: 20%, anhedral, 0.5 - 1 mm. Biotite: 30%, flakes, 0.5 - 1 mm. Chlorite: 1%, alteration

product of biotite. Pyroxene: 1%, anhedral, 0.5 mm. Sphene: trace, subhedral, 0.2 mm.

Mineral	δO^{18} per mil
Quartz	13.0 ± 0.1 (2)
Plagioclase (An_5)	11.5 ± 0.1 (3)
Biotite	7.2 ± 0.0 (2)

BC-23. Biotite schist with intercalated leucocratic layers 3 to 5 mm thick, collected near the margin of the xenolith. The schist is fine-grained (0.2 mm), well foliated, containing biotite 25%, quartz 65%, plagioclase 8%, and chlorite 2%. The leucocratic layers are medium-grained (1 - 2 mm) and contain microcline 60% and quartz 40%.

Mineral	δO^{18} per mil
Quartz (schist)	12.7 ± 0.1 (4)
Biotite (schist)	7.2 ± 0.1 (2)
Quartz (leucocratic layer)	12.5 ± 0.1 (2)

Sillimanite and biotite schists

BC-20. Medium-grained sillimanite schist, 400 feet from intrusive contact. Contains sillimanite 20%, cordierite 9%, andalusite 2%, muscovite 10%, quartz 20%, plagioclase 10%, sericite 20%, chlorite 8%, and opaques 1%. Sericite and chlorite are secondary.

Mineral	δO^{18} per mil
Quartz	17.0 (1)
Whole rock	14.4 (1)

BC-16. Fine-grained biotite schist, 1300 feet from intrusive contact. Quartz: 45%, anhedral, 0.2 mm. Biotite: 35%, flakes, 0.2 mm.

Plagioclase: 15%, anhedral, 0.2 mm. Microcline: 5%, anhedral, 0.3 mm.

Mineral	δO^{18} per mil
Quartz	16.1 ± 0.1 (2)
Biotite	9.3 ± 0.1 (2)
Whole rock	13.3 (1)

BC-15. Fine-grained biotite schist, 2000 feet from intrusive contact. Contains quartz 50%, biotite 30%, white mica 3%, and plagioclase 17%. Average grain size 0.2 mm.

Mineral	δO^{18} per mil
Quartz	14.7 ± 0.1 (2)
Biotite	8.7 ± 0.1 (2)
Whole rock	12.4 (1)

BC-14. Fine-grained biotite schist, 2100 feet from intrusive contact. Mineralogy and texture similar to BC-15.

Mineral	δO^{18} per mil	δD per mil
Quartz	14.9 (1)	
Biotite	8.9 (1)	
Whole rock (H_2O = 1.3%)	12.4 (1)	-86 (1)

BC-26. Fine-grained biotite schist, 3000 feet from intrusive contact. Mineralogy similar to BC-15 except biotite flakes not oriented.

Mineral	δO^{18} per mil	δD per mil
Biotite (H_2O = 3.4%)	9.4 (1)	-83 (1)
Whole rock (H_2O = 1.0%)	12.1 (1)	-85 (1)

Contact metamorphic marbles and skarns

BC-2, BC-10. Irregular massive skarns, adjacent to a tongue-like mass of granite that projects out from the pluton. Consist of large euhedral

crystals (a few mm to 1 cm) of calcite, quartz, epidote, grossularite, diopside, and actinolite.

Sample No.	Rock	Mineral	δO^{18} per mil	δC^{13} per mil
BC-10 E	Granite	Quartz	11.1 ± 0.1 (2)	
BC-10 D	Pure	K-feldspar zone	11.3 ± 0.1 (2)	
BC-10 C	Skarn	Quartz	10.9 ± 0.0 (2)	
		Actinolite	9.0 ± 0.1 (2)	
BC-10 B	Skarn	Calcite	11.2 ± 0.0 (2)	-3.0 ± 0.1 (2)
		Quartz	11.0 ± 0.2 (3)	
		Epidote	7.7 ± 0.1 (2)	
		Grossularite	7.6 ± 0.3 (2)	
BC-2 A	Skarn	Calcite (euhedral)	10.5 (1)	-3.1 (1)
BC-2 B	Skarn	Calcite (matrix)	15.4 ± 0.3 (3)	-2.1 ± 0.1 (2)
BC-10 A	Marble	Calcite	17.4 (1)	-1.0 (1)

BC-32 A, D, E, F. Forsterite marbles, collected 0.5, 2, 16, and 50 feet, respectively, from intrusive contact. Dolomite: 20%, 0.5 - 1 mm, anhedral. Calcite: 60%, 0.5 - 1 mm, anhedral. Forsterite: 20%, 0.1 - 0.4 mm, subhedral to euhedral, fresh in 32 D and E, but completely altered to serpentine in 32 A and F.

Sample No.	Mineral	δO^{18} per mil	δC^{13} per mil
BC-32 A	Calcite	20.5 ± 0.1 (3)	-1.8 ± 0.1 (3)
BC-32 D	Dolomite	23.6 ± 0.1 (2)	-0.9 ± 0.0 (2)
	Calcite	23.4 ± 0.0 (2)	-1.3 ± 0.0 (2)
BC-32 E	Dolomite	24.1 ± 0.0 (2)	-0.8 ± 0.0 (2)
	Calcite	24.0 ± 0.1 (2)	-1.1 ± 0.0 (2)
	Forsterite	20.8 ± 0.5 (2)	
BC-32 F	Dolomite	23.7 ± 0.0 (3)	-0.8 ± 0.0 (3)
	Calcite	21.7 ± 0.1 (2)	-1.2 ± 0.0 (2)

BC-21. Forsterite marble, 0.5 feet from contact. Forsterite completely altered to serpentine. Dolomite 10%; Calcite 70%; Serpentine 20%.

Mineral	δO^{18} per mil	δC^{13} per mil
Dolomite	21.0 (1)	-1.2 (1)
Calcite	21.1 (1)	-1.4 (1)

BC-12. Forsterite marble, 70 feet from intrusive contact. Dolomite 30%; Calcite 50%; Forsterite 20%, unaltered.

Mineral	δO^{18} per mil	δC^{13} per mil
Dolomite	23.6 (1)	-0.7 (1)
Calcite	24.2 (1)	-0.9 (1)

BC-6. Dolomite marble, 125 feet from intrusive contact. Dolomite: 80%, anhedral, 5 mm. Calcite: 20%, anhedral, 5 mm.

Mineral	δO^{18} per mil	δC^{13} per mil
Dolomite	23.7 ± 0.1 (2)	0.0 ±0.1 (2)
Calcite	22.8 (1)	-0.6 (1)

BC-8. Phlogopite-calcite marble, 150 feet from intrusive contact. Calcite: 67%, anhedral, 0.5 mm. Phlogopite: 25%, flakes, 0.3 mm. K-feldspar: 5%, anhedral, 1 mm. Muscovite: 1%, flakes, 0.3 mm. Diopside: 1%, granular, 0.05 mm. Opaques: 1%, granular, 0.02 mm.

Mineral	δO^{18} per mil	δC^{13} per mil	δD per mil
Calcite	19.3 ± 0.0 (2)	-1.0 ± 0.0 (2)	
Phlogopite (H_2O = 4.9%)	14.4 ± (1)		-71 (1)

BC-9. Phlogopite-diopside-calcite marble, 150 feet from intrusive contact. Calcite: 60%, anhedral, 0.2 mm. Diopside: 30%, granular, 0.05 mm. Phlogopite: 10%, flakes, 0.2 mm.

Mineral	δO^{18} per mil	δC^{13} per mil
Calcite	17.4± 0.2 (2)	-1.3 ± 0.0 (2)
Phlogopite	13.5 (1)	

BC-3. Dolomite-calcite marble, 200 feet from intrusive contact. Calcite: 70%, anhedral, 1 - 3 mm. Dolomite: 30%, anhedral, 1 - 3 mm.

Mineral	δO^{18} per mil	δC^{13} per mil
Dolomite	20.0 (1)	0.4 (1)
Calcite	19.2 (1)	-0.3 (1)

Granodiorite

BC-1. Medium-grained hornblende granodiorite, collected 1 mile inside the pluton. Hornblende: 20%, subhedral, 1 - 2 mm. Plagioclase: 56%, subhedral, 1 - 2 mm. Microcline: 10%, anhedral, 1 - 2 mm. Quartz: 8%, anhedral, 1 mm. Pyroxene: 3%, anhedral, 0.5 - 1 mm. Biotite: 1%, anhedral, alteration product of hornblende. Sphene: 1%, euhedral to subhedral, 0.5 — 1 mm. Opaques: 1%, anhedral, 0.5 mm.

Mineral	δO^{18} per mil
Quartz	10.6 ± 0.1 (2)
Pyroxene	7.6 ± 0.0 (2)
Hornblende	6.9 ± 0.1 (2)
Magnetite	2.1 ± 0.0 (2)

4.3 Eldora, Front Range, Colorado

A. Eldora stock contact zone

Biotite samples, Eldora traverse (Hart, 1964)

Sample No.	Rock	Distance from contact, feet	δO^{18} per mil	δD per mil
C 0 A	Quartz monzonite	5	5.4 ± 0.1 (3)	-109 (1)

Sample No.	Rock	Distance from contact, feet	δO^{18} per mil	δ D per mil
C 20 A	Pegmatite	20	6.6 ± 0.0 (2)	
C 58 A	Gneiss	58	6.5 ± 0.1 (2)	
C 248 A	Pegmatite	248	7.0 ± 0.2 (4)	
C 6 B	Pegmatite	1130	6.4 ± 0.2 (2)	
C 7 B	Amphibolite	2400	5.4 ± 0.0 (2)	
C 4 C	Gneiss	3600	7.3 ± 0.2 (2)	-119 (1)
BC-5C	Pegmatite	5200	6.7 ± 0.2 (2)	
C 14 C	Gneiss	14100	6.7 ± 0.1 (2)	
C 12 C	Pegmatite	22500	8.0 ± 0.1 (2)	

Feldspar samples (Steiger and Hart, 1967)

Sample No.	Distance from contact, feet	Proportion of microcline, %	δO^{18} per mil
Chittenden Mountain traverse			
CH-1	75	10 ?	9.1 (1)
CH-4	800	n.d.	10.6 (1)
CH-8	2200	n.d.	9.3 (1)
CH-9a	2890	10 ?	10.0 (1)
CH-10	2900	20	9.6 (1)
CH-11	3100	70	10.4 (1)
CH-12	4300	90-95	10.9 (1)
Ute Mountain traverse			
UM-4	1200	n.d.	9.6 (1)
UM-5	1380	n.d.	9.9 (1)
UM-6	1650	n.d.	10.6 (1)
UM-7	1800	n.d.	9.8 (1)
UM-10	2900	80-90	8.6 (1)
UM-11	3300	80-90	10.0 (1)
UM-12	3900	>95	9.2 (1)

Sample No.	Distance from contact, feet	Proportion of microcline, %	δO^{18} per mil
	Mineral Mountain traverse		
MM-1 a	10	n.d.	9.9 (1)
MM-1 b	30	<20	9.5 (1)
MM-8	1510	60-70	10.4 (1)
	Bryan Mountain traverse		
BM-1	20	n.d.	11.4 (1)
BM-2	200	n.d.	10.6 (1)
BM-3	600	n.d.	10.6 (1)
BM-4	800	90	10.4 (1)
BM-5	900	100	11.6 (1)
BM-6	1000	100	9.7 (1)

Rock samples, Eldora traverse

N-3. Medium-grained quartz monzonite, collected by G. R. Tilton, 450 feet inward from contact. Orthoclase: 10%, euhedral to subhedral phenocrysts, Carlsbad twinning, 5 mm. Plagioclase (An_{25}): 55%, subhedral, zoned, 1 mm. Quartz: 20%, anhedral, 1 mm. Biotite: 8%, flaky or anhedral, 1 mm. Hornblende: 4%, subhedral, 1 mm. Magnetite: 2%, subhedral to granular, 0.2 mm. Sphene: 1%, euhedral, 0.3 mm.

Mineral	δO^{18} per mil
Quartz	9.9 ± 0.0 (2)
Biotite	4.9 ± 0.1 (2)

EL-1. Medium-grained quartz monzonite, collected by S. R. Hart 50 feet inward from contact.

Mineral	δO^{18} per mil
Quartz	9.9 ± 0.1 (2)

Biotite	4.8 ± 0.1 (2)

EL-2. Medium-to coarse-grained gneiss, collected by S. R. Hart, 2 feet from contact. Leucocratic segregation layers common.

Mineral	δO^{18} per mil
Quartz	10.7 ± 0.1 (2)
K-feldspar	9.1 ± 0.0 (2)
Hornblende	6.7 ± 0.0 (2)
Biotite	6.7 ± 0.0 (3)
Magnetite	2.7 ± 0.1 (2)

N-2. Medium-grained amphibolite, collected by G. R. Tilton from same site as EL-2. Hornblende: 65%, ragged, green to brown, 1 - 2 mm. Plagioclase: 25%, subhedral, twinned, 2 mm. Biotite: 5%, anhedral, intergrown as alteration product of hornblende. Quartz: 3%, anhedral, 2 mm. Magnetite: 1%, anhedral, 0.5 mm. Sphene: 1%, subhedral, 0.5 - 1 mm.

Mineral	δO^{18} per mil
Quartz	10.4 ± 0.1 (2)
Plagioclase	9.3 ± 0.1 (2)
Hornblende	7.0 ± 0.1 (2)
Biotite	5.8 ± 0.0 (3)
Magnetite	2.3 ± 0.1 (2)

EL-12. Pegmatite, collected by S. R. Hart, 12 feet from contact.

Mineral	δO^{18} per mil
K-feldspar	9.0 ± 0.1 (2)
Biotite	6.6 ± 0.0 (2)

N-1. Medium-grained amphibolite, collected by G. R. Tilton, 18 feet from contact. Hornblende: 53%, anhedral, 1 - 2 mm, abundant quartz and magnetite inclusions. Plagioclase (An_{45}): 40%, anhedral,

twinned, 1 - 2 mm. Quartz: 5%, anhedral, 1 - 2 mm. Magnetite: 2%, granular, 0.1 mm.

Mineral	δO^{18} per mil
Plagioclase (An_{45})	9.2± 0.1 (2)
Hornblende	7.0± 0.1 (2)

C-20A. Pegmatite, collected by S. R. Hart, 20 feet from contact.

Mineral	δO^{18} per mil
Quartz	10.4 ± 0.1 (2)
K-feldspar	9.2 (1)
Biotite	6.6 ± 0.0 (2)

C4B. Medium-grained gneiss, collected by S. R. Hart, 950 feet from contact. Quartz: 50%, anhedral, 1 mm. Sericite: 25%, pseudomorph after feldspar. Biotite: 15%, ragged, 0.5 -1mm, rutile inclusions, some interleaved chlorite. Plagioclase (An_{25}): 9%, anhedral, 1 mm. Magnetite: 1%, subhedral, 0.5 mm.

Mineral	δO^{18} per mil
Quartz	12.2 ± 0.0 (2)
Biotite	6.9 ± 0.1 (2)
Magnetite	3.7 ± 0.1 (2)
Quartz lens	12.8 (1)

B. Caribou traverse

HES-8. Medium-grained monzonite, 530 feet inward from contact. Plagioclase (An_{25}): 55%, subhedral, 1 mm. K-feldspar: 10%, subhedral to anhedral, 0.5 - 1 mm. Hornblende: 20%, ragged, 1 mm. Biotite: 10%, ragged, 0.5 - 1 mm. Chlorite: 2%, alteration from biotite and hornblende. Magnetite: 1%, subhedral, 0.5 mm. Quartz: 2%, anhedral, 0.5 mm.

Mineral	δO^{18} per mil	
Plagioclase (An_{25})	9.0	(1)
Hornblende	6.5±0.1	(2)
Biotite	4.5±0.0	(2)
Magnetite	1.7±0.1	(2)

HES-4 a, b, c. Gneiss-monzonite contact. The monzonite (HES-4a) is similar to HES-8 except that plagioclase and biotite are more abundant in the near-contact sample. The gneiss (HES-4b, -4c) is medium-grained, containing perthite 60%, biotite 30%, plagioclase 6%, quartz 2%, and magnetite 2%. Quartz graphically intergrown with feldspar near contact. The isotopic data are given in Table 10, section 5.3 - C.

HES-1. Medium-grained sillimanite schist with coarse-grained feldspar and quartz segregations, 1300 feet from contact. Sillimanite: 5%, long needles. Biotite: 20%, flakes, 1 mm. Quartz: 20%, anhedral, 1 - 3 mm. Perthite: 45%, anhedral, 3 - 6 mm. Plagioclase: 9%, subhedral to anhedral, 1 mm. Magnetite: 1%, granular, 0.3 mm.

Mineral	δO^{18} per mil	
Quartz	12.8 ± 0.0	(2)
Perthite	10.9	(1)
Biotite	8.0 ± 0.1	(2)
Magnetite	4.5 ± 0.0	(2)
Whole rock	10.4	(1)

4.4 Marble Canyon, Culberson County, Trans-Pecos Texas

Four samples collected by T. E. Bridge have been isotopically analyzed. The results are shown in Table 11, section 5.4. Bridge has

identified various calc-silicates present in the following samples (personal communication).

A-1. Larnite, rankinite, melilite, spurrite, and merwinite.

A-5. Rankinite and merwinite, with interstitial calcite.

A-6. Diopside, wollastonite, spurrite, rankinite, calcite, and quartz. A sketch of the sample is shown in Figure 30, section 5.4.

A-13. Calcite, chert, and carbonaceous material.

V. DISCUSSION OF ISOTOPIC RESULTS IN INDIVIDUAL AREAS

5.1 Santa Rosa Range, Nevada

A. General statement

The contact metamorphism in the Santa Rosa Range of Nevada has been mapped and studied by Compton (1960). The metamorphic rocks of the area include a 20,000-foot section of Upper Triassic (and Jurassic ?) sediments that was strongly folded, metamorphosed, locally faulted, and intruded by granitic stocks in the late Cretaceous and early Tertiary. The country rocks are dominantly metapelitic; they were converted to metamorphic assemblages of quartz, albite, muscovite, chlorite, and carbonates during the regional metamorphism. There are nine different stocks which vary in composition from sodic granodiorite to adamellite, trondhjemite, and tonalite. Structural relationships show that the stocks are predominantly crosscutting bodies. The distribution of the stocks is shown in Figure 2.

The metamorphic aureoles are divided into two zones by Compton (1960): an outer zone of porphyroblastic phyllite and an inner zone of schist or hornfels where the biotite in the groundmass can be identified megascopically.

Four mineral assemblages were developed in the outer and inner parts of the aureoles:

(1) Cordierite-biotite

(2) Cordierite-andalusite-biotite

(3) Staurolite-andalusite-biotite

(4) Andalusite-biotite

all with quartz, muscovite, and plagioclase.

Figure 2. Map of Santa Rosa Range, Nevada, showing distribution of the granitic stocks (after Compton, 1960).

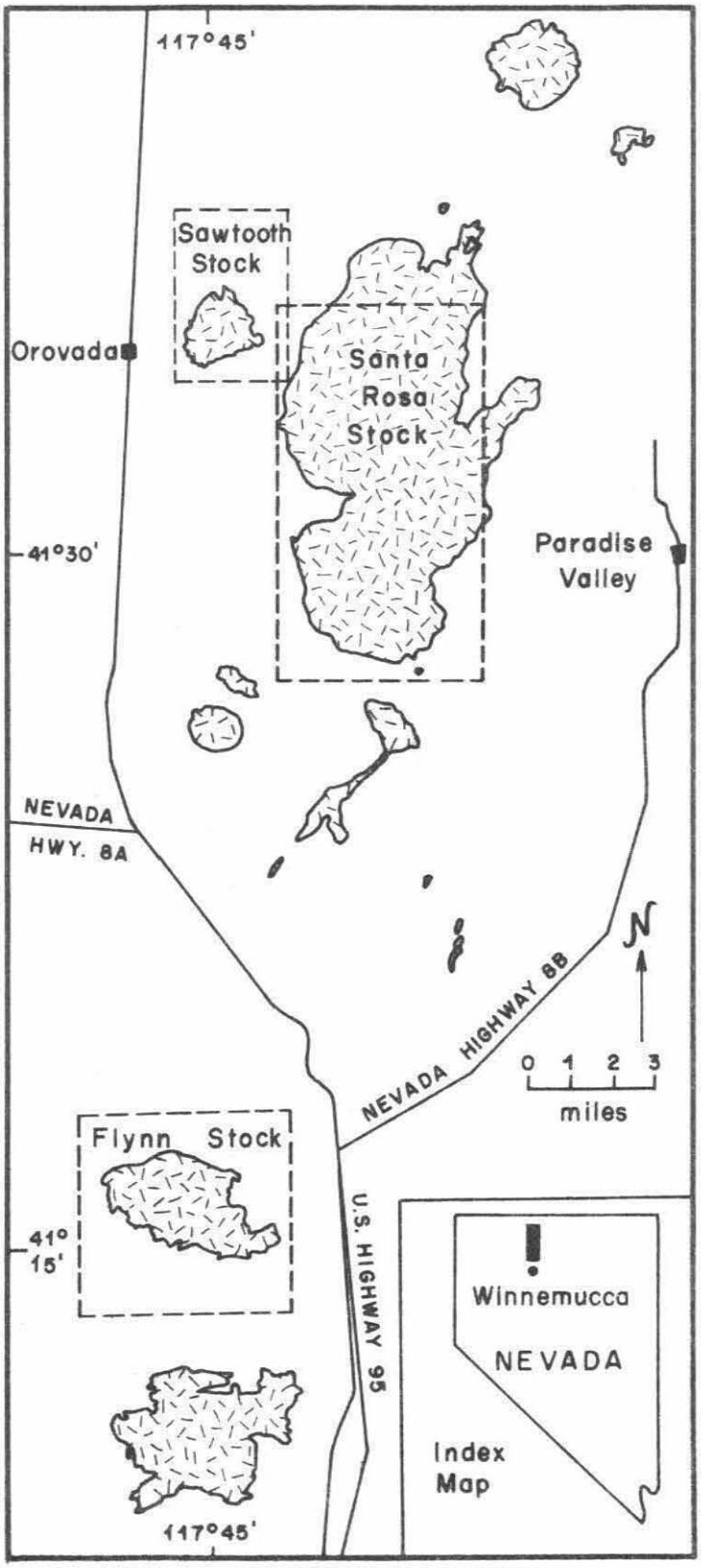
117°45'
Sawtooth Stock
Orovada
Santa Rosa Stock
41°30'
Paradise Valley
NEVADA HWY. 8A
NEVADA HIGHWAY 8B
N
0 1 2 3
miles
Flynn Stock
41° 15'
U.S. HIGHWAY 95
Winnemucca
NEVADA
Index Map
117°45'
WINNEMUCCA 9.5 MILES

Figure 2

Chemical analyses from the metapelites show that besides dehydration, the only metasomatism during progressive contact metamorphism was minor desilication, although addition of Fe occurred in the Sawtooth aureole (Compton, 1960).

B. Sawtooth stock and its aureole

The Sawtooth stock is exposed as a circular body with a diameter of about 1.5 miles. A contact metamorphic aureole was developed around the stock with variable thickness from 1500 to 2500 feet. The stock and its aureole are unique among the stocks in this area in many respects. Among these are: (1) the trondhjemite intrusive produced highly schistose contact metamorphic rocks in the aureole; (2) a sharp, zigzag contact exists between the intrusive and the country rocks; (3) quartz veins and quartzo-feldspathic dikes are abundant; (4) chloritoid and staurolite occur in the aureole; (5) andalusite, muscovite, biotite, and staurolite in the schists are very coarse-grained; (6) muscovite is present in the trondhjemite very near the contact; (7) the country rocks have high Fe_2O_3/FeO ratios compared to other aureoles of the area; and (8) the Fe content of the rocks increases with progressive contact metamorphism.

The mineral assemblages developed in the pelitic rocks are projected on Thompson diagrams (Thompson, 1957) as shown in Figure 3.

Two traverses from the north side of the stock were carefully sampled for isotopic analysis. The geology and sample locations are shown in Figure 4. Traverse I, corresponding to Compton's No. 1 suite, was sampled from the tip of a tongue of the intrusive. Traverse II, corresponding to Compton's No. 2

Figure 3. Observed mineral assemblages in pelitic rocks from the Sawtooth contact metamorphic aureole projected on Thompson diagrams. Solid circles represent chemical analyses by Compton (1960). Note that tie lines can be drawn such that the different mineral assemblages may be explained in terms of differences in bulk chemical composition of the rocks. The following reactions (simplified) are responsible for the change of topology of the diagrams:

I $\rightarrow$ II: chloritoid + chlorite $\rightarrow$ staurolite + biotite + H_2O

II $\rightarrow$ III: staurolite + chlorite $\rightarrow$ andalusite + biotite + H_2O

Figure 4. Generalized geologic map of the Sawtooth stock and its contact aureole, Santa Rosa Range, Nevada, showing sample locations (geology after Compton, 1960).

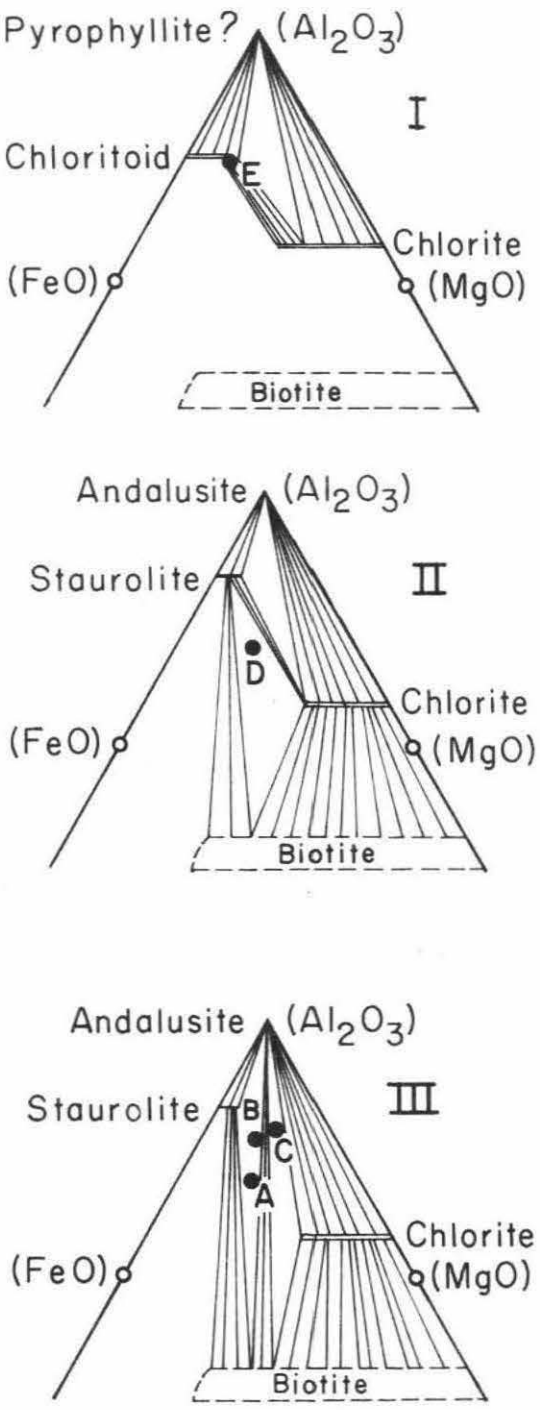

A. SRO-15B, SRO-19B, SRO-19C, SRO-22C, SRO-B

B. SRO-19III, SRO-22A, Compton's 1C, 2B, 4B

C. SRO-19D, Compton's 4A

D. SRO-24, Compton's 3A,3B

E. SRO-25b, Compton's 2A

Figure 3

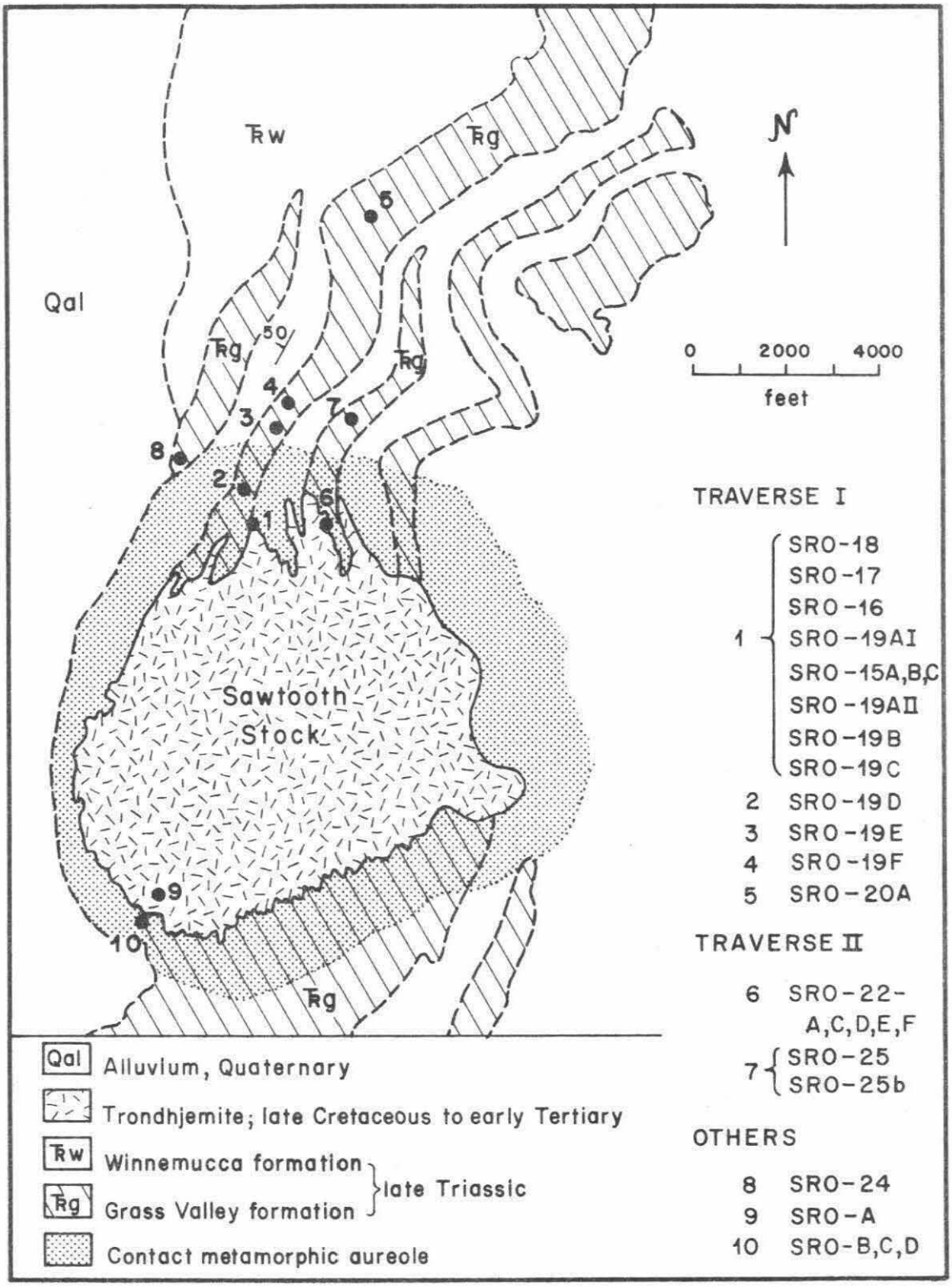
Trw
Trg
Qal
50
Sawtooth
Stock
N
0 2000 4000
feet
TRAVERSE I
1 SRO-18
SRO-17
SRO-16
SRO-19AI
SRO-15A,B,C
SRO-19AII
SRO-19B
SRO-19C
2 SRO-19D
3 SRO-19E
4 SRO-19F
5 SRO-20A
TRAVERSE II
6 SRO-22-A,C,D,E,F
7 SRO-25
SRO-25b
OTHERS
8 SRO-24
9 SRO-A
10 SRO-B,C,D
Qal Alluvium, Quaternary
Trondhjemite; late Cretaceous to early Tertiary
Trw Winnemucca formation
Trg Grass Valley formation
late Triassic
Contact metamorphic aureole

Figure 4

suite, was taken from the center of a re-entrant of the country rock which projects into the intrusive. SRO-24 is equivalent to Compton's sample 3B that contains staurolite. The petrography and isotopic results were presented in Chapter 4, and the isotopic data are plotted in Figures 5, 6, 7, and 8.

Figure 5 is a plot of O^{18}/O^{16} ratios vs. distance from the contact for samples from Traverse I. There are several features worthy of notice: (1) The O^{18}/O^{16} ratios of coexisting minerals from all samples decrease in the following order -- quartz, andalusite, muscovite, biotite, and magnetite; except sample SRO-19D where the order of andalusite and muscovite is reversed. Note that most of the andalusite in this particular sample has altered to muscovite. (2) The O^{18}/O^{16} ratios of individual minerals in the pelitic rocks remain fairly constant beyond 1 foot away from the contact. The same is also observed for samples in the intrusive. Note that the δ-values of quartz in the intrusive are about 1.5 to 2 per mil higher than that in "normal" plutonic igneous rocks (Taylor and Epstein, 1962). (3) The δ-values of quartz in quartz veins or in granitic dikes are similar but not identical to quartz of the adjacent schists and phyllites. They differ by as much as 0.5 to 1.2 per mil. (4) A very steep oxygen isotopic gradient exists within a zone of 1 foot extended on both sides from the contact. (5) The δ-values of the same mineral taken from the country rock and the intrusive 1.5 inches apart are identical within experimental error. (6) There seems to be no noticeable change in the O^{18}/O^{16} ratios of whole-rock samples across the metamorphic zonal boundaries. The only exception is sample SRO-19E, a black phyllite, which shows an abnormally high δ-value (19.8 per mil). It is interesting to note that this rock also shows an abnormally low H_2O content (0.8 wt %)

Figure 5. Plot of O^{18}/O^{16} ratios vs. distance for samples from traverse I of the Sawtooth stock contact zone, Santa Rosa Range (equivalent to Compton's suite 1).

Figure 6. Plot of O^{18}/O^{16} ratios vs. distance for samples from traverse II of the Sawtooth stock contact zone, Santa Rosa Range (equivalent to Compton's suite 2).

Figure 7. Plot of oxygen isotopic fractionations for the mineral pairs quartz-biotite, quartz-muscovite, and muscovite-biotite for samples from traverses I and II of the Sawtooth stock contact zone, arranged in order of sample distances from the contact.

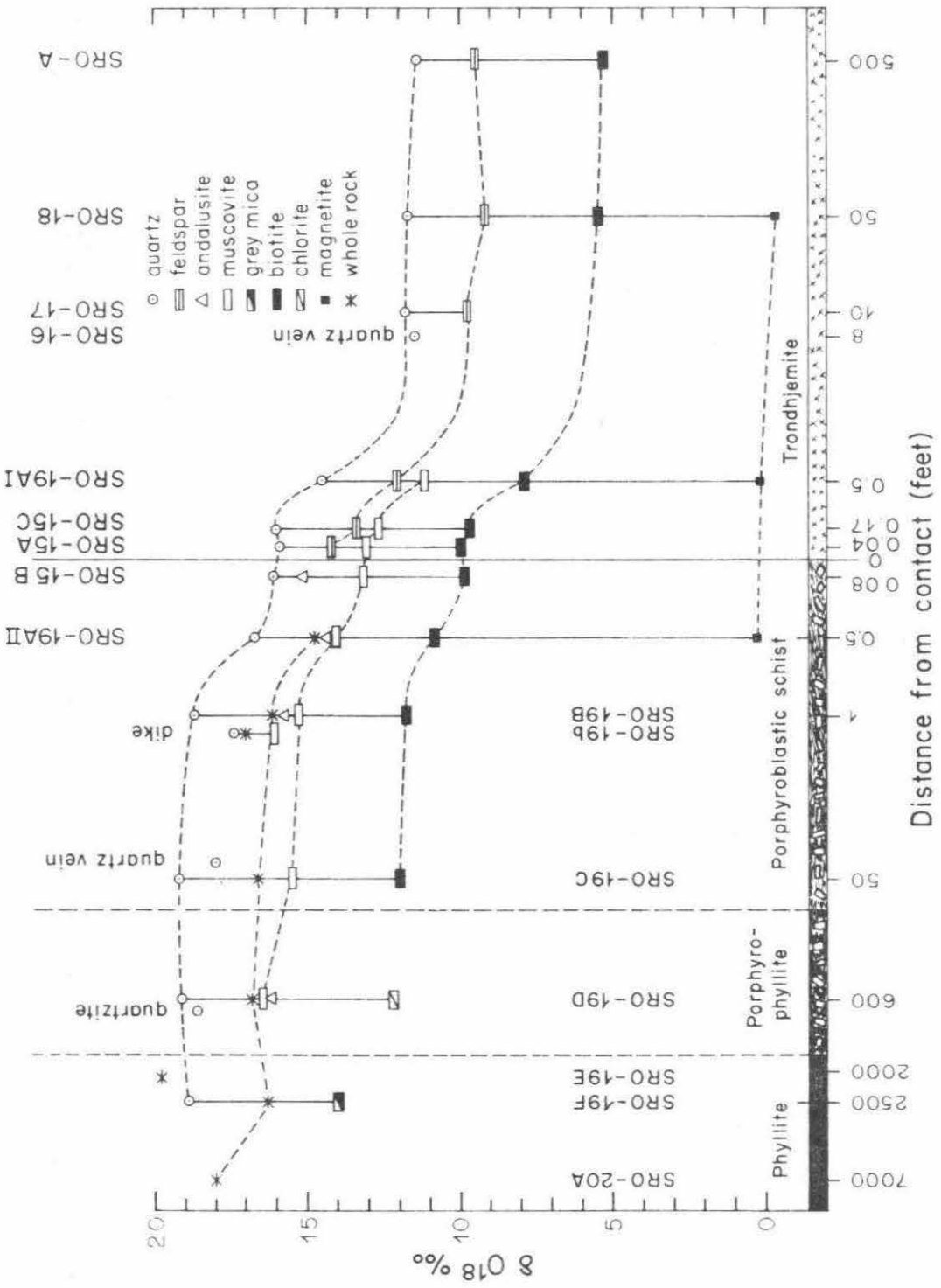
δ O18 ‰
20
15
10
5
0
Distance from contact (feet)
500
50
10
8
0.5
0.17
0.04
0
0.08
0.5
4
50
600
2000
2500
7000
quartz
feldspar
andalusite
muscovite
grey mica
biotite
chlorite
magnetite
whole rock
quartz vein
SRO-A
SRO-18
SRO-17
SRO-16
SRO-19AI
SRO-15C
SRO-15A
SRO-15B
SRO-19AII
dike
quartz vein
quartzite
SRO-19B
SRO-19B
SRO-19C
SRO-19D
SRO-19E
SRO-19F
SRO-20A
Trondhjemite
Porphyroblastic schist
Porphyro-phyllite
Phyllite

Figure 5

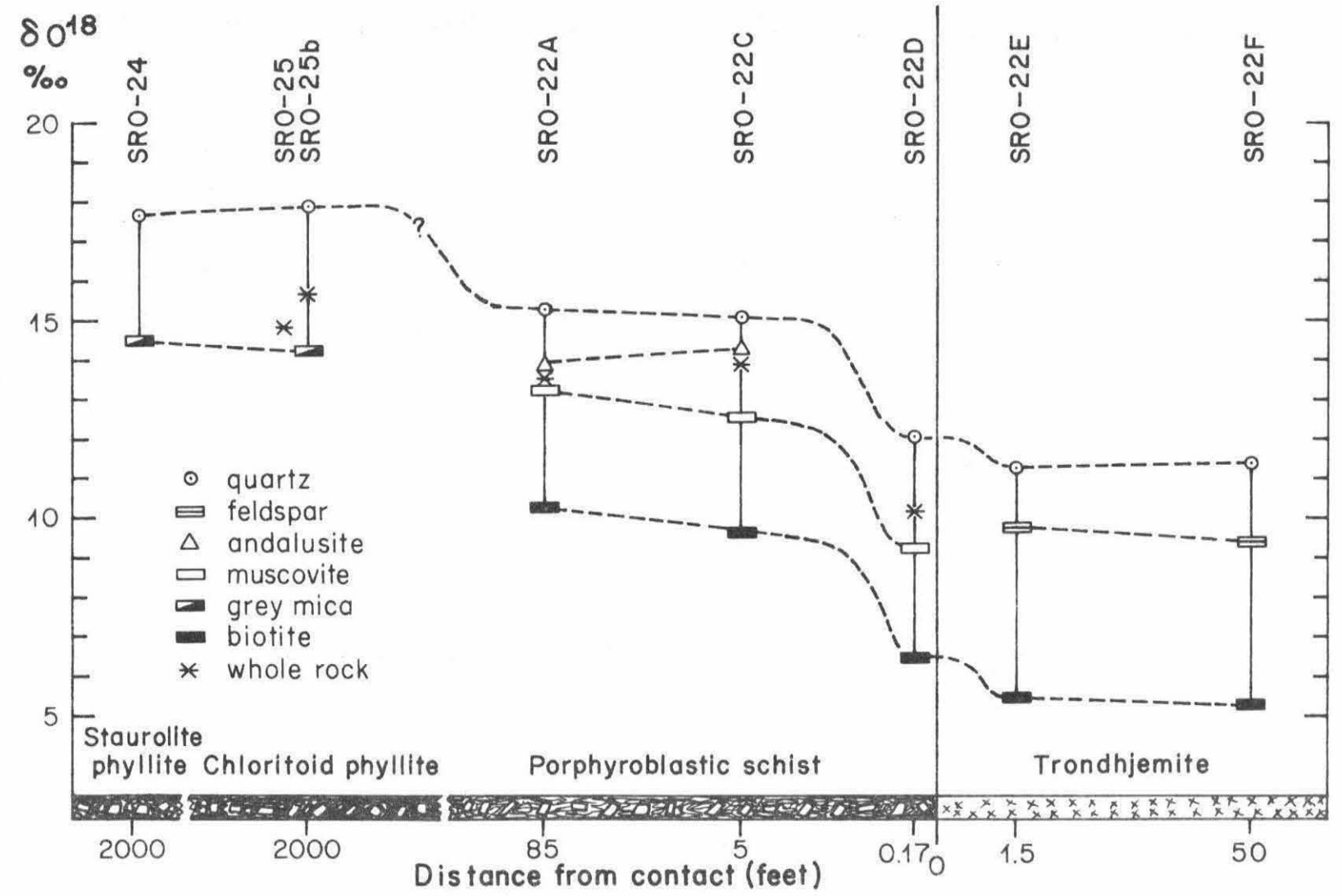
δ O18
‰
20
15
10
5
SRO-24
SRO-25
SRO-25b
SRO-22A
SRO-22C
SRO-22D
SRO-22E
SRO-22F
quartz
feldspar
andalusite
muscovite
grey mica
biotite
whole rock
Staurolite
phyllite
Chloritoid phyllite
Porphyroblastic schist
Trondhjemite
2000
2000
85
5
0.17
0
1.5
50
Distance from contact (feet)

Figure 6

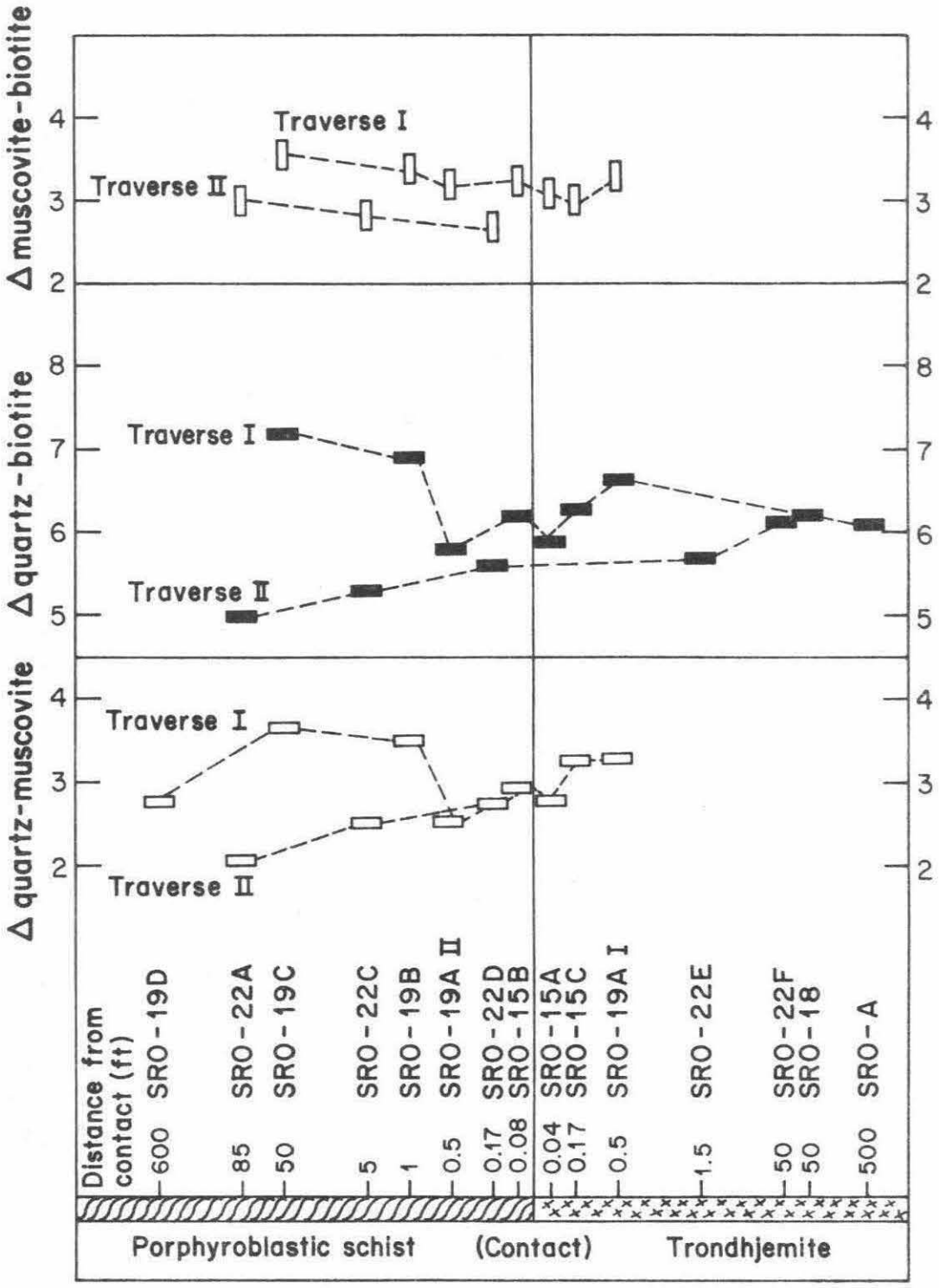
Δ muscovite-biotite
Traverse I
Traverse II
Δ quartz-biotite
Traverse I
Traverse II
Δ quartz-muscovite
Traverse I
Traverse II
Distance from contact (ft)
600 SRO-19D
85 SRO-22A
50 SRO-19C
5 SRO-22C
1 SRO-19B
0.5 SRO-19A II
0.17 SRO-22D
0.08 SRO-15B
0.04 SRO-15A
0.17 SRO-15C
0.5 SRO-19A I
1.5 SRO-22E
50 SRO-22F
50 SRO-18
500 SRO-A
Porphyroblastic schist
(Contact)
Trondhjemite

Figure 7

and high D/H ratio. (7) In contrast with other minerals that show very steep oxygen isotopic gradients near the contact, the O^{18}/O^{16} ratios of 3 magnetites (two occur in the intrusive, one occurs in the schist) are very similar, with a spread of only 0.6 per mil.

Figure 6 is a plot of δO^{18} vs. distance from the contact for traverse II samples. Very similar features as those of traverse I were observed, except that: (1) The δ-values of quartz in the 5-foot and 85-foot samples in the schist of the re-entrant are about 4 per mil lower than the corresponding samples in traverse I. (2) The minerals in the schist 0.17 feet away from the contact have δ-values only about 1 per mil higher than those in the intrusive, whereas a difference of more than 4 per mil is observed in traverse I. Note that in both traverses the δ-values of the minerals in the trondhjemite (excluding those collected within 1 foot from the contact) are almost identical within experimental error.

Another difference between the two traverses is brought out by observing the oxygen isotopic fractionations among coexisting minerals as shown in Table 2 and Figure 7. Apparently, the isotopic fractionations among coexisting minerals in traverse I are consistently larger than in traverse II, suggesting a lower temperature environment in traverse I. Other pertinent features of this aspect of both traverses include: (1) The quartz-biotite and quartz-muscovite fractionations of traverse I decrease quite regularly as a function of sample-distance from the center of the intrusive, if SRO-19D and samples less than 0.5 feet from the contact are disregarded. On the contrary, traverse II shows the opposite trend, which is not compatible with the simple heat flow model discussed in section 2.4. (2) The quartz-

TABLE 2

Oxygen isotopic fractionations among coexisting minerals in the Sawtooth stock contact zone, Santa Rosa Range

Sample No.	Distance from contact, feet	Δ_{Q-Mt}	Δ_{Q-B}	Δ_{Q-Mu}	Δ_{Q-A}	Δ_{A-Mu}	Δ_{Mu-B}	Δ_{F-B}
Traverse I								
Intrusive								
SRO-18	50	12.0	6.2					3.7
SRO-19AI	0.5	14.3	6.6	3.3			3.3	4.2
SRO-15C	0.17		6.3	3.3			3.0	3.7
SRO-15A	0.04		5.9	2.8			3.1	4.2
Country rock								
SRO-15B	0.08		6.2	2.9	0.9	2.0	3.3	
SRO-19AII	0.5	16.4	5.8	2.6	2.3	0.3	3.3	
SRO-19B	1		6.9	3.5	2.9	0.6	3.4	
SRO-19C	50		7.2	3.7			3.6	
SRO-19D	600			2.8	2.9	-0.1		
SRO-19F	2500			3.9 (calc.)				

TABLE 2 (continued)

Sample No.	Distance from contact, feet	Δ_{Q-Mt}	Δ_{Q-B}	Δ_{Q-Mu}	Δ_{Q-A}	Δ_{A-Mu}	Δ_{Mu-B}	Δ_{F-B}
Traverse II								
Intrusive								
SRO-22F	50		6.1					4.1
SRO-22E	1.5		5.7					4.2
Country rock								
SRO-22D	0.17		5.6	2.8			2.7	
SRO-22C	5		5.4	2.5	0.8	1.7	2.9	
SRO-22A	85		5.0	2.0	1.4	0.6	3.0	
South side								
Intrusive								
SRO-A	500		6.1					
Country rock								
SRO-B	1		6.4	3.6	1.0	2.6	2.8	
SRO-D (pegmatite dike)				2.1				

Q=quartz, Mt=magnetite, B=biotite, Mu=muscovite, A=andalusite, F=feldspar

andalusite and muscovite-biotite fractionations in both traverses decrease regularly approaching the contact. (3) Traverse I samples within 0.5 feet of the contact show abnormally small oxygen isotopic fractionations in comparison with the adjacent samples. (4) On the intrusive side there tends to be a decrease in isotopic fractionations approaching the contact. This may indicate that rapid crystallization at the contact has "frozen in" isotopic fractionations at higher temperatures.

From the gross pictures in Figures 5, 6, and 7, we tentatively infer that: (1) There are probably two different kinds of environments or mechanisms responsible for the oxygen isotopic exchange between the country rock and the intrusive, a large-scale exchange occurring over hundreds of feet or more and a small-scale exchange occurring over several inches or 1 foot. (2) The high O^{18}/O^{16} ratios of the intrusive samples compared to "normal" plutonic igneous rocks probably reflect the results of the large-scale exchange mechanism,perhaps due to assimilation and/or isotopic exchange with metasediments prior to solidification. (3) The similarity of the isotopic gradient on both sides of the contact implies that the small-scale isotopic exchange must be still operative after consolidation of the magma, and that consolidation near the contact must have been completed in rather short time after intrusion of the magma. (4) The relatively low and constant O^{18}/O^{16} ratios of 3 magnetites probably reflect the results of continued exchange down to relatively low temperatures, perhaps involving interaction with a low O^{18}/O^{16} source (meteoric water?). Such effects are expected because all the magnetites are exceedingly fine-grained (<0.01 mm) and present in very tiny amounts. (5) While it is true that coexisting minerals usually exhibit their normal sequence of O^{18}/O^{16} ratios, indicating an approach

Figure 8. Plot of D/H ratios and water contents vs. distance for samples from Sawtooth traverse I, Santa Rosa Range.

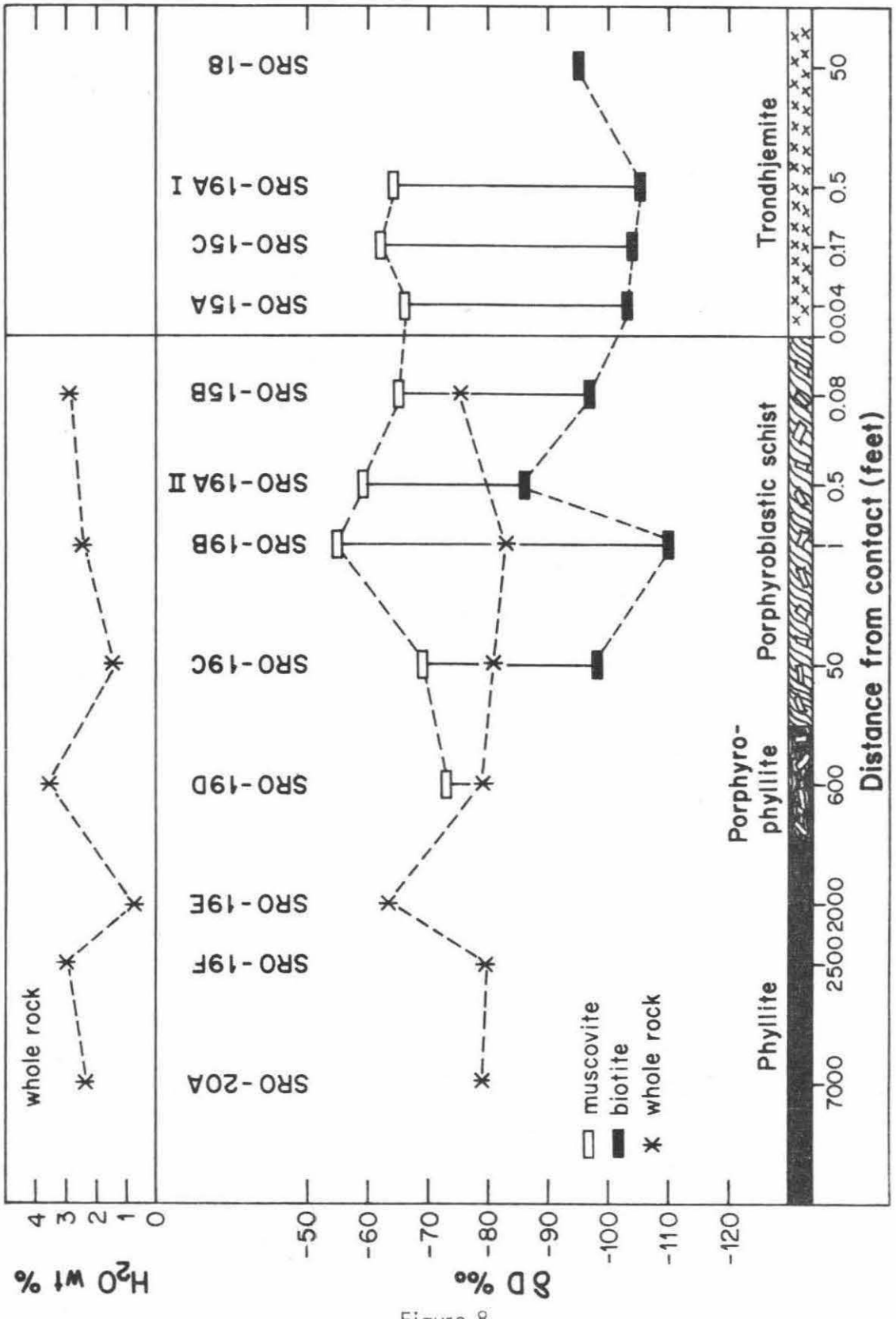
H2O wt %
δD ‰
whole rock
muscovite
biotite
whole rock
SRO-20A
SRO-19F
SRO-19E
SRO-19D
SRO-19C
SRO-19B
SRO-19A II
SRO-15B
SRO-15A
SRO-15C
SRO-19A I
SRO-18
Phyllite
Porphyro-phyllite
Porphyroblastic schist
Trondhjemite
Distance from contact (feet)

Figure 8

to equilibrium, the isotopic fractionations between coexisting mineral pairs are not related to the sample distance in a simple way, suggesting either disequilibrium or that "freeze-in" temperatures are somewhat different for different minerals. (6) Dehydration reactions probably do not appreciably affect the isotopic compositions of the pelitic rocks, as the O^{18}/O^{16} ratios of whole rock samples remain essentially constant throughout the various metamorphic zones.

Hydrogen isotopic compositions and water contents of the minerals and rocks from traverse I are plotted in Figure 8. As can be seen, the D/H ratios of muscovite and biotite are somewhat erratic, showing no definite trend. However, the D/H ratios of the pelitic rocks are rather constant if the black phyllite SRO-19E ($\delta D = -63$) is excluded. The other values range from -83 to -75 per mil (6 samples; 10,000 ft. to 0.08 ft. from the contact). The hydrogen isotopic fractionations between coexisting muscovite and biotite do not show any correlation with sample distance from the contact. The values range from 27 to 53 per mil (7 pairs). Note that the two extremes occur in two schist samples only 6 inches apart. The only obvious systematics in the hydrogen isotope data are that muscovite always concentrates deuterium with respect to coexisting biotite, in agreement with the observations of Taylor and Epstein (1966).

The water contents of the schists and phyllites have a spread from 0.8% to 3.6% by weight (7 samples). These might not be perfectly representative of the samples because of the heterogeneity in mineral proportions of the schists. However, all the values are within the range reported by Compton (1960).

C. Flynn stock and its aureole

The Flynn stock is an oval-shaped body in plan, with an exposed

Figure 9. Generalized geologic map of the Flynn stock and its contact aureole, Santa Rosa Range, Nevada, showing sample locations (geology after Compton, 1960).

Figure 10. Observed mineral assemblages in pelitic rocks from the Flynn contact metamorphic aureole projected on Thompson diagrams. Solid circles represent chemical analyses by Compton (1960). Note that tie lines can be drawn such that the different mineral assemblages may be explained in terms of differences in bulk chemical composition of the rocks. The following reactions (simplified) are responsible for the change of topology of the diagrams:

I $\longrightarrow$ II: andalusite + chlorite $\longrightarrow$ cordierite + biotite + H_2O.

II $\longrightarrow$ III: Chlorite $\longrightarrow$ cordierite + biotite + H_2O.

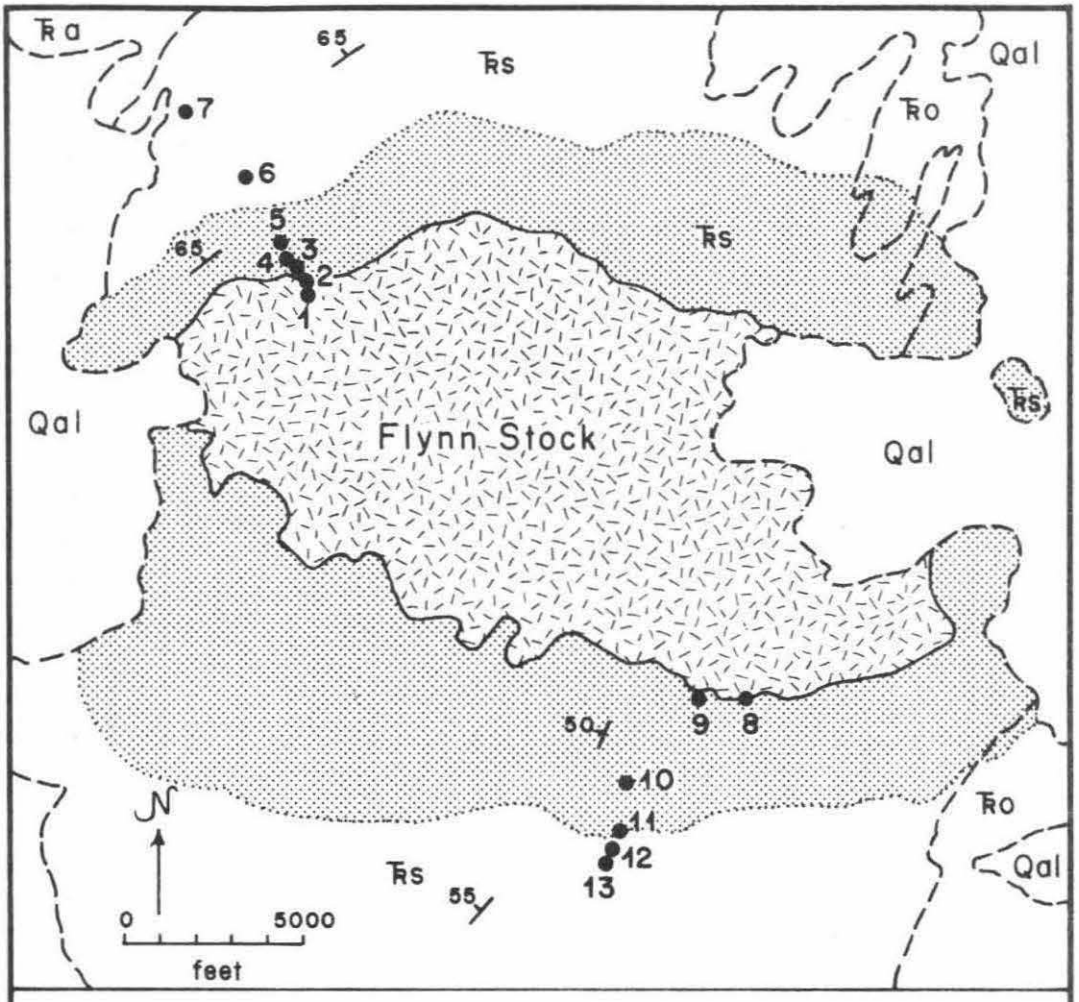

			North traverse	South traverse
Qal	Alluvium, Quaternary		1 SRO-4	8 SRO-39, SRO-38, SRO-37, SRO-36
	Granodiorite, late Cretaceous to early Tertiary		2 SRO-3C, SRO-3AI,II, SRO-3B, SRO-5, SRO-7	9 SRO-42
Ra	Andorno formation	late Triassic	3 SRO-8, SRO-9	10 SRO-46
Rs	Singas formation		4 SRO-10	11 SRO-48
Ro	O'Neil formation		5 SRO-12	12 SRO-49
	Contact metamorphic aureole		6 SRO-11	13 SRO-50
			7 SRO-13	

Figure 9

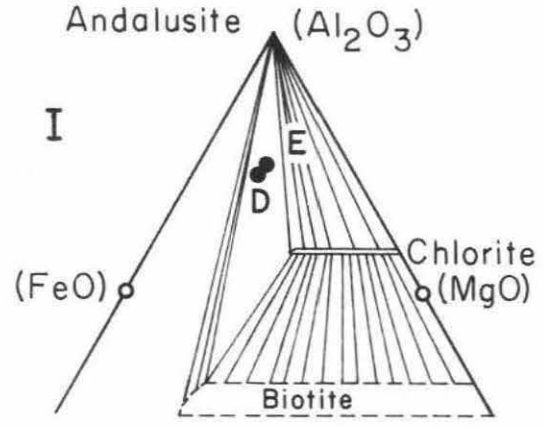

A. SRO-36, SRO-42, Compton's 15C, 15D
B. SRO-37, SRO-5, SRO-7, Compton's 13B
C. SRO-12
D. Compton's 14B, 15B
E. SRO-48

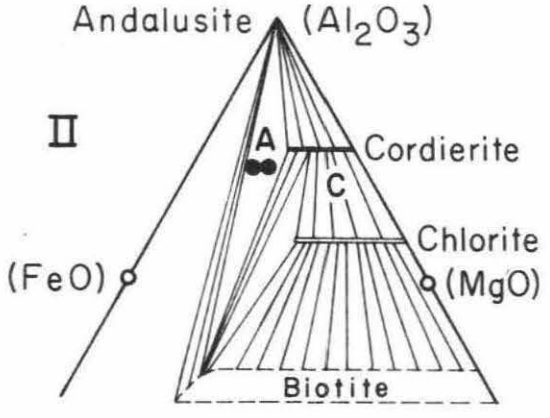

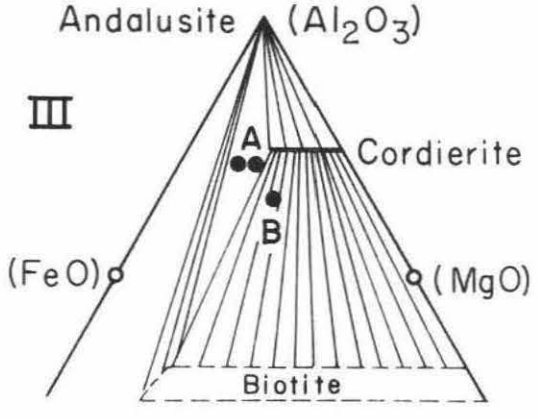

Figure 10

area of about 7 square miles. It is composed mainly of granodiorite, and is surrounded by a contact metamorphic aureole 2500 to 7500 feet in width. The principal rock types in the aureole are hornfels, semi-hornfels, and porphyroblastic phyllite. The simplified geologic map and sample locations are shown in Figure 9. The mineral assemblages of the pelitic rocks developed in the aureole are projected on Thompson diagrams as shown in Figure 10.

The Flynn stock and its aureole differ from the Sawtooth stock and aureole in many ways, among which are:

Flynn	Sawtooth
1. Hornblende-biotite granodiorite.	1. Hornblende-free, biotite trondhjemite.
2. Fine-grained, compact, massive hornfels.	2. Coarse-grained, muscovite-rich schist.
3. Cordierite present, no staurolite or chloritoid.	3. Staurolite and chloritoid present, no cordierite.
4. K-feldspar formed in the hornfels near the intrusive contact.	4. No K-feldspar formed in the schist.

Two traverses were sampled for isotopic analysis (Figure 9). The north traverse was taken from an amphibolite-granodiorite contact. The associated hornfels and semi-hornfels, which are the major rock types, were also collected. The south traverse, which is approximately equivalent to Compton's sample No. 15 suite, was sampled from the unaffected phyllite some 5000 feet away from the contact through the porphyroblastic phyllite to the completely recrystallized, extremely compact hornfels near the intrusive contact. The contact is not well exposed in the south traverse, so samples were not collected within 30 feet of the contact. The isotopic data are illustrated in Figures 11 -

Figure 11. Plot of O^{18}/O^{16} ratios vs. distance for samples from north traverse of Flynn stock contact zone, Santa Rosa Range.

Figure 12. Plot of O^{18}/O^{16} ratios vs. distance for samples from south traverse of Flynn stock contact zone, Santa Rosa Range (equivalent to Compton's suite 15).

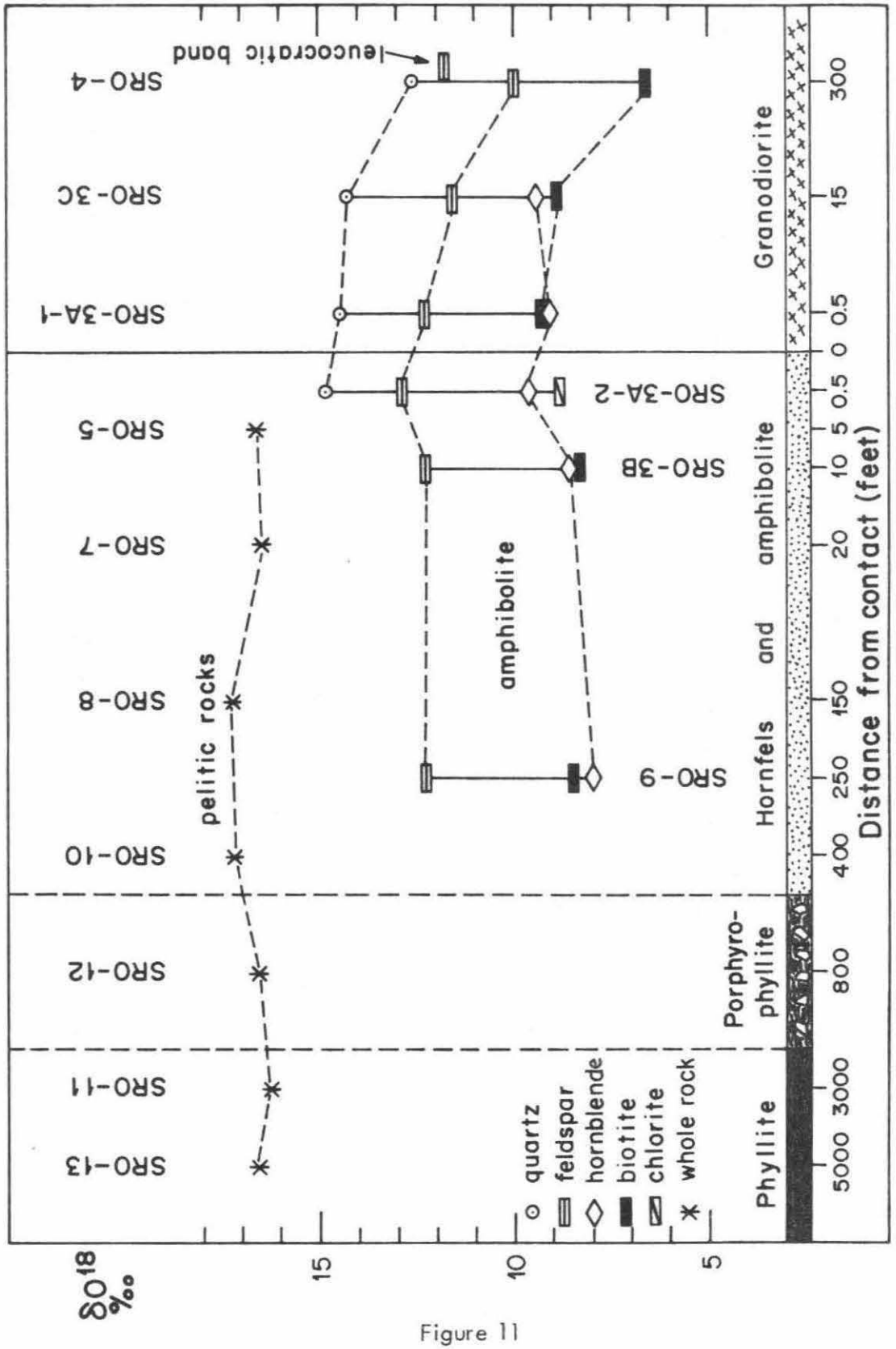
δO^{18} ‰
15
10
5
quartz
feldspar
hornblende
biotite
chlorite
whole rock
SRO-13
SRO-11
SRO-12
SRO-10
SRO-8
SRO-7
SRO-5
SRO-9
SRO-3B
SRO-3A-2
SRO-3A-1
SRO-3C
SRO-4
leucocratic band
pelitic rocks
amphibolite
Phyllite
Porphyro-phyllite
Hornfels and amphibolite
Granodiorite
5000 3000 800 400 250 150 20 10 5 0.5 0 0.5 15 300
Distance from contact (feet)

Figure 11

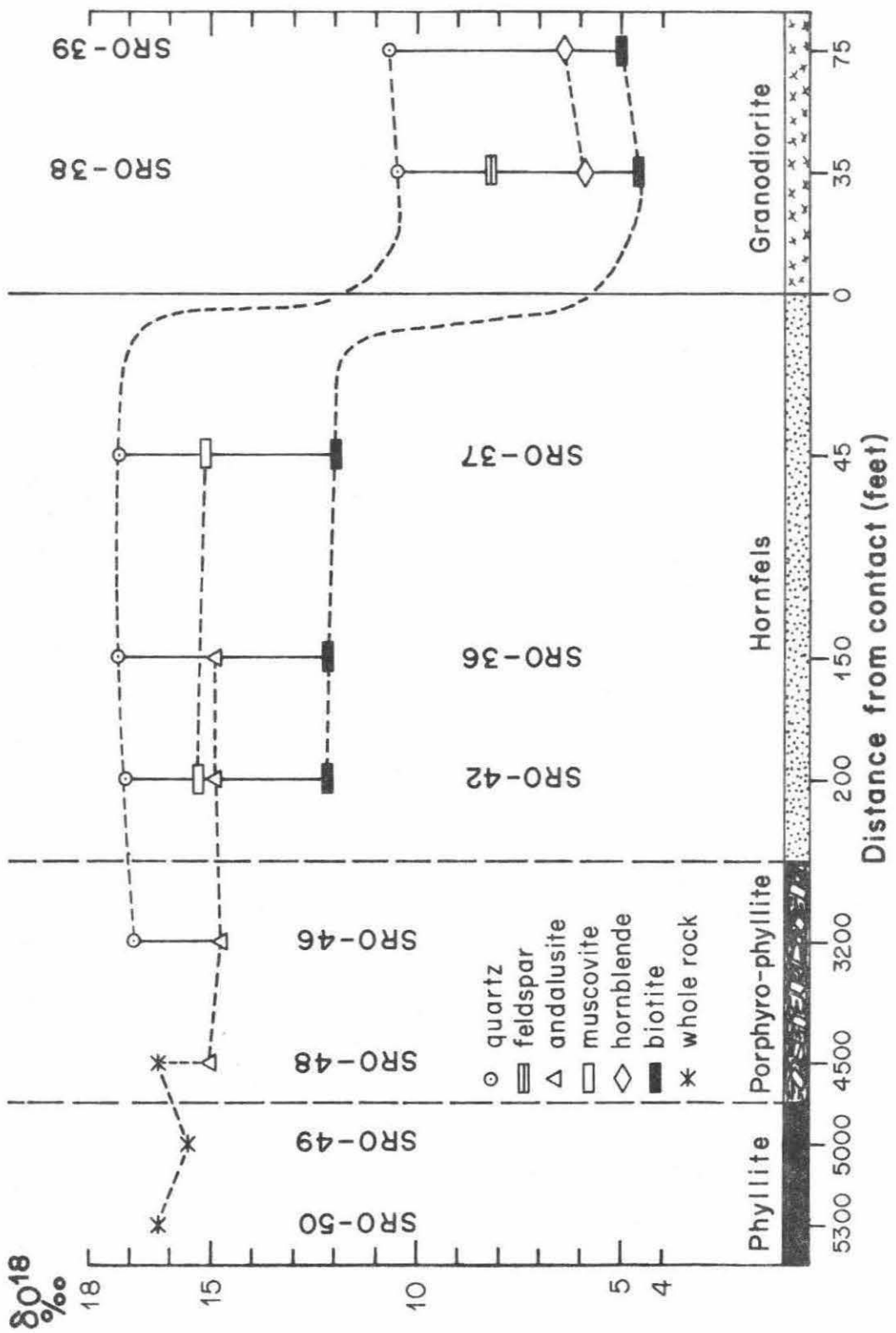
δO^{18} ‰
18
15
10
5
4
SRO-50
SRO-49
SRO-48
SRO-46
SRO-42
SRO-36
SRO-37
SRO-38
SRO-39
quartz
feldspar
andalusite
muscovite
hornblende
biotite
whole rock
Phyllite
Porphyro-phyllite
Hornfels
Granodiorite
5300 5000 4500 3200
200 150 45 0 35 75
Distance from contact (feet)

Figure 12

and 12.

Figure 11 is a δO^{18} vs. distance plot for samples from the north traverse. The δ-values of individual minerals in the amphibolite and in the granodiorite increase slightly toward the contact. However, the relative positions of O^{18}/O^{16} ratios in coexisting hornblende and biotite are not consistent, i.e., a "cross-over" is observed. Note that most of the biotite is an alteration product of hornblende. The O^{18}/O^{16} ratios of the pelitic rocks are rather constant throughout the entire traverse (16.3 - 17.3 per mil). The O^{18}/O^{16} ratios of the marginal intrusive samples are about 4 per mil higher than those in the "normal" plutonic igneous rocks (Taylor and Epstein, 1962).

The oxygen isotopic data from the south traverse are plotted in Figure 12. The O^{18}/O^{16} ratios of individual minerals in the country rock from 4500 feet to 45 feet distant from the contact are exceptionally constant: quartz (16.9 - 17.3 per mil), andalusite (14.8 - 15.1 per mil), muscovite (15.2 - 15.5 per mil), and biotite (12.0 - 12.2 per mil). The same situation is observed for minerals in the intrusive: quartz (10.5 - 10.7 per mil), hornblende (5.9 - 6.4 per mil), and biotite (4.6 - 5.0 per mil). In contrast to the north traverse, the O^{18}/O^{16} ratios of minerals in the marginal intrusive of the south traverse are within or close to the normal igneous range.

The isotopic fractionations among coexisting mineral pairs are listed in Table 3. In the north traverse, the δ-values behave differently for different mineral pairs with respect to sample distance from the contact. In the south traverse, the isotopic fractionations increase rather than decrease toward the contact, incompatible with the presumed temperature gradient. Also, a negative andalusite-muscovite fractionation is observed. All the

TABLE 3

Oxygen isotopic fractionations among coexisting minerals in the Flynn stock contact zone, Santa Rosa Range

Sample No.	Distance from contact, feet	Δ_{Q-B}	Δ_{Q-H}	Δ_{Q-F}	Δ_{F-B}	Δ_{F-H}	Δ_{H-B}
North traverse							
Intrusive							
SRO-4	300	6.1		2.6	3.4		
SRO-3C	15	5.3	4.9	2.6	2.7	2.3	+0.4
SRO-3A-1	0.5	5.3	5.4	2.2	3.1	3.3	-0.1
Country rock							
SRO-3A-2	0.5		5.1	1.8		3.3	
SRO-3B	10				3.8	3.8	0.0
SRO-9	250				3.8	4.2	-0.4
South traverse							
Intrusive							
SRO-39	75	5.7	4.3				+1.4
SRO-38	35	5.9	4.6	2.3	3.6	2.3	+1.3

TABLE 3 (continued)

Sample No.	Distance from contact, feet	Δ_{Q-B}	Δ_{Q-Mu}	Δ_{Q-A}	Δ_{A-Mu}	Δ_{Mu-B}
Country rock						
SRO-37	45	5.3	2.1			3.3
SRO-36	150	5.1		2.3		
SRO-42	200	4.9	1.6	2.1	-0.5	3.3
SRO-46	3200			2.1		

Q = quartz, B = biotite, H = hornblende, F = feldspar, Mu = muscovite, A = andalusite

above data suggest that many of the samples from the Flynn aureole are non-equilibrium mineral assemblages.

In summary: (1) The slight increase in O^{18}/O^{16} ratios of samples near the amphibolite-granodiorite contact may be due to isotopic exchange with the adjacent pelitic rocks. (2) The abnormally high O^{18}/O^{16} ratios of the marginal granodiorite from the north traverse are probably due to the same mechanism(s) that produced similar effects in the marginal zone of the Sawtooth stock. (3) Dehydration reactions apparently did not appreciably alter the oxygen isotopic compositions of the whole rock or the individual minerals.

D. Santa Rosa stock and its aureole

The Santa Rosa stock is the largest stock in the Santa Rosa Range (about 36 square miles in outcrop area). The stock is mainly granodiorite, but tonalite occurs near the contact, and adamellite is commonly present in the core. The stock produced a contact metamorphic aureole 2500 to 10,000 feet in width. The main contact metamorphic rocks are hornfels and semi-hornfels. This is the only aureole that contains all the four mineral assemblages occurring in the area.

A traverse was taken along the southeast side of the stock (see Figure 13). The samples near the intrusive contact are equivalent to Compton's sample No. 9B.

Figure 14 is a plot of δO^{18} vs. distance-to-contact for several samples analyzed. Very similar features to those obtained from the Flynn and Sawtooth traverses are observed: (1) The O^{18}/O^{16} ratios of whole-rock samples in the country rocks remain fairly constant (15.7 to 16.0 per mil) to

Figure 13. Generalized geologic map of the Santa Rosa stock and its contact aureole, Santa Rosa Range, Nevada, showing sample locations (geology after Compton, 1960).

Figure 14. Plot of O^{18}/O^{16} ratios vs. distance for samples from the Santa Rosa stock contact zone, Santa Rosa Range (equivalent to Compton's 9B and 10B).

Figure 15. Plot of O^{18}/O^{16} ratios vs. distance for samples from a granitic dike-hornfels contact in the Santa Rosa aureole, about 30 feet from the main intrusive contact.

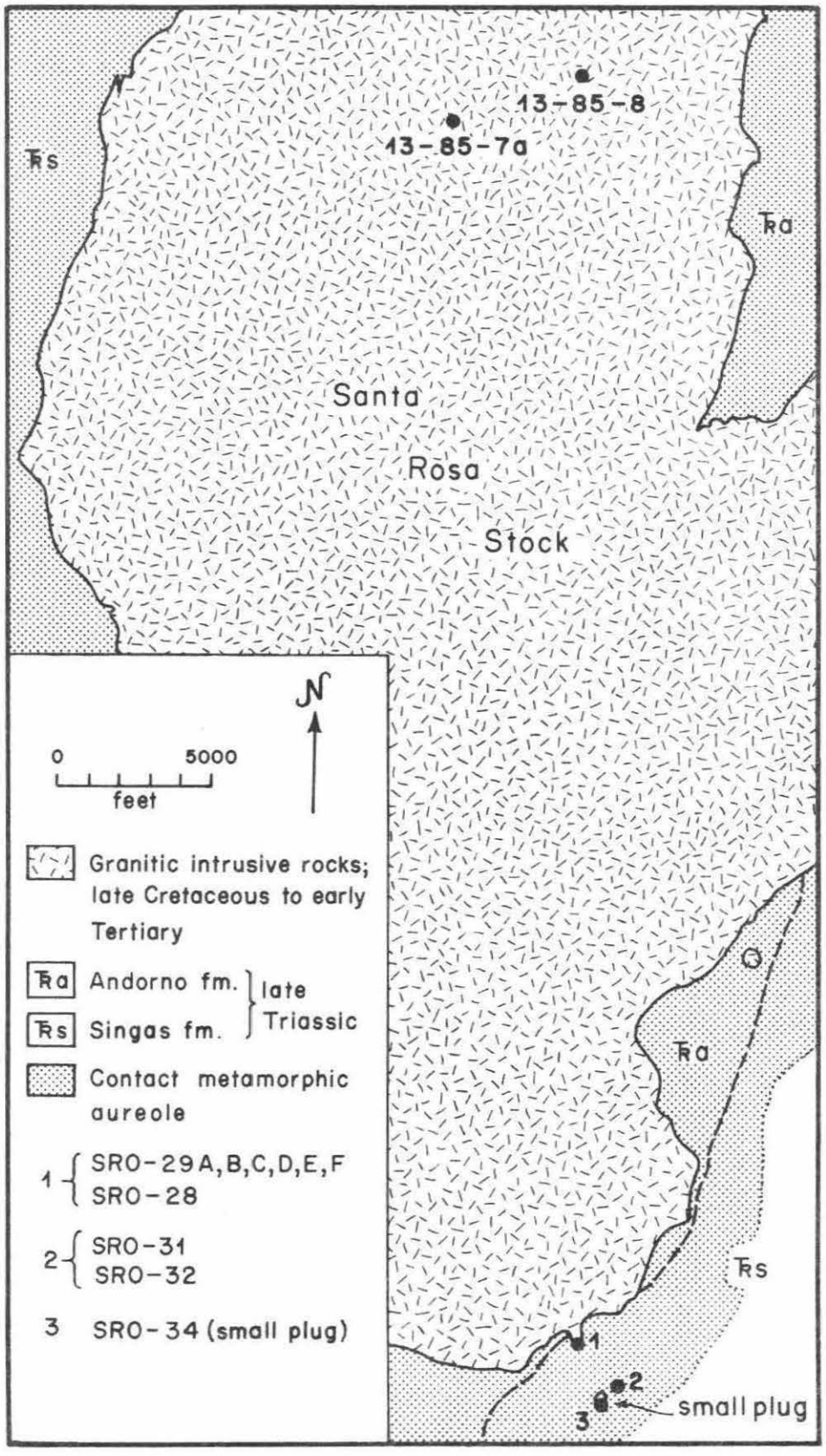
13-85-8
13-85-7a
Trs
Tra
Santa
Rosa
Stock
N
0
5000
feet
Granitic intrusive rocks; late Cretaceous to early Tertiary
Tra Andorno fm.
Trs Singas fm.
late Triassic
Contact metamorphic aureole
1 SRO-29A,B,C,D,E,F
SRO-28
2 SRO-31
SRO-32
3 SRO-34 (small plug)
Q
Tra
Trs
1
2
3
small plug

Figure 13

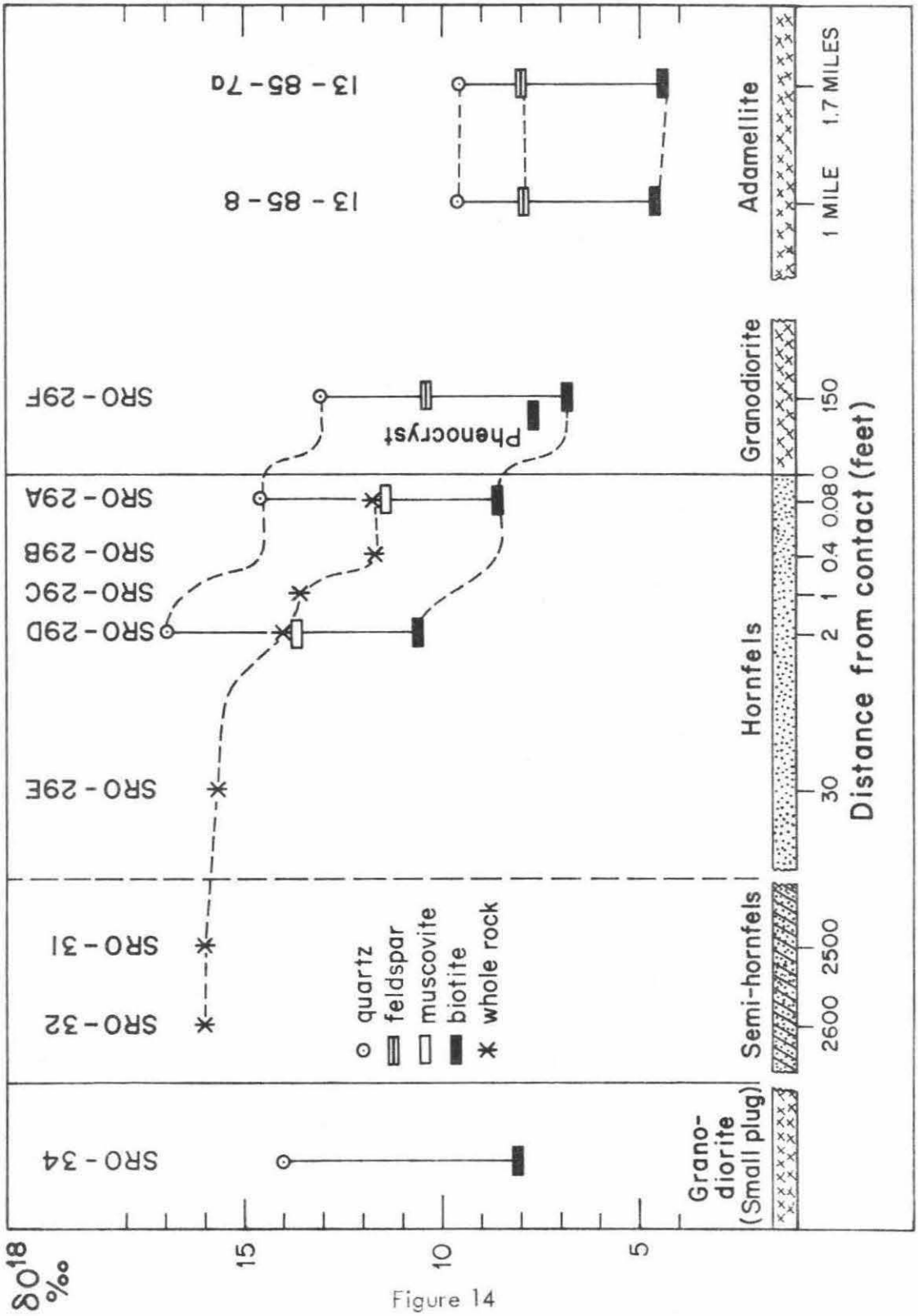
δO18 ‰
15
10
5
SRO - 34
SRO - 31
SRO - 32
SRO - 29E
SRO - 29D
SRO - 29C
SRO - 29B
SRO - 29A
SRO - 29F
13 - 85 - 8
13 - 85 - 7a
Phenocryst
o quartz
feldspar
muscovite
biotite
whole rock
Grano-diorite (Small plug)
Semi-hornfels
Hornfels
Granodiorite
Adamellite
2600 2500
30
2 1 0.4 0.080
150
1 MILE
1.7 MILES
Distance from contact (feet)

Figure 14

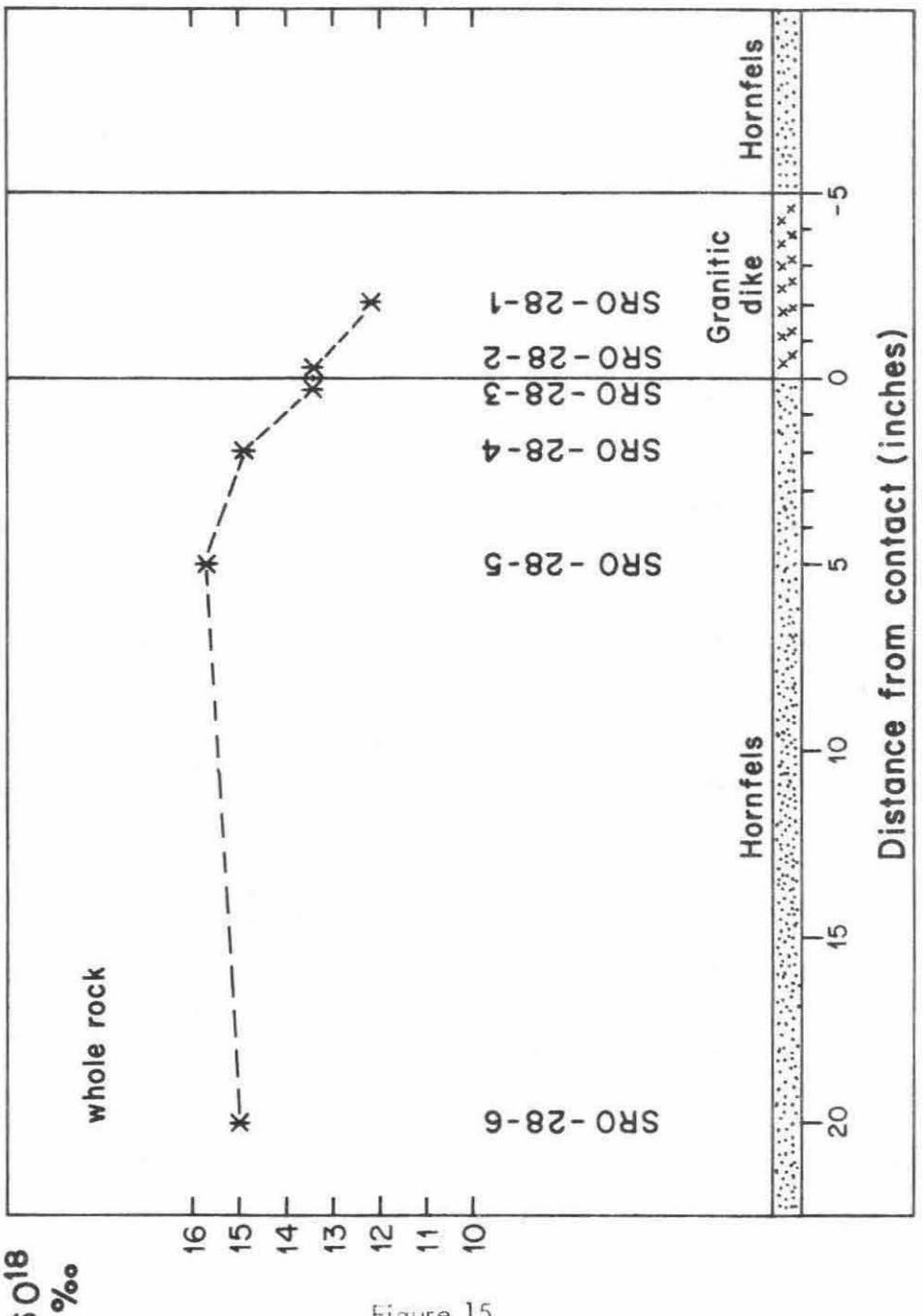
δO18 ‰
16
15
14
13
12
11
10
whole rock
SRO-28-6
SRO-28-5
SRO-28-4
SRO-28-3
SRO-28-2
SRO-28-1
Hornfels
Granitic dike
Hornfels
20
15
10
5
0
-5
Distance from contact (inches)

Figure 15

within about 2 to 5 feet of the contact. (2) Two intrusive samples (SRO-29F and SRO-34, the former collected 150 feet inside the main stock, the latter collected from center of a small plug) have very "abnormal" O^{18}/O^{16} ratios: quartz 13.1 - 14.0, feldspar 10.4, and biotite 6.8 - 8.1 per mil, whereas two other intrusive samples collected 1 to 2 miles inside the stock (13-85-7a and 13-85-8) are quite "normal" in their isotopic compositions: quartz 9.5 - 9.6, feldspar 7.9 - 8.0, and biotite 4.4 - 4.6 per mil. We may therefore infer that samples SRO-29F and SRO-34 have been seriously contaminated by the country rock in some manner.

The change of O^{18}/O^{16} ratios in the vicinity of the contact between hornfels and a small granodiorite dike has also been studied. The result is shown in Figure 15. The dike is 5 inches thick and the contact is extremely sharp. There is no obvious mineralogical or textural change, either in hand specimen or under the microscope, in the hornfels as a result of the intrusion of the dike. However, the 0.2-inch hornfels sample has been lowered in O^{18}/O^{16} ratio by about 2 per mil, and the 2-inch sample by about 0.8 per mil. The 5-inch sample has a δ-value of 15.7 per mil, identical to SRO-29E (30 feet away from the contact); this probably represents the original O^{18}/O^{16} ratio unaffected by the dike. The O^{18}/O^{16} ratios in the dike show a reciprocal response to the hornfels. The 0.1-inch sample of the dike has been dragged up by at least 1.2 per mil by the hornfels.

The oxygen isotopic fractionations among coexisting minerals are given in Table 4. The two hornfels samples collected within 2 feet of the contact show almost identical quartz-biotite and quartz-muscovite fractionations. Two intrusive samples collected 1 to 1.7 miles inside the stock have considerably

TABLE 4

Oxygen isotopic fractionations among coexisting minerals in the Santa Rosa stock contact zone, Santa Rosa Range

Sample No.	Distance from contact	Δ_{Q-B}	Δ_{Q-Mu}	Δ_{Q-F}	Δ_{Mu-B}	Δ_{F-B}
Intrusive						
13-85-7a	1.7 miles	5.1		1.6		3.5
13-85-8	1 mile	4.9		1.7		3.2
SRO-29F	150 feet	6.3		2.8		3.5
Small plug						
SRO-34	100 feet	5.9				
Country rock						
SRO-29A	1 inch	6.0	3.1		2.9	
SRO-29D	2 feet	6.2	3.2		3.0	

Q = quartz, B = biotite, Mu = muscovite, F = feldspar.

smaller quartz-biotite and quartz-feldspar fractionations than samples collected near the margin of the stock.

5.2 Birch Creek, Deep Springs Valley, California

A. General statement

The area of interest is a contact zone between the Inyo batholith and Cambrian sedimentary rocks near Deep Springs Valley, Inyo County, California. The geology of the area and its vicinity has been described by Miller (1928), Nash (1962, 1964), Nelson (1962, 1966), and Nelson and Sylvester (1966). Nash (1962, 1964) made a detailed geologic map of a small, well-exposed contact zone at the mouth of Birch Creek canyon; this is used as a basis for the present study.

The Inyo batholith is an elongate granitic mass exposed over 500 square miles along the northeast flank of the White Mountains. At the mouth of Birch Creek, the Beer Creek quartz monzonite, accompanied by a foliated hornblende granodiorite along the margin, has intruded a sequence of lower Cambrian limestones and fine-grained quartzose and pelitic clastic rocks; the age of emplacement was early to middle Jurassic (McKee and Nash, 1967). A contact metamorphic aureole of marble, hornfels, and schist, approximately 2500 feet in width, was formed. A later phase of unfoliated granite and alaskite was emplaced along the margin of the granodiorite and as dikes and sills within the country rocks, probably in the Cretaceous (McKee and Nash, 1967). The metasomatic skarns studied in the present work were formed during this later phase of intrusion.

Figure 16. Generalized geologic map showing sample locations in the Birch Creek contact aureole, Deep Springs Valley, California (geology after Nash, 1962).

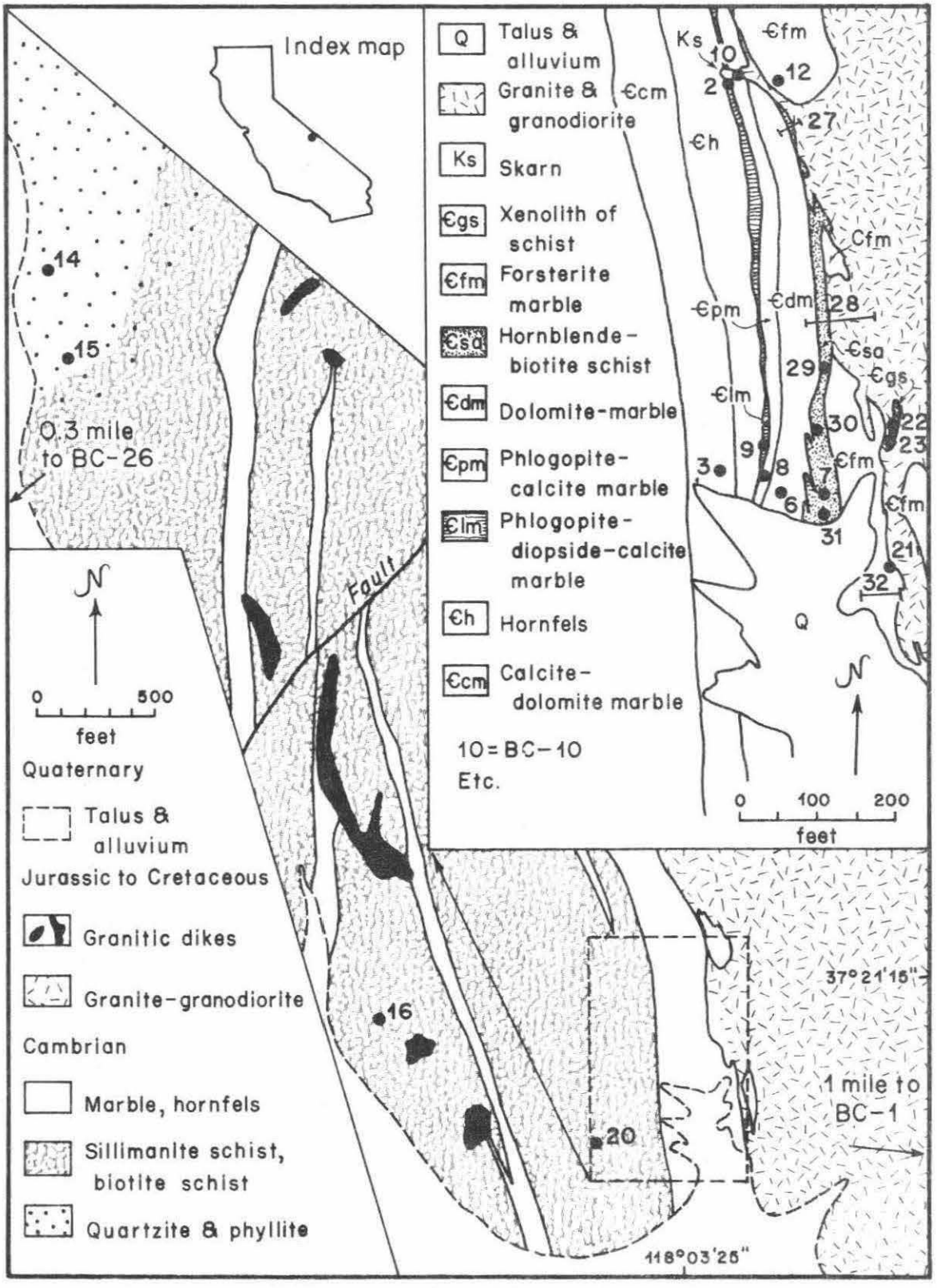
Index map
Q Talus & alluvium
Granite & granodiorite
Ks Skarn
€gs Xenolith of schist
€fm Forsterite marble
€sa Hornblende-biotite schist
€dm Dolomite-marble
€pm Phlogopite-calcite marble
€lm Phlogopite-diopside-calcite marble
€h Hornfels
€cm Calcite-dolomite marble
10 = BC-10
Etc.
0 100 200
feet
0.3 mile to BC-26
Fault
0 500
feet
Quaternary
Talus & alluvium
Jurassic to Cretaceous
Granitic dikes
Granite-granodiorite
Cambrian
Marble, hornfels
Sillimanite schist, biotite schist
Quartzite & phyllite
37°21'15"
1 mile to BC-1
118°03'25"

Figure 16

B. Pelitic contact metamorphic rocks

The present study concentrated on a small, well-exposed contact zone (Figure 16). The metasedimentary rocks within the contact zone are commonly strongly foliated, lenticular units with pronounced mineralogic banding. The metamorphic units strike approximately parallel to the margin of the pluton.

Detailed sampling was carried out on a wedge-shaped, hornblende-biotite schist unit in contact with the intrusive on one side and marble on the other. Two traverses, BC-27 and BC-28, were made starting from inside the intrusive, crossing the schist unit, and terminating in the marble unit. The thickness of the schist unit along traverse BC-27 is 5 feet, and along traverse BC-28 is 17 feet. A diopside-plagioclase zone 3 inches thick is present at the schist-marble contact in traverse BC-27. Samples were also collected along the strike of the schist unit and from a schist xenolith inside the pluton. The mineralogy and textures of all samples collected from the schist unit are similar; each contains biotite, hornblende, plagioclase, microcline, and quartz. However, samples from the schist xenolith are either migmatized or contain leucocratic segregations. In addition, they do not contain hornblende. Representative samples were also collected from different marble units, irregular skarns, and schists several hundred to several thousand feet away from the pluton.

Figures 17 and 18 illustrate the oxygen isotopic results from traverses BC-27 and BC-28, respectively, along with samples from the schist xenolith and granodiorite sample (BC-1) collected about 1 mile inside the pluton. Figure 19 is the plot of oxygen isotopic data for samples from the central part of the hornblende-biotite schist, the phlogopite marble, the forsterite marble, and the sillimanite and biotite schists farther away from the contact.

Figure 17. Plot of O^{18}/O^{16} ratios vs. distance for samples from traverse BC-27, a granite-schist-marble contact zone, Birch Creek.

Figure 18. Plot of O^{18}/O^{16} ratios vs. distance for samples from traverse BC-28, Birch Creek, located 250 feet south of traverse BC-27.

Figure 19. Plot of O^{18}/O^{16} ratios vs. distance for samples which include the sillimanite and biotite schists, the phlogopite marble, the forsterite marble, and the central portion of the schist unit in traverses BC-27 and BC-28, Birch Creek.

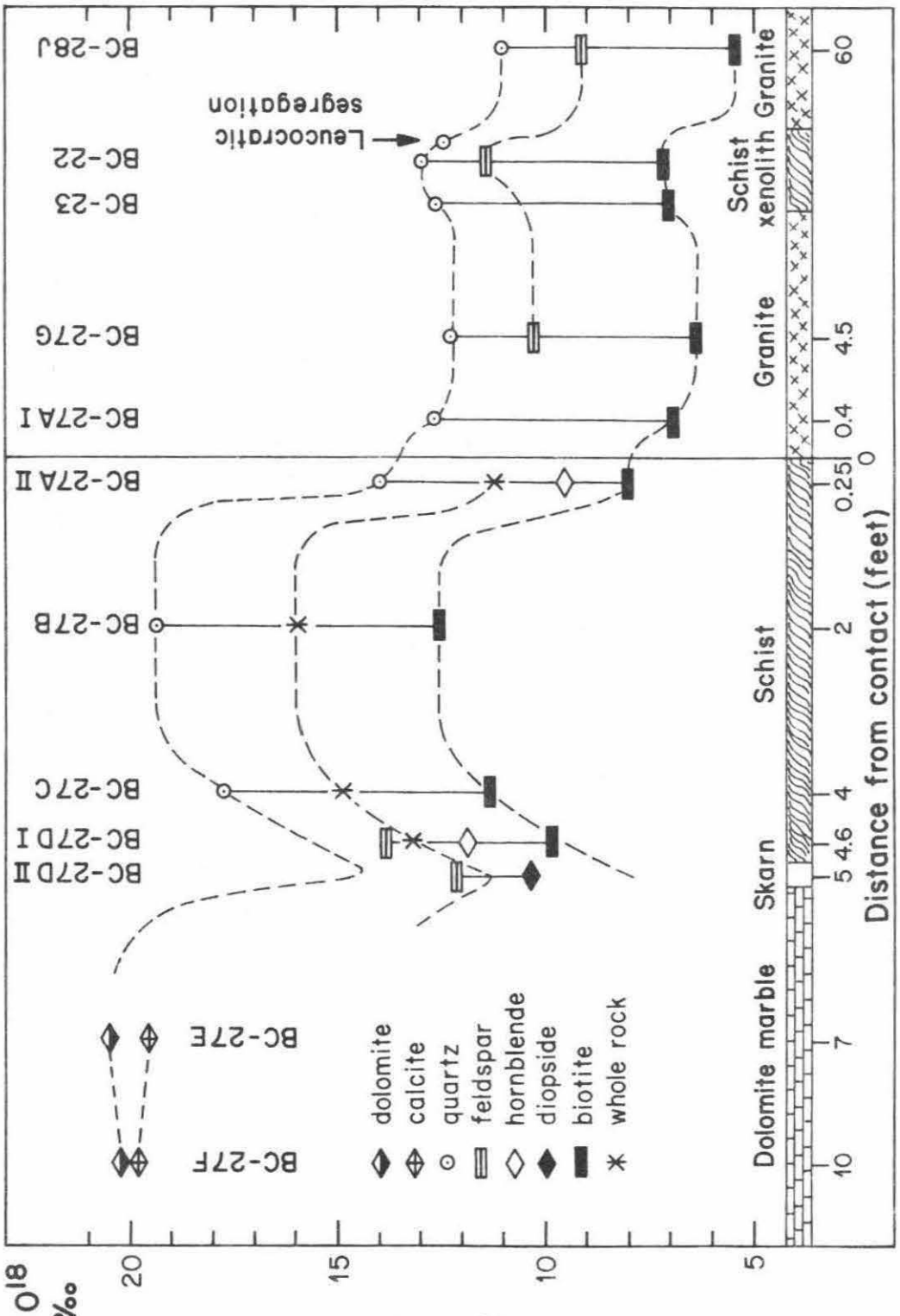
δO18 ‰
20
15
10
5
BC-28J
BC-22
BC-23
BC-27G
BC-27A I
BC-27A II
BC-27B
BC-27C
BC-27D I
BC-27D II
BC-27E
BC-27F
Leucocratic segregation
dolomite
calcite
quartz
feldspar
hornblende
diopside
biotite
whole rock
Dolomite marble
Skarn
Schist
Granite
Schist xenolith Granite
10
7
5 4.6
4
2
0.25
0
0.4
4.5
60
Distance from contact (feet)

Figure 17

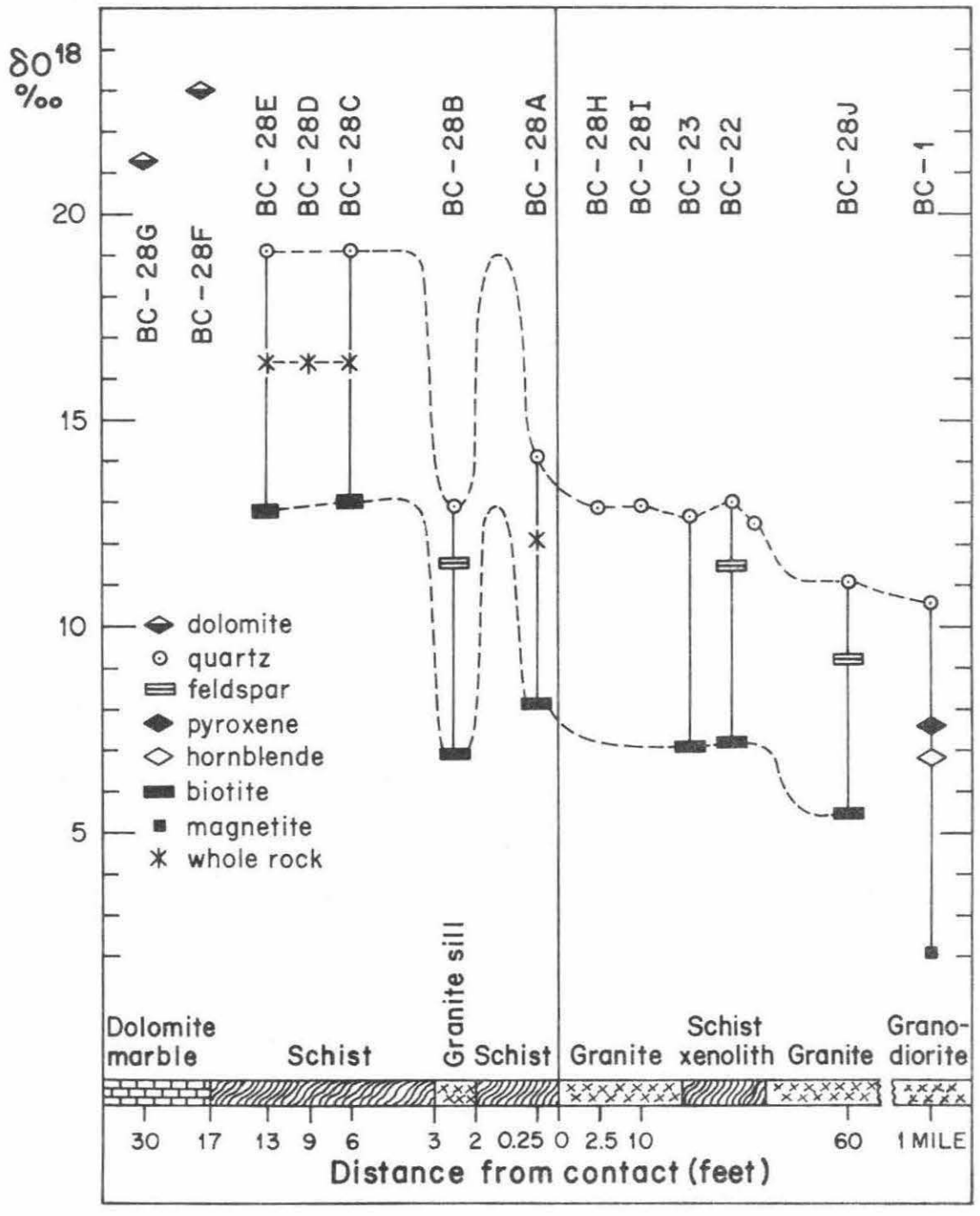
δO18 ‰
20
15
10
5
BC-28G
BC-28F
BC-28E
BC-28D
BC-28C
BC-28B
BC-28A
BC-28H
BC-28I
BC-23
BC-22
BC-28J
BC-1
dolomite
quartz
feldspar
pyroxene
hornblende
biotite
magnetite
whole rock
Granite sill
Dolomite marble
Schist
Schist
Granite
Schist xenolith
Granite
Grano-diorite
30 17 13 9 6 3 2 0.25 0 2.5 10 60 1 MILE
Distance from contact (feet)

Figure 18

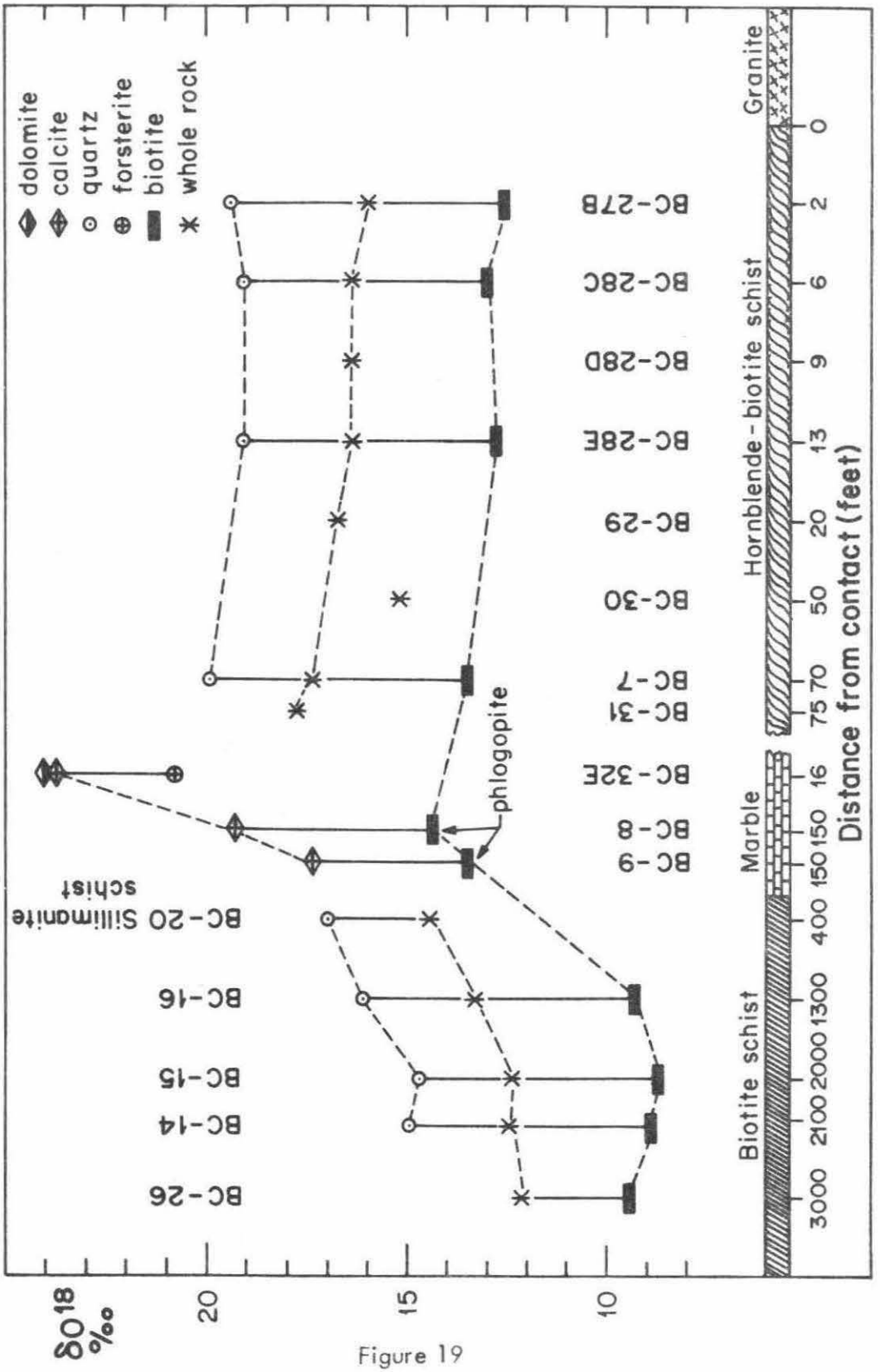
dolomite
calcite
quartz
forsterite
biotite
whole rock
Granite
Hornblende-biotite schist
Marble
Biotite schist
Distance from contact (feet)
0
2
6
9
13
20
50
70
75
16
150
150
400
1300
2000
2100
3000
BC-27B
BC-28C
BC-28D
BC-28E
BC-29
BC-30
BC-7
BC-31
BC-32E
BC-8
BC-9
phlogopite
BC-20 Sillimanite schist
BC-16
BC-15
BC-14
BC-26
10
15
20
δO18 ‰

Figure 19

The O^{18}/O^{16} ratios of the individual minerals and whole-rock samples of the hornblende-biotite schist are very uniform if one disregards those samples 1 foot or less distant from the intrusive or the marbles. Those schist samples less than 1 foot from the intrusive have much lower O^{18}/O^{16} ratios than the central part of the schist unit. The oxygen isotopic compositional gradient in these localities is very steep, about 3 per mil/foot for quartz and 2.5 per mil/foot for biotite. The schist samples adjacent to the zoned skarn also have low O^{18}/O^{16} ratios compared to those from the central portions of the schist unit. Both of the above effects are presumably due to isotopic exchange with the low-O^{18} intrusive or the low-O^{18} skarns.

The O^{18}/O^{16} ratios of individual minerals in the margin of the pluton (at least 10 feet inward from the contact) are rather high: quartz 12.3 - 12.9 and biotite 6.4 - 7.0 per mil. However, BC-1 collected about 1 mile inside the contact has "normal" igneous O^{18}/O^{16} ratios: quartz 10.6, pyroxene 7.6, hornblende 6.9, and magnetite 2.1 per mil.

The O^{18}/O^{16} ratios of minerals in the schist xenolith are almost identical to the corresponding minerals in the marginal pluton itself. A 1-foot thick granite sill intruded into the schist 2 feet away from the main contact also has O^{18}/O^{16} ratios similar to the marginal granite (see Table 5).

The zoned skarns (BC-27 D II) have lower O^{18}/O^{16} ratios than the adjacent marbles and schists, thus producing an "isotopic trough" in Figure 17. The skarns have formed by decarbonation of the marbles, so it may be inferred that decarbonation reactions are probably responsible for lowering the O^{18}/O^{16} ratios of these rocks.

TABLE 5

Comparison of oxygen isotopic compositions of minerals in the schist xenolith, granite sill, and marginal granite from the Birch Creek contact zone.

Rock		Schist xenolith		Granite sill	Marginal granite			
Sample No.		BC-22	BC-23	BC-28B	BC-27AI	BC-27G	BC-28H	BC-28I
δO^{18} per mil	Quartz	13.0	12.7	12.9	12.7	12.2	12.9	12.9
	Feldspar	11.5	-	11.5	-	10.4	-	-
	Biotite	7.2	7.2	6.9	7.0	6.4	-	-

The O^{18}/O^{16} ratios of minerals and whole rocks for samples collected from the outer part of the aureole (a thick biotite schist unit) are consistently 4 to 5 per mil lower than those in the hornblende-biotite schist referred to above. The reason for the low O^{18}/O^{16} ratios of the biotite schist in the outer aureole is not known. It might be inherited from the pre-contact metamorphic O^{18}/O^{16} ratios of the parent rocks. Alternatively, the high O^{18}/O^{16} ratios of the thin hornblende-biotite schist unit may be the result of isotopic exchange with a high O^{18}/O^{16} source (presumably the abundant surrounding marbles). In this connection, it is interesting to note that the O^{18}/O^{16} ratios of the biotite schist increase progressively toward the marble contact.

The oxygen isotopic fractionations among coexisting minerals in the Birch Creek pelitic and plutonic rocks are presented in Table 6, and the quartz-biotite fractionations are plotted in Figure 20. As can be seen, there is a gentle decrease in quartz-biotite fractionations as the intrusive contact is approached; the fractionations in the pluton are very uniform and somewhat

TABLE 6

Oxygen isotopic fractionations among coexisting minerals in the Birch Creek pelitic and plutonic rocks

Sample No.	Distance from contact, feet	Δ_{Q-B}	Δ_{Q-H}	Δ_{Q-F}	Δ_{F-B}	Δ_{H-B}	Δ_{Q-Mt}
Intrusive							
BC-1	5000		3.7				8.5
BC-28J	60	5.6		1.8	3.8		
BC-27G	4.5	5.8		1.8	4.0		
BC-27AI	0.4	5.7					
Granite sill							
BC-28B	2.5	6.0		1.4	4.6		
Schist xenolith							
BC-22	5	5.8		1.5	4.3		
BC-23	1	5.6					
Hornblende -biotite schist							
BC-27AII	0.25	5.9	4.4			1.5	
BC-27B	2	6.8					

TABLE 6 (continued)

Sample No.	Distance from contact, feet	Δ_{Q-B}	Δ_{Q-H}	Δ_{Q-F}	Δ_{F-B}	Δ_{H-B}	Δ_{Q-Mt}
BC-27C	4	6.3					
BC-27DI	4.6				4.0	2.0	
BC-28A	0.25	6.0					
BC-28C	6	6.2					
BC-28E	13	6.3					
BC-7	70	6.4					
Biotite schist							
BC-16	1300	6.8					
BC-15	2000	6.0					
BC-14	2100	6.0					

Q = quartz, B = biotite, H = hornblende, F = feldspar, Mt = magnetite

Figure 20. Oxygen isotopic fractionations between coexisting quartz and biotite plotted vs. distance, for samples from the Birch Creek contact zone.

Figure 21. Plot of D/H ratios and water contents vs. distance for samples from the Birch Creek contact zone.

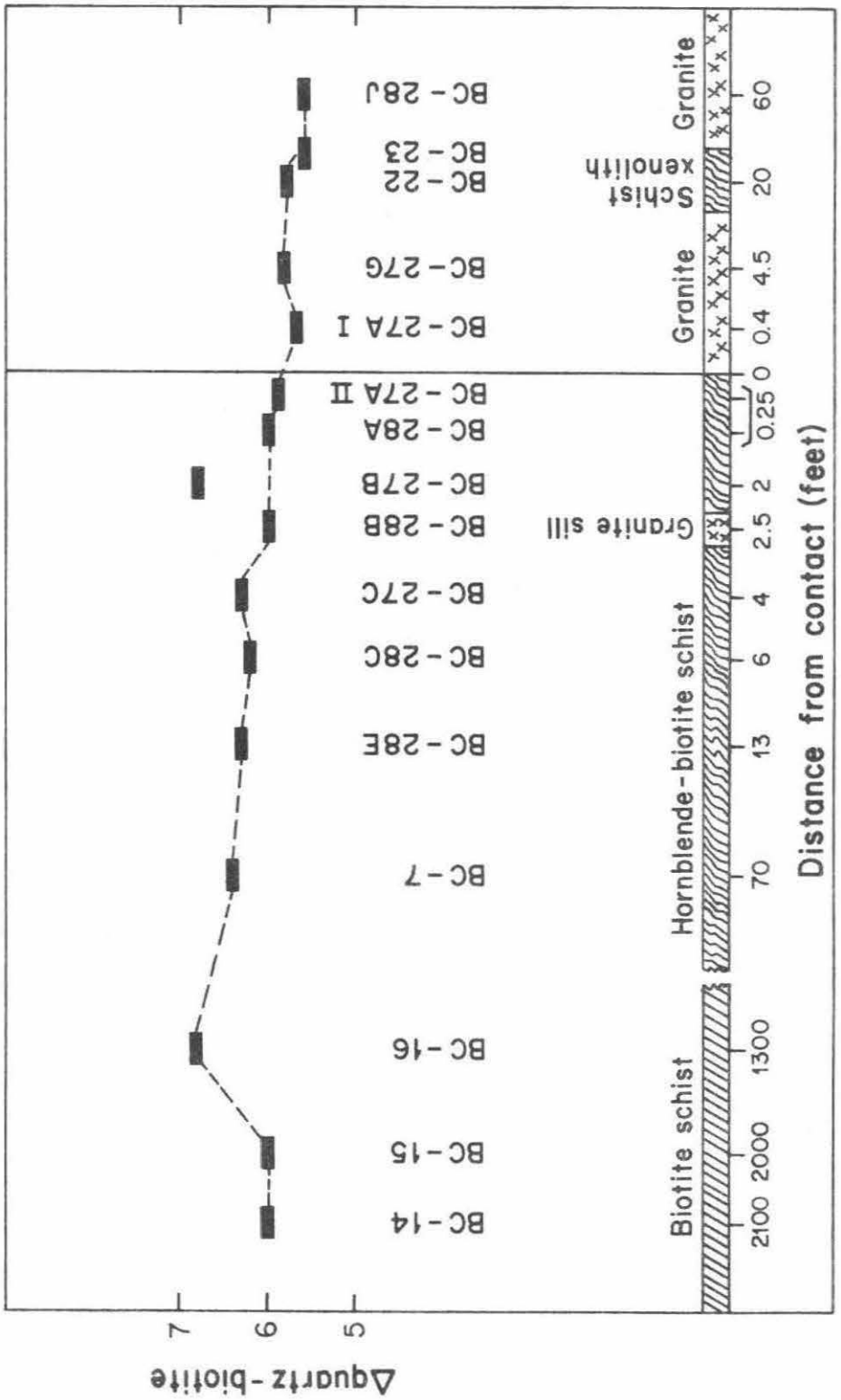
Δquartz-biotite
7
6
5
BC-14
BC-15
BC-16
BC-7
BC-28E
BC-28C
BC-27C
BC-28B
BC-27B
BC-28A
BC-27A II
BC-27A I
BC-27G
BC-22
BC-23
BC-28J
Biotite schist
Hornblende-biotite schist
Granite sill
Granite
Schist xenolith
Granite
2100 2000 1300 70 13 6 4 2.5 2 0.25 0 0.4 4.5 20 60
Distance from contact (feet)

Figure 20

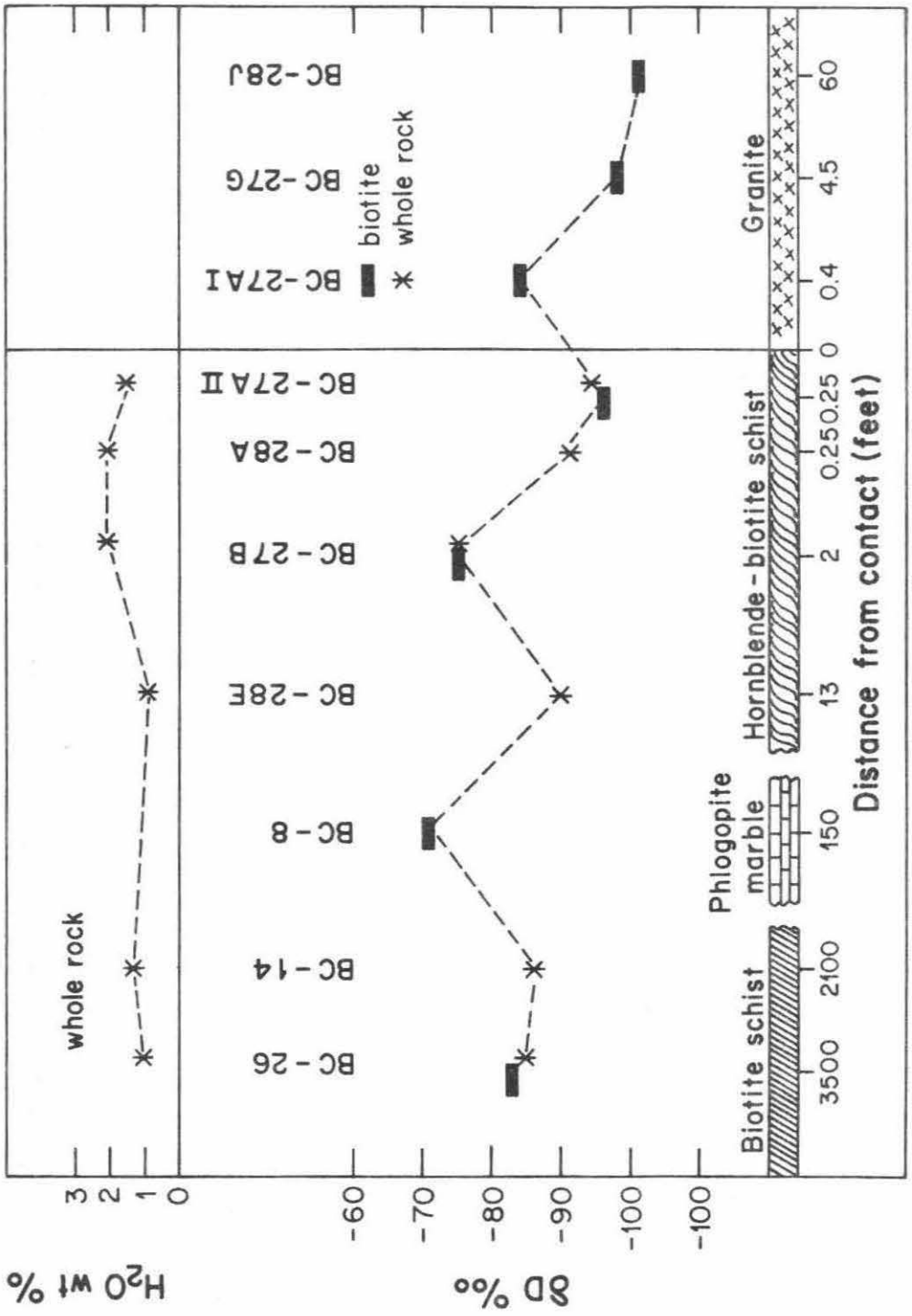
H2O wt %
δD ‰
whole rock
BC-26
BC-14
BC-8
BC-28E
BC-27B
BC-28A
BC-27AII
BC-27AI
BC-27G
BC-28J
biotite
whole rock
Granite
Hornblende-biotite schist
Phlogopite marble
Biotite schist
Distance from contact (feet)

Figure 21

smaller than those in the schists. The exceptions occur in three schist samples: two samples collected 2000 to 2100 feet away from the pluton have very small Δ-values (both 6.0) whereas the third sample collected only 2 feet away from the contact has quite a large Δ-value (6.8). It is also interesting that the quartz-biotite fractionations in the xenolith are identical to those in the pluton.

Hydrogen isotope analyses were made on some of the above samples. The results are illustrated in Figure 21, together with the H_2O-contents of the samples. It is obvious that D/H ratios in the pluton do not differ appreciably from those in the country rocks. The intrusive biotites show a spread from -84 to -101 per mil, whereas the biotites in the country rock have a range from -71 to -96 per mil. The D/H ratios of whole rock samples are essentially identical to those of biotite. Since hornblende and biotite are the only two hydroxyl-bearing minerals in the schist, it confirms the findings of Godfrey (1962) and Taylor and Epstein (1966) that little or no D/H fractionation exists between coexisting biotite and hornblende. The water contents in the schists range from 0.9% to 2.1% by weight, considerably lower than in the schists and phyllites of the Santa Rosa Range.

C. Contact metamorphic marbles

Figures 22 and 23 illustrate the oxygen and carbon isotopic results from the marbles and irregular skarns at Birch Creek. The marble units are, moving outward from the pluton, forsterite marble, dolomite marble, phlogopite marble, and calcite-dolomite marble. The irregular skarns consist of large euhedral crystals (a few mm to 1 cm) of calcite, quartz, epidote, grossularite,

Figure 22. Plot of O^{18}/O^{16} ratios of marbles and irregular massive skarns from the Birch Creek contact zone.

Figure 23. Plot of C^{13}/C^{12} ratios of marbles and irregular massive skarns from the Birch Creek contact zone.

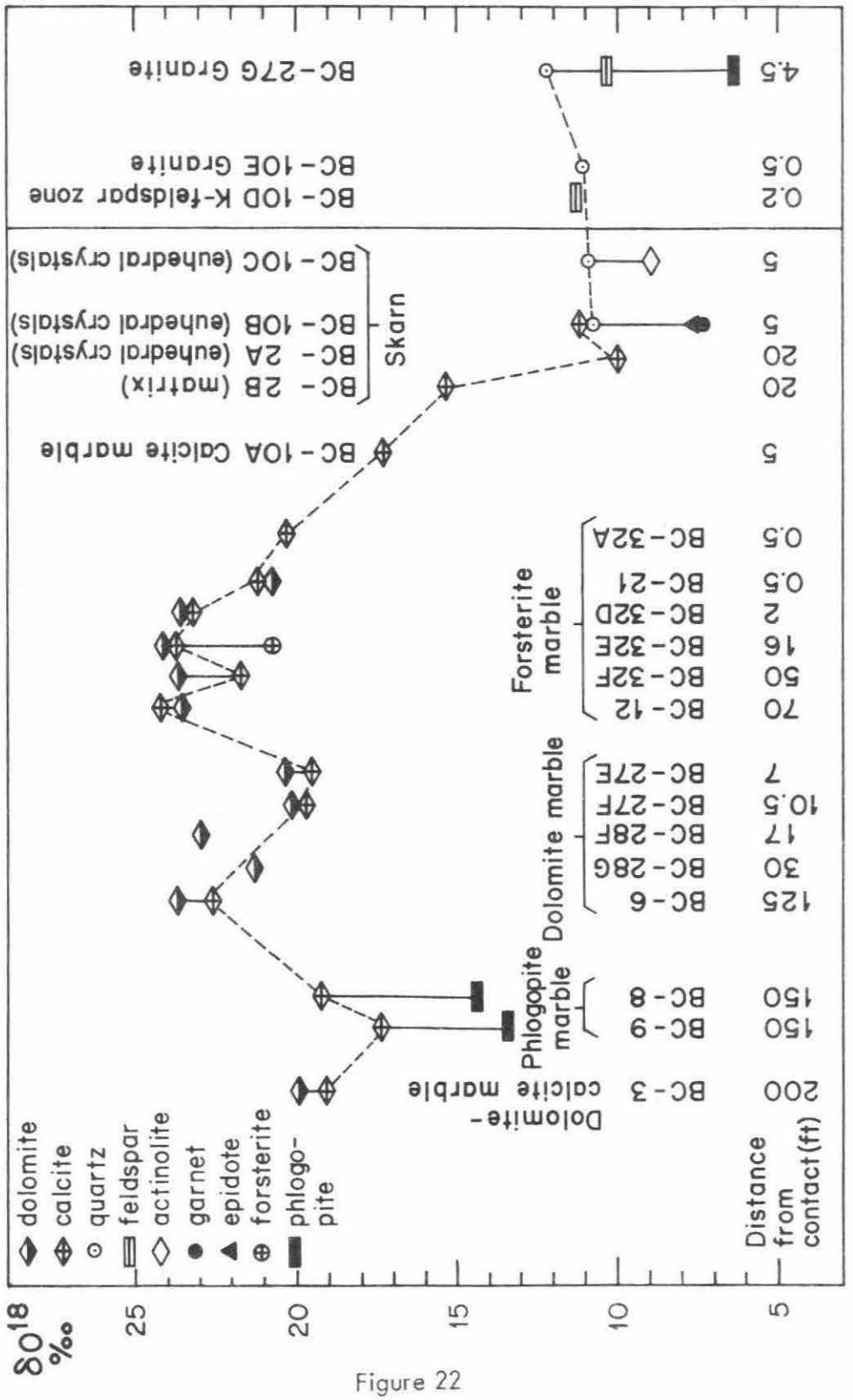
δO18 ‰
25
20
15
10
5
◆ dolomite
◆ calcite
⊙ quartz
▤ feldspar
◇ actinolite
● garnet
▲ epidote
⊕ forsterite
▮ phlogo-pite
Distance from contact(ft)
200 BC-3 Dolomite-calcite marble
150 BC-9
150 BC-8 Phlogopite marble
125 BC-6
30 BC-28G
17 BC-28F
10.5 BC-27F
7 BC-27E Dolomite marble
70 BC-12
50 BC-32F
16 BC-32E
2 BC-32D
0.5 BC-21
0.5 BC-32A Forsterite marble
5 BC-10A Calcite marble
20 BC-2B (matrix)
20 BC-2A (euhedral crystals)
5 BC-10B (euhedral crystals)
5 BC-10C (euhedral crystals) Skarn
0.2 BC-10D K-feldspar zone
0.5 BC-10E Granite
4.5 BC-27G Granite

Figure 22

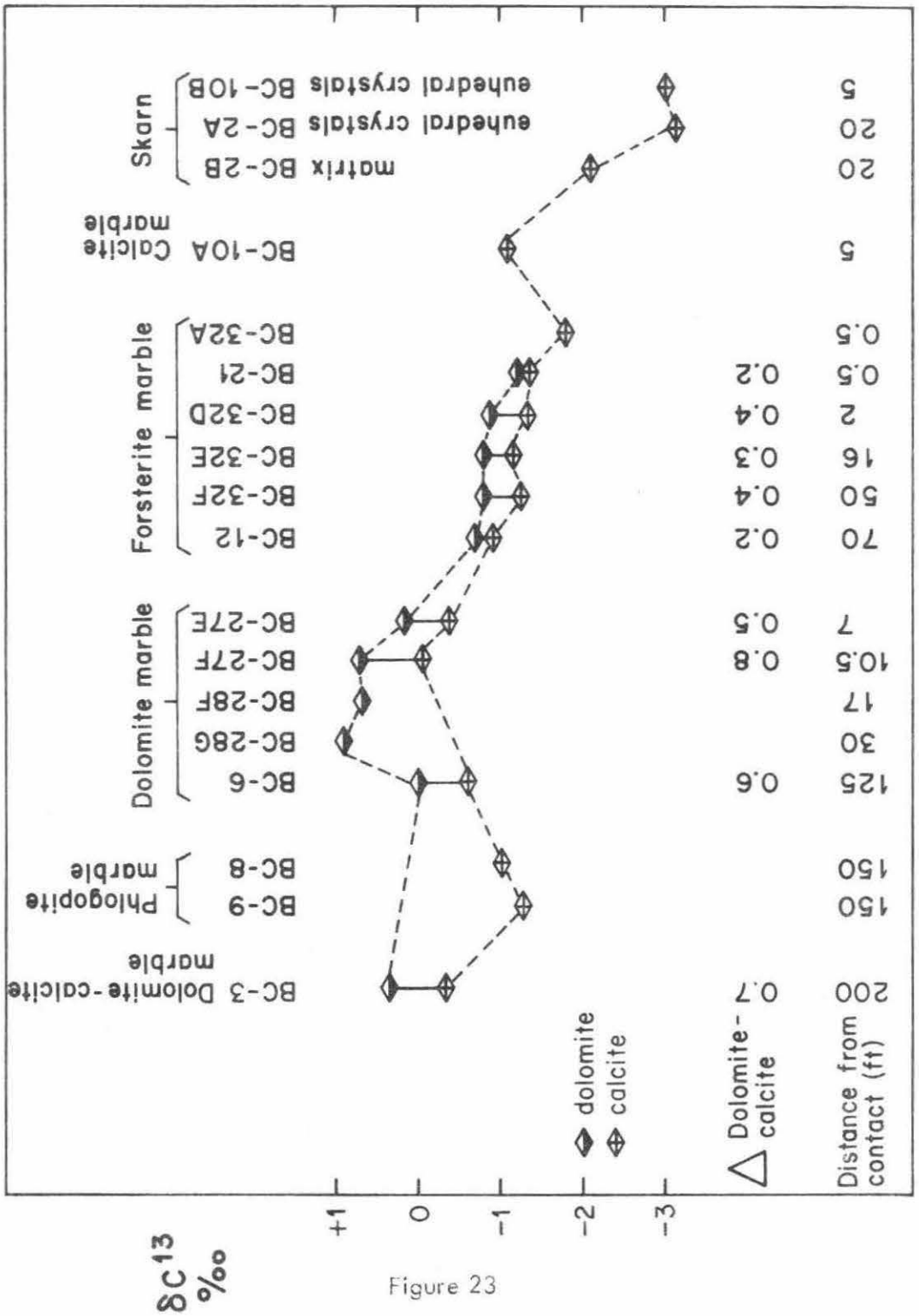
δC13 ‰
+1
0
-1
-2
-3
dolomite
calcite
Dolomite-calcite
Distance from contact (ft)
200 0.7
150
150
125 0.6
30
17
10.5 0.8
7 0.5
70 0.2
50 0.4
16 0.3
2 0.4
0.5 0.2
0.5
5
20
20
5
BC-3 Dolomite-calcite marble
Phlogopite marble
BC-9
BC-8
Dolomite marble
BC-6
BC-28G
BC-28F
BC-27F
BC-27E
Forsterite marble
BC-12
BC-32F
BC-32E
BC-32D
BC-21
BC-32A
Calcite marble
BC-10A
Skarn
matrix BC-2B
euhedral crystals BC-2A
euhedral crystals BC-10B

Figure 23

phlogopite, diopside, wollastonite, and actinolite. The oxygen isotopic ratios are variable in the marbles: calcites 17.4 to 23.9 per mil and dolomites 20.0 to 24.2 per mil; most of these are within the range of normal marine limestone. The calcites with low O^{18}/O^{16} ratios usually occur without co-existing dolomite. The correlation between O^{18}/O^{16} ratios and the presence or absence of calc-silicates is very weak, if any.

The lowest O^{18}/O^{16} ratios are observed in the large, euhedral, well-recrystallized skarns. The δ-value of quartz in the skarns is 1.3 per mil lower than that of quartz in the nearby pluton. Therefore, the $\delta\ O^{18}$-curve exhibits an "isotopic trough" similar to that in Figure 17. The simple isotopic exchange of the skarns with the pluton cannot produce this "isotopic trough" because the skarns are even lower in O^{18} than the intrusive. Inasmuch as the skarns were formed from decarbonation of the marble, it is natural to conclude that the decarbonation reaction is responsible for the lowering of the O^{18}/O^{16} ratios.

The C^{13}/C^{12} ratios in the marbles (Figure 23) show a much narrower range than the O^{18}/O^{16} ratios. They range from +0.9 to -1.2 per mil in dolomites and from -0.1 to -1.8 per mil in calcites. These are typical values for marine limestone. The skarns are about 2 to 3 per mil lower in $\delta\ C^{13}$ than the marbles. The C^{13}/C^{12} ratios correlate well with the presence or absence of the calc-silicates (the presence of calc-silicates is associated with low C^{13}/C^{12} ratios).

The oxygen isotopic fractionations between coexisting dolomite and calcite are small (-0.6 to +2.0), and they show a "cross-over" in two of the forsterite marbles near the contact. No "cross-over" is observed in carbon

TABLE 7

Oxygen and carbon isotopic fractionations between coexisting dolomite and calcite in marbles of the Birch Creek contact zone. dol = dolomite, cal = calcite.

Sample No.	Distance from contact, feet	δO^{18}_{dol}	δO^{18}_{cal}	$\Delta O^{18}_{dol-cal}$	δC^{13}_{dol}	δC^{13}_{cal}	$\Delta C^{13}_{dol-cal}$
Forsterite marble							
BC-21	0.5	21.0	21.1	-0.1	-1.2	-1.4	+0.2
BC-32D	2	23.6	23.4	+0.2	-0.9	-1.3	+0.4
BC-32E	16	24.1	24.0	+0.1	-0.8	-1.1	+0.3
BC-32F	50	23.7	21.7	+2.0	-0.8	-1.2	+0.4
BC-12	70	23.6	24.2	-0.6	-0.7	-0.9	+0.2
Dolomite marble							
BC-27E	7	20.5	19.6	+0.9	+0.1	-0.4	+0.5
BC-27F	10.5	20.2	19.9	+0.3	+0.7	-0.1	+0.8
BC-6	125	23.7	22.8	+0.9	0.0	-0.6	+0.6
Calcite-dolomite marble							
BC-3	200	20.0	19.2	+0.8	+0.4	-0.3	+0.7

Figure 24. Plot of δO^{18} vs. δC^{13} of dolomite and calcite for marbles and skarns from the Birch Creek contact zone.

Figure 25. Plot of δC^{13} of dolomite vs. carbon isotope fractionations between coexisting dolomite and calcite for contact metamorphic marbles at Birch Creek.

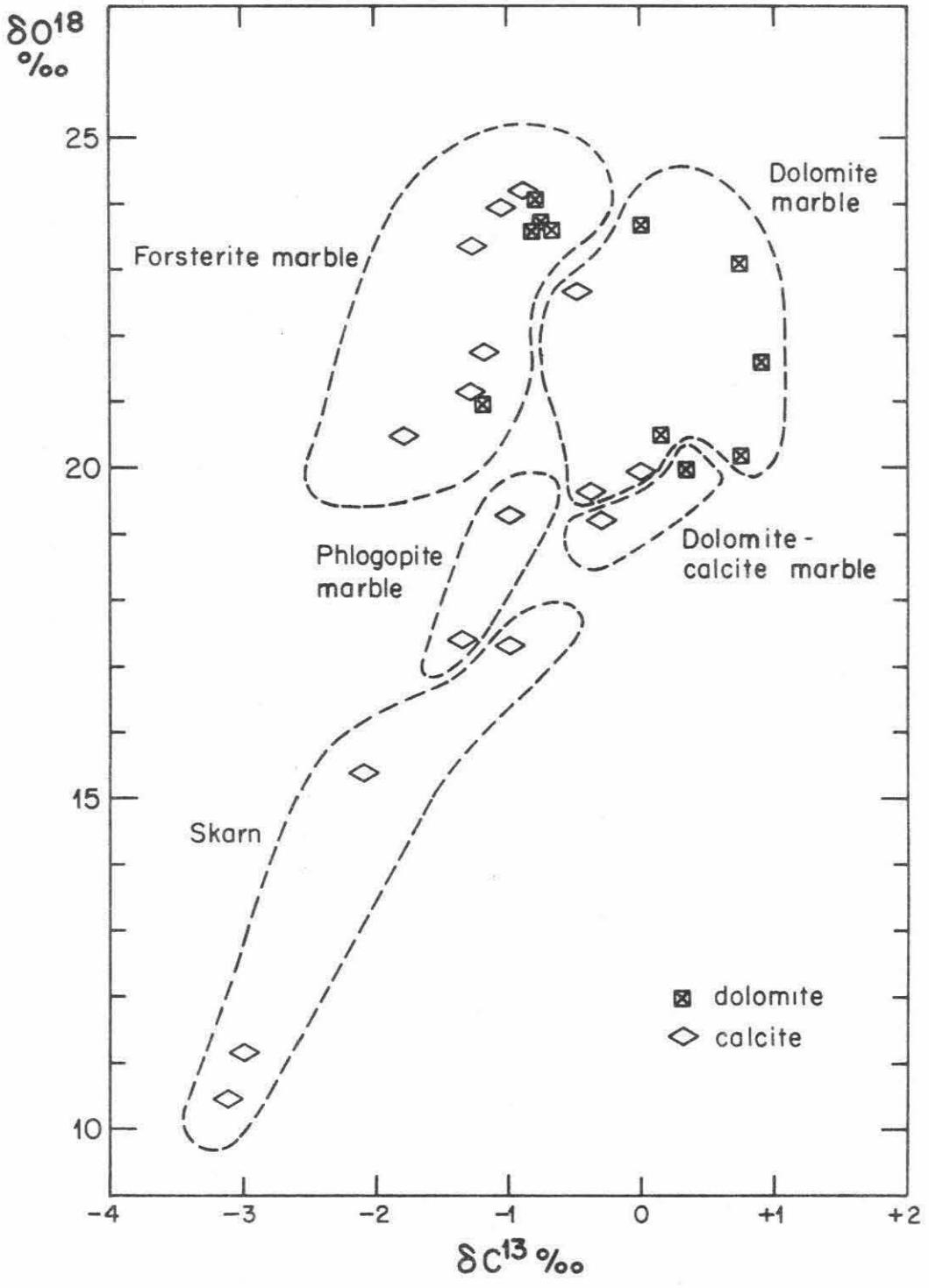
δO18 ‰
25
20
15
10
Forsterite marble
Dolomite marble
Phlogopite marble
Dolomite - calcite marble
Skarn
dolomite
calcite
−4
−3
−2
−1
0
+1
+2
δC13 ‰

Figure 24

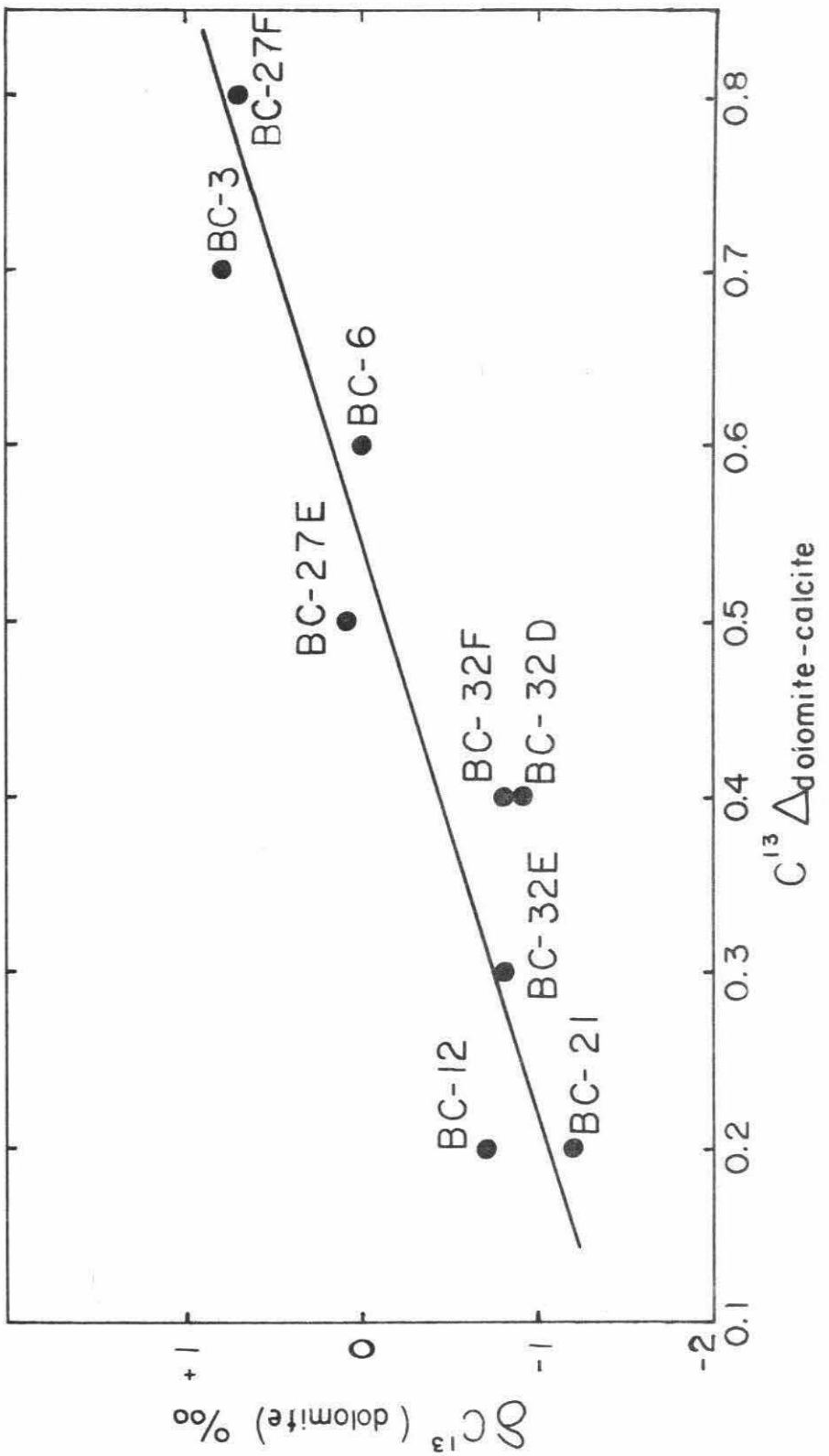
BC-3
BC-27F
BC-6
BC-27E
BC-32F
BC-32D
BC-32E
BC-12
BC-21
+1
0
-1
-2
0.1
0.2
0.3
0.4
0.5
0.6
0.7
0.8
δ C13 (dolomite) ‰
C13 Δdolomite-calcite

Figure 25

isotopes; dolomite is always enriched in C^{13} relative to coexisting calcite, although the fractionations are very small (+0.2 to +0.8). There is no obvious correlation between fractionations (either for oxygen or for carbon) and sample distance from the pluton (Table 7).

One reason for the more regular behavior of the carbon isotopes (no "cross-over", δC^{13} correlates with presen ce or absence of calc-silicates) is perhaps that there is no obvious reservoir of carbon other than the dolomite and calcite of the marble. Therefore, in contrast to oxygen, there is little likelihood of exchange of the carbon isotopes with sources outside the marbles themselves.

In Figure 24, δO^{18} is plotted vs. δC^{13} for coexisting dolomite and calcite. One can delineate five areas which correspond to the four marble units plus skarns. The skarns have the lowest δO^{18} and δC^{13}, whereas the dolomite marbles have the highest. Such a correlation between δO^{18} and δC^{13} was also observed in marbles by Baertschi (1957).

Figure 25 is a plot of δC^{13} of dolomite vs. carbon isotopic fractionations between dolomite and calcite. There is a rough correlation between these two parameters. If decarbonation reactions lower the δC^{13} value of dolomite, one might also expect to observe a smaller dolomite-calcite fractionation in the sample which has undergone decarbonation. At least part of the trend in Figure 25 is probably due to this decarbonation effect.

5.3 Eldora, Front Range, Colorado

A. General statement

The geology in the Front Range has been described by Lovering and Goddard (1950). The oldest rocks in the area are Precambrian schists, gneisses, and amphibolites of the Idaho Springs formation. The rocks were highly and uniformly metamorphosed 1200 to 1500 million years ago (Hart, 1964) to a grade characterized by the sillimanite-almandine subfacies of the almandine-amphibolite facies. The Idaho Springs formation is cut by the Precambrian Boulder Creek granite. These Precambrian crystalline rocks were intruded during Laramide time by a series of stocks extending southwestward across the Front Range. The contact metamorphic zone of the Eldora stock was chosen by Doe and Hart (1963) and Hart (1964) for studies on the effects of contact metamorphism on isotopic mineral ages of different minerals. Steiger and Hart (1967), and Wright (1967) carried out studies on the microcline-orthoclase transition within the Eldora contact zone.

In the present study, oxygen isotopic analyses were made on the samples originally used by Hart (1964), and Steiger and Hart (1967). In addition, G. R. Tilton (personal communication) supplied three samples collected from Hart's Eldora traverse. The present writer collected an additional traverse from the Caribou stock contact zone about 1 mile north of the Eldora stock. The geology and sample locations are shown in Figure 26.

B. Eldora stock contact zone

The Eldora stock and its contact zone has been geologically studied by Cree (1948). The intrusive is a quartz monzonite with an exposed diameter of about 2 miles. There are also numerous small pegmatites of a few feet or inches in thickness occurring concordantly along the foliations of the country-

Figure 26. Generalized geologic map showing sample locations of Eldora and Caribou stock contact zones (geology after Lovering and Goddard, 1950; and Steiger and Hart, 1967).

Figure 27. Variation of mineral ages (upper figure; after Hart, 1964) and O^{18}/O^{16} ratios (lower figure) as a function of distance from the intrusive contact for the Eldora traverse.

Figure 28. Plot of O^{18}/O^{16} ratios vs. distance, for the identical K-feldspar samples used by Steiger and Hart (1967) for their microcline-orthoclase transition studies (Eldora stock contact zone).

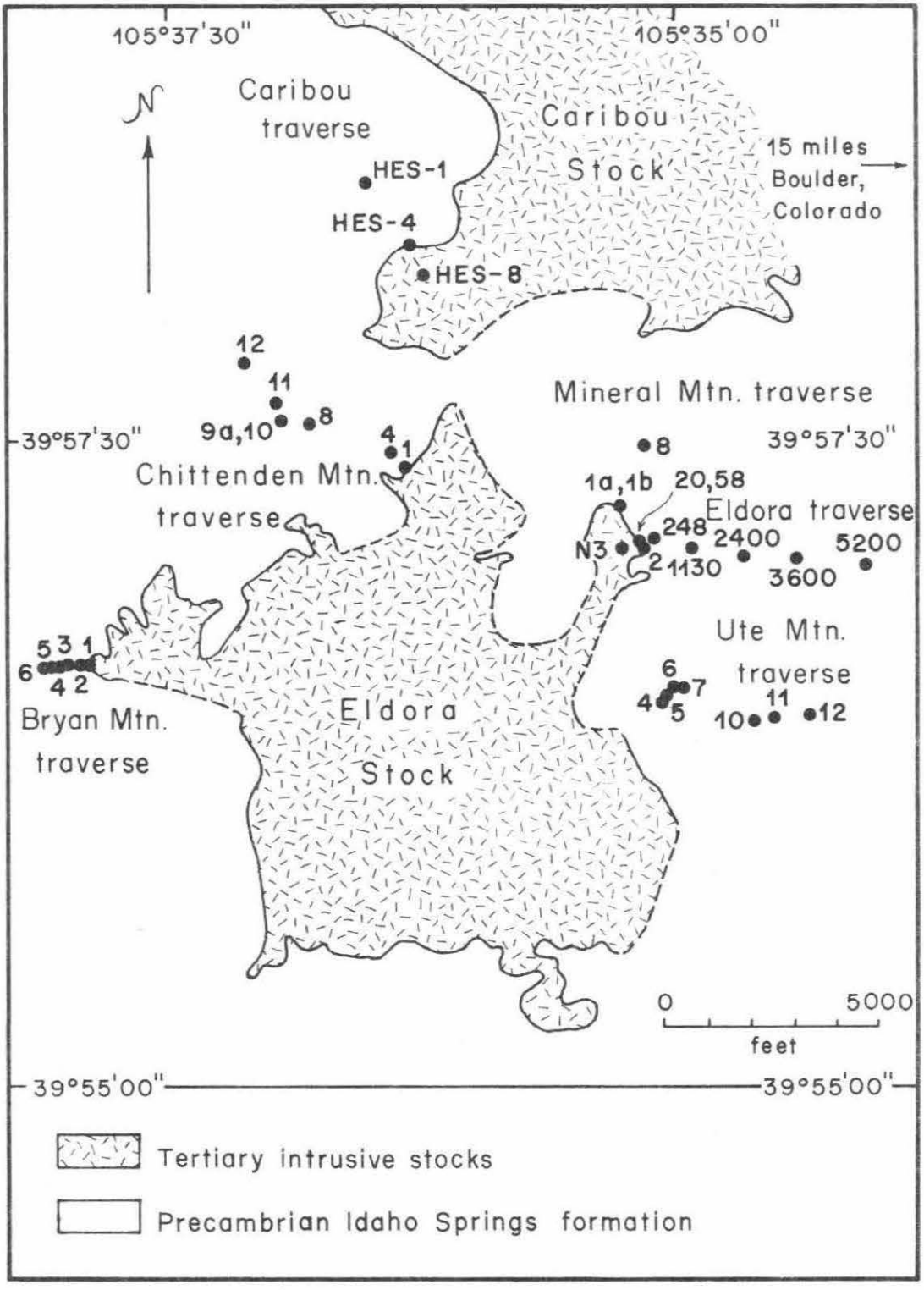
105°37'30"
105°35'00"
N
Caribou traverse
Caribou Stock
15 miles Boulder, Colorado
HES-1
HES-4
HES-8
12
11
9a,10
8
4
1
39°57'30"
Chittenden Mtn. traverse
Mineral Mtn. traverse
8
1a,1b
20,58
248
N3
2
1130
2400
5200
3600
Eldora traverse
Ute Mtn. traverse
6
7
4
5
10
11
12
5 3 1
6
4 2
Bryan Mtn. traverse
Eldora Stock
0
5000
feet
39°55'00"
Tertiary intrusive stocks
Precambrian Idaho Springs formation

Figure 26

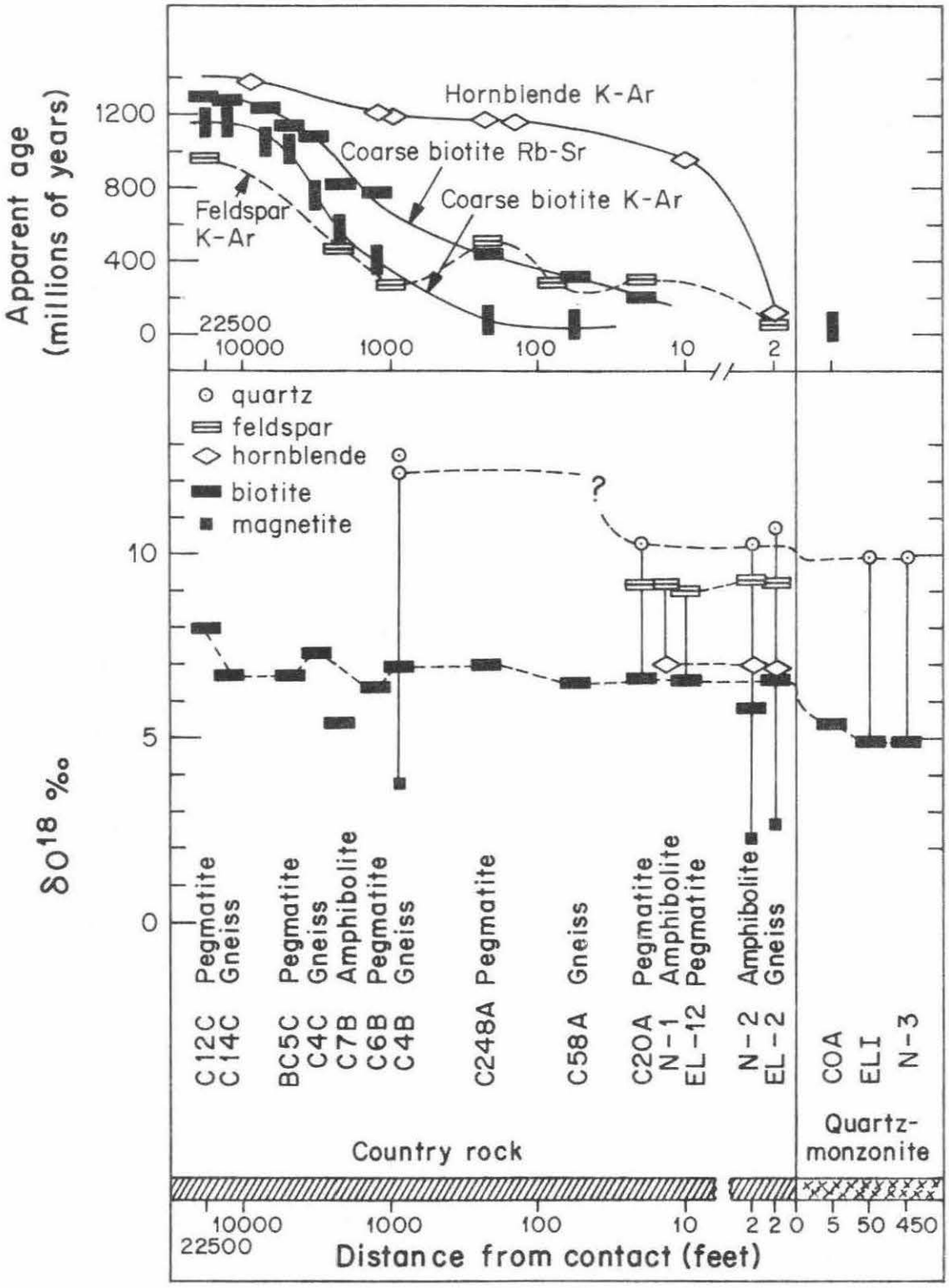
Apparent age (millions of years)
1200
800
400
0
Hornblende K-Ar
Coarse biotite Rb-Sr
Coarse biotite K-Ar
Feldspar K-Ar
22500
10000
1000
100
10
2
quartz
feldspar
hornblende
biotite
magnetite
?
10
5
0
δO18 ‰
C12C Pegmatite
C14C Gneiss
BC5C Pegmatite
C4C Gneiss
C7B Amphibolite
C6B Pegmatite
C4B Gneiss
C248A Pegmatite
C58A Gneiss
C20A Pegmatite
N-1 Amphibolite
EL-12 Pegmatite
N-2 Amphibolite
EL-2 Gneiss
COA
ELI
N-3
Country rock
Quartz-monzonite
10000
22500
1000
100
10
2 2 0
5
50
450
Distance from contact (feet)

Figure 27

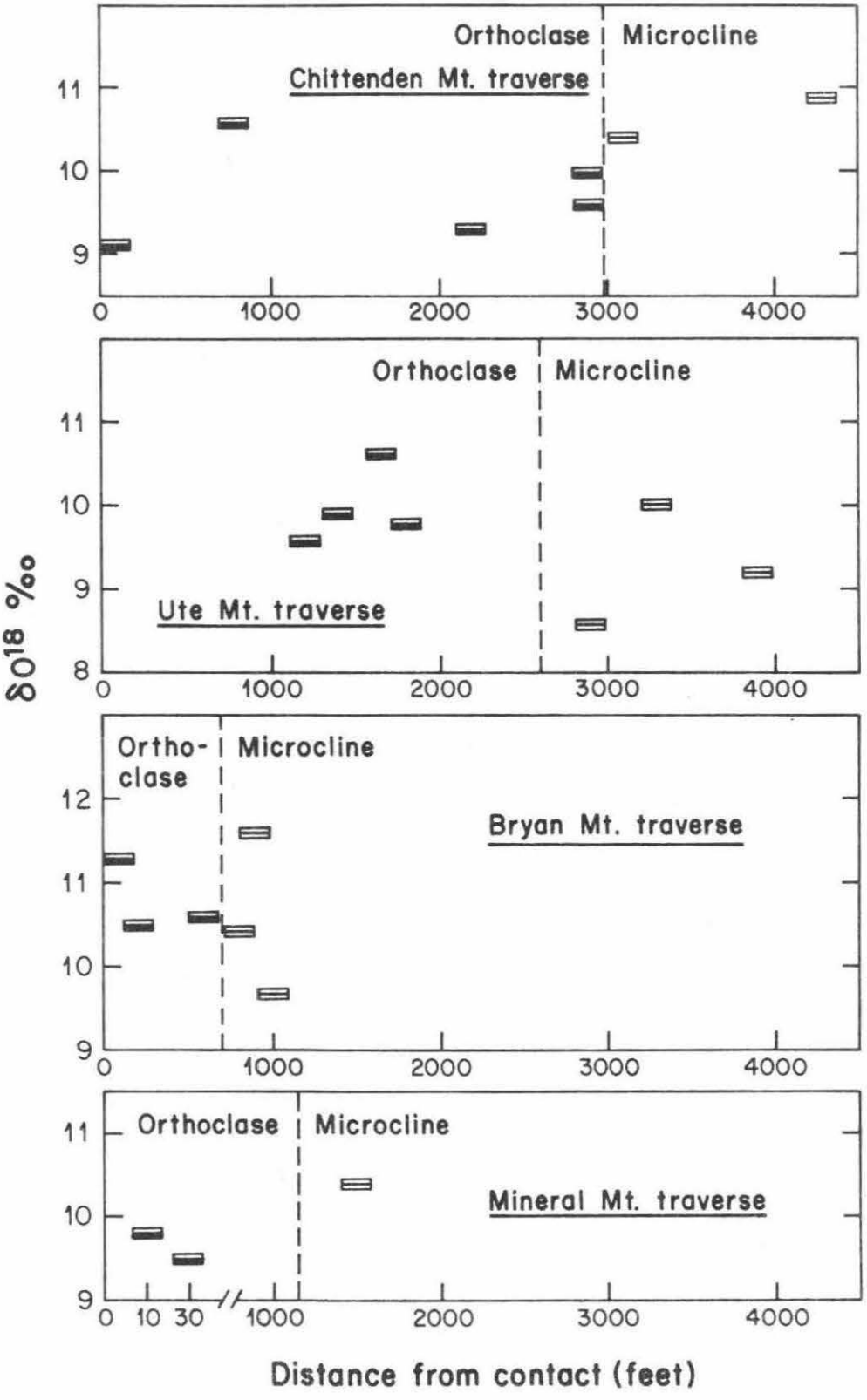
Orthoclase
Microcline
Chittenden Mt. traverse
Ute Mt. traverse
Ortho-
clase
Bryan Mt. traverse
Mineral Mt. traverse
δO18 ‰
Distance from contact (feet)

Figure 28

rock gneisses and schists. Hart (1964) observed some minor contact metamorphic effects in the country rocks. Within a few feet from the contact, hornblende has been partially altered to biotite and twinned oligoclase has untwinned sodic overgrowths. However, the only major mineralogical change observed by Hart (1964) and Steiger and Hart (1967) is the transition of the alkali feldspar from a perthitic microcline of high obliquity in the unaffected country rock to non-perthitic orthoclase near the contact. The transition could be sharp or gradational, and the width of the orthoclase zone is variable, depending strongly upon the configuration of the contact. The mineralogic age of different minerals also responded differently due to the contact heating (Doe and Hart, 1963; Hart, 1964). The results of Hart (1964) are shown in the upper half of Figure 27.

The oxygen isotopic results of the Eldora traverse are shown in the lower half of Figure 27 and the isotopic fractionations among coexisting minerals are listed in Table 8. There are several pertinent features: (1) The quartz monzonite has quite "normal" igneous O^{18}/O^{16} ratios. (2) The O^{18}/O^{16} ratios of biotite in the country rocks, excluding those in the amphibolites and pegmatite C 12 C, are very uniform (δ = 6.4 to 7.3 per mil, 10 samples); note that the biotite occurs in samples collected 2 feet to 14,000 feet away from the intrusive contact. The biotites in amphibolites are distinctly lower in O^{18}/O^{16} ratio than those in gneisses and pegmatites, but it should be noted that the biotites in the amphibolites are alteration products of hornblendes. The biotite in sample C 12 C is high in O^{18}/O^{16} ratio compared to other biotites, and it is interesting that this pegmatite differs from the other pegmatites in that it contains muscovite and the Or-

TABLE 8

Oxygen isotopic fractionations among coexisting minerals in the Eldora stock contact zone.

Q = quartz, Mt = magnetite, B = biotite, H = hornblende, F = feldspar

Sample No.	Rock	Distance from contact, feet	Δ_{Q-Mt}	Δ_{Q-B}	Δ_{Q-H}	Δ_{Q-F}	Δ_{F-B}	Δ_{F-H}	Δ_{B-Mt}	Δ_{F-Mt}
N-3	Quartz monzonite	450		5.0						
EL-1	Quartz monzonite	50		5.1						
EL-2	Gneiss	2	8.0	4.0	4.0	1.6	2.4	2.4	4.0	6.4
N-2	Amphibolite	2	8.1	4.6	3.4	1.1	3.5	2.3	3.5	7.0
EL-12	Pegmatite	12					2.4			
N-1	Amphibolite	18						2.2		
C20A	Pegmatite	20		3.6		1.2	2.4			
C4B	Gneiss	950	8.5	5.3					3.2	

content in its K-feldspar is lower than other K-feldspars (Hart, 1964). (3) Although the variations of O^{18}/O^{16} ratios in biotite are less than 1 per mil, the variations in quartz are bigger (δ= 10.4 - 12.8 per mil). However, quartz within 20 feet away from the contact has quite a uniform O^{18}/O^{16} ratio, similar to that of quartz in the intrusive. (4) The oxygen isotopic fractionations among coexisting minerals in the country rocks are, in most cases, smaller than those in other areas studied in this research, and are very uniform through the whole traverse, perhaps indicating that uniformly high temperatures were attained during regional metamorphism. (5) The quartz-biotite fractionations in the intrusive samples are identical to those obtained from the central portion of the Santa Rosa stock, and similar to those in "normal" plutonic granitic rocks (Taylor and Epstein, 1962).

Figure 28 shows the O^{18}/O^{16} ratios measured on the identical K-feldspar samples used by Steiger and Hart (1967) for their microcline - orthoclase transition studies. A spread of about 2 per mil is observed in each of the four traverses studied, and the δ -values show no apparent change across the microcline-orthoclase transition zone. Although the oxygen isotopic data do not clarify the mechanism of the transition (see Steiger and Hart, 1967), there is little doubt that the O^{18}/O^{16} ratios of the orthoclase must be inherited from the regionally metamorphosed rocks.

C. Caribou traverse

The Caribou stock is exposed about one-half mile north of the Eldora stock. A traverse was taken along the west side of the stock where the intrusive is a monzonite and the country rocks are sillimanite schist,

Figure 29. Plot of O^{18}/O^{16} ratios vs. distance for samples from the Caribou stock contact zone.

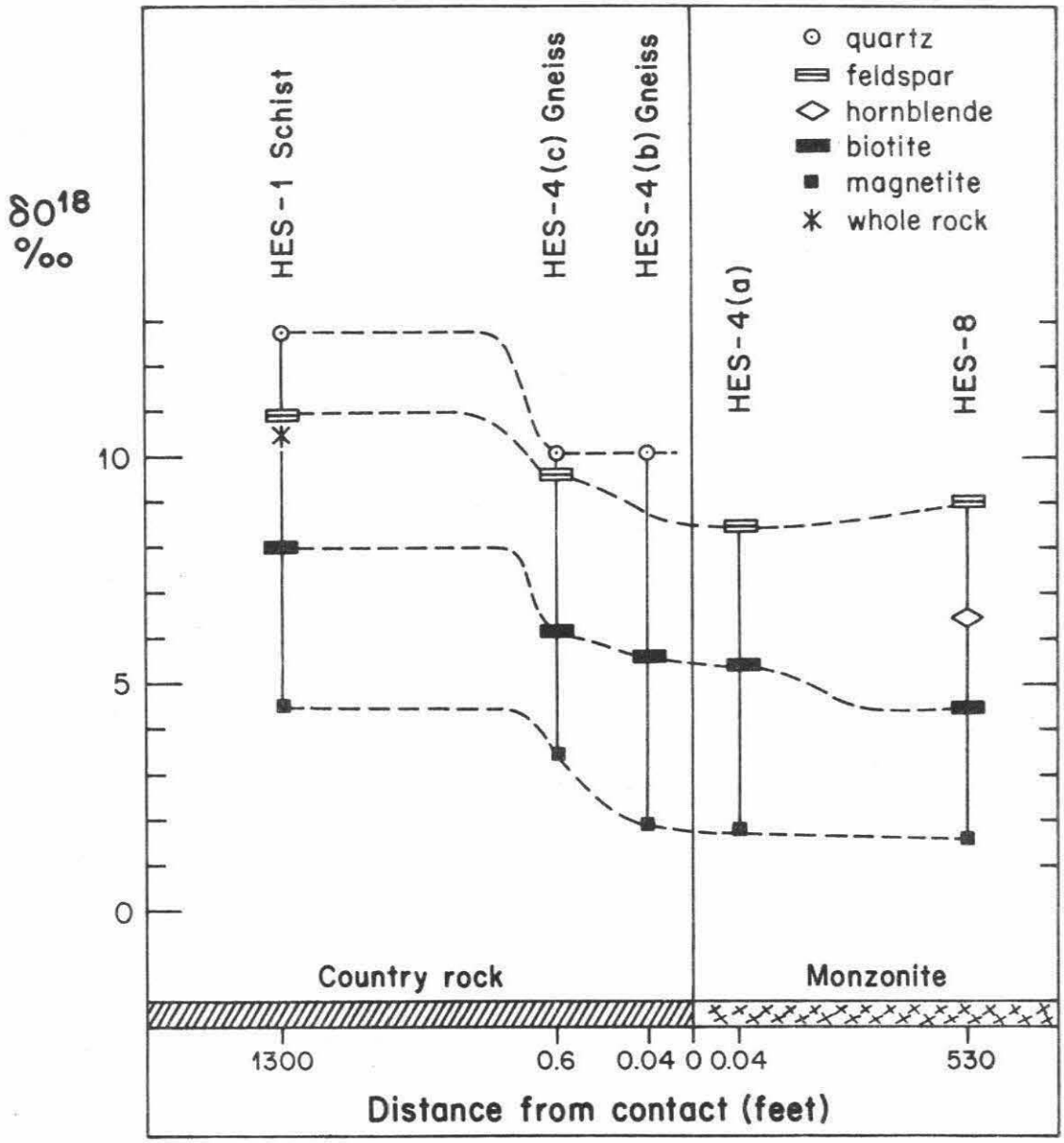
δO18 ‰
HES-1 Schist
HES-4(c) Gneiss
HES-4(b) Gneiss
HES-4(a)
HES-8
quartz
feldspar
hornblende
biotite
magnetite
whole rock
10
5
0
Country rock
Monzonite
1300
0.6
0.04
0
0.04
530
Distance from contact (feet)

Figure 29

TABLE 9

Oxygen isotopic fractionations among coexisting minerals in the Caribou stock contact zone.

Q = quartz, Mt = magnetite, B = biotite, F = feldspar, H = hornblende

Sample No.	Rock	Distance from contact, feet	$\Delta_{Q\text{-}Mt}$	$\Delta_{Q\text{-}B}$	$\Delta_{F\text{-}Mt}$	$\Delta_{F\text{-}B}$	$\Delta_{F\text{-}H}$	$\Delta_{B\text{-}Mt}$	$\Delta_{Q\text{-}F}$
HES-8	Monzonite	530			7.3	4.5	2.5	2.8	
HES-4a	Monzonite	0.04			6.7	3.1		3.6	
HES-4b	Gneiss	0.04	8.2	4.6				3.6	
HES-4c	Gneiss	0.6	6.7	4.0	6.2	3.5		2.7	0.5
HES-1	Schist	1300	8.3	4.8	6.4	2.9		3.5	1.9

TABLE 10

O^{18}/O^{16} ratios in 3 closely-spaced samples at the gneiss-monzonite contact of Caribou traverse.

Sample No.	Rock	Distance from contact, inch	δ quartz	δ feldspar	δ biotite	δ magnetite
HES-4a	Monzonite	0.5	------	8.5± 0.0 (2)	5.4±0.1 (2)	1.8±0.0 (2)
HES-4b	Gneiss	0.5	10.1 (1)	-----	5.5±0.0 (2)	1.9±0.0(2)
HES-4c	Gneiss	7.0	10.1±0.0 (2)	9.6 (1)	6.1±0.2 (2)	3.4±0.0(2)

Analytical error shown is average deviation from the mean. Numbers in parentheses indicate the number of separate determinations.

gneiss, pegmatite, and amphibolite. The sample locations are shown in Figure 26. The isotopic data are illustrated in Figure 29 and listed in Table 9.

The intrusive sample collected 530 feet inside the stock, and the sillimanite schist sample 1300 feet away from the contact have O^{18}/O^{16} ratios similar to the corresponding samples from the Eldora traverse. Three closely-spaced samples sliced from a large hand specimen containing the gneiss-monzonite contact have slightly different δ-values as shown in Table 10. HES-4a (monzonite) and HES-4b (gneiss), separated from each other by 1 inch, show almost identical O^{18}/O^{16} ratios in the individual minerals. The 0.1 per mil differences in biotite and magnetite between the two samples may be real, instead of due to experimental errors, since the δ-values vary in the right direction. HES-4c, however, is distinctly higher by 0.6 per mil in biotite and 1.5 per mil in magnetite than HES-4b collected only 6.5 inches away. The difference in the O^{18}/O^{16} ratios in the 3 samples indicate that the dimensions of the oxygen isotopic equilibrium system are very small in the Eldora area. It is definitely less than 7 inches, and probably very close to 0.5 inches. The relatively small size of such an equilibrium system compared with the Santa Rosa and Birch Creek areas may be due to the presence of only minor amounts of pore-fluids in an already highly regionally metamorphosed country rock; also, the intrusion itself appears to have been relatively "dry."

5.4 Marble Canyon, Culberson County, Trans-Pecos Texas

The Marble Canyon contact aureole has been described by Bridge (1964, 1966a, 1966b). An elliptical intrusion of composition ranging from syenite to olivine monzonite has intruded siliceous limestone and dolomite, producing a contact aureole 150 to 300 feet in width. A complete sequence of anhydrous calcium-and magnesium-silicates (see Bowen, 1940; Tilley, 1951) was developed in the country rocks.

Four samples collected by T. E. Bridge (personal communication) have been isotopically analyzed. The results are given in Table 11. Sample A-6 contains various monomineralic layers; a sketch with isotopic data is shown in Figure 30.

Although only three calcite samples were analyzed, they have δO^{18}-values of 14.2 to 23.4 per mil and δC^{13}-values of +0.1 to -9.2 per mil; the lowest δ-values, both in O^{18} and C^{13}, are found in sample A-5 where the calcite occurs interstitially to the calc-silicates. Note that both δO^{18} and δC^{13} in A-5 are about 10 per mil lower than in typical marine limestone. Sample A-1 consists exclusively of calc-silicates (no carbonate is identified), indicating that decarbonation reactions have gone to completion. This rock gives the lowest O^{18}/O^{16} ratio (δ = 8.9 per mil) of any of the 4 samples.

The O^{18}/O^{16} ratios in sample A-6 are complex. The calcite layer gives δO^{18} = 23.3 and δC^{13} = 0.1; both are typical values for marine-limestone. The calc-silicate and quartz layers give quite low δO^{18}-values, presumably due to decarbonation. Three wollastonite layers separated

TABLE 11

O^{18}/O^{16} and C^{13}/C^{12} ratios in minerals and rocks in Marble Canyon contact aureole, Culberson County, Trans-Pecos, Texas.

Sample No.	Distance from contact, feet	Rock	Mineral	δO^{18} per mil	δC^{13} per mil
A-1	4	Calc-silicates	whole rock	8.9	
A-5	15	Calc-silicates with calcite	whole rock	14.2	-9.2
A-6	25	Monomineralic layers of calc-silicates, quartz and calcite	(b) Wollastonite	16.4	
			(c) Quartz	15.0	
			(cd) Quartz	14.7	
			(d) Wollastonite	11.3	
			(e) Diopside	13.0	
			(h) Quartz	14.8	
			(i) Wollastonite	14.4	
			(j) Calcite	23.3	+0.1
A-13	130	chert and carbonate	chert	23.4	
			calcite	17.0	-2.3

Figure 30. Sketch of a monomineralic layered skarn, sample A-6, from the Marble Canyon contact aureole, showing oxygen and carbon isotopic analyses of various minerals.

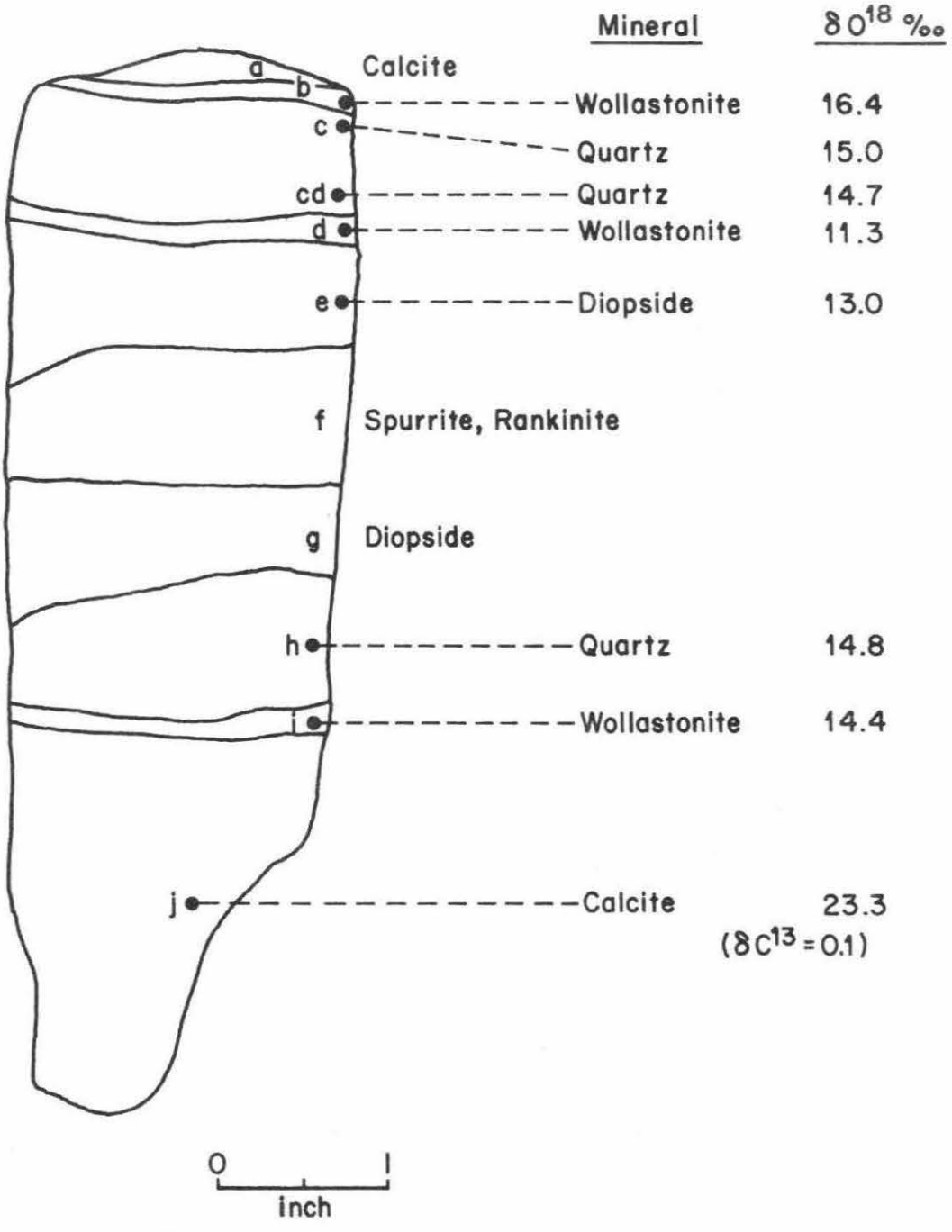
Mineral
δ O18 ‰
a
b
Calcite
c
Wollastonite
16.4
Quartz
15.0
cd
Quartz
14.7
d
Wollastonite
11.3
e
Diopside
13.0
f
Spurrite, Rankinite
g
Diopside
h
Quartz
14.8
i
Wollastonite
14.4
j
Calcite
23.3
(δC13 = 0.1)
0
1
inch

Figure 30

a few cm from one another have three different δO^{18}-values (16.4, 11.3, and 14.4, respectively), whereas two quartz layers are quite similar in their δO^{18}-values (14.7 and 15.0). Some of the adjacent layers are obviously not in isotopic equilibrium. For example, quartz layer (c) is lower in δO^{18} than wollastonite layer (b) by 1.4 per mil. Quartz layer (h) is almost identical in δO^{18} to wollastonite layer (i) (14.8 vs. 14.4). It is therefore inferred that a "dry" decarbonation of this type usually results in isotopic disequilibrium, and that any subsequent re-equilibrations were not powerful enough to restore equilibrium even on a scale of a few millimeters.

VI. GENERAL DISCUSSION AND INTERPRETATION

6.1 Relative O^{18}/O^{16}, C^{13}/C^{12}, and D/H ratios in coexisting minerals of contact metamorphic rocks

A. Oxygen isotopes

One of the most striking systematics observed in the present research is the consistent order of O^{18}-enrichment in the coexisting minerals in a given rock. Listed in order of decreasing O^{18}/O^{16}, the minerals are:

Quartz
Feldspar
Andalusite
Muscovite
Pyroxene
Hornblende
Biotite
Magnetite

The above sequence is identical to those reported by Taylor et al. (1963), Garlick and Epstein (1967), and Taylor and Coleman (1968) in regional metamorphic rocks, except that andalusite is added in the present study. If one assumes that the Al_2SiO_5 polymorphs andalusite and kyanite do not fractionate oxygen isotopes, the order of muscovite and kyanite suggested by Garlick and Epstein (1967), and Taylor et al. (1963) is reversed from the present sequence. However, note that only three kyanite analyses were made in the above references; two of them do not coexist with muscovite, and the third is based on only a 50 - 60 percent oxygen yield.

Only five rocks in the present study exhibit an "abnormal" oxygen isotopic sequence for their coexisting minerals. Two rocks (an amphibolite and a granodiorite) in the north traverse of the Flynn stock show

reversal in the positions of hornblende and biotite. Note that the biotite in the amphibolite (SRO-9) is an alteration product of the hornblende. The granodiorite was collected 6 inches inward from the contact with another amphibolite sample which also shows biotite altering from hornblende. The isotopic positions of andalusite and muscovite are reversed in two rocks: one occurs in the fine-grained hornfels of the south traverse of Flynn stock and the other in the porphyroblastic phyllite of traverse I of the Sawtooth stock. The former rock also shows an unreasonably small quartz-muscovite fractionation (Δ = 1.6), and in the latter rock most of the muscovite is a retrograde product of andalusite porphyroblasts. Most of the above examples of isotopic disequilibrium can therefore be correlated with textural or mineralogical evidence of disequilibrium.

The fifth "abnormal" rock is a pegmatite dike (SRO-D) crosscutting country rock on the south side of the Sawtooth stock in which K-feldspar is lower in δO^{18} than coexisting muscovite by 3.3 per mil. Also, the pure quartz core of this pegmatite is 0.5 per mil higher in δO^{18} than the outer-zone quartz associated with the feldspar and muscovite. It appears that the K-feldspar has become depleted in O^{18} relative to the coexisting quartz, because this quartz is isotopically similar to adjacent metasedimentary quartz. The extremely large quartz- K-feldspar fractionation (Δ = 5.4) implies an absurdly low temperature of less than 100° C (see Figure 42), so this is unquestionably a non-equilibrium pair. On the other hand, the quartz-muscovite fractionation (Δ = 2.1), corresponding to a temperature of 830° C does not appear to be far away from equilibrium. The δ-values of quartz and

muscovite are similar in both the pegmatite and the country rock, suggesting that the isotopic composition of the pegmatite is controlled by isotopic exchange with the adjoining metasedimentary rock. The δ-value of the feldspar then must be a result of exchange down to what appear to be unreasonably low temperatures, or it must be a result of interaction with low - O^{18} fluids. The plausible sources of such O^{18} - depleted fluids are meteoric water that may have been present in the metasediments, or relatively low-temperature fluids derived from a late stage of crystallization of the trondhjemite. Such fluids may also be responsible for the very low O^{18}/O^{16} ratios of magnetite in the Sawtooth aureole, as mentioned in section 5.1 - B.

The coexisting minerals in the analyzed marbles generally exhibit the following oxygen isotopic sequence, listed in order of decreasing O^{18}/O^{16}:

Dolomite
Calcite
Forsterite
Phlogopite

The only exceptions occur in two forsterite marble samples where the relative positions of dolomite and calcite are reversed. This type of oxygen isotopic reversal between dolomite and calcite has also been observed quite commonly in the regional metamorphic marbles studied by Sheppard (1966) and Schwarcz (1966). Such a relation is most commonly observed in the high-grade marbles. Inasmuch as the laboratory-calibrated curve for isotopic equilibrium between dolomite and calcite does not show any "cross-over" within the temperature range 350 - 610° C (O'Neil and Epstein, 1966) and 300 - 510° C (Northrop and Clayton, 1966), it may be inferred that the two forsterite marbles represent non-equilibrium assemblages.

B. Carbon isotopes

Carbon isotopes were analyzed only in the dolomite and calcite of the present study. It is found, without exception, that C^{13} is always concentrated preferentially in the dolomite compared to coexisting calcite by 0.2 to 0.8 per mil, in agreement with the results of Schwarcz (1966), and Sheppard (1966) for regional metamorphic marbles. The two samples with the smallest ΔC^{13}-values are the same forsterite marbles referred to above that show the oxygen isotopic "reversal."

C. Hydrogen isotopes

Muscovite, biotite and hornblende are the three hydroxyl-bearing minerals analyzed in the present study. It is found, without exception, that muscovite concentrates deuterium relative to coexisting biotite; and hornblende and biotite have almost identical D/H ratios, in agreement with the results of Taylor and Epstein (1966) and Godfrey (1962).

In Figure 31 is shown the δO^{18} vs. δ D plot for biotite and muscovite of igneous and contact metamorphic rocks from the Santa Rosa Range, Birch Creek, and the Eldora area. Except that muscovite is always higher in O^{18}/O^{16} and D/H ratios, there is no clear-cut correlation between the O^{18}/O^{16} and D/H ratios among the biotites and the muscovites.

6.2 Isotopic fractionations among coexisting minerals

A. Oxygen isotopic fractionations in silicates and oxides

After demonstrating the consistency of relative O^{18}/O^{16} ratios among coexisting minerals, it is desirable to know if the fractionations among

Figure 31. Plot of δO^{18} vs. δD for biotites and muscovites in igneous and contact metamorphic rocks of the Santa Rosa Range, Birch Creek, and the Eldora area.

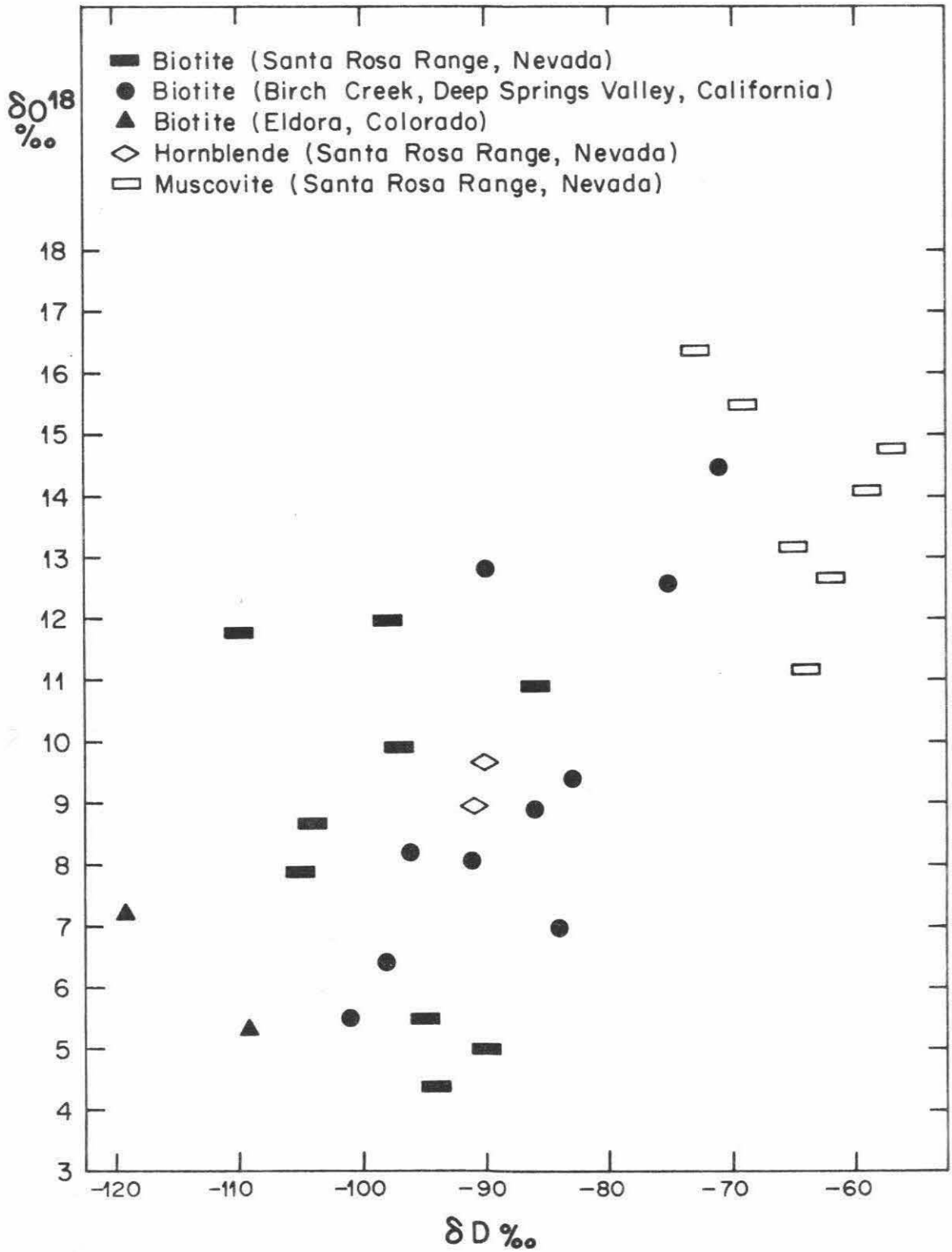
Biotite (Santa Rosa Range, Nevada)
Biotite (Birch Creek, Deep Springs Valley, California)
Biotite (Eldora, Colorado)
Hornblende (Santa Rosa Range, Nevada)
Muscovite (Santa Rosa Range, Nevada)
δO18 ‰
18
17
16
15
14
13
12
11
10
9
8
7
6
5
4
3
-120
-110
-100
-90
-80
-70
-60
δ D ‰

Figure 31

coexisting minerals are internally consistent. One way to test this is by plotting the isotopic fractionations of two coexisting minerals against those of another pair. In Figures 32 to 36 are shown such plots. The data of Taylor and Epstein (1962), Taylor et al. (1963), Garlick and Epstein (1967), and Taylor (1968 b) are also included. The fractionations quartz-muscovite vs. quartz-biotite, feldspar-biotite vs. quartz-biotite, and quartz-biotite vs. quartz-magnetite show good correlations; therefore most of these assemblages must represent approximate isotopic equilibrium. The plot muscovite-biotite vs. quartz-biotite shows a faint correlation. No correction has been made for the An-contents of the plagioclase feldspars, and part of the scatter in Figure 34 is undoubtedly due in part to this effect (see O'Neil and Taylor, 1967). The plot quartz-muscovite vs. andalusite-muscovite shows no correlation (Figure 36). However, judging from other isotopic data and textural evidence, samples SRO-22C, SRO-15B, and SRO-B are more likely to represent mineral assemblages in isotopic equilibrium than are the rest of the samples. A straight line best fitting these three samples also passes through the origin. One might therefore infer that the rest of the samples are non-equilibrium assemblages in which the δ-values of muscovite have become progressively heavier so as to cause isotopic "reversal" in two cases (SRO-19D and SRO-42). The increase in O^{18}/O^{16} ratios of muscovite may be accounted for if the alteration of andalusite to muscovite occurred during the temperature decline, because at lower temperatures the isotopic fractionation between muscovite and water becomes progressively larger. It is also interesting to note that the ratios Δ quartz-muscovite $/\Delta$ quartz-biotite from the present research are consistently smaller than those obtained by Garlick and Epstein (1967) in regional meta-

Figure 32, 33. Plot of oxygen isotopic fractionations Δ quartz-muscovite vs. Δ quartz-biotite and Δ muscovite-biotite vs. Δ quartz-biotite for quartz-muscovite-biotite assemblages from contact metamorphic, regional metamorphic and granitic igneous rocks. Slope A is derived from average values in contact metamorphic and granitic igneous rocks. Slope B is derived from average values in regional metamorphic rocks.

Figure 34. Plot of oxygen isotopic fractionations Δ feldspar-biotite vs. Δ quartz-biotite for quartz-feldspar-biotite assemblages from contact metamorphic, regional metamorphic, granitic plutonic and volcanic rocks. The slope is derived from the average values of all samples.

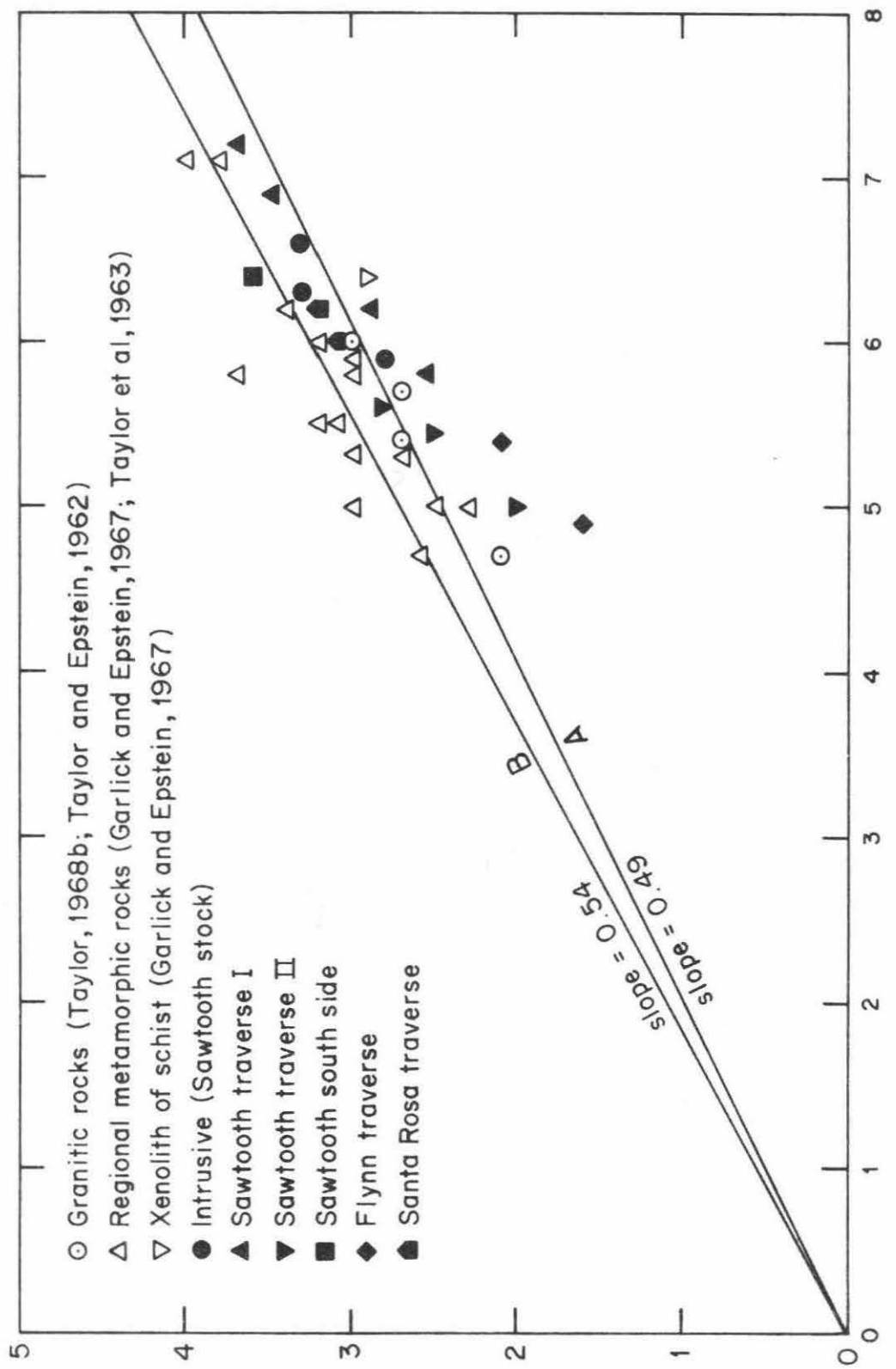
⊙ Granitic rocks (Taylor, 1968b; Taylor and Epstein, 1962)
△ Regional metamorphic rocks (Garlick and Epstein, 1967; Taylor et al, 1963)
▽ Xenolith of schist (Garlick and Epstein, 1967)
● Intrusive (Sawtooth stock)
▲ Sawtooth traverse I
▼ Sawtooth traverse II
■ Sawtooth south side
◆ Flynn traverse
⬟ Santa Rosa traverse
slope = 0.54
slope = 0.49
A
B
Δquartz - muscovite
Δquartz - biotite
0
1
2
3
4
5
6
7
8

Figure 32

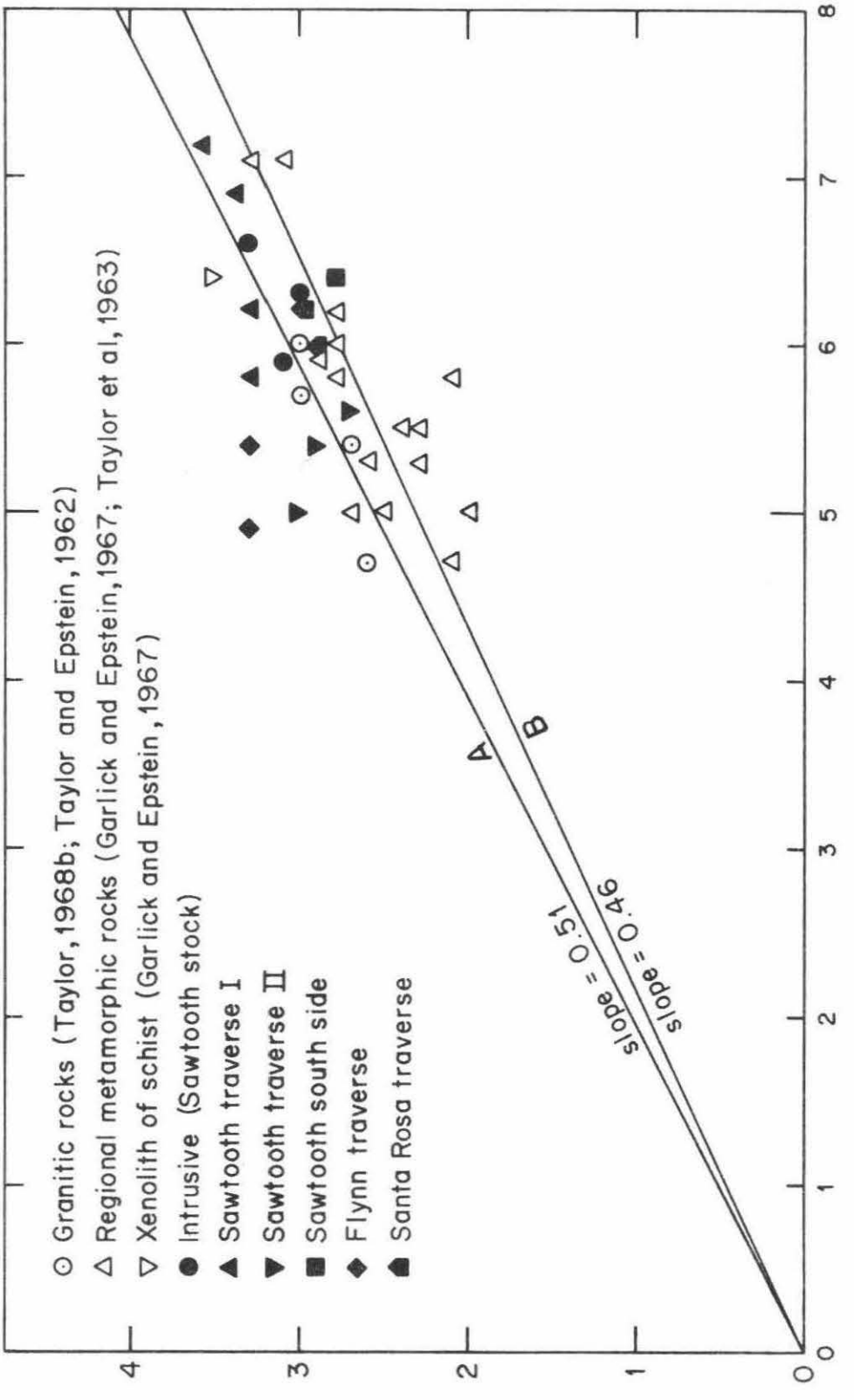
⊙ Granitic rocks (Taylor, 1968b; Taylor and Epstein, 1962)
△ Regional metamorphic rocks (Garlick and Epstein, 1967; Taylor et al, 1963)
▽ Xenolith of schist (Garlick and Epstein, 1967)
● Intrusive (Sawtooth stock)
▲ Sawtooth traverse I
▼ Sawtooth traverse II
■ Sawtooth south side
◆ Flynn traverse
◀ Santa Rosa traverse
A
B
slope = 0.51
slope = 0.46
Δ muscovite - biotite
Δ quartz - biotite
0
1
2
3
4
5
6
7
8

Figure 33

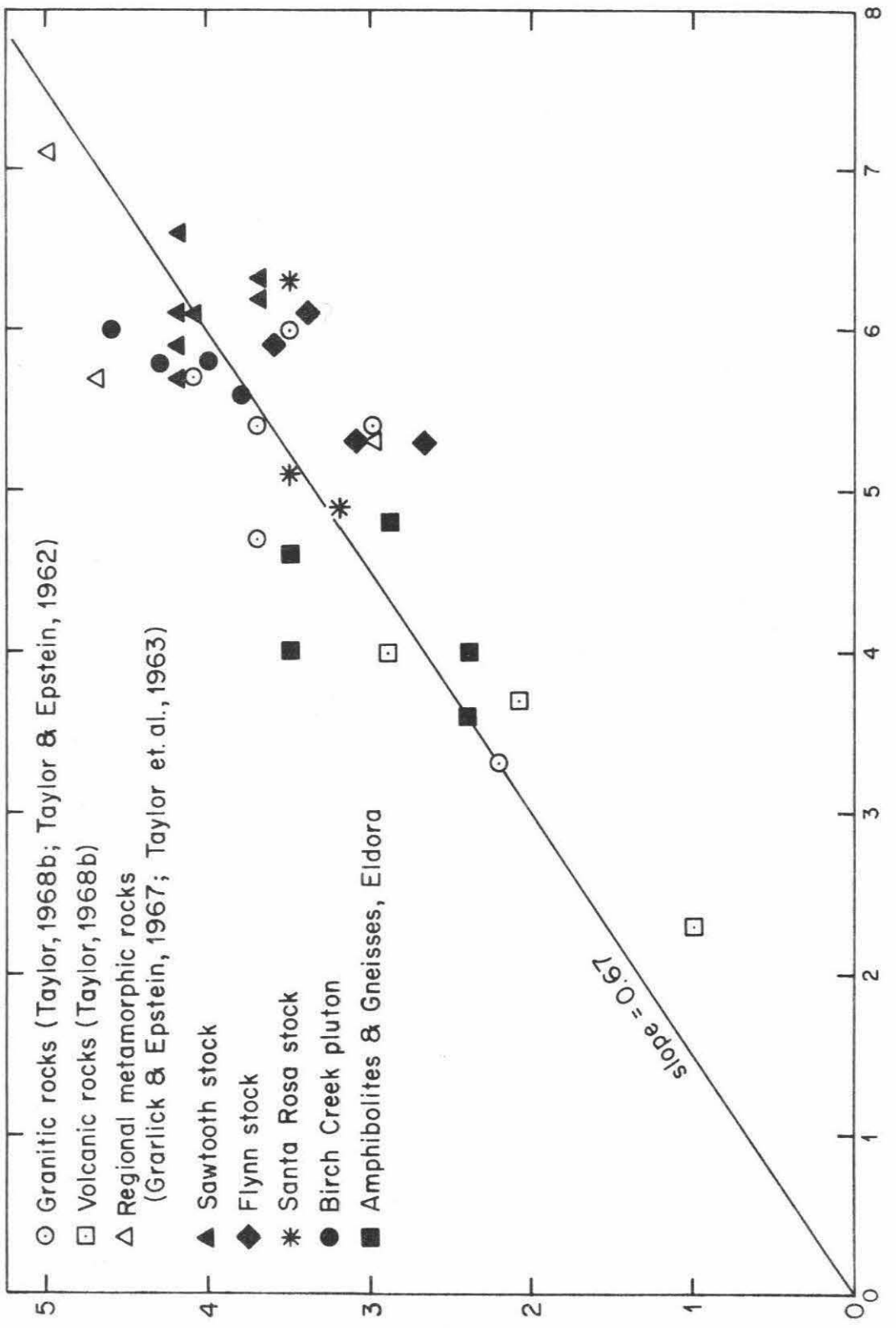
⊙ Granitic rocks (Taylor, 1968b; Taylor & Epstein, 1962)
⊡ Volcanic rocks (Taylor, 1968b)
△ Regional metamorphic rocks (Grarlick & Epstein, 1967; Taylor et. al., 1963)
▲ Sawtooth stock
◆ Flynn stock
✱ Santa Rosa stock
● Birch Creek pluton
■ Amphibolites & Gneisses, Eldora
slope = 0.67
Δfeldspar - biotite
Δquartz - biotite
0
1
2
3
4
5
6
7
8

Figure 34

Figure 35. Plot of oxygen isotopic fractionations Δ quartz-biotite vs. Δ quartz-magnetite for quartz-biotite-magnetite assemblages from contact metamorphic, regional metamorphic, granitic and volcanic rocks. Slope after Taylor (1968 b).

Figure 36. Plot of oxygen isotopic fractionations Δ quartz-muscovite vs. Δ andalusite-muscovite for quartz-andalusite-muscovite assemblages from contact metamorphic rocks. Samples SRO-B, 15B, and 22C are more likely to represent mineral assemblages in isotopic equilibrium than are the rest of the samples. A straight line best fitting these three samples also passes through the origin.

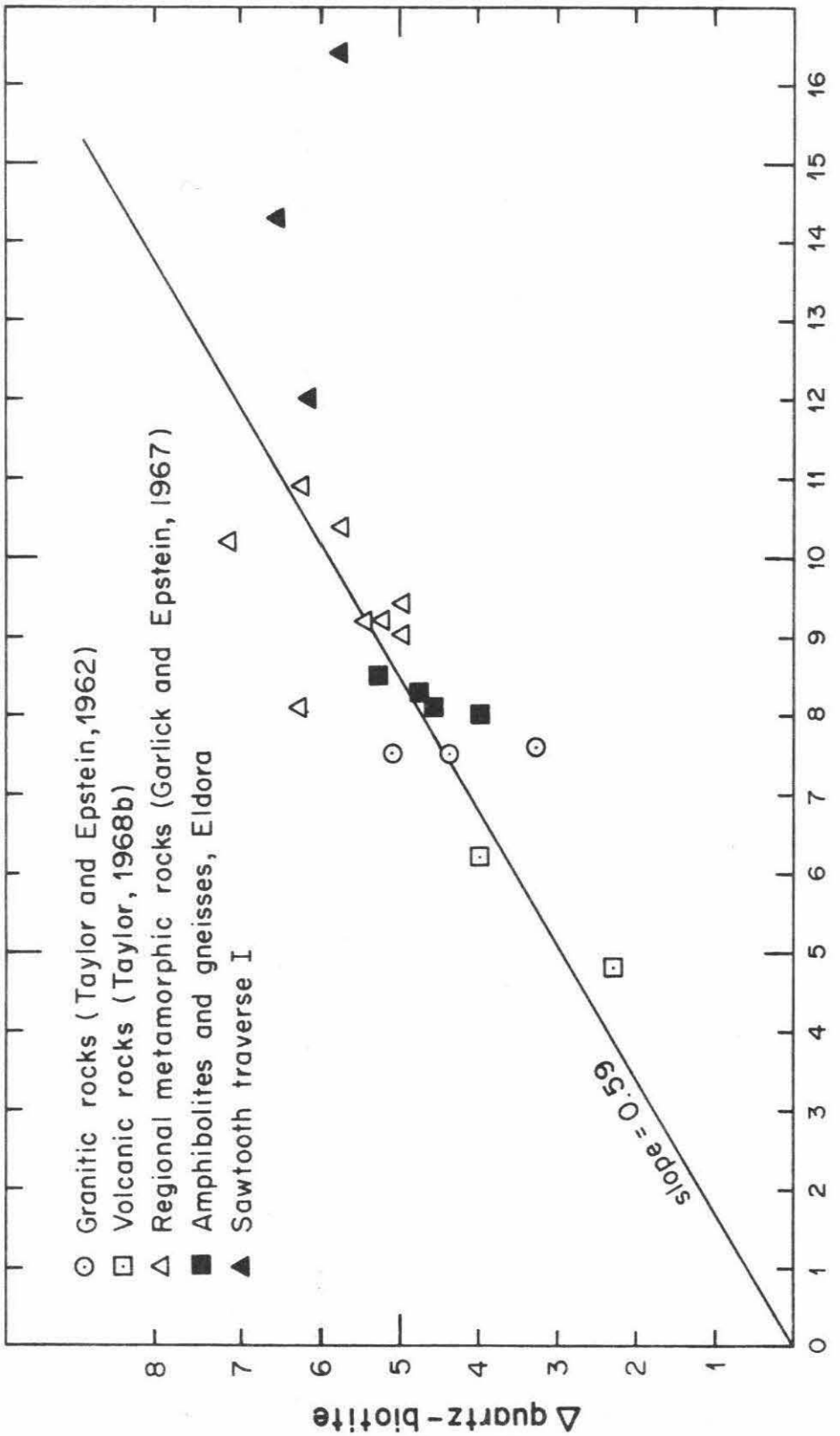
⊙ Granitic rocks (Taylor and Epstein, 1962)
⊡ Volcanic rocks (Taylor, 1968b)
△ Regional metamorphic rocks (Garlick and Epstein, 1967)
■ Amphibolites and gneisses, Eldora
▲ Sawtooth traverse I
slope = 0.59
Δ quartz - biotite
Δ quartz - magnetite
0 1 2 3 4 5 6 7 8 9 10 11 12 13 14 15 16
1 2 3 4 5 6 7 8

Figure 35

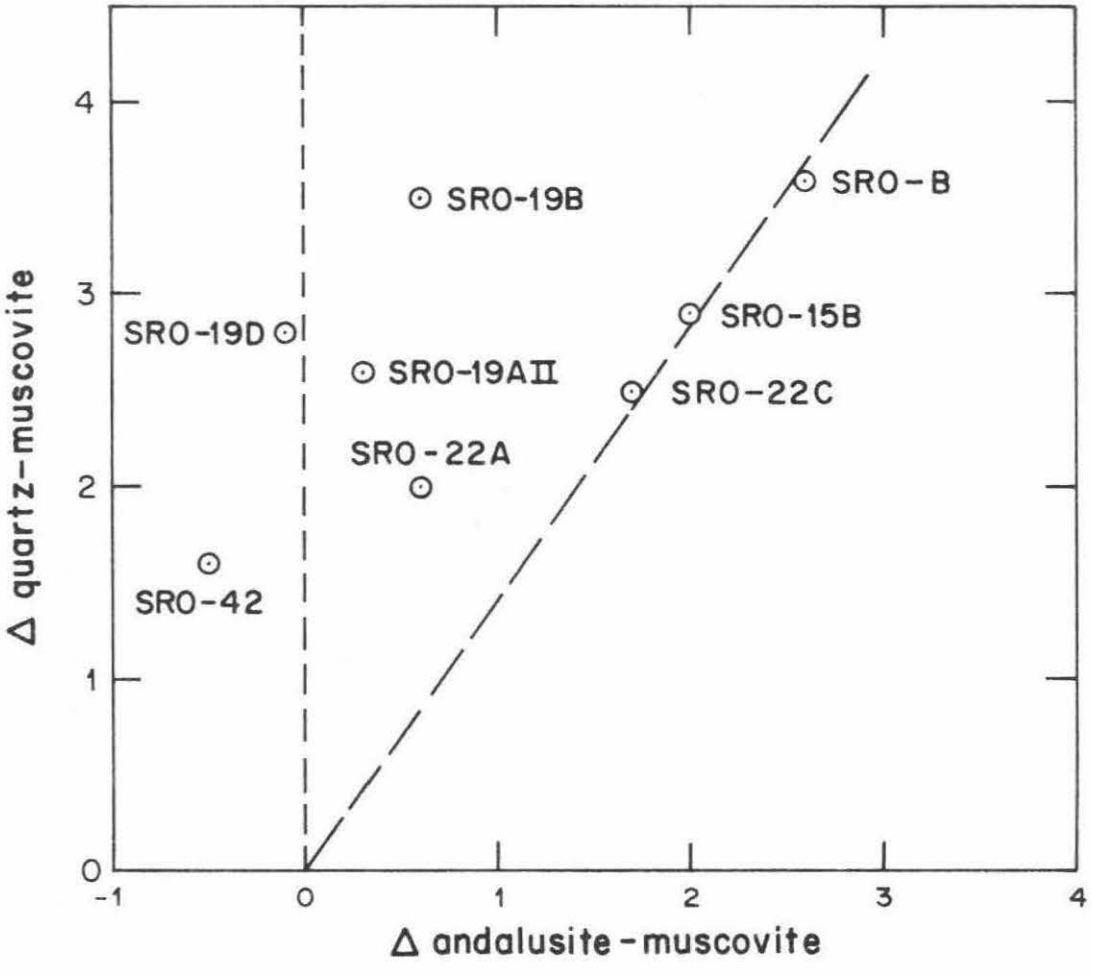
SRO-19B
SRO-B
SRO-15B
SRO-19D
SRO-19AII
SRO-22C
SRO-22A
SRO-42
Δ quartz-muscovite
Δ andalusite-muscovite
0
1
2
3
4
-1

Figure 36

morphic rocks, but almost identical to those reported by Taylor (1968 b), and Taylor and Epstein (1962) in granitic igneous rocks (Figure 32 and Table 12). The lowest ratio (0.45) in the assemblages analyzed by Garlick and Epstein (1967) occurs in a schist xenolith in trondhjemite. The reason for the difference in the ratios is not clear, but an inspection of Figure 33 shows that the discrepancy in part comes from the larger muscovite-biotite fractionations in contact metamorphic and granitic igneous rocks. This would be explained if: (1) The muscovite and biotite in contact metamorphic and granitic igneous rocks continue to re-equilibrate down to somewhat lower temperatures than those in regional metamorphic rocks. (2) In contact metamorphic and granitic igneous rocks, the degree of substitution of OH by F may be more extensive in muscovite than in biotite, or, conversely, in regional metamorphism F may be relatively lower in muscovite. This could produce the observed effects because hydroxyl oxygen is believed to be much more O^{18}-depleted than the SiO_4 tetrahedra oxygen (Taylor and Epstein, 1962).

TABLE 12

Comparison of the ratios of quartz-muscovite and quartz-biotite fractionations in different rock types.

Rock type	Δ quartz-muscovite/ Δ quartz-biotite	Ave. Dev.	No. Samples
Contact metamorphic	0.49	0.03	12 *
Regional metamorphic	0.54	0.03	15**
Granitic igneous	0.48	0.02	4***

* This work, excluding samples SRO-37 and SRO-42 which show evidence of isotopic disequilbrium.

** Garlick and Epstein (1967), excluding the schist xenolith which has a ratio of 0.45.

*** Taylor (1968 b), and Taylor and Epstein (1962).

B. Oxygen and carbon isotopic fractionations between dolomite and calcite

Figure 37 shows a plot of the oxygen vs. carbon isotopic fractionations between coexisting dolomite and calcite; included also are data from regionally metamorphosed marbles analyzed by Sheppard (1966), and Schwarcz (1966). Except for samples BC-32 F and BC-27 F, all other samples, including the two forsterite marbles that show oxygen isotopic "reversal" referred to earlier, fall very close to the line derived by Sheppard (1966) from regional metamorphic marbles. The fairly good correlation between ΔO^{18} and ΔC^{13} of samples from different areas and from different metamorphic rocks is suggestive of an approach to isotopic equilibrium. It is to be noted that in contact metamorphic marbles, neither ΔO^{18} nor ΔC^{13} is correlated well with sample distance from the igneous contact. Except for one very peculiar sample, BC-32 F, the forsterite marbles consistently give the smallest ΔO^{18} and ΔC^{13} values in the Birch Creek area.

C. Oxygen and hydrogen isotopic fractionations between muscovite and biotite

In Figure 38 is shown the plot of oxygen vs. hydrogen isotopic fractionations between coexisting muscovite and biotite from the Sawtooth traverse. Also included are data from regional metamorphic and plutonic granitic rocks analyzed by Garlick and Epstein (1967), and Taylor (unpublished data). There is no

Figure 37. Plot of C^{13} Δ dolomite-calcite vs. O^{18} Δ dolomite-calcite for dolomite-calcite assemblages from contact metamorphic and regional metamorphic marbles. Diagonal line is derived from regional metamorphic marbles (after Sheppard, 1966).

Figure 38. Plot of Δ muscovite-biotite (O^{18}/O^{16}) vs. Δ muscovite-biotite (D/H) for coexisting muscovite and biotite from contact metamorphic, regional metamorphic, and plutonic granitic rocks.

Figure 39. Plot of δ D of biotite vs. Δ muscovite-biotite (D/H) for coexisting muscovite and biotite from the schists and trondhjemites of the Sawtooth stock and contact zone.

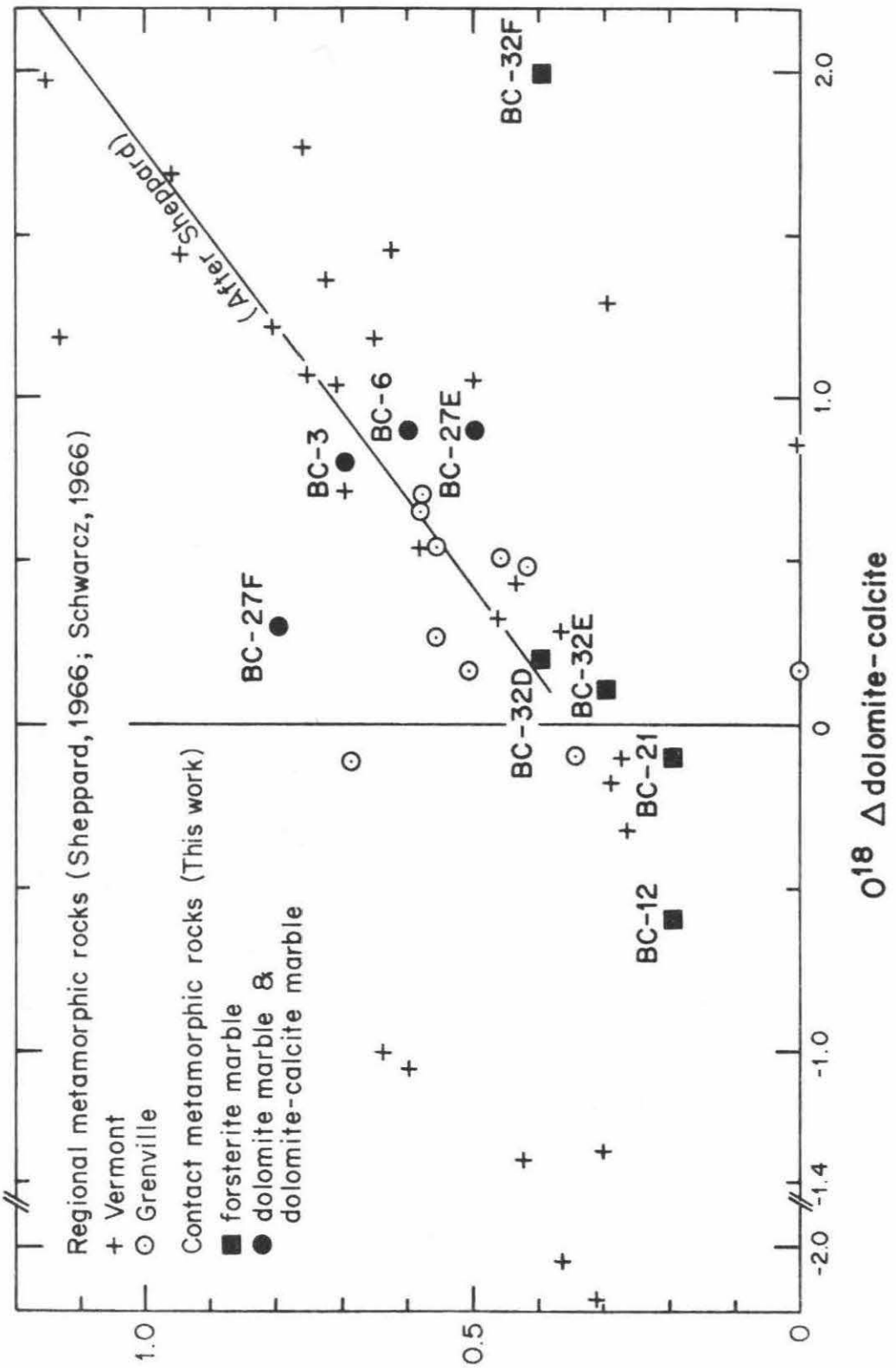
Regional metamorphic rocks (Sheppard, 1966; Schwarcz, 1966)
+ Vermont
⊙ Grenville
Contact metamorphic rocks (This work)
■ forsterite marble
● dolomite marble &
dolomite-calcite marble
(After Sheppard)
BC-27F
BC-3
BC-6
BC-27E
BC-32F
BC-32D
BC-32E
BC-21
BC-12
1.0
0.5
0
-2.0
-1.4
-1.0
0
1.0
2.0
C13 Δdolomite-calcite
O18 Δdolomite-calcite

Figure 37

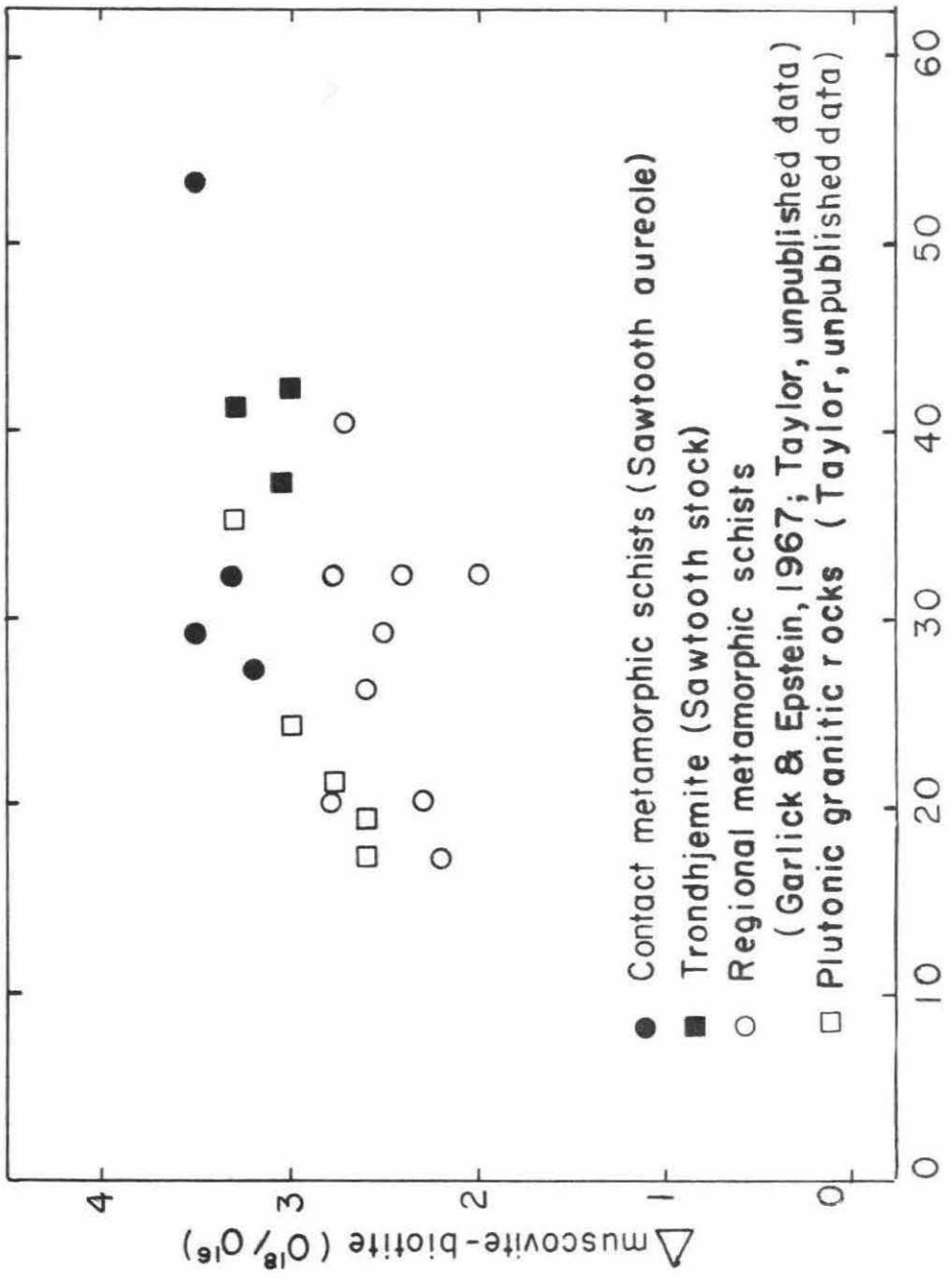
● Contact metamorphic schists (Sawtooth aureole)
■ Trondhjemite (Sawtooth stock)
○ Regional metamorphic schists
(Garlick & Epstein, 1967; Taylor, unpublished data)
□ Plutonic granitic rocks (Taylor, unpublished data)
Δ muscovite-biotite (O18/O16)
Δ muscovite-biotite (D/H)
0
1
2
3
4
0
10
20
30
40
50
60

Figure 38

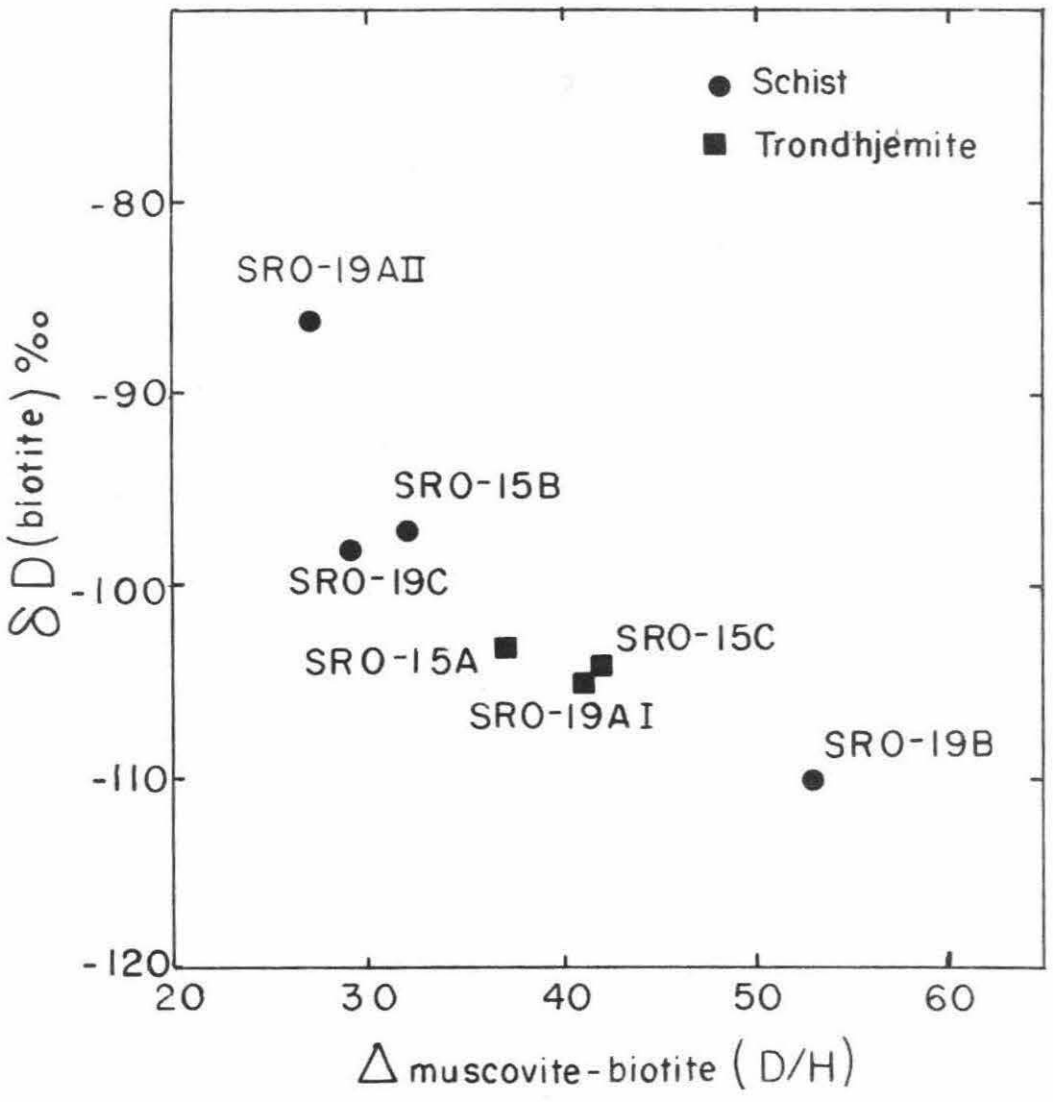
Schist
Trondhjémite
SRO-19AII
SRO-15B
SRO-19C
SRO-15A
SRO-15C
SRO-19AI
SRO-19B
-80
-90
-100
-110
-120
20
30
40
50
60
δ D (biotite) ‰
Δ muscovite-biotite (D/H)

Figure 39

obvious correlation between ΔO^{18} and ΔD, except that both oxygen and hydrogen isotopic fractionations are somewhat larger in the present study. It should be noted that the three intrusive samples and three schist samples plot very near one another, but another schist SRO-19B, which is only 0.5 feet away from SRO-19 AII, has the largest ΔD-value ($\Delta = 53$) yet obtained for a muscovite-biotite pair. Since the muscovites show only a small range of D/H ratios, the variation of ΔD-values is essentially due to the variation in the biotites. In Figure 39, δD of biotite is plotted vs. ΔD muscovite-biotite. The correlation between the two parameters is very good. One may thus speculate that meteoric water may be responsible for the lowering of the D/H ratios of biotite, because the present day surface waters in the surrounding region have D/H ratios from -112 to -165 per mil (see Figure 50, section 6.8); these waters are much more deuterium-depleted than the micas. In addition, during the temperature decline following metamorphism, biotite would become unstable first relative to muscovite. For example, we might expect biotite to alter to chlorite or at least be out of equilibrium with the adjacent pore fluids. This might in part explain why the D/H ratios of biotite are more easily affected by meteoric water than the D/H ratios of muscovite.

6.3 Geothermometry

A. General statement

From the previous section, it was shown that the isotopic behavior of different minerals is in general different. Complete isotopic equilibrium is not commonly attained. As a consequence, extreme caution should be taken

when any isotopic geothermometer is applied to natural mineral pairs. The isotopic temperature is meaningless unless one can demonstrate that the coexisting mineral pair is an equilibrium assemblage with respect to isotopic partitioning. In this section, an attempt will be made to estimate the temperatures of formation of certain mineral assemblages which are most likely to have been formed in isotopic equilibrium. Some simple heat flow calculations will also be considered to gain some insight into the thermal history of the rocks. Finally, the isotopic temperatures are compared with temperatures calculated from heat flow models and from mineral parageneses.

B. Laboratory equilibration curves

Laboratory calibrations of oxygen isotopic fractionations in various mineral-water systems have been done by several workers: calcite-water by Clayton (1961), dolomite-water by Northrop and Clayton (1966), quartz-water and magnetite-water by O'Neil and Clayton (1964), alkali feldspar-water and anorthite-water by O'Neil and Taylor (1967), and muscovite-water by O'Neil and Taylor (1966). Their results are shown in Figure 40. The quartz-water curve in the figure is the revised curve recently done by Clayton et al. (1967). The magnetite-water curve of O'Neil and Clayton (1964) is probably in need of revision, and is therefore not shown in Figure 40.

The experimentally calibrated calcite-CO_2 and dolomite-CO_2 oxygen isotopic fractionation curves by O'Neil and Epstein (1966) are shown in Figure 41.

C. Oxygen isotopic temperatures in contact metamorphic rocks and intrusions

The data presented in Chapter 5 and in section 6.2 indicate that

Figure 40. Oxygen isotope calibration curves experimentally determined for the systems calcite-water (Clayton, 1961), dolomite-water (Northrop and Clayton, 1966), alkali feldspar-water and anorthite-water (O'Neil and Taylor, 1967), muscovite-water (O'Neil and Taylor, 1966), and quartz-water (Clayton et al., 1967).

Figure 41. Oxygen isotope calibration curves experimentally determined for CO_2-calcite and CO_2-dolomite (O'Neil and Epstein, 1966).

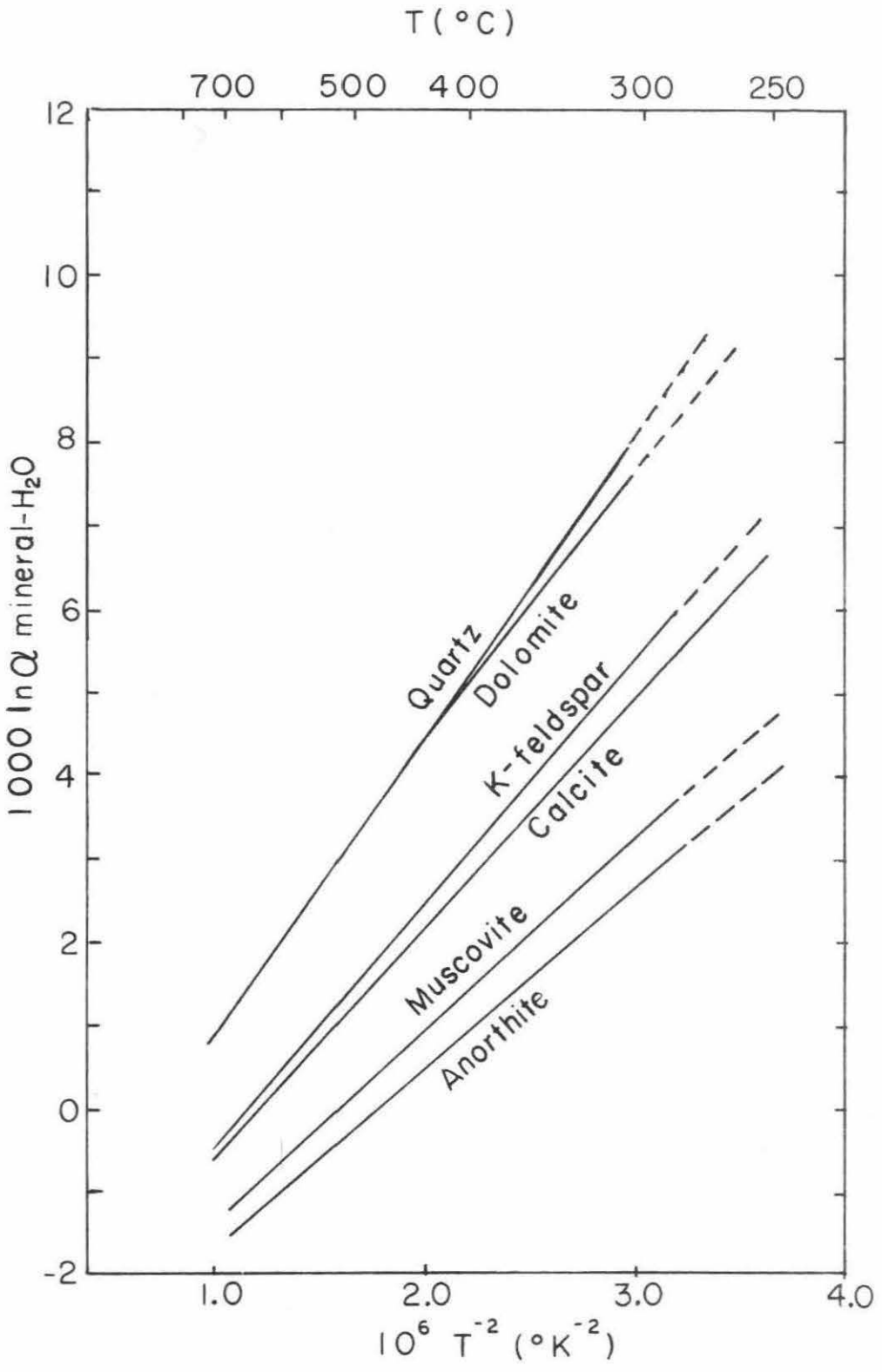
T(°C)
700
500
400
300
250
12
10
8
6
4
2
0
-2
1000 lnα mineral-H2O
Quartz
Dolomite
K-feldspar
Calcite
Muscovite
Anorthite
1.0
2.0
3.0
4.0
10^6 T^-2 (°K^-2)

Figure 40

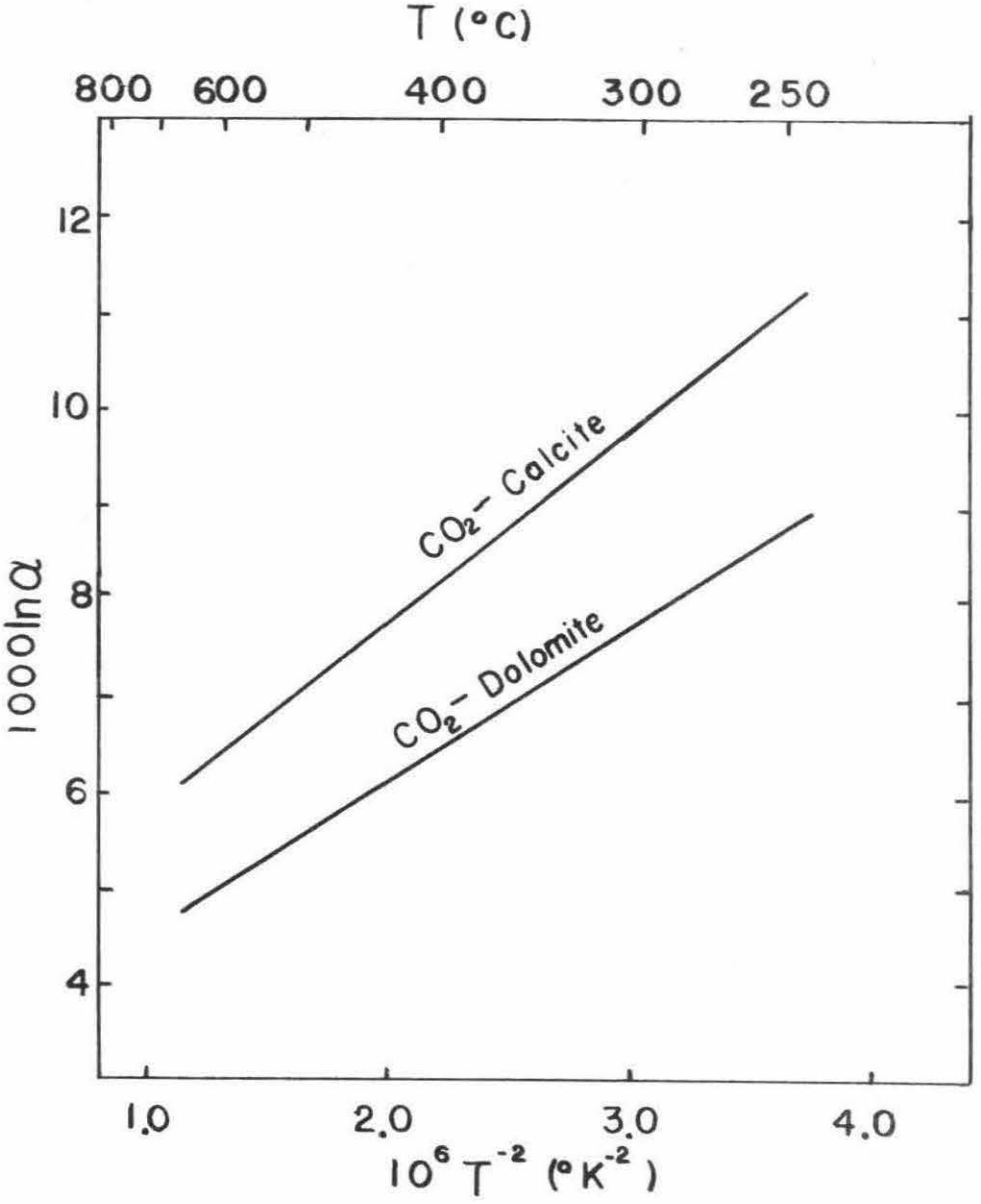
T (°C)
800
600
400
300
250
12
10
8
6
4
1000lnα
CO_2 - Calcite
CO_2 - Dolomite
1.0
2.0
3.0
4.0
$10^6 T^{-2}$ ($°K^{-2}$)

Figure 41

although the isotopic fractionations among coexisting minerals tend to approach equilibrium, complete equilibrium is commonly not attained. The data also show that the isotopic compositions of individual minerals were probably "quenched in " in a complicated way, or some of the minerals exchange their isotopes subsequently, as a correlation between the isotopic fractionations of a coexisting mineral pair and distance from an intrusive contact is only rarely observed in the present study. Perry and Bonnichsen (1966) found that the quartz-magnetite oxygen isotopic fractionations in the metamorphosed Biwabik iron formation varied systematically as a function of distance of the sample from the Duluth gabbro contact; this is the only previous study of oxygen isotope fractionations in a contact aureole. On the basis of the present work, however, it is possible that the lack of an obvious correlation between isotopic fractionations and sample distance from the intrusive contact may be the rule rather than the exception. In order to obtain meaningful isotopic temperatures, it is probably legitimate to consider only those samples which on the basis of other criteria most likely represent isotopic equilibrium.

In the present study, all the country rock samples showing any incomplete isotopic exchange with the intrusive, or vice versa, probably indicate a non-equilibrium situation. In order for such assemblages to represent equilibrium, all the coexisting minerals would have had to undergo isotopic exchange at the same rate and for the same period of time, which seems unlikely. The optimum situation is probably represented by samples collected right at the contact. In these samples, the coexisting minerals usually show 100% isotopic exchange between the country rock and the intrusive, and have attained the same isotopic composition from opposite directions, in the same way that true

equilibrium is demonstrated in the laboratory.

In Table 13 are listed the oxygen isotopic temperatures of various assemblages, together with the isotopic compositions of waters in equilibrium with these assemblages, based on the experimentally determined quartz-muscovite curve. Since quartz-biotite and quartz-magnetite fractionation curves have not yet been determined experimentally, or are in need of revision, tentative curves were derived from natural assemblages. The quartz-biotite curve was derived by assuming 1000 ln α quartz-muscovite = 0.49 x 1000 ln α quartz-biotite (see Figure 32); the quartz-magnetite curve utilized is the one estimated by Taylor and Coleman (1968) from mineral assemblages in regional metamorphic rocks. These curves are shown in Figure 42 together with the experimentally determined quartz-muscovite and quartz-K-feldspar curves. The quartz-magnetite curve derived by Taylor and Coleman (1968) gives temperatures about 50-80°C lower than the quartz-magnetite temperatures of Garlick and Epstein (1967) in the range Δquartz-magnetite = 8 to 11.

The samples in Table 13 are separated into three groups:

Group I - those samples showing complete oxygen isotopic exchange between the intrusive and the country rocks.

Group II. - those showing no evidence of exchange.

Group III - those showing incomplete exchange.

As would be expected, samples in group I show the most reasonable and concordant temperatures. The quartz-mica isotopic contact temperature at Sawtooth stock is about 555°C, at Santa Rosa stock 525°C, and at Birch Creek pluton 540°C. The quartz-magnetite isotopic contact temperature at

Figure 42. Oxygen isotope fractionation curves for quartz-K-feldspar, quartz-muscovite, quartz-biotite, and quartz-magnetite. The quartz-K-feldspar and quartz-muscovite curves are experimentally determined; the quartz-biotite and quartz-magnetite curves are based on data from natural samples. The quartz-magnetite curve is after Taylor and Coleman (1968).

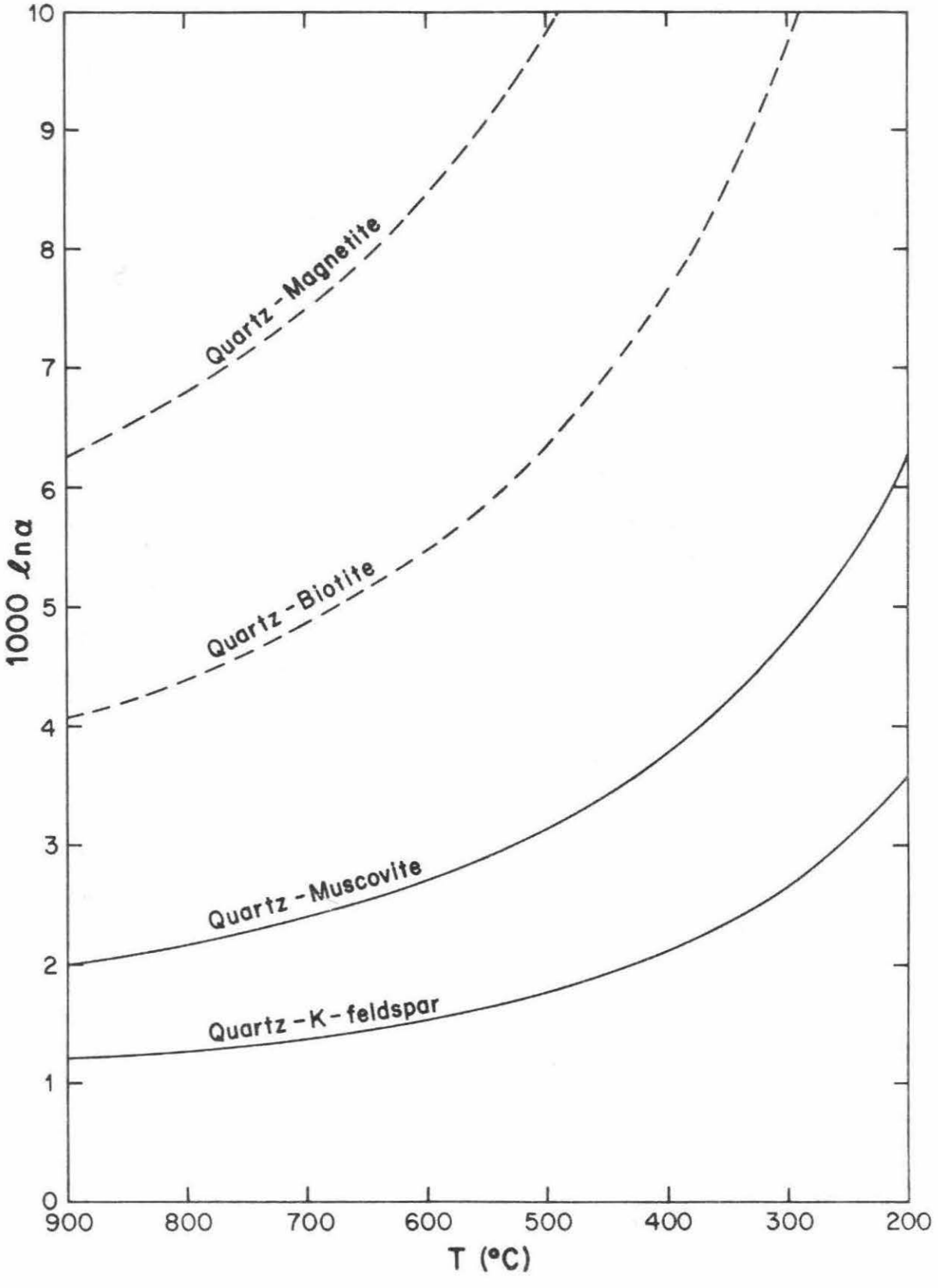
10
9
8
7
6
5
4
3
2
1
0
1000 lna
Quartz - Magnetite
Quartz - Biotite
Quartz - Muscovite
Quartz - K - feldspar
900
800
700
600
500
400
300
200
T (°C)

Figure 42

Caribou stock is 625°C, but the quartz-biotite temperature of 750°C is probably too high. The size of the intrusives does not seem to appreciably affect the isotopic contact temperatures. Two samples collected from a xenolith at the margin of the pluton in Birch Creek give quartz-biotite temperatures of 560 and 590°C, being 20 to 50°C higher than the main contact temperature. This is reasonable because a xenolith enclosed in the magma should in general have a higher temperature than the intrusive contact.

Many of the samples in group II could also be expected to have equilibrium isotopic fractionations, because similar samples usually give similar quartz-mica isotopic temperatures and these temperatures are geologically reasonable. Examples are: the trondhjemites in the Sawtooth stock average at 535°C, the granodiorites in the Flynn stock 560°C, the granodiorite in the margin of the Santa Rosa stock 505°C, the adamellites in the central portion of the Santa Rosa stock 680°C, the quartz-monzonite in the Eldora stock 670°C, and the granite in the pluton of Birch Creek 570°C. The country rock temperatures are rather uniform from 1 foot to 70 feet: at Birch Creek 500 to 515°C and at Sawtooth 425 to 445°C. The temperatures at the Sawtooth appear to be abnormally low in comparison with the contact temperatures (see discussion in section 6.3-E). The schists and gneisses in the Caribou and Eldora traverses give rather high quartz-biotite temperatures (630 to 710°C) for samples 1000 feet away from the contact, but the quartz-magnetite temperatures (595 to 615°C) seem more reasonable, as these conceivably could represent the original regional metamorphic temperatures.

Group III consists of samples with incomplete isotopic exchange.

TABLE 13

Oxygen isotope temperatures of formation of mineral pairs in the intrusions and contact metamorphic aureoles compared with heat flow temperatures and the oxygen isotopic compositions of waters in equilibrium with the mineral pairs.

Group I: Samples showing complete isotopic exchange between intrusive and country rock

Sample No.	Rock	Distance from contact, feet	Isotopic temperature °C			Heat flow temperature °C	δH_2O *
			Q-Mu	Q-B	Q-Mt		
Sawtooth							
SRO-15A	Trondhjemite	0.04	570	545			13.6
SRO-15B	Schist	0.08	550	520		550	13.5
SRO-22D	Gneiss	0.17	570	580		550	9.7
Santa Rosa							
SRO-29A	Hornfels	0.08	510	535		650	11.5
Birch Creek							
BC-27AII	Schist	0.25		545		550	11.4
BC-28A	Schist	0.25		535		550	11.5
BC-22	Xenolith	5		560		>550	10.6
BC-23	Xenolith	1		590		>550	10.6

TABLE 13 (continued)

Sample No.	Rock	Distance from contact, feet	Isotopic temperature °C Q-Mu	Q-B	Q-Mt	Heat flow temperature °C	δH_2O*
Caribou							
HES-4b	Gneiss	0.04		750	625	650	9.5

Group II: Samples showing no evidence of isotopic exchange between intrusive and country rock

Sample No.	Rock	Distance from contact, feet	Isotopic temperature °C Q-Mu	Q-B	Q-Mt	Heat flow temperature °C	δH_2O*
Sawtooth							
SRO-19B	Schist	1	440	450		550**	14.4
SRO-19C	Schist	50	420	430		535**	14.5
SRO-22E	Trondhjemite	1.5		570			9.0
SRO-22F	Trondhjemite	50		530			8.6
SRO-18	Trondhjemite	50		515	390		8.8
SRO-A	Trondhjemite	500		525			8.6
Flynn							
SRO-37	Hornfels	45	830	630		640	15.6
SRO-38	Granodiorite	35		550			7.9
SRO-39	Granodiorite	75		570			8.4

TABLE 13 (continued)

Sample No.	Rock	Distance from contact, feet	Isotopic temperature °C Q-Mu	Q-B	Q-Mt	Heat flow temperature °C	δH_2O *
Santa Rosa							
SRO-29F	Granodiorite	150		505			10.0
13-85-8	Adamellite	5000		695			8.4
13-85-7a	Adamellite	9000		660			8.2
Eldora and Caribou							
EL-2	Gneiss	2		940	645	650	11.0
N-2	Amphibolite	2		750	635	650	9.8
C4B	Gneiss	950		630	595	480	10.5
HES-1	Schist	1300		710	615	450	11.9
EL-I	Q Monzonite	50		660			8.6
N-3	Q Monzonite	450		680			8.7
Birch Creek							
BC-27B	Schist	2		460		550	15.6
BC-28C	Schist	6		515		548	16.3
BC-28E	Schist	13		505		546	16.0
BC-7	Schist	70		500		530	16.8

TABLE 13 (continued)

Sample No.	Rock	Distance from contact, feet	Isotopic temperatures °C Q-Mu	Q-B	Q-Mt	Heat flow temperature °C	δH_2O*
BC-16	Schist	1300		460			12.3
BC-15	Schist	2000		535			11.9
BC-14	Schist	2100		535			12.1
BC-28B	Sill	2.5		535			10.3
BC-27G	Granite	4.5		560			9.8
BC-28J	Granite	60		580			9.0
BC-1	Granodiorite				595		8.5

Group III: Samples showing incomplete isotopic exchange between intrusive and country rock

Sample No.	Rock	Distance from contact, feet	Isotopic temperatures °C Q-Mu	Q-B	Q-Mt	Heat flow temperature °C	δH_2O*
Santa Rosa Range							
SRO-15C	Trondhjemite	0.17	470	505			12.2
SRO-19AI	Trondhjemite	0.5	470	475	315		10.7
SRO-19AII	Schist	0.5	630	560	265	550 **	15.0
SRO-19D	Porphyro-phyllite	600	570			445 **	16.9

TABLE 13 (continued)

Sample No.	Rock	Distance from contact, feet	Isotopic temperatures °C Q-Mu	Q-B	Q-Mt	Heat flow temperature °C	δH_2O*
SRO-22C	Schist	5	665	610		549	13.7
SRO-22A	Schist	85	900	680		527	15.7
SRO-D	Pegmatite		830				17.6
SRO-3A-1	Granodiorite	0.5		630			12.8
SRO-42	Hornfels	200	>1000	700		610	16.0
SRO-29D	Hornfels	2	490	505		650	13.4
Birch Creek							
BC-27C	Schist	4		505		549	14.6
Caribou							
HES-4c	Gneiss	0.6		940	810	650	10.4

Q = Quartz, Mu = Muscovite, B= Biotite, Mt = Magnetite.

* Isotopic compositions of waters based on quartz-muscovite temperature, or if no muscovite in the assemblage, based on quartz-biotite temperature.

** Based on heat flow model E, see section 6.3-E for discussion.

Most of these probably represent non-equilibrium situations. The indicated isotopic temperatures show a large scatter and are probably meaningless.

D. Temperatures calculated from heat flow models

The temperature distribution in the neighborhood of an intrusive-country rock contact is governed by (1) the temperature of intrusion, (2) the temperature range of solidification of magma, (3) the thermal properties of intrusion and country rock, (4) the latent heat of solidification, (5) the extent of convection in the magma, (6) the heat of metamorphic reactions in the country rocks (including heat of vaporization of pore-water), and (7) amount of heat carried away by material transport or by radiation.

If all the factors mentioned above are considered together, the heat flow problem would become an extremely complex one. Fortunately, some of the above factors may be eliminated or simplified in the calculation for the reasons mentioned below:

Factor (2) may be simplified to a definite melting point at the liquidus temperature, because Jaeger (1957) found that the width of the range of solidification is not important to the contact temperature or to the temperatures outside the intrusion.

For factor (5) one may take the extreme case by keeping the whole of the magma well stirred so that its temperature is uniform over its volume until solidification is completed. This will give an upper limit of contact temperature and an over-estimate of temperatures in the country rock near the contact.

Factor (7) may be neglected because the isotopic data do not

allow any appreciable massive movement of aqueous fluids from the intrusive into the country rock because of the very steep oxygen isotopic gradient (3 per mil per foot) preserved near the contact (see section 6.4). Also, radiation is probably not important in a deep-buried body at the temperature of interest.

In factor (6), if the metamorphic reaction is exothermic, the country rock temperatures would be higher; if it is endothermic, the temperature would be lower. The vaporization of pore-water would also lower the temperature, but Jaeger (1959) has shown that the lowering of contact temperatures is not important for moderate to low values of rock porosity. Most of the rocks studied in this research probably have low porosities because of the antecedent regional metamorphism and depth of burial. For simplicity, factor (6) will not be considered in the calculations.

Even with the simplifications as stated above, the heat flow problem still remains a very complex one and can only be solved by a numerical method (Jaeger, 1957; 1959).

Since we are particularly interested in the contact temperatures, because of our greater confidence in the oxygen isotopic geothermometers in these regions, the various contact "temperatures" based on different heat flow models are listed in Table 14 (Jaeger, 1959).

In the Sawtooth stock, the trondhjemite magma probably intruded below 750°C, and in the Santa Rosa and Flynn stocks the initial magma temperatures were probably close to 900°C (Compton, 1960). The thermal properties of granite and shale give a value for σ around 2 (Lovering, 1936), but for a phyllite-granite contact, the σ-value is probably less than 2. If we

TABLE 14

Initial contact temperatures of an infinite dike based on different heat flow models

Heat flow model	Contact temperature °C	
	Magma = 700	Magma = 900
1. Equal thermal properties of country rock and intrusive, no latent heat of crystallization ($\sigma = 1$, $L = 0$).	400	500
2. Equal thermal properties of country rock and intrusive, with latent heat of crystallization ($\sigma = 1$, $L = 100$).	504	614
3. Equal thermal properties of country rock and intrusive, latent heat accounted for by exaggerating the magma temperature ($\triangle T = L/C = 300^{\circ}C$, $\sigma = 1$)	550	650
4. Same as model 1, except different σ ($\sigma = 2$, $L = 0$)	500	633
5. Same as model 2, except different σ ($\sigma = 2$, $L = 100$)	610	760
6. Convection (extreme case)	700	900

Initial country rock temperature = 100°C, $C_1 = C_2 = 0.25$ cal/gm°C

L = latent heat (cal/gm) $\quad \sigma = \left(\frac{K_2 \rho_2 C_2}{K_1 \rho_1 C_1} \right)^{1/2}$

K = thermal conductivity, ρ = density, C = specific heat, subscript 1 referred to country rock, 2 referred to solidified magma.

assume the magma intruded at 700°C where the country rock was 100°C, the contact temperatures in Table 14 range from 700° to 400°C, according to different heat flow models. Model 1 assumes no latent heat; therefore it would give too low a temperature. Model 6 assumes the extreme case of convection; this would give too high a temperature. If the above two cases are disregarded, then the most probable initial contact temperature would lie somewhere between 500 and 610°C. If one assumes the magma temperature to be 900°C, the initial contact temperature probably would lie between 610 and 750°C, depending on the different kinds of heat flow models used. Since model 3, in which the latent heat is accounted for by exaggeration of the intrusion temperature, is mathematically very simple and gives a contact temperature almost in the middle of the most probable temperature range, it is the model utilized to construct the thermal history of the country rock. This is shown in Figure 1 of section 2.4, and in Figures 43 and 44.

Figure 43 shows two graphs containing various temperature vs. time curves. Model E was constructed by assuming an infinite cylinder of square cross section 8000 x 8000 feet, with initial intrusive temperature 700°C, country rock temperature 100°C, thermal diffusivity 0.009 cm^2/sec and an exaggeration of the intrusive temperature by 300°C to account for the latent heat of solidification. The model should be closely analogous to the conditions of intrusion of the Sawtooth stock. The heat contribution from the nearby Santa Rosa stock was also taken into account by assuming another parallel infinite cylinder of dimensions 20,000 feet x 20,000 feet and magma temperature 900°C located 15,000 feet away. Model D was constructed similar

Figure 43. Temperature vs. time curves for various infinite cylinder heat flow models, assuming initial country rock temperature = 100°C and diffusivity = 0.009 cm^2/sec. Latent heat of solidification accounted for by exaggeration of intrusive temperature by 300°C. Model D is constructed analogous to the conditions of intrusion of the Flynn stock, and model E of the Sawtooth stock.

Figure 44. Maximum temperature vs. distance curves for various heat flow models constructed in Figure 1 and Figure 43.

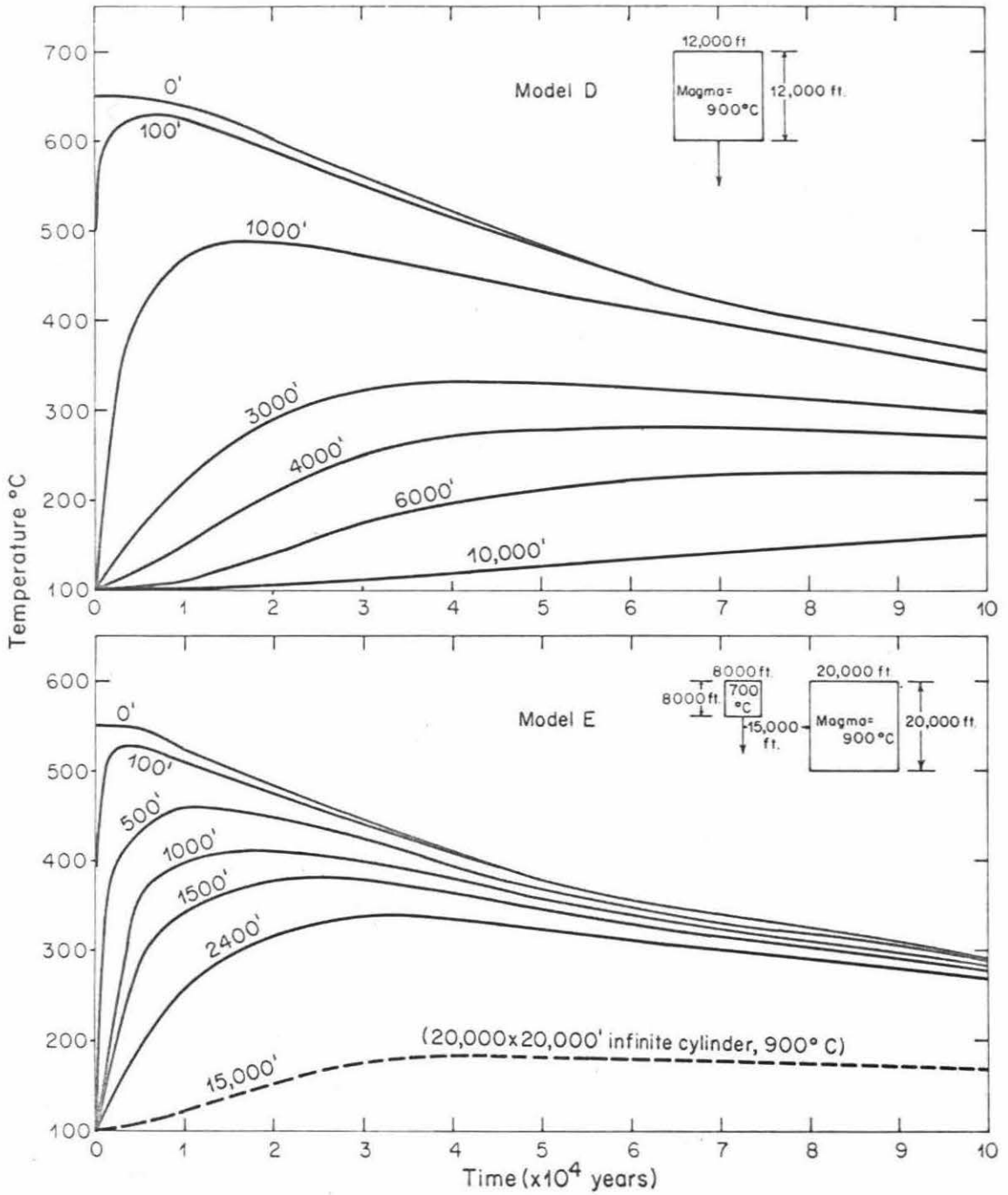
Model D
12,000 ft
Magma = 900°C
12,000 ft.
0'
100'
1000'
3000'
4000'
6000'
10,000'
Model E
8000 ft.
8000 ft.
700 °C
15,000 ft.
20,000 ft.
Magma = 900 °C
20,000 ft.
0'
100'
500'
1000'
1500'
2400'
15,000'
(20,000x20,000' infinite cylinder, 900° C)
Temperature °C
Time (x10⁴ years)

Figure 43

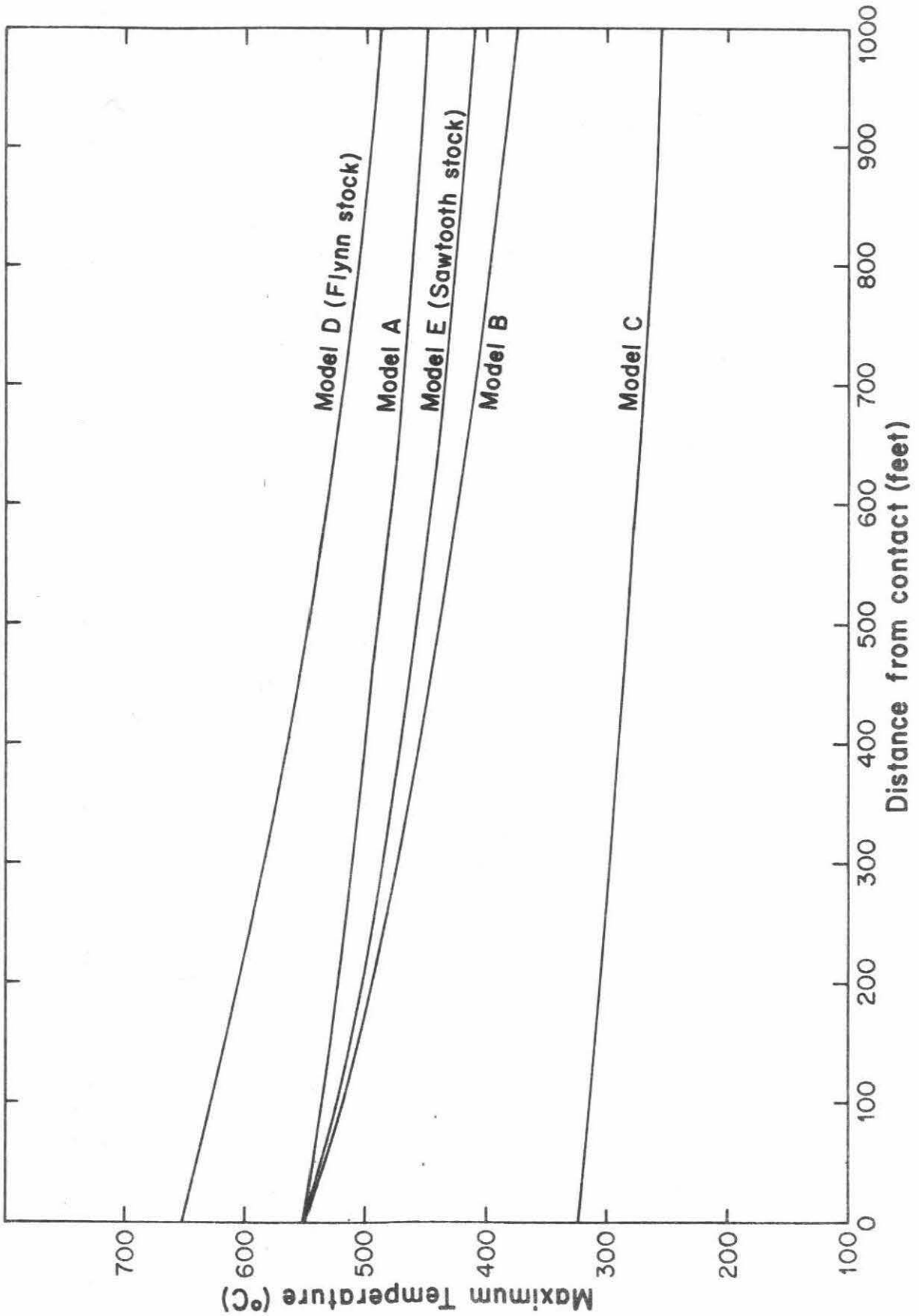
Model D (Flynn stock)
Model A
Model E (Sawtooth stock)
Model B
Model C
Maximum Temperature (°C)
Distance from contact (feet)
100
200
300
400
500
600
700
0
100
200
300
400
500
600
700
800
900
1000

Figure 44

to model B in section 2.4 except of different dimensions (12,000 x 12,000 feet) and of different intrusive temperature (900°C). The model should be analogous to the conditions of intrusion of the Flynn stock. All the above infinite cylinder models are based upon a square cross section instead of the perhaps more realistic circular or elliptic cross section, only because the numerical calculations are much simpler in the former case. Also, the isotherms tend to smooth out near a corner, such that after a short period of time the isotherms in a square cross-section model closely approach the case of a circular cross section (see Jaeger, 1961).

Figure 44 is a plot of maximum temperature vs. distance for models D and E, together with models A, B, and C constructed in section 2.4. It should be noted that regardless of what model is used, the maximum temperature attained at a distance 100 feet away from the contact is no more than 30°C lower than the initial contact temperature, and the maximum temperature attained at a distance 1000 feet away from the contact is no more than 175°C lower than the initial contact temperature. To take a specific case, model E, constructed in analogue to the Sawtooth stock (Figure 43), indicates that the maximum temperature attained at the contact is 550°C, at 100 feet 530°C, and at 1000 feet 410°C. The contact sample will remain above 540°C for 7000 years; the 100-foot sample will remain above 520°C for 5000 years; and the 1000-foot sample will remain above 400°C for 20,000 years. The outer limit of the Sawtooth metamorphic aureole (~1500 feet) will attain a maximum temperature of 380°C, and that of Flynn aureole (~3000 feet) will be 340°C. These seem to be "reasonable" temperatures for the beginning of metamorphic reactions in

the lowest-grade rocks in the Santa Rosa Range, because the experimentally investigated reaction

$$\text{Pyrophyllite} = \text{andalusite} + \text{quartz} + H_2O$$

at $P H_2O$ = 1 Kb occurs at about 380°C (Kerrick, 1966 , quoted by Turner, 1968, p. 256).

E. Comparison of oxygen isotopic temperatures with heat flow calculations and with mineral parageneses

The oxygen isotopic temperatures and the temperatures calculated from heat flow models for a variety of samples are given in Table 13.

The oxygen isotopic temperatures at the contacts of the Sawtooth and Birch Creek plutons are very similar: 555 and 540°C, respectively. These temperatures are quite close to those calculated from heat flow models 2, 3, 4,and 5 in Table 14, assuming an initial magma temperature of 700°C and country rock temperature of 100°C. The quartz-magnetite temperature of 625°C at the contact of the Caribou stock is also very close to the heat flow temperatures calculated from models 2, 3, and 4, assuming an initial intrusive temperature of 900°C and country rock temperature of 100°C.

The central part of the Santa Rosa stock exhibits quartz-biotite temperatures of 660 to 695°C. These data, in conjunction with the heat flow models, suggest that the isotopic contact temperature of the Santa Rosa stock (525°C), is abnormally low, but this might reflect the peculiar geometry of the intrusive at this locality, similar to the situation at Sawtooth traverse I as discussed below.

The isotopic temperatures in the marginal zones of all the intrusions except the Birch Creek pluton are lower than the isotopic contact temperatures.

For example, the quartz-biotite isotopic temperature difference between the marginal intrusive and the contact is about 80°C at the Eldora and Caribou stocks, about 15°C at the Sawtooth stock, and about 30°C at the Santa Rosa stock; the Birch Creek contact temperature, on the other hand, is about 30°C lower than in the marginal intrusive. It is thus possible that the oxygen isotopic fractionations might be "quenched in" not far below the temperature maximum at the various contacts, but might continue to re-equilibrate in the marginal portions of the intrusions until a lower temperature is reached. Kennedy (1955) has suggested that the marginal portions of the magma could have crystallized at much lower temperature than the central portion because of the higher water pressure in the margins. As will be discussed later (sections 6.4-C and 6.6), the migration of water from the country rocks into the intrusive might be significant in certain stocks.

The oxygen isotopic temperatures of SRO-19B and SRO-19C, two schist samples collected 1 foot and 50 feet, respectively, away from the contact of the Sawtooth stock, are far too low compared with that of SRO-15B, a schist sample collected 0.08 feet away from the contact. SRO-19B gives a temperature of 445°C and SRO-19C of 425°C, about 90° to 110°C lower than the temperature of SRO-15B. Such a steep temperature gradient is not compatible with any of the heat flow models. Why the oxygen isotopes of the above two samples were "quenched" at such low temperatures is not completely understood. However, because the intrusive at this locality forms a narrow wedge projecting into the country rock, the temperatures in the country rock should be considerably lower than the temperatures in the case of a plane

contact. A more realistic model (F) may be constructed by placing two additional infinite cylinders of square cross sections 500 x 500 feet and 50 x 50 feet side by side at the surface of the 8000 x 8000 foot cylinder of the original model E, as illustrated in Figure 44A. The temperature vs. time curves in the 1-foot and 50-foot samples can then be calculated by superimposing temperatures obtained from Model E and the two additional cylinders. As may be seen in Figure 44A, the 1-foot sample attains a maximum temperature of 510°C, but it stays above 500°C for only 2 months; it cools below 400°C and then gradually rises to a maximum of 460°C and remains above 450°C for about 12,000 years. The 50-foot sample reaches a maximum temperature of 455°C, and remains above 450°C for about 9000 years. These temperatures are in much better agreement with the quartz-mica isotopic temperatures (see footnote in Table 13).

The geometry of the intrusive in the Santa Rosa traverse also closely resembles that of Model F (see Figure 13); the abnormally low oxygen isotopic temperatures in the country rock (0.08-foot sample 525°C and 2-foot sample 500°C) may also be explained in terms of a heat flow model similar to Model F.

In Birch Creek, three schist samples collected 6 to 70 feet away from the intrusive contact give quartz-biotite isotopic temperatures from 500 to 515°C. These are 20 to 35°C lower than the temperature obtained from BC-28A (0.25 feet from contact). The isotopic temperature gradient in this case is 35°C/70 feet; this is in good agreement with a heat flow temperature gradient of 20°C/70 feet, based on the cooling of a magma body (initial temperature = 700°C) in the shape of an infinite cylinder of square cross section 8000 x 8000 feet with plane contact. The geometry of the latter cylinder

Figure 44A. Temperature vs. time curves for heat flow model F. The model is constructed by placing two additional infinite cylinders of square cross sections 500 x 500 feet and 50 x 50 feet side by side at the surface of the 8000 x 8000 foot cylinder of model E. Solid lines: cooling curves for 1-foot and 50-foot samples in model F. Dashed lines: cooling curves for 1-foot and 50-foot samples in model E. The maximum temperatures for the 1-foot and 50-foot samples are about 80 to 90°C lower in model F than in model E. Note that there are two maximum temperatures for the 1-foot sample in model F (510°C and 460°C), but the first maximum lasts for only a short time (the sample remains above 500°C for only 2 months). Model F closely resembles the intrusive geometry at the localities represented by Sawtooth traverse I and the Santa Rosa traverse (see Figures 4 and 13), and may explain the abnormally low country-rock isotopic temperatures near both contacts.

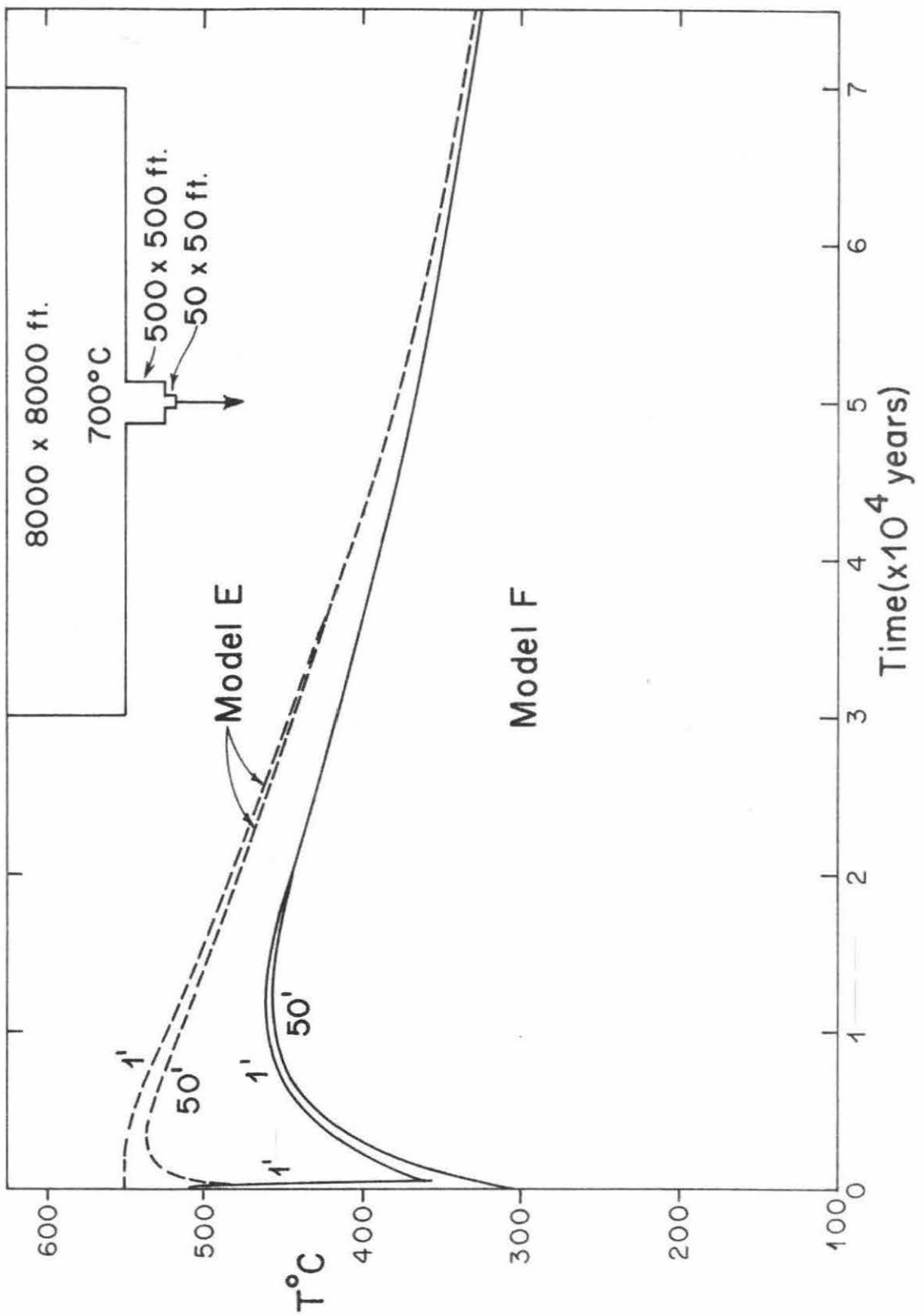
8000 x 8000 ft.
700°C
500 x 500 ft.
50 x 50 ft.
Model E
Model F
1'
50'
1'
50'
1'
T°C
600
500
400
300
200
100
0
1
2
3
4
5
6
7
Time(x10^4 years)

Figure 44A

is similar to that of the southern tip of the composite pluton in Birch Creek (see McKee and Nash, 1967, Figure 2).

It was observed by Compton (1960) and by the present writer that in the innermost part of the Flynn and Santa Rosa aureoles K-feldspar has formed from muscovite and biotite, and sillimanite has apparently formed by breakdown of both andalusite and micas. In the Sawtooth aureole no K-feldspar has been found, but sillimanite has formed at the contact from some biotite and andalusite grains. Using the experimentally determined muscovite plus quartz breakdown curve (Evans, 1965), and the Al_2SiO_5 polymorphic transition curves (Weill, 1966; Fyfe and Turner, 1966; Richardson et al. 1967), and assuming that P_{H_2O} is approximately equal to P_{TOTAL}, it can be determined that the temperature near the contacts of the Flynn and Santa Rosa stocks was probably between 550 and 600°C, and the water pressure was between 1000 and 1500 bars (see Turner, 1968,p. 248-252). These mineralogical " temperatures" are in good agreement with temperatures derived from oxygen isotopic geothermometers and from heat flow models. The P_{TOTAL} also agrees with the independent estimate of 1 to 2 Kb by Compton (1960) based on geological evidence. Inasmuch as no K-feldspar has been found in the Sawtooth aureole, and sillimanite has formed from andalusite, it is inferred that either the temperature was lower or P_{H_2O} somewhat higher in the Sawtooth aureole than in the Flynn and Santa Rosa aureole.

6.4 Extent of isotopic exchange and dimensions of the isotopic equilibrium system

A. General statement

Studies of the variations of oxygen isotopes in the contact zone offer an excellent opportunity to investigate the extent and possibly the mechanism of isotopic exchange between the intrusive and the country rock, because the oxygen isotopic compositions of the igneous rocks and minerals are quite different from those of the sedimentary and low-grade regional metamorphic rocks and minerals. There is always a tendency for different isotopes to undergo exchange in the presence of an isotopic compositional gradient. Isotopic equilibrium is established in a system only if the isotopic compositions of a particular mineral are equal everywhere in that system, provided that system is everywhere at a constant temperature.

Carbon and hydrogen isotopes were studied to a lesser extent in the present research. Insufficient data prevent us from drawing any definite conclusions concerning the size of the equilibrium systems for these isotopes.

Three types of oxygen isotopic exchange will be distinguished in the following discussion. The small-scale oxygen isotopic exchange observed in the vicinity of the contact involves a steep isotopic gradient that extends less than 2 to 3 feet on both sides of the contact. This exchange probably took place essentially in the solid state through a diffusion-controlled process. The large-scale oxygen isotopic exchange is observed in the marginal zones of the stocks or plutons where "abnormally" high O^{18}/O^{16} ratios exist; this probably took place when the intrusions were largely molten. A third type of isotopic exchange is observed in the Birch Creek xenolith and Sawtooth

re-entrant. The movement of aqueous fluids is probably an important factor in the isotopic exchange between the xenolith or re-entrant and the intrusion.

B. Small-scale oxygen isotopic exchange

The small-scale oxygen isotopic exchange occurs at the immediate contact between the intrusion and the country rocks where a steep (1 to 3 per mil per foot) oxygen isotopic compositional gradient is observed. Beyond a few feet away from the contact, both on the intrusive side and on the country rock side, the O^{18}/O^{16} ratios of the individual minerals or whole rock samples remain quite constant (see the various $\delta\ O^{18}$-distance plots in Chapter 5). Note that the steep isotopic gradient does not prevent attainment of a "normal" sequence of O^{18}-enrichment of the coexisting minerals in all the traverses studied. The shape of the curves in the $\delta\ O^{18}$-distance plot indicates that the oxygen isotopes have undergone exchange between the intrusive and the country rock to a varying degree depending upon their distances from the contact. If 100% exchange occurs, the O^{18}/O^{16} ratios of a particular mineral in the intrusive and in the country rock will be equal. If no exchange occurs at all, the O^{18}/O^{16} ratios of a particular mineral should retain their original values. Inasmuch as the O^{18}/O^{16} ratios of the individual minerals remain quite constant beyond a few feet away from the contact, they are assumed to represent 0% exchange. The percentage of isotopic exchange for different minerals from various traverses has been calculated. The results are presented in Table 15 and Figure 45.

The extent of oxygen isotopic exchange in most cases does not exceed 25% for samples beyond 2 feet from the contact, possibly with the exception of

TABLE 15

Percent oxygen isotope exchange between intrusive and country rock for samples from different traverses.

Sample No.	Distance from contact, feet	Rock	Mineral	δO^{18} per mil	%Exchange
Sawtooth traverse I					
SRO-18	50	Trondhjemite	Quartz	11.7	0
			Biotite	5.5	0
			Feldspar	9.2	0
SRO-17	10	Trondhjemite	Quartz	11.8	0
			Feldspar	9.7	0
SRO-19AI	0.5	Trondhjemite	Quartz	14.5	65
			Biotite	7.9	53
			Feldspar	12.1	55
SRO-15C	0.17	Trondhjemite	Quartz	16.0	100
			Biotite	9.7	93
			Feldspar	13.4	83
SRO-15A	0.04	Trondhjemite	Quartz	15.9	100
			Biotite	10.0	100
			Feldspar	14.2	100
SRO-15B	0.08	Schist	Quartz	16.1	100
			Muscovite	13.2	100
			Biotite	9.9	100
SRO-19AII	0.5	Schist	Quartz	16.7	78
			Muscovite	14.1	61

TABLE 15 (continued)

Sample No.	Distance from contact, feet	Rock	Mineral	δO^{18} per mil	%Exchange
			Biotite	10.9	52
SRO-19B	1	Schist	Quartz	18.7	16
			Muscovite	15.3	9
			Biotite	11.8	10
SRO-19C	50	Schist	Quartz	19.2	0
			Muscovite	15.5	0
			Biotite	12.0	0
Sawtooth traverse II					
SRO-22F	50	Trondhjemite	Quartz	11.4	0
			Biotite	5.3	0
			Feldspar	9.4	0
SRO-22E	1.5	Trondhjemite	Quartz	11.3	0
			Biotite	5.6	25
			Feldspar	9.8	0
SRO-22D	0.17	Gneiss	Quartz	12.1	100
			Muscovite	9.2	100
			Biotite	6.5	100
SRO-22C	5	Schist	Quartz	15.1	6
			Muscovite	12.6	17
			Biotite	9.7	16
SRO-22A	85	Schist	Quartz	15.3	0

TABLE 15 (continued)

Sample No.	Distance from contact, feet	Rock	Mineral	δO^{18} per mil	%Exchange
			Muscovite	13.3	0
			Biotite	10.3	0
Flynn south traverse					
SRO-38	35	Granodiorite	Quartz	10.5	0
			Biotite	4.6	0
SRO-37	45	Hornfels	Quartz	17.3	0
			Muscovite	15.2	0
			Biotite	12.0	0
Santa Rosa traverse					
SRO-29A	0.08	Hornfels	Whole rock	11.8	100
SRO-29B	0.4	Hornfels	Whole rock	11.8	100
SRO-29C	0.9	Hornfels	Whole rock	13.6	56
SRO-29D	2	Hornfels	Whole rock	14.0	48
SRO-29E	30	Hornfels	Whole rock	15.7	0
Santa Rosa dike					
SRO-28-1	0.17	Dike	Whole rock	12.2	?
SRO-28-2	0.008	Dike	Whole rock	13.4	100

TABLE 15 (continued)

Sample No.	Distance from contact, feet	Rock	Mineral	δO^{18} per mil	%Exchange
SRO-28-3	0.017	Hornfels	Whole rock	13.6	100
SRO-28-4	0.17	Hornfels	Whole rock	14.9	38
SRO-28-5	0.42	Hornfels	Whole rock	15.7	0
Birch Creek traverses					
BC-27G	4.5	Granite	Quartz	12.2	0
			Biotite	6.4	0
BC-27AI	0.4	Granite	Quartz	12.7	42
			Biotite	7.0	54
BC-27AII	0.25	Schist	Quartz	14.0	90
			Biotite	8.1	92
BC-27B	2	Schist	Quartz	19.4	0
			Biotite	12.6	0
BC-28I	10	Granite	Quartz	12.9	0
BC-28H	2.5	Granite	Quartz	12.9	0
BC-28A	0.25	Schist	Quartz	14.1	90
			Biotite	8.1	89
BC-28B	2	Dike	Quartz	12.9	0
BC-28C	6	Schist	Quartz	19.2	0
			Biotite	13.0	0

TABLE 15 (continued)

Sample No.	Distance from contact, feet	Rock	Mineral	δO^{18} per mil	%Exchange
Caribou traverse					
HES-8	530	Monzonite	Biotite	4.5	0
			Magnetite	1.7	0
HES-4a	0.04	Monzonite	Biotite	5.4	100
			Magnetite	1.8	100
HES-4b	0.04	Gneiss	Quartz	10.1	100
			Biotite	5.5	100
			Magnetite	1.9	100
HES-4c	0.6	Gneiss	Quartz	10.1	100
			Biotite	6.1	76
			Magnetite	3.4	42
HES-1	1300	Schist	Quartz	12.8	0
			Biotite	8.0	0
			Magnetite	4.5	0

Figure 45. Percent oxygen isotope exchange between intrusive and country rock as a function of distance from contact for the Santa Rosa traverse, Sawtooth traverses I and II, Birch Creek traverse, Caribou traverse, and a granitic dike-hornfels contact 30 feet from the main contact of the Santa Rosa stock.

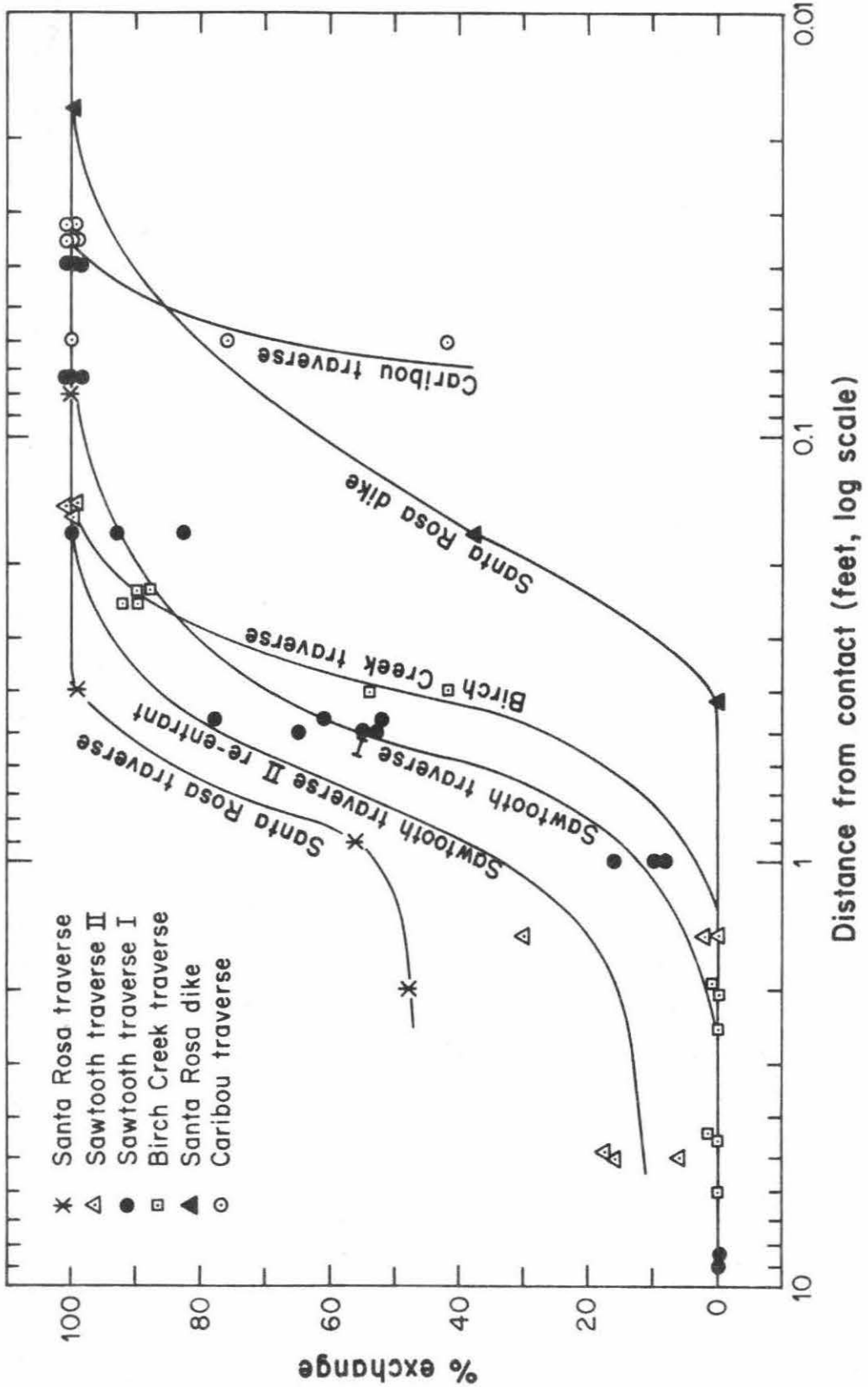
% exchange
100
80
60
40
20
0
10
1
0.1
0.01
Distance from contact (feet, log scale)
Santa Rosa traverse
Sawtooth traverse II
Sawtooth traverse I
Birch Creek traverse
Santa Rosa dike
Caribou traverse
Santa Rosa traverse
Sawtooth traverse II re-entrant
Sawtooth traverse I
Birch Creek traverse
Santa Rosa dike
Caribou traverse

Figure 45

the Santa Rosa stock where a 2-foot country-rock sample appears to have undergone 50% exchange; however, the latter case is less reliable because it is based only on one whole-rock analysis. There is no marked difference in the degree of exchange among the coexisting minerals analyzed in a rock, except for the 7-inch sample from the Caribou traverse in which quartz has undergone 100% exchange, whereas magnetite has apparently only experienced 40% exchange. It should be pointed out that this magnetite is much coarser - grained than the Sawtooth magnetite discussed in section 5.1-B.

Garlick and Epstein (1966, 1967) analyzed the O^{18}/O^{16} ratios of coexisting minerals in a schist xenolith enclosed in trondhjemite and the hydrothermal wall-rock alteration envelopes at Butte, Montana. They found that garnet undergoes oxygen isotopic exchange in the xenolith only with difficulty, whereas ilmenite, muscovite, and biotite are the easiest minerals to exchange. In the hydrothermally altered envelope at Butte, K-feldspar has experienced much isotopic exchange whereas quartz is not appreciably affected by the alteration process. The same effects have also been observed by Taylor (1968b) in red-rock granophyres. No garnet was analyzed in the present study, but the feldspar samples analyzed from two traverses in the Sawtooth stock show essentially the same degree of exchange as coexisting quartz and biotite. The discrepancy between the present result and that of Taylor (1968b) and Garlick and Epstein (1967) is not understood. However, it is known that differences in the alkali concentrations of the hydrothermal fluids can have important effects on such exchange processes (see O'Neil and Taylor, 1967).

The dimensions of the oxygen isotopic equilibrium system during such small-scale oxygen isotopic exchange can be determined by measuring the

maximum distance between samples that have undergone essentially 100% isotopic exchange, such that a particular mineral has attained essentially the same O^{18}/O^{16} ratio in the samples. It is found that such an equilibrium system is quite small, being about 1 foot in the Santa Rosa traverse, 0.5 feet in Sawtooth traverse II, 0.2 feet in Sawtooth traverse I, 0.3 feet in Birch Creek, 0.1 feet in Caribou traverse, and 0.05 feet in the Santa Rosa dike.

The size of such an exchange system may depend upon (1) temperature, (2) time of heating, and (3) availability of an exchange medium (oxygen-bearing fluids). The dimensions of oxygen isotopic equilibrium systems estimated above correlate quite well with combinations of such parameters. For example, the Santa Rosa stock is the biggest stock; as a consequence, the country rock should be held above a specific temperature for much longer time than in the case of the smaller stocks (see section 2.4-B). The Sawtooth stock is probably the "wettest" of the intrusives. Traverse II of Sawtooth is in the re-entrant where the temperature should have been abnormally high. All these factors (higher temperatures, longer heating, and higher water pressure) should facilitate the isotopic exchange. On the other hand, the Caribou stock contact zone was probably the "driest" because the country rock had already been regionally metamorphosed to sillimanite grade prior to the contact metamorphism, and the Caribou traverse shows the smallest extent of exchange. The Santa Rosa dike is about 5 inches thick, and crosscuts hornfels about 30 feet away from the main intrusive contact; the heating effect of the country rock by the dike must have been very small.

It is interesting to inquire into the mechanism of such small-scale isotopic exchange. Isotopic exchange may occur through the mechanism of

(1) recrystallization, perhaps by diffusion along cleavage cracks or crystal imperfections, accompanied by oxygen isotopic equilibration in a fluid film at the interface between exchanged and unexchanged portions of mineral grains, as proposed by O'Neil and Taylor (1967) in their experiments on the oxygen and cation exchange of the feldspars; or by (2) solid-state diffusion through the crystal lattice of each mineral. Mechanism (2) is a very slow process. The diffusion coefficient of oxygen in quartz parallel to the c-axis was determined by Choudhury et al. (1965) at 667°C and 820 bars to be 4×10^{-12} cm^2/sec, using the nuclear reaction O^{18} (p, α) N^{15}; it was determined by Verhoogen (1952) at 500°C to be 3×10^{-11} cm^2/sec, using electric conductivity measurements. For example, using $D = 4 \times 10^{-12}$ cm^2/sec and $t = 1 \times 10^4$ years, the average distance travelled by the oxygen along the c-axis of quartz would be only 1.6 cm. The distance would be much smaller at temperatures of 500° to 600°C. On the other hand, mechanism (1) is a very effective process, because intergranular or surface diffusion coefficients are several orders of magnitude larger than lattice diffusion coefficients, particularly in the presence of a fluid film; essentially complete isotopic exchange is possible within reasonable experimental times (see O'Neil and Taylor, 1967). Another argument against the effectiveness of simple solid-state diffusion is the fact that the isotopic fractionations among coexisting minerals apparently were "frozen in" at approximately equilibrium values at or near the maximum contact temperatures. This suggests that the mineral assemblages have undergone recrystallization during the small-scale exchange, and that only minor adjustments of O^{18}/O^{16} ratios occurred by solid diffusion during the further temperature

decline.

The oxygen isotopic data in the present study do not seem to allow any transfer mechanisms which require abundant or massive movement of solution or fluid phase across the contact, because of the existence of steep isotopic gradients (as steep as 3 per mil/ft.) and the very narrow zone (less than a few feet) that has taken part in the isotopic exchange. It is more likely that the oxygen isotopes were transferred from the intrusive to the country rock, and vice versa, by diffusion along grain-boundaries in the presence of an essentially static interstitial fluid film.

Oxygen isotopic zoning of mineral grains in the exchanged zones probably does not exist as far as the present experimental accuracy is concerned. The steepest isotopic gradient observed in the present study is about 0.015 per mil/mm, and the largest average grain-size of minerals other than andalusite is about 2 mm. Therefore, the maximum δ-value difference between two adjacent grains of a mineral is not more than 0.03 per mil.

In all of the traverses studied except Sawtooth traverse I, the maximum $\delta\ O^{18}$-lowering in the country rock is greater than the maximum $\delta\ O^{18}$-enrichment in the intrusive in the small-scale isotopic exchange zones (Table 16). This presumably is due to the fact that such small-scale isotopic exchange would begin to take place as soon as the country rock is intruded, but the isotopic gradient on the intrusive side would not be well preserved until after the magma has become solidified. In traverse I of the Sawtooth stock, where the intrusion forms a narrow wedge surrounded by the country rock, the $\delta\ O^{18}$-lowering in the country rock is less than the $\delta\ O^{18}$-increase of the intrusive, in keeping

TABLE 16

Comparison of maximum δO^{18}-lowering in the country rock vs. δO^{18}-increase in the intrusive for various small-scale isotopic exchange zones.

Traverse	Mineral	δO^{18}-lowering (Country rock)	δO^{18}-increase (intrusive)	Ratio of δO^{18}-lowering/to δO^{18}-increase
Sawtooth I	Quartz	3.2 per mil	4.3 per mil	0.7
	Biotite	2.0	4.5	0.4
Sawtooth II	Quartz	3.2	0.8	4.0
	Biotite	3.8	1.2	3.2
Santa Rosa	Quartz	3.4	1.5	2.3
	Biotite	3.2	1.8	1.9
Birch Creek	Quartz	6.0	1.2	5.0
	Biotite	4.9	1.3	3.8
Caribou and Eldora	Quartz	2.7	0.2	13.0
	Biotite	2.5	0.9	2.8
	Magnetite	2.6	0.2	13.0

with the probably more rapid crystallization of the trondhjemite near this contact. It is also noted that the ratio δO^{18}-lowering/δO^{18}-increase is slightly greater in quartz than in biotite for all the traverses studied in this research.

C. Large-scale oxygen isotopic exchange in the igneous rocks

Large-scale oxygen isotopic exchange effects are here defined as those observed over a scale of hundreds of feet or more. Unlike the small-scale exchange discussed above, except for two examples discussed in section 6.4-D, these effects are confined to the igneous rocks. They have been observed in the marginal portions of the Santa Rosa, Flynn, Sawtooth, and Birch Creek plutons as much as 300 to 500 feet inward from the contact. A small intrusive plug (300 x 600 feet) in the outer aureole of the Santa Rosa stock shows even more marked effects than the examples mentioned above.

The evidence for such large-scale isotopic exchange is the "abnormally" high O^{18}/O^{16} ratios of minerals in the marginal portions of the intrusives compared to those obtained from the central portion of the Santa Rosa stock and from the "normal" plutonic granitic rocks reported by Taylor and Epstein (1962), as shown in Table 17.

It seems certain that the "abnormally" high O^{18}/O^{16} ratios of the marginal parts of these intrusions are the result of contamination of an originally "normal" igneous granitic rock (mostly in a molten state) with O^{18}-rich material. The only logical source of such O^{18}-rich material is the metasedimentary country rock that has been intruded. A "normal" igneous rock (or magma) can be isotopically contaminated by the country rock in the following ways: (1) simple melting or assimilation of stoped blocks, (2) exchange with xenoliths

TABLE 17

Comparison of O^{18}/O^{16} ratios of quartz and biotite from marginal portions of various intrusions with those from the central portion of the Santa Rosa stock and from "normal" plutonic granitic rocks

Pluton	δ quartz (per mil)	δ biotite (per mil)
Central zones of plutons		
"Normal" plutonic granitic rocks (Taylor and Epstein, 1962)	9.9 ± 0.3 (6)	5.0 ± 0.4 (5)
Central portion of Santa Rosa stock	9.5 ± 0.0 (2)	4.5 ± 0.1 (2)
Marginal zones of plutons		
Sawtooth stock	11.5 ± 0.1 (4)	5.4 ± 0.1 (4)
Flynn stock — North	13.5 ± 0.8 (2)	7.8 ± 1.1 (2)
Flynn stock — South	10.6 ± 0.1 (2)	4.8 ± 0.2 (2)
Santa Rosa stock	13.1 (1)	6.8 (1)
Small intrusive plug	14.0 (1)	8.1 (1)
Birch Creek pluton	12.3 ± 0.6 (4)	6.0 ± 0.4 (2)
Eldora and Caribou stocks	9.9 ± 0.0 (2)	4.8 ± 0.2 (3)

The uncertainty shown is average deviation from the mean.
Numbers in parentheses represent number of samples.

enclosed in the magma, (3) exchange with country rock by means of aqueous fluids, and (4) absorption of water from the country rock.

Simple melting or assimilation of country rock will be important if the magma is intruded at high temperatures. There is geologic evidence that many of the stocks in the Santa Rosa Range are dominantly crosscutting (and stoped) bodies (Compton, 1960, p. 1397). Some assimilation of the country rock by the magma almost certainly occurred at the time of intrusion. However, the compositional pattern of the Santa Rosa stock does not support the idea of simple assimilation of appreciable quantities of country rock at the present level of exposure (Compton, 1960, p. 1401). A material-balance calculation from the oxygen isotopic data shows that sample SRO-29F, collected 150 feet inward from the Santa Rosa stock, requires that 30 atom per cent of its oxygen be derived from the country rock if simple assimilation is the only mechanism. Such large amounts of assimilated metasediments would certainly have been reflected in the compositional pattern of the intrusion.

Mechanism (2) should be very effective for large-scale oxygen isotopic exchange. A xenolith immersed in the magma may undergo isotopic exchange to such an extent that the O^{18}/O^{16} ratios of minerals in the xenolith become essentially identical to the ratios in the intrusive without melting the xenolith. An example of such an exchange mechanism has been observed in a schist xenolith in the Birch Creek pluton (see section 6.4-D).

O^{18}-enrichment of a magma can also be the result of isotopic exchange with country rock by means of aqueous fluids (i.e., mechanism 3). Two examples will serve to illustrate this effect. Sample SRO-D is a pegmatite

dike 3 inches thick crosscutting schist of the Sawtooth aureole. The pegmatite consists of a pure quartz core about 0.5 inch thick bordered on both sides by very coarse-grained K-feldspar, muscovite and minor quartz. The δO^{18}-values are: quartz (core) 18.3, quartz (border) 17.8, K-feldspar 12.4 and muscovite 15.7 per mil. As discussed in section 6.1-A, the O^{18}/O^{16} ratios of the quartz and muscovite in this pegmatite are similar to those of the corresponding minerals in the schist. This is almost certainly not the result of simple small-scale isotopic exchange with the schist after solidification of the pegmatite, because the quartz in the core is even more O^{18}-rich than in the border zone and the quartz and muscovite are both extremely coarse-grained. In addition, the same effects observed in the pegmatite can also be seen in a 0.5 inch thick aplite dike crosscutting SRO-19B (schist). The aplite is fine-grained (0.3 mm) and is composed of quartz (δ = 17.4), feldspar, and muscovite (δ = 16.1). The quartz in the aplite is 1.3 per mil lower in δO^{18} than the quartz in the adjoining schist. However, inasmuch as the muscovite in the aplite is 0.8 per mil higher in δO^{18} than the muscovite in the schist, this cannot have been the result of simple isotopic exchange in the crystalline state. The fact that similar effects occur in two granitic dikes with such vastly different grain sizes and textures is evidence that isotopic exchange in both occurred with liquid magma.

Mechanism (4), the absorption of water from the metasedimentary rocks into the magma, can also be significant if the magma is relatively "dry" (i.e., if it is highly undersaturated in H_2O). There is geologic evidence that the Santa Rosa and Flynn stocks were "drier" than the Sawtooth stock when emplaced (Compton, 1960, p. 1408); a much larger quantity of water might migrate

from the country rocks into the "dry" stocks than into the "wet" stock. This is apparently borne out by the oxygen isotopic data, because the marginal portions of the Santa Rosa stock, the north side of the Flynn stock, and the whole portion of the small plug in the Santa Rosa aureole show the greatest O^{18}-enrichment in the minerals. As the Sawtooth stock was presumably much more nearly saturated in H_2O, there would have been less tendency for influx of H_2O from the country rocks, and the Sawtooth stock shows significantly less marginal isotopic contamination. In the Eldora and Caribou stocks the country rocks were regionally metamorphosed to very high grade prior to the intrusions of the stocks; therefore one would not expect any appreciable influx of water from the country rocks, and the marginal intrusive samples in fact show no signs of isotopic contamination (Table 17).

In summary, each of the four mechanisms discussed above may be in part responsible for the O^{18}-enrichment of the minor intrusions and the marginal portions of the larger igneous bodies. The relative importance of each mechanism will depend largely upon the physical conditions of emplacement of the plutons. It should be pointed out that very significant oxygen isotopic effects have occurred with little or no evidence of bulk chemical changes in the rocks. In most of the stocks examined, xenoliths are very rare. Therefore, it seems likely that mechanisms (3) and (4) are predominant. In the Birch Creek pluton, however, xenoliths are abundant near the contact and they have undergone extensive isotopic exchange, suggesting that mechanism (2) prevails at this locality.

D. Large-scale isotopic exchange in xenolith and re-entrant

The only places where large-scale oxygen isotopic exchange effects were found in metasedimentary rocks are in the Birch Creek xenolith and in the Sawtooth re-entrant. BC-22 and BC-23 are two samples collected from the center and the margin, respectively, of a schist xenolith having an exposed area 10 x 50 feet. The O^{18}/O^{16} ratios of minerals in these two samples are essentially identical to those of the same minerals in the adjacent granite (see Table 5, section 5.2-B). If we assume that the xenolith originally had O^{18}/O^{16} ratios similar to the schist outside the pluton, then a lowering of δ-values by about 6 per mil is indicated; the size of the oxygen isotopic equilibrium system in the xenolith is at least 10 feet (the width of the xenolith). This is at least 30 times larger than at the main contact.

In the re-entrant of Sawtooth traverse II where an embayment of country rock projects into the intrusive, the O^{18}/O^{16} ratios of quartz in two schist samples collected 5 and 85 feet away from the contact show a uniform lowering of about 3 per mil in comparison with O^{18}/O^{16} ratios for samples outside the re-entrant. This cannot be due to the same mechanism responsible for small-scale isotopic exchange discussed earlier because a further abrupt lowering of O^{18}/O^{16} ratios, which is characteristic of the small-scale exchange, occurs within 1 foot of the contact.

It is likely that the samples collected from the xenolith and the re-entrant were maintained at high temperatures for very long periods of time. Both heat flow considerations (Jaeger, 1961) and oxygen isotopic data (smaller fractionations among coexisting minerals) support this view. Although

diffusion would be faster in such an environment than at the main contact because of the higher temperatures involved, the widths of the isotopically exchanged zones would not be expected to be vastly different. Therefore, a much more effective method of material transport seems to be required to explain the large-scale exchange in the xenolith and re-entrant. In this connection, it may be significant that the Sawtooth and Birch Creek plutons appear to have been relatively "wet" compared with the other intrusions studied in this work. It is logical to infer that a low-density aqueous fluid would tend to move upward in a gravitational field even if it were present only as a fluid film in the pore spaces of rocks. Therefore, one can expect much larger-scale effects in country rocks that are underlain by or surrounded by an intrusive igneous rock that is a source of volatiles. The only two examples of such geometry that were studied in the present research are the xenolith and re-entrant; for all other cases, the intrusive-country rock contact is essentially vertical, and upward-moving volatiles would produce no isotopic exchange between the intrusive and country rock. Thus, whereas horizontal outward movement of H_2O from the magma is negligible (see section 6.6), upward transport may be very important. In certain cases, it is even possible that H_2O has migrated into the intrusive, exchanged oxygen with it, and then moved upward out of the magma system.

6.5 Isotopic fractionations in dehydration reactions

The effect of dehydration reactions upon the oxygen isotopic compositions of the pelitic rocks can be studied by examining the variations of the oxygen isotopes across the metamorphic zones. The best sets of samples on

which to study such isotopic effects are those from the Santa Rosa Range. The O^{18}/O^{16} ratios, either of whole rock or of individual minerals, do not show any noticeable change across the metamorphic zones in any of the traverses studied. Three explanations are possible: (1) Fractionations of oxygen isotopes between water and pelitic rock do not accompany dehydration reactions. (2) Oxygen isotopic fractionations occur during dehydration reactions but the amount of water escaping from the system is negligible compared with the total oxygen in the rock. (3) Isotopic fractionations occurred, but later isotopic homogenization has swept out all the isotopic inequalities.

The last possibility is unlikely because of the small size of the country rocks that have undergone homogenization of oxygen isotopes (see section 6.4-B).

Possibility (1) can be evaluated in terms of experimental data. Table 18 shows the oxygen isotopic compositions of pelitic rocks and coexisting waters in equilibrium with the mineral assemblages; the latter have been calculated for both the isotopic temperatures and heat flow temperatures, utilizing the muscovite-water calibration curve. We see that δ rock and δ H_2O are similar, particularly for samples close to the contact. The few samples collected from the main parts of the contact aureoles show δ rock higher than δ H_2O by about 2 to 4 per mil. Therefore, if the dehydrated water is equilibrated with the rock before escaping, the dehydration process will either produce no effect, or at most will increase the δ rock by only 0.2 to 0.4 per mil (see below). There is a faint suggestion in the isotopic data that rocks in the aureole are slightly richer in O^{18} than their unmetamorphosed equivalents (see Figure 11).

Possibility (2) can be evaluated by calculating the proportion of oxygen liberated during the dehydration reactions. Compton (1960, p. 1408) has derived the following balanced dehydration reactions in which the actual stoichiometric amounts

TABLE 18

O^{18}/O^{16} ratios of pelitic rocks and coexisting waters in equilibrium with the mineral assemblages

Sample No.	Distance from contact, feet	δ rock	δH_2O (based on isotopic temp.)	δH_2O (based on heat flow temp.)
	Sawtooth aureole			
SRO-22D	0.17	10.2	9.7	9.5
SRO-22C	5	14.3	13.7	12.5
SRO-22A	85	13.9	15.7	12.5
SRO-15B	0.08	13.5	13.5	13.5
SRO-19B	1	15.9	14.4	14.9 (460°C) *
SRO-19C	50	16.6	14.5	15.2 (455°C) *
SRO-19D	600	16.8	16.9	14.0
	Santa Rosa aureole			
SRO-29A	0.08	11.8	11.5	13.3
SRO-29D	2	14.0	13.4	15.6
	Flynn aureole			
SRO-37	45	15.5	15.6	15.7
SRO-46	3200	15.5	--	9.7
	Birch Creek aureole			
BC-27AII	0.25	11.3	11.4	11.4
BC-27B	2	16.0	15.6	16.8
BC-28C	6	16.4	16.3	16.6
BC-28E	13	16.4	16.0	16.4
BC-7	70	17.4	16.8	17.1
BC-16	1300	13.3	12.3	--
BC-15	2000	12.4	11.9	--
BC-14	2100	12.4	12.1	--

*: Based on heat flow model F

of reactants and products are taken into account:

(1) 1.1 chlorite + 1 muscovite = 1 biotite + 1.5 andalusite + 0.25 staurolite + 1.2 quartz + 4.1 H_2O

(2) 1.4 chlorite + 1 muscovite + 1.3 quartz = 1 biotite + 1 cordierite + 1 andalusite + 5.6 H_2O

(3) 1 chlorite + 1 muscovite = 1 biotite + 2.5 andalusite + 1 quartz + 4 H_2O

From the above dehydration reactions, it is calculated that the percent of oxygen liberated as dehydrated water relative to the total oxygen in the rock is 9.3%, 10.8%, and 9.5%, respectively, for these three reactions. Therefore, any kinetic fractionation during dehydration would have to exceed 10 per mil in order to produce as much as a 1 per mil change in the country rock.

In summary, both the actual oxygen isotopic data and material-balance considerations indicate that dehydration reactions would not produce any significant oxygen isotopic changes during contact metamorphism.

The D/H ratios of the pelitic rocks also do not show any obvious change across the contact metamorphic zones. Fractionations of hydrogen isotopes probably do not accompany dehydration reactions.

6.6 Source and movement of water during contact metamorphism

Water in contact metamorphism can be derived either from the country rock or from the intrusive. Water in the country rock probably comes mainly from metamorphic dehydration reactions, but meteoric water may also be present in the pore spaces and fissures of the country rock. The amount of water in the magma depends in part upon the solubility of water in the magma. The solubility of water in albite and pegmatite melts has been determined

recently by Burnham and Jahns (1962); in the temperature range 660° to 720°C at a pressure of 4 Kb, the solubility of water in a pegmatite melt is 10% by weight and at 7 Kb about 14%. Inasmuch as the solubility of water in silicate melt is strongly pressure-dependent, an ascending magma may separate an aqueous phase during its course of intrusion. The total pressure on the stocks in the Santa Rosa Range during their intrusion is estimated to be about 1 to 2 Kb (Compton, 1960); a H_2O-saturated granitic melt under such conditions would contain only about 5.5 weight percent H_2O (Burnham, 1967).

In many books of petrology, it is generally conceded without much justification that "near granite contacts a permeable rock undergoing metamorphism may be continuously flushed with outward-flowing water" (Turner, 1968, p. 244). Similar statements emphasising the idea of outward movement of water through contact metamorphic aureoles from granitic intrusions can be found in Harker (1939, p. 23), Barth (1962, p. 262), and Turner and Verhoogen (1960, p. 658). The oxygen isotopic data are pertinent to the questions as to the source and movement of water during contact metamorphism, because the water equilibrated with the magma can definitely be distinguished from that equilibrated with the sediments or low-grade metamorphic rocks.

The oxygen isotopic compositions of waters in equilibrium with the minerals of various rocks studied in this research are given in Table 13, calculated from the experimentally calibrated quartz-H_2O and muscovite-H_2O oxygen isotopic fractionation curves. The range of O^{18}/O^{16} ratios of waters in Group I and Group II samples, in which the oxygen isotopes show either 100% exchange or no evidence of exchange, are presented in Table 19. It is seen that the O^{18}/O^{16} ratios of the waters are distinctly different in the intrusive

TABLE 19

Range of O^{18}/O^{16} ratios of waters in equilibrium with the intrusive, the country rock, and the contact samples from different localities.

Location	Intrusive	Country rock	Contact
Sawtooth	8.6 - 9.0	14.4 - 14.5	13.5 - 13.6 (Traverse I) 9.7 (Traverse II)
Flynn	7.9 - 8.4	15.6	----
Santa Rosa	10.0 (margin) 8.2 - 8.4 (Center)	14.0	11.5
Birch Creek	9.0 - 9.8	15.6 - 16.8	11.4 - 11.5
Eldora and Caribou	8.6 - 8.7	9.8 - 11.9	9.5

and the country rocks. Also note that the O^{18}/O^{16} ratios of waters are quite uniform within the intrusive or within the country rocks in an individual contact zone, and that intermediate O^{18}/O^{16} ratios are obtained at the contacts. Inasmuch as the exchanged zone at the intrusive-country rock contact is less than a few feet wide, horizontal outward movement of large quantities of water across the contact during the crystallization of the magma is ruled out. The idea that a large amount of water is expelled outward through the entire contact aureole from the granitic intrusions, or that water acts as a significant heat carrier, that is, "heat is carried from the cooling magma into the country rock by transfer of steam as well as by conduction" (Fyfe, Turner, and Verhoogen, 1958, p. 190) is not compatible with the isotopic data presented here.

The oxygen isotopic data, however, are compatible with the concept that upward movement of water is probably far more important and operative at a much larger scale than the horizontal outward movement of water from the magma. The large-scale isotopic exchange observed in the xenolith and in the re-entrant was cited earlier as evidence of appreciable upward movement of water (see section 6.4-D).

If a "dry" (i.e., undersaturated with respect to H_2O) magma is emplaced into "wet" sediments or metasedimentary rocks, migration of water from the country rocks to the magma may be significant. The abnormally high O^{18}/O^{16} ratios of samples from the marginal portion of the Santa Rosa stock, the northwest portion of the Flynn stock, and the whole portion of the small plug in the Santa Rosa aureole may in part be due to such an effect (see section 6.4-C).

The rough correlation between the D/H ratios of biotite and that of local surface water as is discussed in section 6.8-C may be interpreted to mean that meteoric water may also be incorporated into all of the shallow intrusions studied in the present research. Taylor (1968 b) has shown on the basis of O^{18}/O^{16} data that much larger quantities of ground water have been incorporated into certain other shallow plutons such as the Mull, Skye, Ardnamurchan, and Skaergaard intrusions. Except perhaps for the SRO-D pegmatite feldspar and magnetites of the Sawtooth contact zone, no oxygen isotopic evidence for meteoric water has been found in the present study. However, much smaller quantities of meteoric water are necessary to produce a change in D/H ratio than O^{18}/O^{16} ratio in a rock.

6.7 Isotopic fractionations in decarbonation reactions

Three examples of contact metamorphic decarbonation reactions are:

$$CaCO_3 + SiO_2 = CaSiO_3 + CO_2$$

calcite silica wollastonite

$$2CaMg(CO_3)_2 + SiO_2 = 2CaCO_3 + Mg_2SiO_4 + 2CO_2$$

dolomite silica calcite forsterite

$$3CaMg(CO_3)_2 + KAlSi_3O_8 + H_2O = KMg_3AlSi_3O_{10}(OH)_2 + 3CaCO_3 + 3CO_2$$

dolomite K-feldspar phlogopite calcite

The CO_2 liberated in the above reactions will escape out of the rock; therefore it is interesting to inquire into the isotopic effects that accompany such processes.

It was pointed out in chapter 5 that skarns usually have the lowest O^{18}/O^{16} and C^{13}/C^{12} ratios in comparison with the adjacent rock units. In

other words, an "isotopic trough" is usually observed in such localities. Also, low C^{13}/C^{12} ratios in carbonates are correlated with the presence of calc-silicates. Inasmuch as the skarns and calc-silicates have formed by decarbonation of the marbles, it is natural to infer that the decarbonation reactions are at least in part responsible for the lowering of the O^{18}/O^{16} and C^{13}/C^{12} ratios of the rocks. Taylor (1968 a) has shown that some of the calc-silicate skarns in the Adirondack anorthosite massif have exceedingly low δO^{18}-values (e.g., wollastonite = -0.9 to +0.5 per mil; diopside = +0.2 per mil). A correlation of O^{18}/O^{16} or C^{13}/C^{12} ratios of carbonates vs. modal abundance of calc-silicates in marbles and calcareous schists samples from Vermont was also observed by Sheppard (1966).

It is desirable to know the isotopic composition of the liberated CO_2. If the liberated CO_2 is in equilibrium with the carbonate before escaping, the oxygen isotopic composition of the CO_2 can be estimated from the laboratory calibration curves (O'Neil and Epstein, 1966). For example, in the temperature range 500 - 700°C, the CO_2 in equilibrium with dolomite would be about 5.5 to 4.5 per mil higher in O^{18}/O^{16} ratio than the dolomite. If the isotopic fractionations during decarbonation reactions are kinetically controlled, the situation may be more complex. Sharma and Clayton (1965) have measured the oxygen isotopic fractionation between CO_2 and dolomite during thermal decomposition of dolomite in vacuum. They found that O^{18} is concentrated in the CO_2 phase and the fractionation decreased with increasing temperature: Δ = 6.0 at 519°C, 5.6 at 532° C, 5.1 at 570°C, and 4.6 at 600°C. Note that the kinetic fractionations between CO_2 and dolomite at the temperature range studied are almost identical to those of equilibrium

fractionations.

If it is assumed that the only constituent lost during contact metamorphic decarbonation is CO_2, then the amount and the isotopic composition of CO_2 can be calculated from material balance considerations. A forsterite marble (BC-32E), a phlogopite marble (BC-8), and a multi-layered skarn (A-6) were used to make such calculations because of the rather simple mineralogy in these rocks. The results for BC-32E and BC-8 are given in Table 20. The main uncertainty of the calculations comes from the uncertainty of the initial isotopic compositions of minerals. In making the calculations for BC-32E and BC-8, the O^{18}/O^{16} ratios of dolomite and calcite that were used are the highest values observed in the nearby dolomite marble. The δO^{18} in silica was assigned a value 4 per mil higher than the δO^{18}-value in the carbonate, which is a probable fractionation at sedimentary temperatures. K-feldspar was assigned $\delta = 17.0$; H_2O was assigned $\delta = 0$. Note that minor changes in the δ-values of the minerals other than the carbonates will not appreciably affect the results because of the relatively small amount involved in the calculation.

The calculations show that the liberated CO_2 would have the following isotopic compositions:

BC-32E	$\delta O^{18} = 29.0$,	$\delta C^{13} = 4.4$
BC-8	$\delta O^{18} = 61.0$,	$\delta C^{13} = 5.4$

In terms of fractionations between CO_2 and calcite, they are:

BC-32E	$\Delta O^{18} = 5.1$,	$\Delta C^{13} = 5.5$
BC-8	$\Delta O^{18} = 41.7$,	$\Delta C^{13} = 6.4$

The carbon isotopic fractionations are quite similar in the two samples, but the oxygen isotopic fractionations are vastly different. BC-32E is close to equilibrium

TABLE 20

Calculated isotopic compositions of CO_2 liberated during decarbonation reactions by material balance

BC-32E Forsterite Marble

$$2\,CaMg(CO_3)_2 + SiO_2 \rightleftharpoons 2CaCO_3 + Mg_2SiO_4 + 2CO_2$$

dolomite silica calcite forsterite

		Dolomite	Silica	Calcite	Forsterite	CO_2
After Decarbonation	Mode (vol %)	20	0	60	20	?
	Molecular proportion	1.55	0	8.15	2.30	4.60
	Oxygen (atom %)	17.8	0	47.0	17.6	17.7
	Carbon (atom %)	19.5	0	51.5	0	29.0
	δO^{18} per mil	24.2	--	23.9	20.8	29.0
	δC^{13} per mil	-0.8	--	-1.1	--	4.4
Before Decarbonation	Molecular proportion	6.15	2.30	3.55	0	0
	Oxygen (atom %)	70.8	8.8	20.4	0	0
	Carbon (atom %)	79.0	0	21.0	0	0
	δO^{18} per mil	24.0	28.0	24.0	--	--
	δC^{13} per mil	0.7	--	0	--	--

TABLE 20 (continued)

BC-8 Phlogopite Marble

$$3CaMg(CO_3)_2 + KAlSi_3O_8 + H_2O \rightleftharpoons KMg_3AlSi_3O_{10}(OH)_2 + 3CaCO_3 + 3CO_2$$

dolomite — K-feldspar — phlogopite — calcite

		Dolomite	K-feldspar	H_2O	Phlogopite	Calcite	CO_2
After Decarbonation	Mode (vol %)	0	5	0	25	70	?
	Molecular proportion	0	0.36	0	1.20	14.0	3.60
	Oxygen (atom %)	0	4.2	0	21.8	63.2	10.8
	Carbon (atom %)	0	0	0	0	80	20
	δO^{18} per mil	--	19.0	--	14.4	19.3	61.0
	δC^{13} per mil	--	--	--	--	-1.0	5.4
Before Decarbonation	Molecular proportion	3.60	1.56	1.2	0	10.4	0
	Oxygen (atom %)	33.0	19.0	2.0	0	46.0	0
	Carbon (atom %)	40.0	0	0	0	60.0	0
	δO^{18} per mil	24.0	17.0	~0	--	24.0	--
	δC^{13} per mil	0.7	--	--	--	0	--

decarbonation but BC-8 is completely out of equilibrium. It has been shown in the laboratory that CO_2 and calcite can easily attain isotopic equilibrium in the temperature range 350 to 610°C within a few days (O'Neil and Epstein, 1966). Even if decarbonation involves very large kinetic oxygen isotopic fractionation, re-equilibration between CO_2 and carbonates would probably bring the ΔO^{18} to near-equilibrium values provided the liberated CO_2 does not escape rapidly out of the rock. Therefore, some of the assumptions used in the calculation for BC-8 may not be valid. For example, the original dolomite and calcite might have had lower O^{18}/O^{16} ratios than those used in the calculation.

A much simpler case of contact metamorphic decarbonation was observed in sample A-6 from Marble Canyon, Trans-Pecos Texas (Figure 30). The calculation was made on a mono-mineralic wollastonite layer with δO^{18} = 14.4, which was bounded by a quartz layer with δO^{18} = 14.8 on one side and a calcite layer with δO^{18} = 23.3 on the other side. The wollastonite apparently has formed from the reaction:

$$CaCO_3 + SiO_2 = CaSiO_3 + CO_2$$

Material balance shows that the liberated CO_2 would have O^{18} = 28.2 per mil, or $\Delta_{CO_2 - CaCO_3} = 4.9$. The value is very similar to that in BC-32E and probably close to the equilibrium fractionation value.

It is thus concluded that the CO_2 liberated from decarbonation of carbonates during contact metamorphism is very significantly richer in O^{18} and C^{13} than the original carbonates. Inasmuch as most marine limestones have δC^{13}-values close to zero, one would expect that decarbonation of the limestones would give off CO_2 with δC^{13}-values greater than zero. However,

most of the CO_2 gas samples from Yellowstone Park (Craig, 1953, 1963), Utah and New Mexico (Zartman et al., 1961), and other places (Hulston and McCabe, 1962; Lang, 1959)) have negative δC^{13} -values (average about -5 per mil). Unless there is evidence for isotopic exchange with other carbon with very light isotopic values (e.g., organic carbon), the CO_2 gas samples mentioned above can hardly be expected to be simply derived from the decarbonation of marine limestones as most authors suggested. A more plausible source for such CO_2 samples is "juvenile" CO_2 emanations from igneous rocks (see Taylor et al., 1967).

It should also be pointed out that most of the irregular skarn bodies in the Birch Creek contact zone are clearly formed by metasomatic reactions between the carbonate rock and the volatiles evolving from the magma. In this case, the combination of isotopic exchange with the volatiles together with the decarbonation effects would greatly enhance the lowering of the isotopic values.

6.8 Comparison of isotopic relationships in contact and regional metamorphic rocks

A. Oxygen isotopes

One of the major problems in metamorphic petrology is whether truly magmatic or "juvenile" water plays an important role during metamorphism. Oxygen isotopic analysis of metamorphic rocks may help to unravel the problem. If the metasedimentary rocks have undergone isotopic exchange with significant quantities of pore-fluids in communication with or derived from plutonic rocks during metamorphism, one should expect a decrease in O^{18}/O^{16} ratios with

increasing metamorphic grade. If metamorphism involves only simple loss of water through dehydration reactions, then the O^{18}/O^{16} ratios of metasedimentary rocks should essentially remain constant during progressive metamorphism (see section 6.5).

Figure 46 shows a plot of the O^{18}/O^{16} ratios of pelitic rocks from different metamorphic grades and zones of regional and contact metamorphism. The O^{18}/O^{16} ratios from regional metamorphic rocks were taken or calculated from data analyzed by Garlick and Epstein (1967), Clayton and Mayeda (1963), and Taylor (1968 a). A few garnet-grade pelitic schists from southeastern Vermont were excluded because of the abnormally low O^{18}/O^{16} ratios in the rocks. The O^{18}/O^{16} ratios of shale were taken from Taylor and Epstein (1964) and Savin (1967). For contact metamorphic rocks, only the pelitic rocks from the Santa Rosa Range and Birch Creek (including the schist xenolith) were plotted in the figure because these are the only samples studied for which distinct metamorphic zones are recognizable.

It is rather striking from Figure 46 that in regional metamorphic rocks, the O^{18}/O^{16} ratios of pelitic rocks tend to decrease with increasing metamorphic grade. In contact metamorphic rocks, the O^{18}/O^{16} ratios remain exceedingly constant throughout the entire contact aureole except for samples from the very narrow exchanged zones, the re-entrant, and the xenolith, where the O^{18}/O^{16} ratios are considerably lower. Except for the latter samples, it is also noted that the O^{18}/O^{16} ratios of pelitic rocks in the contact metamorphic aureoles are within range of the O^{18}/O^{16} ratios of shale and chlorite-grade regional metamorphic rocks. The O^{18}/O^{16} ratios of samples from the xenolith, the re-entrant, and the exchanged zones lie in

Figure 46. O^{18}/O^{16} ratios of pelitic rocks plotted against metamorphic grade for both regional and contact metamorphism. Data are from the present study, Garlick and Epstein (1967), Clayton and Mayeda (1963), Taylor (1968 a), Taylor and Epstein (1964) and Savin (1967).

Figure 47. O^{18}/O^{16} ratios of contact metamorphic and regional metamorphic marbles plotted against metamorphic grade. The upper amphibolite facies in the Grenville may be equivalent to sillimanite grade. The general range of O^{18}/O^{16} ratios of normal marine limestones are also included for reference. Data are from the present study, Sheppard (1966), and Schwarcz (1966).

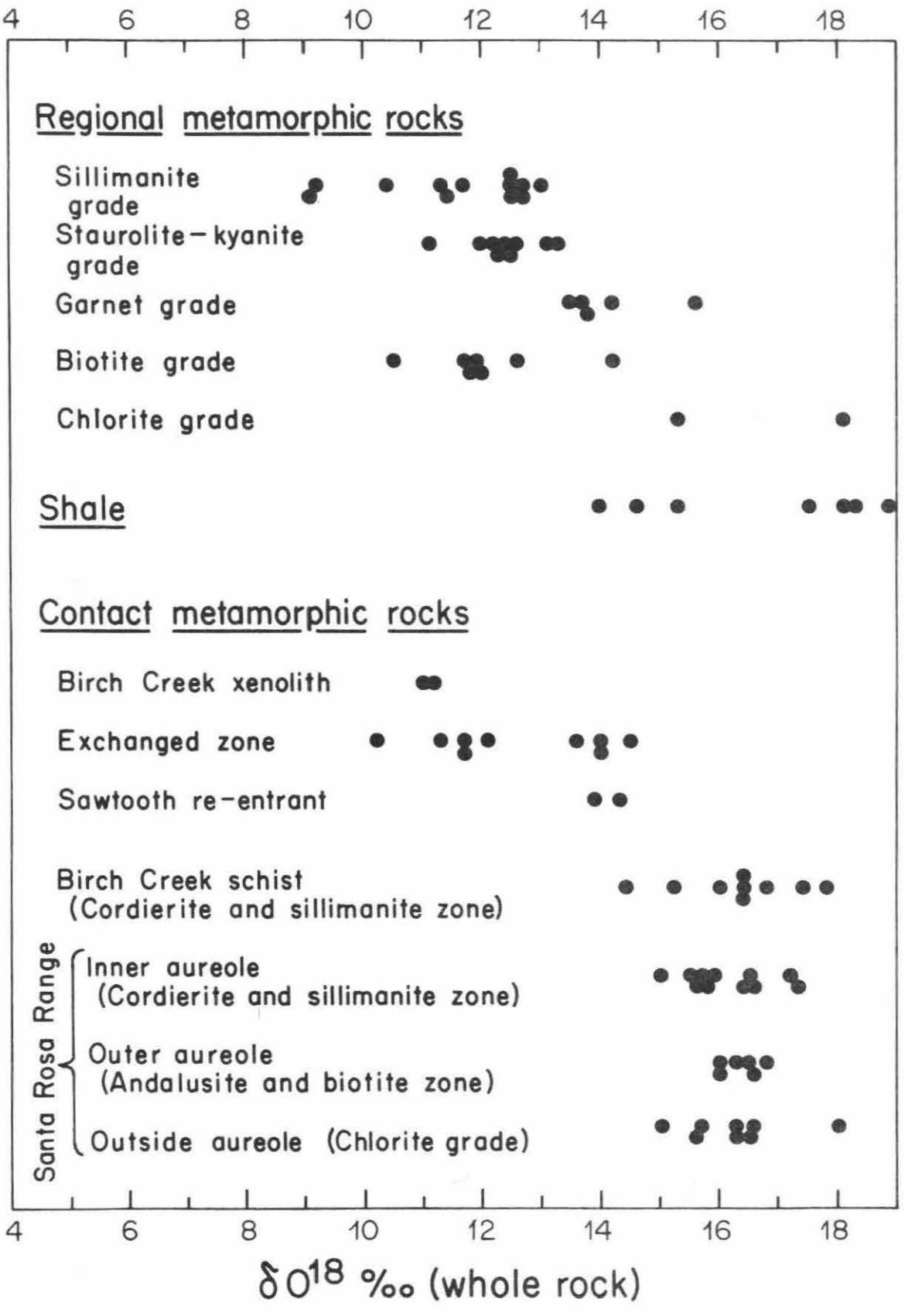
4
6
8
10
12
14
16
18
Regional metamorphic rocks
Sillimanite grade
Staurolite – kyanite grade
Garnet grade
Biotite grade
Chlorite grade
Shale
Contact metamorphic rocks
Birch Creek xenolith
Exchanged zone
Sawtooth re-entrant
Birch Creek schist (Cordierite and sillimanite zone)
Santa Rosa Range
Inner aureole (Cordierite and sillimanite zone)
Outer aureole (Andalusite and biotite zone)
Outside aureole (Chlorite grade)
δ O18 ‰ (whole rock)

Figure 46

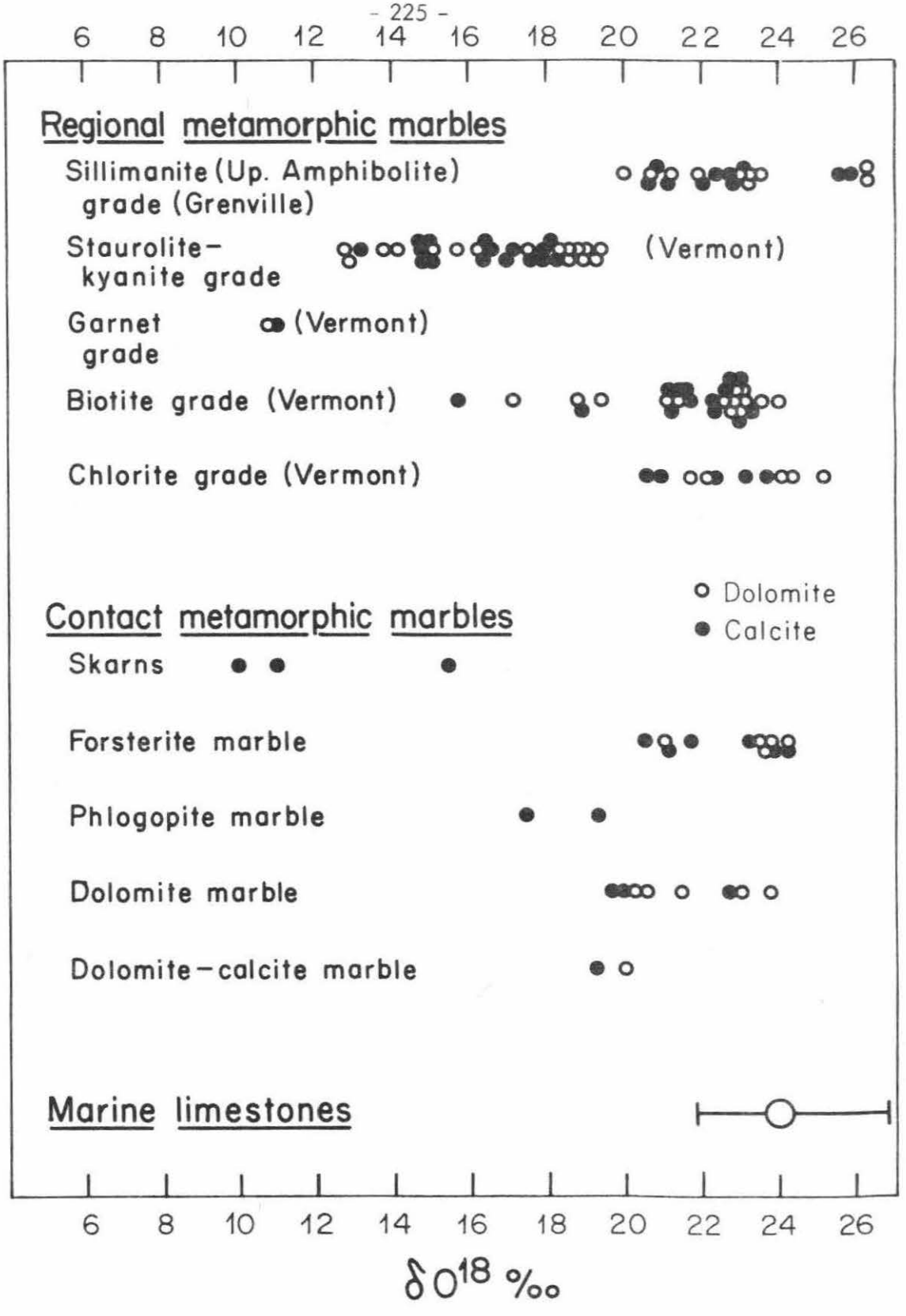
6 8 10 12 14 16 18 20 22 24 26
Regional metamorphic marbles
Sillimanite (Up. Amphibolite) grade (Grenville)
Staurolite–kyanite grade
(Vermont)
Garnet grade
(Vermont)
Biotite grade (Vermont)
Chlorite grade (Vermont)
Dolomite
Calcite
Contact metamorphic marbles
Skarns
Forsterite marble
Phlogopite marble
Dolomite marble
Dolomite–calcite marble
Marine limestones
6 8 10 12 14 16 18 20 22 24 26
δO18 ‰

Figure 47

about the same range as those in the higher-grade regional metamorphic rocks.

The O^{18}/O^{16} ratios of contact and regional metamorphic marbles from various metamorphic grades are shown in Figure 47. The regional metamorphic marbles from Vermont and the Grenville Province were analyzed by Sheppard (1966) and Schwarcz (1966). There is a tendency for the Vermont samples to decrease in O^{18}/O^{16} ratios from lower to higher grade. However, the sillimanite-grade samples from the Grenville show O^{18}/O^{16} ratios identical to the chlorite-grade samples from Vermont, and are within the range of normal marine limestones. The contact metamorphic marbles from Birch Creek show O^{18}/O^{16} ratios within or very close to the range of normal marine limestones, but the skarns are considerably O^{18}-depleted. It appears that the relation between the O^{18}/O^{16} ratios of marbles and metamorphic grade is complex. It seems plausible that oxygen isotopic exchange with an external reservoir may be the main process controlling the O^{18}/O^{16} ratios of the pelitic rocks. However, in carbonate rocks, in addition to the possibility of open-system isotopic exchange, the isotopic fractionations accompanying decarbonation are also of prime importance (see section 6.7), and the extent of decarbonation in marbles is not necessarily proportional to metamorphic grade.

B. Carbon isotopes

The C^{13}/C^{12} ratios of contact and regional metamorphic marbles from various metamorphic grades are plotted in Figure 48. Nearly all of the samples lie in the range of normal marine limestones. In regional metamorphic marbles, the C^{13}/C^{12} ratios show a large scatter and remain essentially

Figure 48. C^{13}/C^{12} ratios of contact metamorphic and regional metamorphic marbles plotted against metamorphic grade. Also included is the general range of C^{13}/C^{12} ratios of normal marine limestones. Data are from the present study, Sheppard (1966), and Schwarcz (1966).

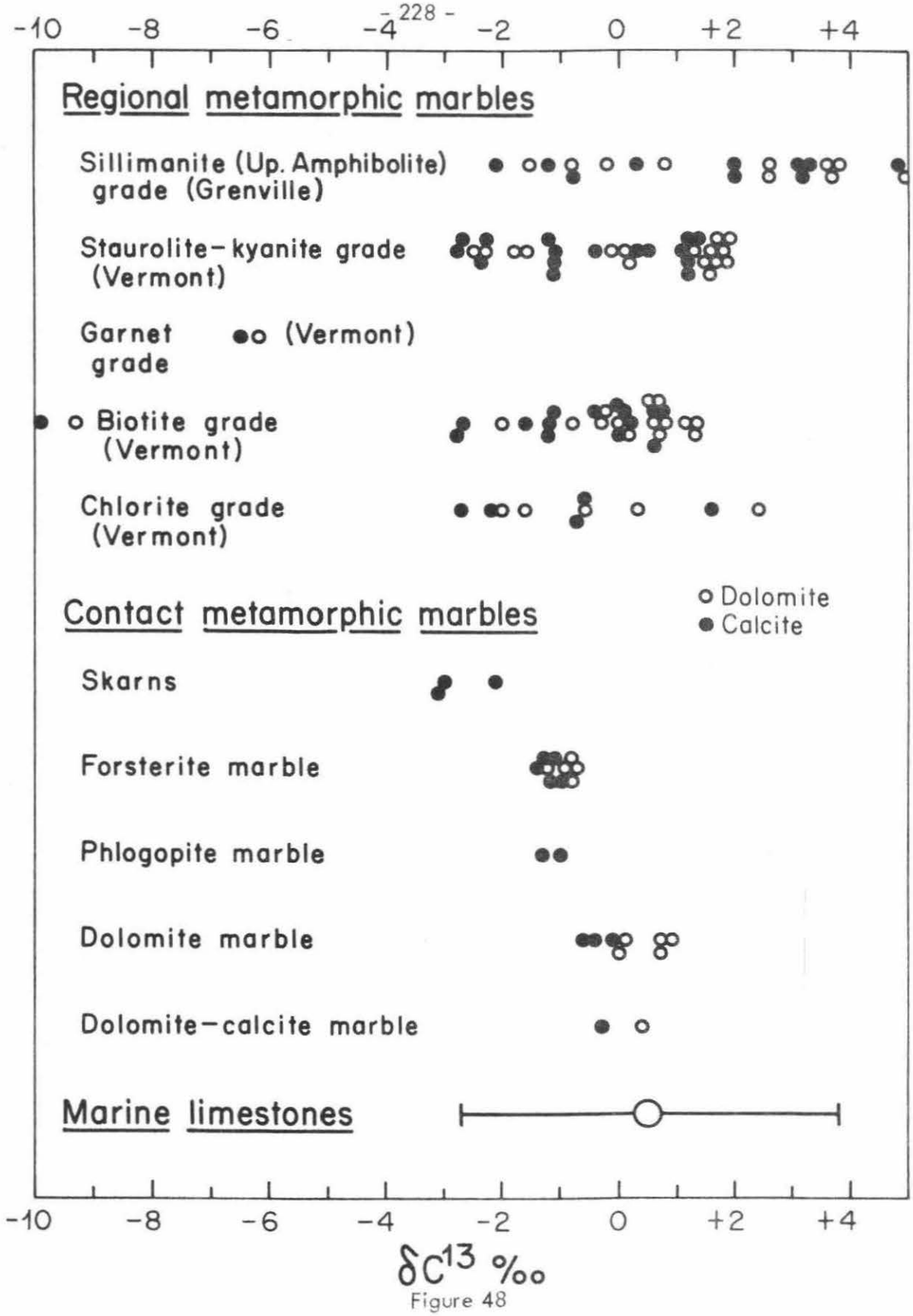
-10
-8
-6
-4
-2
0
+2
+4
Regional metamorphic marbles
Sillimanite (Up. Amphibolite) grade (Grenville)
Staurolite–kyanite grade (Vermont)
Garnet grade (Vermont)
Biotite grade (Vermont)
Chlorite grade (Vermont)
Contact metamorphic marbles
Dolomite
Calcite
Skarns
Forsterite marble
Phlogopite marble
Dolomite marble
Dolomite–calcite marble
Marine limestones
δC13 ‰

Figure 48

constant throughout various metamorphic grades. In the Birch Creek contact metamorphic marbles, the C^{13}/C^{12} ratios show a correlation with metamorphic grade. However, this is fundamentally a correlation with the presence or absence of calc-silicate minerals, a feature which is also observed in certain regionally metamorphosed samples from Vermont (Sheppard, 1966).

C. Hydrogen isotopes

The range of D/H ratios for samples analyzed in the present research and for samples from regional metamorphic rocks (Taylor and Epstein, 1966) are shown in Figure 49. The minerals in contact metamorphic rocks and in the associated plutons in general tend to have lower D/H ratios than regional metamorphic rocks. The D/H ratios in the country rocks surrounding the Sawtooth, Flynn, Birch Creek, and Eldora plutons are almost indistinguishable from the D/H ratios in the intrusives.

In contact metamorphic rocks and the associated plutons, there is a rough correlation between the D/H ratios and geographic locations of samples, as the Rocky Mountain samples (e.g., the Eldora stock in Colorado) tend to be low in deuterium. Friedman et al. (1964 b) showed that the D/H ratios of continental surface water tend to decrease with the latitude and the altitude of the ground surface. The D/H ratios of surface waters in the Western United States as determined by Friedman et al. are shown in Figure 50. The Rocky Mountain surface waters are most depleted in deuterium, the intermountain plateau waters next, and the Sierra Nevada waters least depleted, of the three general areas studied in the present work. Geographically

Figure 49. Plot of D/H ratios of muscovite, biotite and hornblende for contact metamorphic rocks and the associated intrusions from Birch Creek, Santa Rosa Range, and Eldora. The range of D/H ratios of regional metamorphic muscovites, chlorites, and biotites analyzed by Taylor and Epstein (1966) are also included for comparison.

Figure 50. Range and mean of D/H ratios of surface waters in the Western United States (after Friedman et al., 1964 b).

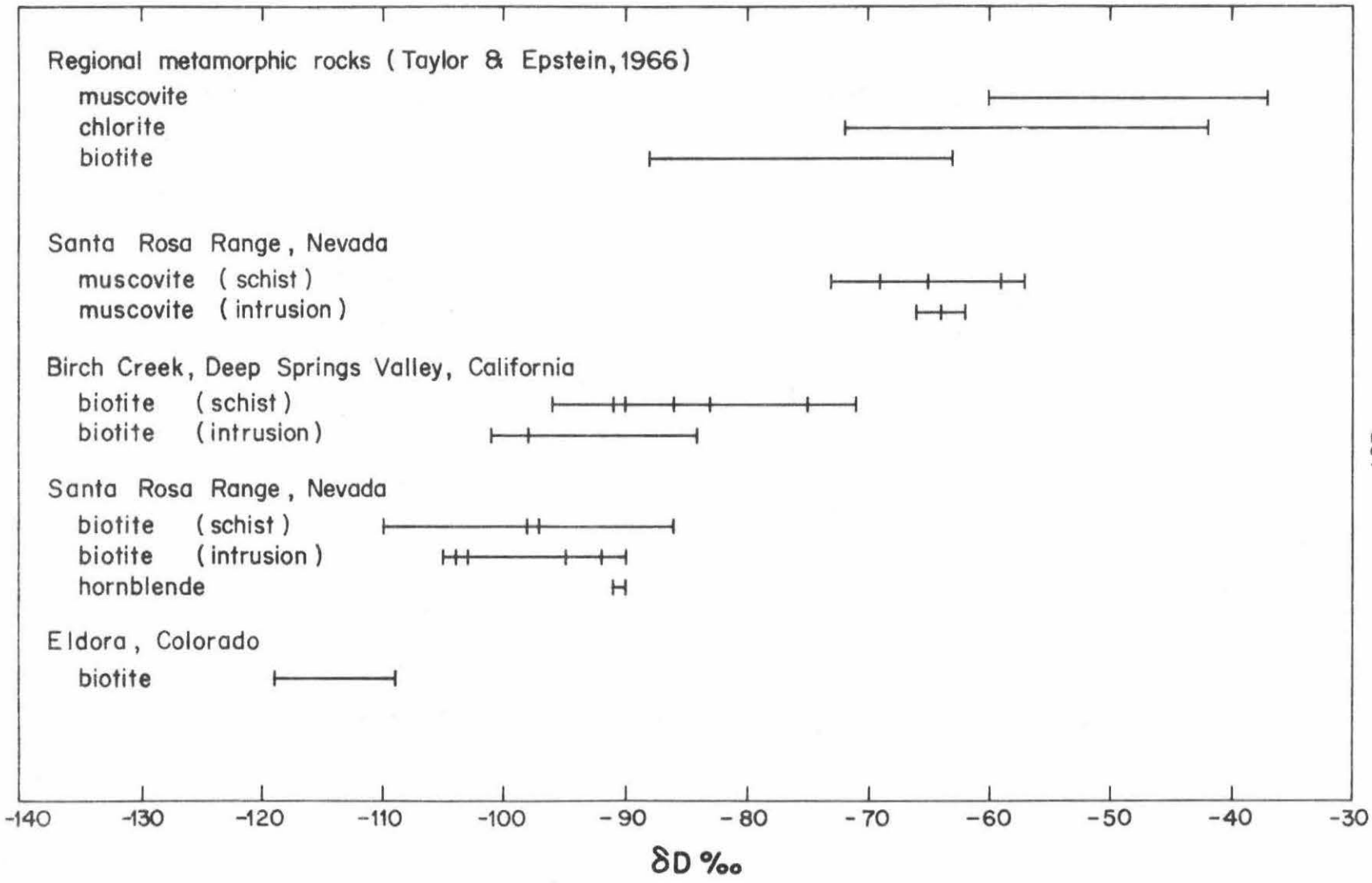
Regional metamorphic rocks (Taylor & Epstein, 1966)
muscovite
chlorite
biotite
Santa Rosa Range, Nevada
muscovite (schist)
muscovite (intrusion)
Birch Creek, Deep Springs Valley, California
biotite (schist)
biotite (intrusion)
Santa Rosa Range, Nevada
biotite (schist)
biotite (intrusion)
hornblende
Eldora, Colorado
biotite
-140
-130
-120
-110
-100
-90
-80
-70
-60
-50
-40
-30
δD ‰

Figure 49

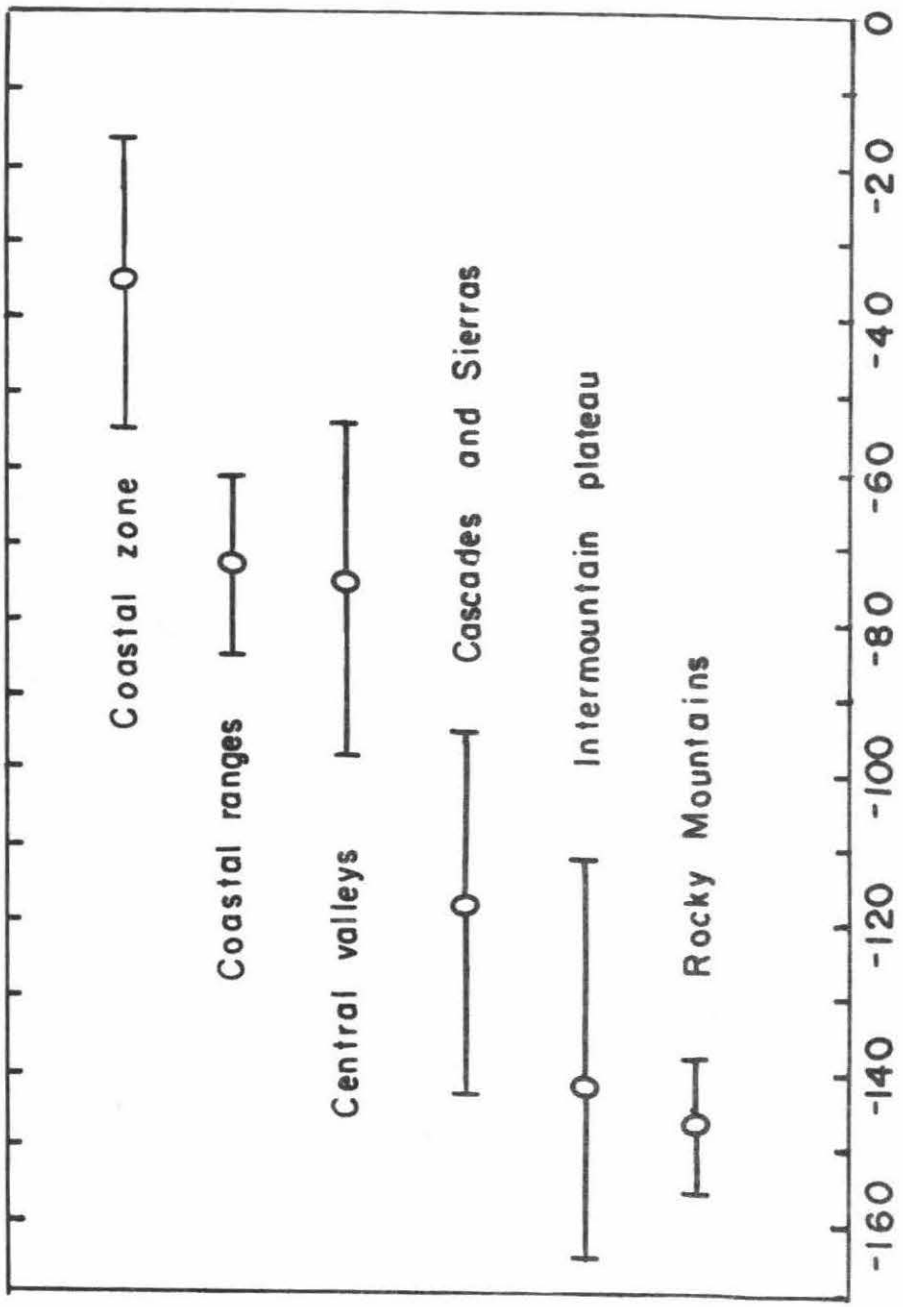
Coastal zone
Coastal ranges
Central valleys
Cascades and Sierras
Intermountain plateau
Rocky Mountains
0
-20
-40
-60
-80
-100
-120
-140
-160
δD ‰

Figure 50

these areas correspond, respectively, to the Eldora, Santa Rosa, and Birch Creek localities; it is therefore conceivable that the rough correlation between the D/H ratios in these contact metamorphic minerals and the nearby surface waters may be a result of control by local meteoric ground waters. From isotopic analyses of hydrated volcanic glass, Taylor (1968 b) has shown that, even as far back as the early Tertiary, meteoric water patterns in the Western United States were apparently similar to those prevailing today.

VII. SUMMARY AND CONCLUSIONS

1. The consistent order of O^{18}/O^{16}, C^{13}/C^{12}, and D/H enrichment in coexisting minerals of contact metamorphic rocks is similar to relationships previously observed in regional metamorphic and igneous rocks; this strongly suggests that mineral assemblages in general tend to approach isotopic equilibrium during contact metamorphism.

2. The correlation between isotopic fractionations among coexisting mineral pairs is also indicative of isotopic equilibrium. In the present study, the following relationships are observed:

$$\Delta O^{18}_{\text{quartz-muscovite}} = 0.49\, \Delta O^{18}_{\text{quartz-biotite}}$$

$$\Delta O^{18}_{\text{feldspar-biotite}} = 0.67\, \Delta O^{18}_{\text{quartz-biotite}}$$

$$\Delta O^{18}_{\text{quartz-biotite}} = 0.59\, \Delta O^{18}_{\text{quartz-magnetite}}$$

$$\Delta C^{13}_{\text{dolomite-calcite}} = 0.37\, \Delta O^{18}_{\text{dolomite-calcite}} + 0.35$$

The ratio Δ quartz-muscovite/Δ quartz-biotite is apparently different for different rock types; it is 0.54 for regional metamorphic rocks, 0.48 for plutonic granitic rocks, and 0.49 for contact metamorphic rocks.

3. A correlation between oxygen isotopic fractionations and sample distance from contact is observed in certain cases in the present study; the best traverse in this respect is at Birch Creek where a regular decrease of quartz-biotite fractionations (from 6.8 to 5.9) is observed in 8 samples collected from 1300 feet to 0.25 feet of the contact.

4. Small-scale oxygen isotope exchange effects between igneous intrusions and adjacent country rocks are observed within 0.5 to 3 feet of the intrusive contacts. The existence of a steep isotopic gradient (about 3 per mil

per foot) in the exchanged zones, on both the intrusive side and the country rock side of the contact, suggests that the small-scale isotopic exchange occurred essentially in the crystalline state by a diffusion-controlled recrystallization process. This presumably took place by grain-boundary diffusion in a static interstitial fluid film.

5. The degree of small-scale oxygen isotope exchange is essentially identical for different coexisting minerals, except for 3 exceedingly fine-grained magnetites and one pegmatite K-feldspar; these have undergone much more extensive isotopic exchange, perhaps with meteoric water.

6. The size of the oxygen isotope equilibrium system in the small-scale exchanged zones is very small; it ranges from about 1.5 cm to 30 cm. The size of such an equilibrium system shows a good correlation with the presumed physical conditions at each contact during magmatic intrusion. The larger-size systems are associated with higher temperatures, larger intrusions, longer times of heating, and greater availability of aqueous fluids.

7. Samples at the intrusive-country rock contacts have been demonstrated to contain mineral assemblages in oxygen isotope equilibrium, because identical O^{18}/O^{16} ratios of a particular mineral were attained by approaching isotopic equilibrium from opposite directions. At the contacts we typically observe a lowering of the country rock O^{18}/O^{16} ratios by about 3 to 4 per mil and an increase in the intrusive O^{18}/O^{16} ratios by about 1 to 2 per mil.

8. Based on oxygen isotope fractionation calibration curves, the contact temperatures are estimated to be 555°C at the Sawtooth stock, 525°C

at the Santa Rosa stock, 540°C at the Birch Creek pluton, and 625°C at the Caribou stock. Except at the contact of the Santa Rosa stock, the isotopic contact temperatures agree well with temperatures estimated from heat flow calculations and from mineral parageneses.

9. The abnormally low isotopic country rock temperatures in the Santa Rosa and Sawtooth I traverses are compatible with a heat flow model (F) based on their occurrence at the tips of tongue-like portions of the intrusives that project outward into the country rock. The isotopic temperatures obtained from samples in a xenolith and a re-entrant of country rock that projects inward into the intrusion are higher than those obtained on samples collected in the vicinity of planar contacts; this also agrees with heat flow considerations.

10. Samples from tiny intrusive bodies and dikes and from the marginal portions of most of the larger plutons have unusually high O^{18}/O^{16} ratios relative to "normal" igneous rocks from the central portions of plutons. This is interpreted to be the result of large-scale oxygen isotopic exchange between essentially molten igneous rock and metasedimentary country rock, either through a medium of aqueous fluids or by contamination with xenolithic blocks of country rock. Direct influx and absorption of water from the country rock may also be significant in certain intrusive stocks that are initially undersaturated with respect to H_2O.

11. The fact that only a very narrow zone of country rock has undergone isotopic exchange with the intrusive implies that horizontal outward movement of water into the contact metamorphic aureole is almost negligible during crystallization of the granitic magmas studied in this research.

12. The oxygen isotope exchange effects in a xenolith and in a re-entrant were found to be much more extensive than the exchange effects observed at main intrusive-country rock contacts, indicating that large-scale isotopic homogenization can occur in such instances, probably through upward transfer of H_2O-rich volatile fluids.

13. The O^{18}/O^{16} and D/H ratios of pelitic rocks do not show any appreciable change across the various mineralogical and textural zones in the contact metamorphic aureoles, suggesting that no significant oxygen and hydrogen isotope fractionations accompany metamorphic dehydration reactions.

14. The O^{18}/O^{16} ratios of pelitic rocks throughout all the contact metamorphic aureoles, except for the re-entrant, xenolith, and small-scale exchanged zones, are within the range of O^{18}/O^{16} ratios of shale and chlorite-grade regional metamorphic rocks. This is in contrast to the behavior of pelitic rocks in regional metamorphism, in which a decrease of O^{18}/O^{16} ratios generally accompanies increasing metamorphic grade.

15. The contact metamorphic marbles that are low in O^{18}/O^{16} ratios also tend to be low in C^{13}/C^{12} ratios, and they are frequently associated with calc-silicate minerals, indicating that the CO_2 liberated during metamorphic decarbonation reactions is enriched in both O^{18} and C^{13} relative to the carbonates. Material balance calculations show that the liberated CO_2 is about 5 per mil richer in O^{18} and about 6 per mil richer in C^{13} than coexisting calcite. Therefore, it is unlikely that most occurrences of CO_2 gas in nature, which are commonly similar to or slightly lower in C^{13} than limestones, can be a result of contact metamorphic decarbonation reactions.

16. The D/H ratios of muscovite and biotite are lower in contact metamorphic rocks than in regional metamorphic rocks. Also the D/H ratios of contact metamorphic biotites in the western United States show a geographic correlation that is roughly similar to that shown by the D/H ratios of meteoric surface waters.

17. The O^{18}/O^{16} ratios of the K-feldspars in the Eldora contact zone do not show any appreciable change across the microcline-orthoclase transition boundary.

18. The chemical analyses of pelitic rocks from the Sawtooth aureole and the Flynn aureole (Compton, 1960), when plotted on Thompson diagrams, suggest that the different mineral assemblages that are developed in the aureoles may be explained in terms of differences in bulk chemical compositions of the rocks.

REFERENCES

Anderson, A. T., The dimensions of oxygen isotopic equilibrium attainment during prograde metamorphism, J. Geol., 75, 323-332, 1967.

Baertschi, P., Isotopic composition of the oxygen in silicate rocks, Nature, 166, 112-113, 1950.

Baertschi, P., Messung und Deutung relativer Haufigkeitsvariationen von O^{18} und C^{13} in Karbonatgesteinen und Mineralien, Schweiz. Min. Petr. Mitt., 37, 73-152, 1957.

Baertschi, P. and S. R. Silverman, The determination of the relative abundance of the oxygen isotopes in silicate rocks, Geochim. et Cosmochim. Acta 1, 317, 1951.

Barth, T. F. W., Theoretical Petrology, John Wiley and Sons, New York, 1962.

Bigeleisen, J., The relative reaction velocities of isotopic molecules, J. Chem. Phys. 17, 675, 1949.

Bigeleisen, J. and M. G. Mayer, Calculation of equilibrium constants for isotopic exchange reactions, J. Chem. Phys. 15, 261, 1947.

Bowen, N. L., Diffusion in silicate melts, J. Geol. 29, 295-317, 1921.

Bowen, N. L., Progressive metamorphism of siliceous limestone and dolomite, J. Geol., 48, 225-274, 1940.

Bridge, T. E., Contact metamorphism in the siliceous limestones and dolomites and the geology of the related intrusion in Marble Canyon, Culberson County, Trans-Pecos Texas, Geol. Soc. Am. Spec. Paper 82, 19, 1965.

Bridge, T. E., Contact metamorphism in the siliceous limestones and dolomites and the geology of the related intrusion in Marble Canyon, Culberson County, Trans-Pecos Texas, Ph.D. Thesis, Univ. Texas, 1966 a.

Bridge, T. E., Bredigite, larnite, and γ dicalcium silicates from Marble Canyon, Am. Mineral., 51, 1766-1774, 1966 b.

Burnham, C. W., Hydrothermal fluids at the magmatic stage, in Geochemistry of Hydrothermal Ore Deposits, ed., H. L. Barnes, New York, Holt, Rinehart and Winston, 34-76, 1967.

Burnham, C. W., and R. H. Jahns, A method for determining the solubility of water in silicate melts, Am. J. Sci., 260, 721-745, 1962.

Carslaw, H. S., and J. C. Jaeger, Conduction of Heat in Solids, 2nd. ed., Oxford, Oxford University Press, 1959.

Choudhury, A., et al., Study of oxygen diffusion in quartz by using the nuclear reaction O^{18} (p, α) N^{15}, Solid State Comm., 3, 119-122, 1965.

Clayton, R. N., Oxygen isotope fractionation between calcium carbonate and water, J. Chem. Phys. 34, 724-726, 1961.

Clayton, R. N., and S. Epstein, The relationships between O^{18}/O^{16} ratios in coexisting quartz carbonate and iron oxides from various geologic deposits, J. Geol. 66, 352, 1958.

Clayton, R. N., and T. D. Mayeda, The use of bromine pentafluoride in the extraction of oxygen from oxides and silicates for isotopic analysis, Geochim. et Cosmochim. Acta 27, 43, 1963.

Clayton, R. N., J. R. O'Neil, T. Mayeda, 1967, unpublished data.

Compton, R. R., Contact metamorphism in Santa Rosa Range, Nevada, Geol. Soc. Am. Bull., 71, 1383-1416, 1960.

Craig, H., The geochemistry of the stable carbon isotopes, Geochim. et Cosmochim. Acta, 3, 53-92, 1953.

Craig, H., Isotopic standards for carbon and oxygen and the correction factors for mass spectrometric analysis of carbon dioxide, Geochim. et Cosmochim. Acta 12, 133, 1957.

Craig, H., Standards for reporting concentrations of deuterium and oxygen O^{18} in natural water, Science 133, 1833, 1961.

Craig, H., The isotopic geochemistry of water and carbon in geothermal areas, Symp. Nuclear Geol. Geothermal Areas, Spoleto, Italy, 17-53, 1963.

Cree, A., Tertiary intrusives in the Hessie-Tolland area, Boulder and Gilpin Counties, Colorado, Ph.D. thesis, Univ. Colorado, 1948.

Doe, B. R., and S. R. Hart, The effect of contact metamorphism on lead in potassium feldspars near the Eldora stock, Colorado, J. Geophys. Res. 68, 3521-3530, 1963.

Engel, A. E. G., R. N. Clayton and S. Epstein, Variations in isotopic composition of oxygen and carbon in Leadville limestone (Mississippian, Colorado) and its hydrothermal metamorphic phases; J. Geol. 66, 374, 1958.

Epstein, S., D. L. Graf, and E. T. Degens, Oxygen isotope studies on the origin of dolomites, in Isotopic and Cosmic Chemistry (Urey volume), ed. by H. Craig et al., North-Holland Pub. Co., Amsterdam, 169-180, 1964.

Evans, B. W., Application of a reaction-rate method to the breakdown equilibria of muscovite and muscovite plus quartz, Am. J. Sci., 263, 647-667, 1965.

Friedman, I., Deuterium content of natural waters and other substances, Geochim. et Cosmochim. Acta, 4, 89-103, 1953.

Friedman, I., R. L. Smith, B. Levin, and A. Moore, The water and deuterium content of phenocrysts from rhyolitic lavas, in Isotopic Cosmic Chemistry (Urey volume), ed. by H. Craig et al., North- Holland Publ. Co., Amsterdam, 200-204, 1964 a.

Friedman, I., A. C. Redfield, B. Schoen, and J. Harris, The variation of the deuterium content of natural waters in the hydrologic cycle, Rev. Geophys., 2 (1), 177-224, 1964 b.

Fyfe, W. S., F. J. Turner, and J. Verhoogen, Metamorphic reactions and metamorphic facies, Geol. Soc. Am., Memoir 73, 1958.

Fyfe, W. S., and F. J. Turner, Reappraisal of the metamorphic facies concept, Contrib. Mineral. Petrol., 12, 354-365, 1966.

Garlick, G. D., Oxygen isotope ratios in coexisting minerals of regionally metamorphosed rock, Ph.D. thesis, California Institute of Technology, 1964.

Garlick, G. D., and S. Epstein, The isotopic composition of oxygen and carbon in hydrothermal minerals in Butte, Montana, Econ. Geol., 61, 1325-1335, 1966.

Garlick, G. D., and S. Epstein, Oxygen isotope ratios in coexisting minerals of regionally metamorphosed rocks, Geochim. et Cosmochim. Acta, 31, 181-214, 1967.

Godfrey, J. D., The deuterium content of hydrous minerals from the east-central Sierra Nevada and Yosemite National Park, Geochim. et Cosmochim. Acta, 26, 1215-1245, 1962.

Harker, A., Metamorphism, 2nd ed., E. P. Dutton & Co., New York, 1939.

Hart, S. R., The petrology and isotopic-mineral age relations of a contact zone in the Front Range, Colorado, J. Geol. 72, 493-523, 1964.

Haul, R., and G. Dümbgen, Untersuchung der Sauerstoffbeweglichkeit in Titandioxyd, Quarz und Quarzglas mit Hilfe des hetergenen Isotopenaustausches, Zeitschift für Elcktrochemie, 1962.

Hoering, T. C., The physical chemistry of isotopic substances, Ann. report of the Director of the Geophysical laboratory, 201, 1960-1961.

Hulston, J. R., and W. J. McCabe, Mass spectrometer measurements in the thermal areas of New Zealand, Part 2, Carbon isotopic ratios, Geochim.et Cosmochim. Acta, 26, 399-410, 1962.

Jaeger, J. C., The temperature in the neighborhood of a cooling intrusive sheet, Am. J. Sci., 255, 306-318, 1957.

Jaeger, J. C., Temperatures outside a cooling intrusive sheet, Am. J. Sci., 257, 44-45, 1959.

Jaeger, J. C., The cooling of irregularly shaped igneous bodies, Am. J. Sci., 259, 721-734, 1961.

Jaeger, J. C., Thermal effects of intrusions, Rev. Geophys. 2, 443-466, 1964.

James, H. L. and R. N. Clayton, Oxygen isotope fractionation in metamorphosed iron formations of the Lake Superior region and in other iron-rich rocks, Geol. Soc. Am. Buddington Volume, 217, 1962.

Kennedy, G. C., Some aspects of the role of water in rock melts, Geol. Soc. Am. Spec. Paper 62, 489-503, 1955.

Lang, W. B., The origin of some natural carbon dioxide gases, J. Geophys. Res., 64, 127-131, 1959.

Lovering, T. S. Heat conduction in dissimilar rocks and the use of thermal models, Geol. Soc. Am. Bull. 47, 87-100, 1936.

Lovering, T. S. and E. N. Goddard, Geology and ore deposits of the Front Range, Colorado, U. S. Geol. Survey Prof. Paper 223, 1950.

McCrea, J. M., The isotopic chemistry of carbonates and a paleotemperature scale, J. Chem. Phys. 18, 849-857, 1950.

McKee, E. H., and D. B. Nash, Potassium-argon ages of granitic rocks in the Inyo Batholith, east-central California, Geol. Soc. Am. Bull., 78, 669-680, 1967.

McKinney, C. R. et al., Improvements in mass spectrometers for the measurement of small differences in isotopic abundance ratios, Rev. Sci. Instr. 21, 724, 1950.

M iller, W. J., Geology of Deep Springs Valley, California, J. Geol., 36, 510-525, 1928.

Nash, D. B., Contact metamorphism at Birch Creek, Blanco Mountain quadrangle, Inyo County, California, M.S. thesis, University California, Berkeley, 1962.

Nash, D. B.,Metamorphism along a composite granite-sedimentary contact zone at Birch Creek, Deep Springs Valley, California, Geol. Soc. Am. Spec. Paper 76, 216 (abstract), 1964.

Nelson, C. A., Lower Cambrian-Precambrian succession, White-Inyo Mountains, California, Geol. Soc. Am. Bull.,73, 139-144, 1962.

Nelson, C.A.,Geological map of the Blanco Mountain quadrangle, Inyo and Mono Counties, California, U.S. Geol. Survey GQ-529, 1966.

Nelson, C. A., and A. G. Sylvester, Forceful emplacement of the Birch Creek pluton, White Mountains, California, Geol. Soc. Am. Spec. Paper 87, 220-221, 1966.

Nier, A. O. C., A mass spectrometer for isotope and gas analysis, Rev. Sci. Instr. 18, 398, 1947.

Northrop, D. A., and R. N. Clayton, Oxygen-isotope fractionations in systems containing dolomite, J. Geol., 74, 174-196, 1966.

O'Neil, J. R., and R. N. Clayton, Oxygen isotope geothermometry, in Isotopic and Cosmic Chemistry (Urey volume), ed. by H. Craig, et al., North-Holland Publishing Company, Amsterdam, 157-168, 1964.

O'Neil, J. R., and S. Epstein, Oxygen isotope fractionation in the system dolomite-calcite-carbon dioxide, Science, 152, 198-201, 1966.

O'Neil, J. R., and H. P. Taylor, Jr., The oxygen isotope and cation exchange chemistry of feldspars, Amer. Mineralogist, 52, 1414-1437, 1967.

O'Neil, J. R., and H. P. Taylor, Jr., Oxygen isotope fractionation between muscovite and water (abstract), Trans. Am. Geophys. Union, 47 (1), 212, 1966.

Perry, E. C., Jr., and B. Bonnichsen, Quartz and magnetite-oxygen 18-oxygen 16 fractionation in metamorphosed Biwabik iron formation, Science, 153, 528-529, 1966.

Richardson, S. W., P. M. Bell, and M. C. Gilbert, Kyanite-sillimanite relations, Carnegie Inst. Wash. Yr. Book, 65, 247-248, 1966.

Savin, S. M., Oxygen and hydrogen isotope ratios in sedimentary rocks and minerals, Ph.D. thesis, California Institute of Technology, 1967.

Schwander, H., Bestimmung des relativen Sauerstoffisotopen-Verhältnisses in Silikatgesteinen und Mineralien, Geochim. et Cosmochim. Acta 4, 261, 1953.

Schwarcz, H. P., Oxygen and carbon isotopic fractionation between coexisting metamorphic calcite and dolomite, J. Geol., 74, 38-48, 1966.

Sharma, T., and R. N. Clayton, Measurement of O^{18}/O^{16} ratios of total oxygen of carbonates, Geochim. Cosmochim. Acta, 29, 1347-1354, 1965.

Sharma, T., Mueller, R. F., and R. N. Clayton, O^{18}/O^{16} ratios of minerals from the iron formations of Quebec, J. Geol., 73, 664-667, 1965.

Sheppard, S. M. F., Carbon and oxygen isotope studies in marbles, Ph.D. thesis, McMaster University, 1966.

Silverman, S. R., The isotope geology of oxygen, Geochim. et Cosmochim. Acta 2, 26, 1951.

Steiger, R. H., and S. R. Hart, The microcline-orthoclase transition within a contact aureole, Am. Mineral., 52, 87-116, 1967.

Taylor, H. P., Jr., Oxygen isotope studies of anorthosites, with special reference to the origin of bodies in the Adirondack Mountains, New York, in Origin of Anorthosites, N. Y. State Museum Spec. Publ., in press, 1968 a.

Taylor, H. P., Jr., The oxygen isotope geochemistry of igneous rocks, Contrib. Mineral. Petrol., in press, 1968 b.

Taylor, H. P., and S. Epstein, Relationship between O^{18}/O^{16} ratios in coexisting minerals of igneous and metamorphic rocks, Part I: Principles and experimental results, Bull. Geol. Soc. Am. 73, 461, 1962.

Taylor, H. P. and S. Epstein, Relationship between O^{18}/O^{16} ratios in coexisting minerals of igneous and metamorphic rocks, Part 2: Applications to petrologic problems, Bull. Geol. Soc. Am. 73, 675, 1962.

Taylor, H. P., Jr., and S. Epstein, Comparison of oxygen isotope analyses of tektites, soils and impactite glasses, in Isotopic and Cosmic Chemistry (Urey volume), ed. by H. Craig et al., North-Holland Publ. Co., Amsterdam, 181-199, 1964.

Taylor, H. P., Jr., and S. Epstein, Deuterium-hydrogen ratios in coexisting minerals of metamorphic and igneous rocks, Trans. Am. Geoph. Union

(abstract), 47, 213, 1966.

Taylor, H. P., Jr. A. L. Albee, and S. Epstein, O^{18}/O^{16} ratios of coexisting minerals in three assemblages of kyanite-zone pelitic schist, J. Geology, 71, 513-522, 1963.

Taylor, H. P., Jr., J. Frechen, and E. T. Degens, Oxygen and carbon isotope studies of carbonatites from the Laacher See District, West Germany and the Alno District, Sweden, Geochim. et Cosmochim. Acta, 31, 407-430, 1967.

Taylor, H. P., Jr., and R. G. Coleman, O^{18}/O^{16} ratios of coexisting minerals in glaucophane-bearing metamorphic rocks, Bull. Geol. Soc. Am., (in press), 1968.

Tilley, C. E., A note on the progressive metamorphism of siliceous limestones and dolomites, Geol. Mag. 88, 175-178, 1951.

Thompson, J. B., Jr., The graphical analysis of mineral assemblages in pelitic schists, Am. Mineral., 42, 842, 1957.

Turner, F. J., and J. Verhoogen, Igneous and Metamorphic Petrology, McGraw-Hill, New York, 1960.

Turner, F. J., Metamorphic Petrology: Mineralogical and Field Aspects, McGraw-Hill, New York, 1968.

Urey, H. C., The thermodynamic properties of isotopic substances, J. Chem. Soc. 562-581, 1947.

Verhoogen, J., Ionic diffusion and electrical conductivity in quartz, Am. Min., 37, 637-655, 1952.

Verbeek, A. A., and G. D. L. Schreiner, Variations in $^{39}K/^{41}K$ ratio and movement of potassium in a granite-amphibolite contact region, Geochim. Cosmochim. Acta, 31, 2125-2133, 1967.

Weill, D. F., Stability relations in the Al_2O_3-SiO_2 system calculated from solubilities in the Al_2O_3-SiO_2-Na_3AlF_6 system, Geochim. et Cosmochim. Acta, 30, 223-238, 1966.

Wright, T. L., The microcline-orthoclase transformation in the contact aureole of the Eldora stock, Am. Mineral., 52, 115-134, 1967.

Zartman, R. E., G. J. Wasserburg, and J. H. Reynolds, Helium, argon, and carbon in some natural gases, J. Geophys. Res. 66, 277-306, 1961.

APPENDIX: ISOTOPIC REPRODUCIBILITY OF ST. PETER SANDSTONE STANDARD

During the course of this research, a working standard SPS (St. Peter sandstone) was routinely included in each set of six samples analyzed. The δ-value of St. Peter sandstone is taken as 10.9 per mil (see Garlick and Epstein, 1967) relative to Standard Mean Ocean Water (SMOW). The δ-value of a particular sample x relative to SMOW is then calculated by the following formula:

$$\delta_{x\text{-SMOW}} = 1.05 \left(\delta_x^{raw} - \delta_{sps}^{raw} \right) + 10.9$$

where δ_{sps}^{raw} is the mean value of one of four groups of St. Peter sandstone samples measured against the mass spectrometer reference gas (see list below); for example, if a sample analyzed during the period of group I, a value of -13.58 was used, etc. The factor 1.05 is the total correction factor arising from change of standards, background and valve-leak in the mass spectrometer, and C^{13} and O^{17} correction (see p. 22).

In the following are listed the δ raw of St. Peter sandstone in four groups. The slight differences in the average δ-values among groups I, II, and III were due to variations in the isotopic composition of the mass spectrometer reference gas and/or to secular drifts in the mass spectrometer. However, during the experimental period of group IV, an anomalous systematic lowering of δ-values of all the samples was observed. The effect was ultimately found to be due to the improper splitting of the CO_2 gas sample when introduced into the mass spectrometer (due to a quick freezing-defrost procedure) such that the isotopically light portion of the CO_2 sample was analyzed (this was

checked by analyzing the other portion of the sample which was isotopically heavier). After the discovery of this effect, the freezing-defrost procedure was discarded. All samples measured during the period of group IV were reanalyzed at least once, and when converted into the final $\delta_{x\text{-SMOW}}$-values using appropriate values of δ^{raw}_{sps}, the results agreed within 0.2 per mil.

Run No.	Yield %	δraw per mil
Group I (Apr. 13, 1966 - Feb. 17, 1967)		
46	99	-13.13
52	102	-13.67
58	101	-13.59
63	100	-13.30
64	104	-13.69
86	99	-13.10
87	106	-13.39
93	98	-13.68
99	100	-13.52
106	99	-13.73
112	100	-13.69
118	101	-13.99
155	100	-13.28
160	100	-13.57
166	100	-13.57
169	100	-13.74
177	99	-13.75
182	100	-13.77
197	100	-13.63
223	99	-13.69
238	100	-13.38
241	98	-13.57
244	100	-13.96
Average: -13.58 ± 0.17 (23)		
Group II (Feb. 20, 1967 - May 24, 1967; June 27, 1967 - Nov. 7, 1967)		
247	99	-13.34
251	100	-13.10
257	96	-13.19
261	99	-13.25
269	98	-13.15
271	101	-13.15
279	99	-13.22
282	99	-13.11
293	99	-13.13
334	97	-13.08
340	101	-13.04
346	101	-12.92
351	100	-13.35
367	101	-13.24
388	98	-13.37
400	98	-13.46
406	102	-13.32
427	101	-13.20
451	103	-13.06
523	102	-13.35
544	101	-13.15
561	100	-13.23
582	102	-13.18
584	103	-13.52
599	102	-13.16
613	101	-13.18
629	100	-13.55
649	102	-13.09
655	101	-13.59
674	102	-13.18
678	102	-13.18
696	101	-13.01
Average: -13.22 ± 0.12 (32)		

Run No.	Yield %	δ raw per mil
Group III (Nov. 20, 1967 - May 20, 1968)		
731	101	-12.87
735	97	-12.99
738	101	-13.13
744	100	-13.02
762	98	-12.95
780	100	-13.04
785	99	-13.11
792	98	-13.15
888	98	-12.82
913	99	-12.99
A verage:		-13.01 ± 0.08 (10)
Group IV (May 26, 1967 - June 20, 1967)		
462	100	-13.84
464	102	-13.88
473	100	-13.72
478	102	-13.86
484	102	-13.81
495	99	-13.86
504	101	-13.72
510	102	-14.10
514	102	-14.07
Average:		-13.87 ± 0.09 (9)